# Spontaneous Segregation of Adaptive Agents in Auctions

Aloric, Aleksandra

*Awarding institution:*
King's College London

KING'S COLLEGE LONDON

DOCTORAL THESIS

# Spontaneous Segregation of Adaptive Agents in Auctions

*Author:*
Aleksandra ALORIĆ

*Supervisor:*
Prof. Peter SOLLICH

*A thesis submitted in fulfillment of the requirements*
*for the degree of Doctor of Philosophy*

*in the*

Disordered Systems Group
Department of Mathematics

March, 2017

# Declaration of Authorship

I, Aleksandra ALORIĆ, declare that this thesis titled, "Spontaneous Segregation of Adaptive Agents in Auctions" and the work presented in it are my own. I confirm that:

- This work was done wholly or mainly while in candidature for a research degree at this University.
- Where any part of this thesis has previously been submitted for a degree or any other qualification at this University or any other institution, this has been clearly stated.
- Where I have consulted the published work of others, this is always clearly attributed.
- Where I have quoted from the work of others, the source is always given. With the exception of such quotations, this thesis is entirely my own work.
- I have acknowledged all main sources of help.
- Where the thesis is based on work done by myself jointly with others, I have made clear exactly what was done by others and what I have contributed myself.

Signed:

_____

Date:

_____

*"You cannot hope to build a better world without improving the individuals. To that end each of us must work for his own improvement, and at the same time share a general responsibility for all humanity, our particular duty being to aid those to whom we think we can be most useful."*

Marie Sklodowska Curie

KING'S COLLEGE LONDON

# *Abstract*

**Spontaneous Segregation of Adaptive Agents in Auctions**

by Aleksandra ALORIĆ

When a population of agents divides into subgroups, and subsequently interactions happen between largely fixed subgroups, we regard the population as segregated. The segregated state might confer benefits, e.g. a buyer who has a strong preference for a particular seller has shorter exploration time when buying. As it might also add vulnerability to a system, understanding how segregation emerges is essential.

To investigate whether the segregation can arise spontaneously, as a consequence of repeated interaction and co-adaptation among the agents, a stylised model of double auction markets and traders is developed and investigated. We show that in a system with two discrete-time double auctions and a large population of adaptive traders a collaborative segregated state emerges.

When the typical scale of market returns become higher than some threshold, the preferred state of the system is segregated: both buyers and sellers are segmented into subgroups that are persistently loyal to one market over another. The segregated state is stabilised by some agents acting cooperatively to enable trade and provides higher rewards than its unsegregated counterpart both for individual traders and the population as a whole. Realising that the agent's adaptation is the key promoter of the segregation, we investigate the robustness of our findings in continuous double auctions with sophisticated trading strategies – adaptive agents still prefer to segregate. Accordingly, to create informed regulations e.g. in large financial systems, we believe it is necessary to investigate benefits and risks that segregation brings and consequently how to promote or suppress it.

# *Acknowledgements*

Apart from the tremendous efforts of myself, this research relied largely on the support and guidelines of many others. I take this opportunity to express my gratitude to the people who have been instrumental in the successful completion of this project. My intellectual debt is to my supervisor, Prof. Peter Sollich for enlightening discussions and endurance of continually increasing phenomenology emerging from a model that seemed so trivial at the beginning. Physics intuition and knowledge that he shared have been greatly appreciated. I owe my deepest gratitude to Prof. Peter McBurney whose empirical insights inspired this research and who kept helping me put my research into the wider context. I am indebted by his kind words of encouragement during times when the end seemed unattainable. I would also like to thank Dr Tobias Galla for stimulating discussions and fruitful collaboration.

My research and time spent in the Disordered Systems Group would not be the same without the "disordered girls". Silvia, I am especially grateful for all the endless discussions about our oscillating research success, our amazing students and King's experience, for the sleepless nights we were working together before deadlines, and for all the fun we have had living and working together. Barbara, thanks for so many inspiring moments while travelling, visiting art galleries and discussing politics.

For being a scientist I am greatly indebted to Petnica Science Center that already during highschool formed me as a researcher with integrity, a critical thinker and an idealist in constant pursuit of better scientific society.

Nemanja, I am grateful for all the drawings of Sale that made me laugh when it was the hardest. Thanks for supporting me and believing in me, despite blaming my thesis for the last four years of our long-distance life.

Finally, I must express my very profound gratitude to my family for providing me with unfailing support and continuous encouragement throughout so many years of study. This accomplishment would not have been possible without Sofija, Teodora, Stanija and Ratko. Thank you.

# Contents

# List of Figures

# List of Abbreviations

| | |
|---|---|
| **TAC** | **T**rading **A**gent **C**ompetition |
| **CAT** | CATallactics; CAT tournament is a mechanism design tournament |
| **EWA** | **E**xperience **W**eighted **A**ttraction |
| **ZI** | **Z**ero **I**ntelligence |
| **NE** | **N**ash **E**quilibrium |
| **APA** | **A**ll-**P**ay **A**uctions |
| **SAPA** | **S**econd highest bid **A**ll-**P**ay **A**uctions |
| **ESS** | **E**volutionary **S**table **S**trategy |

# List of Symbols

| | |
|---|---|
| $a$ | ask value |
| $a(s, s_1, \ldots, s_{k-1})$ | payoff function |
| $A_\gamma$ | attraction to an action $\gamma$ |
| $A_\gamma^i$ | denotes single agent's ($i$) attraction |
| $A_\gamma^{(g)}$ | denotes group's ($g$) attraction |
| $\mathbf{A}$ | vector of attractions |
| $b$ | bid value |
| $B$ | Binder cumulant |
| $C_{\gamma\delta}$ | autocovariance function |
| $k$ | number of players in an auction |
| $L$ | number of discrete strategies |
| $M_n$ | $n$-th jump moment |
| $n$ | trading period counter |
| $n(s)$ | number of agents playing strategy $s$ |
| $N$ | number of agents |
| $N_\gamma$ | number of agents taking an action $\gamma$ |
| $p_\tau$ | probability to trade in a role $\tau \in \{\mathcal{B}, \mathcal{S}\}$, e.g. buyer or seller |
| $r$ | forgetting rate |
| $Q_\gamma$ | probability that an order is valid |
| $s$ | strategy |
| $S$ | return, specially $S_\gamma$ return at action $\gamma$ |
| $t$ | rescaled time, $t = nr$ |
| $T_\gamma$ | trading probability, e.g. probability of finding a trading partner |
| $V$ | value of reward in evolutionary auctions |

| | |
|---|---|
| $\alpha$ | forgetting rate interpolating parameter (Chapter 4) |
| $\alpha$ | reward ratio (Chapter 5) |
| $\beta$ | intensity of choice, specially $\beta_s$ is segregation threshold |
| $\gamma$ | action, $\gamma = \{m, \tau\}$ where $m$ denotes market, $\tau$ denotes order type |
| $\Delta$ | attraction difference $\Delta = A_1 - A_2$, $\Delta^i$ and $\Delta^{(g)}$ as for attractions $A$ |
| $\theta_m$ | bias of a market $m$ |
| $\theta()$ | Heaviside step function |
| $\mu$ | distribution mean, specially $\mu_a$ mean ask, $\mu_b$ mean bid |
| $\pi_m$ | trading price at market $m$, specially $\pi^{eq}$ is an equilibrium price |
| $\pi(s)$ | fitness when playing strategy $s$ |
| $\sigma$ | distribution standard deviation |
| $\sigma_\beta()$ | sigmoid function $\sigma_\beta(x) = 1/(1 + \exp(-\beta x))$ |
| $\phi(s)$ | strategy cumulative distribution |
| $\psi(s)$ | strategy probability density distribution |
| $\omega$ | frequency |

*Sofiji, Teodori, Staniji i Ratku*

# Chapter 1

# Introduction

## 1.1 Motivation

When a population of agents divides into subgroups, and subsequently interactions happen between largely fixed subgroups, we regard the population as segregated. For instance: buyers who always buy from the same type of merchants, airline companies who target only a subset of a buying population, individuals who trade books on Amazon, but when trading electronic devices their choice is eBay.

An argument can be made that a segregated state develops as a consequence of some attributes exogenously imposed, such as wealth distribution (airline companies are grouped based on targeting customers of different budget constraints) or geographical distribution (all conditions being equal an agent will probably prefer to buy from a vendor in his/her geographical vicinity). However, changes in the economic system – such as e-commerce or cryptocurrencies – raise the question if segregated states can emerge endogenously.

Especially, the increasing fraction of global trades that now takes place online in the form of high-frequency algorithmic trading (around $30\%$ of equity trading in the UK and around $60\%$ in the USA [1]) raises many challenges for market regulations. To make regulation as informed as possible more research is needed to understand the possible long-run states of systems of coevolving markets and traders. The segregated population of traders is one possible long-run state and although it might confer benefits, e.g. an agent who has a strong preference for a particular seller has shorter exploration time when buying, it might also add vulnerability to a system, for example by reducing market

liquidity.

Market consolidation versus market fragmentation is another term very closely related to the questions of segregation. In a consolidated or concentrated market, majority of trades occur in one (or a few) as opposed to numerous trading venues. With proliferation of trading venues, especially with online marketplaces and darkpools[1], the question whether market fragmentation confers advantages or disadvantages is a widely researched topic (see e.g. [3]). Trading costs, liquidity, execution times, latency arbitrage are among investigated consequences of market fragmentations. Whether market fragmentation aids or hinders these effects is a long standing debate [4–9]. Specially, in an already fragmented financial markets that mostly employ continuous trading, authors of [10] argue that latency arbitrage needs to be considered and they show that it negatively affects market efficiency. Conversely, discrete-time market is proposed as a way to improve efficiency which motivates our investigation of stylized discrete time double auctions.

Understanding if states like segregation emerge in large systems of adaptive agents is a challenging question in the domain of engineering sciences, too. Technological advances created the need for development and management of extensive automated systems (e.g. online marketplaces with algorithmic traders, but also systems for monitoring and control of urban traffic flow, etc. [11]). For optimal design and control of such systems, it is essential that an engineer knows about possible collective states as e.g. segregation and how to induce them (if beneficial) or suppress them (if risky). All things considered, we believe investigating how segregation emerges is necessary.

To understand the segregation-like phenomena we believe the first step is to reproduce it under controlled conditions. This would allow us to isolate causes and effects and gain possible insights into benefits of such state. In this thesis, I develop one such model of interacting adaptive agents using which we can observe and analyse spontaneous segregation. In most of what follows, I focus on the emergence of segregation in a population of adaptive traders who choose among different markets, e.g. eBay or

[1] Alternative trading venues that guarantee anonymity, which among other things prevents price drops when large quantities of shares are sold, see e.g. [2].

Amazon, New York Stock Exchange or London Stock Exchange, or across various currency exchange markets, etc. The central questions this thesis addresses are: Under what conditions does the segregation emerge? Does the segregation bring benefits to a population? When does a competition between markets lead to market coexistence and when does a subset of markets or monopoly arise? We extend the list of questions and describe further the aims and approaches taken in this research after a brief review of existing work.

## 1.2 Review of existing work

The emergence of collective behaviour among autonomous agents has been a prolific research topic among physicists during the last couple of decades. The main reason for this is a presumption that statistical physics techniques that contributed to the understanding of macroscopic phenomena built from an understanding of large systems of interacting microscopic entities can be applied to various biological, economic and social systems. A large body of work exists on collective motion of animals [12–14], mass movement of people [15, 16], but also voting patterns [17, 18] (for a detailed overview of physics application in the domain of social sciences see e.g. Castellano *et al.* [19]), etc.

In a similar vein, in this thesis, I address a macroscopic effect – **segregation**, i.e. the emergence of group structure within an initially homogeneous population, investigating whether it can arise spontaneously, just as a consequence of interactions at the agents' level and individual adaptation. It is worth nothing that, differently from the Schelling segregation [20], i.e. the emergence of spatial separation between different types of agents, especially different ethnicities, we address segregation in the form of group formation in the space of preferences or some other individual attribute, rather than the actual physical space. Nevertheless, the remarkable result from the Schelling model informs us that, contrary to intuition that a strongly racially segregated society must be a signal of intense racism, a small preference to be surrounded by neighbours of the same ethnicity gets pronounced by interactions and the population tends towards full segregation.

Another interesting cellular automata based model is the *sugarscape*, a model of artificial societies developed by Epstein and Axtell [21]. The authors study many phenomena emerging out of a few simple update rules based on nearest neighbour interactions, but especially, they address the evolution of a system when trading is introduced. The agents need two commodities for survival, sugar and spice, both initially scattered across space and can be acquired either directly or by trade. The study offers a decentralised perspective into trading assuming that neighbours locally bargain until a mutually agreeable deal is reached, investigating this way the questions of efficient markets and equilibrium trading prices. In the simulated system, it was shown that trade often occurs among the same agents and some agents would persistently obtain one of the commodities through trade while the other will be directly extracted from the surrounding space.

Other authors focus on the Minority game [22], a mathematical formalisation of the "El Farol" bar [23] problem, because of its simplicity, yet rich phenomenology [24]. In the simplest form of the game, an agent needs to decide whether to go to the bar or not and only if (s)he is in the minority group (either as an agent in the bar or at home) (s)he wins. Typically agent's strategies are formalised in terms of instructions how to act based on the history. Although apparently the game does not have any relation to financial markets, it is commonly used as a market toy model because the choices to go or to stay can be interpreted as to buy or to sell and if the price is determined based on the relation between the demand and supply, an agent in the minority will receive higher returns. Many extensions to the game exist, and while some are known to reproduce market stylised facts such as volatility clustering and fat tails in the return distribution [25], others aim to replicate segregation-like effects. Especially, in the study [26] it was noted that "...a population of competing agents with similar capabilities and knowledge will tend to self-segregate into opposing groups characterised by extreme behaviour". The variant of the minority game used in this study supposes that agents can choose to follow a global strategy based on collective memory – this is the primary driver of segregation. Another group of authors consider multi-asset minority games [27] and show that in a system of agents who have the option of copying a winning (minority) strategy from their neighbourhood with some probability $p$, a self-organized grouping of strategies arises when

the probability $p$ is large enough. Grouping was only found when the underlying interaction network is well connected, and when agents have perfect information about the success of their neighbours. Compared to these studies where the minority game is used as a metaphor for financial markets and a large amount of public information is shared among agents, in this thesis I focus on studying segregation effects among agents who participate in auctions with different types of mechanisms and the information they have at their disposal will always be only their own history.

Specialisation or grouping in agent's strategy space was studied in the paper by Hanaki *et al.* [28] with a focus on a system of agents competing for parking spots in a one-way street. As in the model we propose in the following chapters, the authors study the development of agents' preferences when they learn based on their trials with rewards (the closer to the city centre the better) and penalties (an agent is punished if (s)he reaches the centre without parking). When an agent's strategy is the distance at which they start searching for the first available spot where they will park, the authors notice that at high choice intensities[2] specialization in the population occurs – some agents learn to be lucky, they always start searching for parking space very close to the target location, while the others settle for parking far from the city centre aiming to avoid disappointment of not finding a parking spot in the locations closer to the city centre. Although this study focuses on a different problem, the techniques we use, primarily to analyse interactions of only a few players, resemble their analysis very closely with a difference in the details of return mechanisms.

A more closely related model with adaptive agents in a financial market was studied by Brock and Hommes [29]. They examine the dynamics of agents who have to decide whether to purchase a sophisticated price predictor or use a freely available naive predictor of price. Even though the agents are faced with a choice that might be related to our investigation goals, this scenario differs from our model in a number of ways; apart from the more sophisticated trading strategies of the agents, it assumes perfect information about previous prices and the performance of any price predictor. What is important

[2]Intensity of choice is a parameter of agent's learning dynamics that will be defined and used through the thesis. In its essence it describes how strongly agents rely on the choices that were the most rewarding in the past.

in the analysis of Ref. [29], however, is that the limit of a large population of agents is implicitly taken, so that the system can be described entirely in terms of the fraction of agents choosing a given action (price predictor) at any instant in time, with these fractions evolving deterministically in time. The authors of Ref. [29] show that depending on the intensity of choice, these two fractions can exhibit rich dynamics. The origin of this is that when all traders use sophisticated predictors, the cost of this predictor leads some agents to start choosing the free predictors, while there is a reverse effect from positive feedback when all traders use the simple predictor.

Kirman and Vriend [30] study emergence of loyalty between buyers and sellers in a fish market in Marseille. Motivated by two empirical facts, buyer-seller loyalty and a large price dispersion, the authors develop a stylised model to describe the observed phenomena. In its core question, this work is very closely related to ours, as stated previously: once segregated, the population largely interact within specific subgroups that indeed resembles a long lasting loyalty. However, aiming to address very particular market, the authors have made several assumptions that we will avoid later: the number of sellers is an order of magnitude smaller than the number of buyers, and there is an assumed difference between buying and selling strategy, not only in the order price (as we will later consider as well), but the seller is supposed to make a decision how (s)he will address a loyal buyer. These assumptions are reasonable in the type of market the authors are discussing, where the interaction is direct, but when modelling interactions over an anonymous market such as the currency exchange, there is no reason for the disparity of buyer and seller numbers, and similarly most of the markets will hide traders identity. Finally, it is not entirely clear whether the observed loyalty is only a consequence of a special strategy trait that is loyalty related. Nevertheless, the authors replicated stylised facts observed in the real market and found that the loyal buyers receive an overall higher benefit as opposed to buyers who randomise their choice of sellers. Contrary to this model the loyalty we observe between traders and markets is signalled by persistence in market visitation patterns, but the markets do not distinguish between loyal or randomising agents. As we will argue in more detail later, the benefit the segregation will bring is stability in the number of trades.

The Trading Agent Competition [31] was developed to instigate more research into optimal automated trading strategies evaluated against fixed market rules. Similarly but in the reverse direction, the CAT market design tournaments [32–35] were aimed at promoting development and investigation of more sophisticated market specialists strategies. As TAC tournament organisers provided the market setup at which trading strategies competed against each other, CAT tournament organisers populated the system with automated traders who had a variety of trading and market choosing strategies. Submitted market designs in CAT tried to attract many traders, but also to maximise the profit from the traders taking place under their governance. Some of the trading strategies that participated in the CAT tournaments were the ones we use extensively in our study (e.g. Zero Intelligence Traders), but other types of strategies had more sophisticated order pricing mechanisms, e.g. chartists or fundamentalists. Similarly, a variety of market choosing strategies were implemented ranging from random market selection to sophisticated learning strategies. During the five consecutive successful competitions (2007-2011) a pool of different market strategies was acquired, which made it a useful tool for development and evaluation of new market mechanisms (see e.g. [33, 36]). But even more interestingly in the context of this study, in an *in silico* experiment based on CAT Market Design tournaments segregated states were observed in the co-adaptation of markets and traders [34]. Some markets ended up focusing on attracting specific traders, and some traders preferred to trade at a specific market, although no such fixed propensities were imposed from the beginning. Further signals of segregation like phenomena include persistence in customer visitation patterns [37], segmentation in credit markets in the Philippines [38], specialisation and herding in financial markets [39], etc. As mentioned before, it can be argued that something else in these systems (geographic, wealth or other heterogeneity) prompted the segregation-like effect. However, the observations made in CAT-based experiments suggest that an endogenously developed segregation is possible too. This encouraged us to develop an analytically tractable model to investigate such possibility.

More research focuses on the exploration of the already segmented population, in order to target the product to a particular, previously untargeted niche of customers.

These lines of work are a continuation of Adam Smith's [40] postulate that specialisation leads to better exploitation (see for example [34, 41–43]).

Finally, authors such as Ellison *et al.* [44] and Shi *et al.* [36] focus on studying competition of markets and conditions under which this contest might lead to multiple market coexistence and conversely when it will lead to monopoly. The authors name two significant effects in the competition of double auctions, one of them is the positive size effect, i.e. agents prefer trading in a market where there are already many traders of the opposite type (e.g. sellers like trading at markets where there are many buyers), as the choice among offers is better. The authors additionally suggest the existence of the negative size effect in a double auction market, as agents will prefer being in the minority group to trade more often (e.g. buyers see the benefit of trading at a market where there are not many buyers, see e.g. [45]). Ellison *et al.* [44] point out that due to the negative size effects coexistence of many markets is possible. On the other hand Shi *et al.* [36] investigate which of the two effects is stronger and finds that due to more substantial positive effects in many situations monopoly will be a favoured end-state. When there is a strong market differentiation, the authors of [36] argue that market coexistence is possible, especially for markets that have different pricing policies, e.g. one market charges a fixed participation fee versus the market that charges a profit fee.

Although in what follows we will consider markets without fee charging policies, we will find that various system parameters enable markets coexistence, e.g. both markets will be populated with roughly the same numbers of traders, but we also identify the parameters for which one market is dominant. Interestingly we will find out that coexistence of the two markets will be driven by agents' learning parameters and it can happen even when the two markets are identical. Important to note is that in principle these different results are not necessarily comparable, because not only do we avoid considering fee charging policies, but the previous works focused on finding either the Nash Equilibria or states favoured by the replicator dynamics while we look into dynamics based on agent's learning, which we believe is more appropriate in the context of agents engaging in economic interactions[3].

[3]We believe a more relevant update mechanism in a social system is related to adaptation by learning rather than by natural selection. Although it might be argued that some basic reflex strategies could have emerged as favoured by evolution, in repeated interactions such as the ones we will study, the time scales

We are additionally fascinated by segregation-like effects in an ecological context. Namely, there are many collective phenomena that share similarities with the segregated states, e.g. generalist vs. specialist in virus-host relationships [47], compartmentalization in food webs [48], emergence of mutualistic networks and hierarchical structures between species [49], nestedness in networks of mutualistic relationships [50], etc. All these examples signal some segregation within the population indicated with interactions that primarily take place within specific subgroups. All these effects are argued to offer stability and robustness to ecological systems (see e.g. [49]). Another segregation-like effect is related to one of the fundamental questions of evolution – speciation, i.e., emergence of new species. Besides what is called *allopatric speciation* (that assumes a geographic barrier in species interaction which is crucial for the speciation), empirical evidence also asks for models and understanding of sympatric speciation, where speciation happens even without geographical barriers (e.g., in Lakes Malawi and Victoria [51]). A large body of work is devoted to mathematical understanding of mechanisms that could lead to this phenomena, including various concepts that are themselves similar to segregation: polymorphism (occurrence of two or more alternative phenotypes that cannot be explained by mutation only; the distinctive types are assumed to coexist in the same habitat with random mating [52]), disruptive selection (where selection favours the coexistence of two extremal trait values rather than an averaged one), but also specialization in either choosing mating partners or mutualist partners [53] (an example of speciation model in a plant-pollinator system can be found in [54]). All these examples are fascinating phenomena on their own and their investigation helps in building a deeper understanding of speciation.

Our attention was especially attracted by evolutionary auction games [55] in which the authors report that when many rewards are offered specialisation in the population occurs. Early on authors [56–59] realized that many interactions in a biological context have forms of auctions, too, for example: energy investment in competition for resources

are those more suitable for learning. Additionally, Sato and Crutchfield [46] show that an equation similar to the replicator dynamics can be developed starting by learning rather than the birth/death process under natural selection.

(e.g., competition of tree height to reach most of the sunlight) or development of ornament or weapon traits in males to attract a female or defend a territory. The main difference between evolutionary auctions and auctions studied in an economic context for a very long time lie in the fact that in the biological context a realistic assumption is that everyone pays their bid. Compared to early works [59, 60], Reiter *et al.* [55] extend evolutionary games asking how the bidding strategies change when competitors are offered more than one reward. Interestingly, already the introduction of the second reward suggests that the evolutionary stable state is such that the population is specialised in low and high bidders. What additionally differs evolutionary auctions compared to games studied to a large extent such as prisoner's dilemma or the hawk-dove game is that its strategy space is continuous - an agent in a contest for the reward can bid any real value $s$. Contrary to the discrete strategy games where evolution is studied with evolutionary dynamics methods, such as replicator and similar equations, such formalism has not been developed for continuous strategy games, but the games have been studied only by means of static tools, such as evolutionary stable strategies [56, 57]. Building on the works of [61–64], we develop a macroscopic equation describing evolutionary dynamics starting from a microscopic birth-death process of players. Our goal is hence to investigate whether under evolutionary adaptation agents who interact via evolutionary auctions will specialise and if such states are stable under the dynamics we study.

## 1.3 Aims and approach

The central question of this thesis is the possibility of segregation emergence among adaptive traders who interact via auctions. In particular, can we develop a stylised model of the double auction markets and traders aiming to reproduce phenomena observed in CAT tournaments [34]? Can we identify segregation drivers? Are there benefits that segregation brings to a population? Are the findings robust under changes of model assumptions?

As opposed to the paradigm of a rational, fully informed, utility maximising, representative agent, in pursuing answers to those questions we will start from an agent-based model (for a detailed review, see [65]), which is a growing new economic paradigm trying

to allow for all the heterogeneity that exists in financial systems. Many existing models already showed a good level of success in reproducing market stylised facts (e.g. [66–68]), but also offering insights into the emergence of collective effects like herding and trade-following (e.g. [69, 70]). Although there is growing interest in developing larger and empirically tuned Agent Based Models to allow for direct comparison with financial data, we will take a different route and build a simple, stylised model hoping to unravel prevalent driving forces behind phenomena, without overspecialization to any type of market interaction.

Different possible double auction mechanisms that prompted our research are described here [35, 71, 72]; In particular we start with a discrete time, global price setting market, that we can fully describe analytically. We proceed and test our findings in the more realistic continuous double auction markets. When modelling agent's trading strategies we follow the route proposed by previous authors [73–75] and assume that agents are trading at random [76]. This assumption is often motivated by the desire to reduce system complexity in the space of trading strategies to be able to investigate system properties that are the consequence of market mechanisms or intrinsic to the system. Once we have developed an analytical description and understanding of the system adaptation with these stylised traders, as in the case of market mechanisms, we also probe robustness of our findings with more sophisticated trading strategies – the fundamentalists.

Finally, when modelling how agents choose between the markets we rely on the Experience Weighted Attraction learning [77, 78]. The two main paradigms in agent's adaptation are reinforcement and belief-based learning [74]. The belief-based paradigm assumes agents are acutely aware of the existence of other players: often an agent is able to keep track of other agent's scores, infer their strategy and base his/her choices on that belief, all of which we assume should not be taken for granted in the system we address. Instead, we suppose agent's actions are based on the reinforcement learning - trial and error and decision making based only on agent's own history. This approach does not even assume the agent is aware of the market mechanisms nor existence and numbers of other players. Agent only tries different options and based on those forms attraction

to these choices in the future that are with the *logit* function transformed into a market choosing strategy, e.g. probability of visiting any of the markets. As we do not assume market mechanisms nor other players' choices are always easily accessible information available to each agent, in what follows we focus on investigating adaptation based on reinforcement learning, though we address different versions of it.

As concluded in the review by Duffy [74], despite the abundance of literature on different learning models, the consensus between reinforcement learning vs. belief-based learning only exist in as much that both of the learning mechanisms are better predictors of the agent's adaptation than previously used static analysis such as the Nash equilibrium. On the question which of the paradigms is more justified results are less conclusive as often the two lead to experimentally indistinguishable results, or experiments were not as long as necessary to demarcate between the two. Thus, we believe that the choice must be made case by case, depending on the context in which the learning is implemented (for example in our model we argue belief-based model is not appropriate) until more conclusive experimental findings are available.

In the domain of agents in the ecological context whose interactions we model by evolutionary auctions, in this thesis we ask when the specialisation is possible. When is the specialised population a fixed state of the evolutionary dynamics? We aim to address the emergence of specialisation among agents who adapt through the natural selection. We focus on previously reported evolutionary stable states that show the emergence of specialisation in a population of agents playing evolutionary auctions. We develop macroscopic equations of evolutionary dynamics from the underlying birth-death process driven by the repeated interactions. This result was not previously extended to games with continuous strategy space, while now it enables us to study dynamics of the evolutionary auctions. We analyse the fixed points, their stability and other dynamical phenomena such as noise induced cycles for different type of evolutionary auctions.

## 1.4 Structure of thesis

The remainder of this thesis progresses as follows. In Chapter 2, a novel model of double auction markets and adaptive traders is developed. Compared to similar models which

study the emergence of grouping or specialised agents, this model considers the possibility of the emergence of segregation in the context of double auction markets. We show results of the numerical simulations that demonstrate the existence of a segregated steady state in a domain of large intensity of choice - agent's learning parameter. The detailed analytical description that retrieves numerical results with remarkable precision and gives insights into benefits that segregation brings to the whole population are presented.

Chapter 3 continues an analytical investigation of the system of agents and markets introduced in Chapter 2; especially, we address the large memory limit where the transition between an unsegregated and the segregated state is sharp. Firstly we analyse small systems of two and four agents that are tractable and easy to interpret, yet nevertheless show a variety of steady states of synchronised and segregated type. We continue analysis on a large homogeneous population where we introduce all necessary techniques to detect and categorise different types of steady states. We conclude by returning to the numerical model to analyse stability and the existence of a variety of segregated states the theory predicts.

In Chapter 4 we address robustness of our findings by extending our model to probe effects of various simplifying assumptions we have introduced. We show that a more realistic trading models (e.g. agents with budget constraints, fundamentalist trading strategies, continuous double auction market with limit order books, etc.) share qualitative features of the simplified model – there is a threshold intensity of choice above which the population of agents segregates. We re-examine the learning mechanism proposed and show that our results are robust under a wide variety of reinforcement learning models. Finally, we address segregation in systems with more than two markets and show that not all traders will visit all types of market, i.e. markets will appear specialised even when there is no intention to target subsets of traders.

In Chapter 5 we turn to adaptive agents in a biological context. Instead of learning we consider evolutionary dynamics of agents who interact in the form of k-player all-pay auctions. We extend existing methods of deriving macroscopic equations of the replicator type for the games with continuous strategy space. In particular, for the finite system

sizes we analyse effects of demographic noise on the fixed points of the dynamics. Finally, we investigate under which conditions an analogue of segregation – specialisation – occurs and study stability of such states.

Chapter 6 draws conclusions based on the research carried out within the thesis, reviews the contributions that this thesis has made and discusses how this work can be extended in the future.

## 1.5 Previously published work

1. Alorić, A., Sollich, P., & McBurney, P. (2015). Spontaneous segregation of agents across double auction markets. In *Advances in Artificial Economics* (Lecture Notes in Economics and Mathematical Systems 676). Springer International Publishing.

2. Alorić, A., Sollich, P., McBurney, P., & Galla, T. (2016). Emergence of Cooperative Long-Term Market Loyalty in Double Auction Markets. *PLoS One* , 11(4).

**Autor contributions**: A.A., P.S. and P.M. conceived the study. A.A. and P.S. carried out the research, A.A. developed the simulations, carried out the analytical calculations and prepared the figures. A.A., P.S. and T.G. interpreted the data and shaped the study. All authors wrote and reviewed the manuscripts.

Published papers cover the content of Chapter 2 and parts of Chapters 1 and 4. Chapter 5 is collaborative work with Tobias Galla who devised the study and developed the method presented in section 5.2.1, I have carried out the research, developed the simulations and carried out the analytical calculations and prepared figures and other relevant results presented in the chapter and supporting material.

# Chapter 2

# Model for spontaneous segregation of adaptive agents facing choice of double auctions

While the CAT tournament results referred to in Chapter 1 provide a clear impetus to study spontaneous segregation, they are difficult to analyse theoretically due to the complexity of both the agents' trading strategies and the market mechanisms of the competing markets. We therefore devise and analyse a stylized individual-based model of a double auction. We focus on agents using experience-weighted attraction learning (EWA) [77] to learn from the payoffs received for past actions and thus optimise future trading. By developing a stylized model we obtain an intuitive and analytically tractable tool for understanding whether and when segregation can emerge spontaneously in a system of competing double auction markets. We start with a desription of the Model and then provide Numerical results, summarizing the main findings from our numerical simulations. In the following subsections we develop an Analytical description in the large market limit, using a Fokker-Planck approach to investigate the steady states of the system mathematically and in particular to develop insights into the properties of the segregated state.

## 2.1 Model of learning at double-auction markets

To address the question of spontaneous segregation, we study a stylized model of a population of adaptive traders and two double auction markets. We hypothesize that segregation can arise as a product of co-adaptation of traders, and construct on this basis a minimal model for both traders and markets. We investigate this in detail by numerical simulation, and provide a full theoretical understanding and characterisation of the observed segregation effects.

**Traders.** Following the works of Gode and Sunder [76], Ladlay [73] and Duffy [74], we populate our system with agents without sophisticated trading strategies, essentially zero-intelligence traders. This is done because our aim is to investigate whether market loyalty can arise as an intrinsic property of a system of interacting agents without reliance on complex trading strategies. The orders to buy at a certain price (bids) and orders to sell at a certain price (asks) are assumed to be unrelated to previous trading success or any other information. We assume that bids, $b$, and asks, $a$, are normally distributed ($a \sim \mathcal{N}(\mu_a, \sigma_a^2)$ and $b \sim \mathcal{N}(\mu_b, \sigma_b^2)$), and that their means satisfy $\mu_b > \mu_a$.

The assumption that the average bid is higher than the average ask is not crucial; it mainly allows a larger number of successful trades as the resulting trading price is typically below the average bid and above the average ask. In the work of Gode and Sunder (Ref. [76]) various demand and supply curves were used and thus both orderings of average bids and asks, $\langle a \rangle > \langle b \rangle$ and $\langle a \rangle < \langle b \rangle$, were investigated: they lead qualitatively to the same results. We similarly explored the case $\mu_a > \mu_b$, and apart from the obvious quantitative consequence that a smaller fraction of orders is valid for trade and consequently the number of successful trades is smaller, the qualitative results remain the same.

In the spirit of the work of Gode and Sunder [76], $a, b$ can be thought of as cost and redemption values for each trader. These values are private to each trader but correspond to order prices if submitted bids and asks are truthful and reflect the actual valuation of goods by the agents. Traders will not accept any price from the market: sellers will trade

only if the trading price $\pi$ is no less than their asking price ($\pi \geq a$), and buyers require that the trading price is no greater than what they bid ($\pi \leq b$)[1].

After each round of trading each agent receives a score, reflecting their payoff in the trade. The scores of agents who do trade are assigned as in works of previous authors [76, 79]: buyers value paying less than they offered ($b$), and so their score is $S = b - \pi$. Sellers value trading for more than their ask ($a$), and so $S = \pi - a$ is a reasonable model for their payoff. We note that these scores are based on a linear model and do not reflect effects such as diminishing returns. Traders who do not get to trade in a given round receive return $S = 0$. The assignment of returns that we are using was introduced in Ref. [76], where it is associated with budget constraints of "Zero Intelligence-Constrained" traders. Exactly these agents were shown to reproduce the efficiency of human traders in double auction markets. Although the assignment of returns is the same in our model, we do not use the term budget constrained in the description as our agents are allowed to persistently buy (or sell), which is possible only if there is no overall wealth constraint[2].

**Markets.** The role of a market is to facilitate trades so we define markets in terms of their price-setting and order matching mechanisms; for an in-depth review of possible double auction market mechanisms see [35, 80]. We consider a single-unit discrete time double auction market where all orders arrive simultaneously and market clearing happens once every period after the orders are collected. (Note that each period consist of one round only, which is why we will talk only in terms of periods.)

We also assume that a uniform price is set by the market – once all orders have arrived, these are used to determine average bid $\langle b \rangle$ and average ask $\langle a \rangle$ and set the global trading price between:

$$\pi = \langle a \rangle + \theta(\langle b \rangle - \langle a \rangle) \tag{2.1}$$

where $\theta$ fixes the price closer to the average bid ($\theta > 0.5$) or the average ask ($\theta < 0.5$);

[1] This is in line with Gode and Sunder [76] where the traders that turned out to be more similar to human traders were the zero-intelligence ones with budget constraint, i.e. traders who were not allowed to trade at loss – higher than the redemption value for buyers and lower than the cost value for sellers.

[2] We note that also in Ref. [76], agents were preassigned the role of a buyer or a seller and were not allowed to change this during trading, thus acting as if there was no overall constraint on the possession of money/goods for trade.

the parameter $\theta$ thus represents the bias of the market towards buyers or sellers[3]. Once the trading price has been set, all bids below this price, and all asks above it, are marked as invalid orders as they cannot be executed at the current trading price. The remaining orders are executed by randomly pairing buyers and sellers; the execution price is $\pi$. Note that we assume here that each order is for a single unit of the good traded.

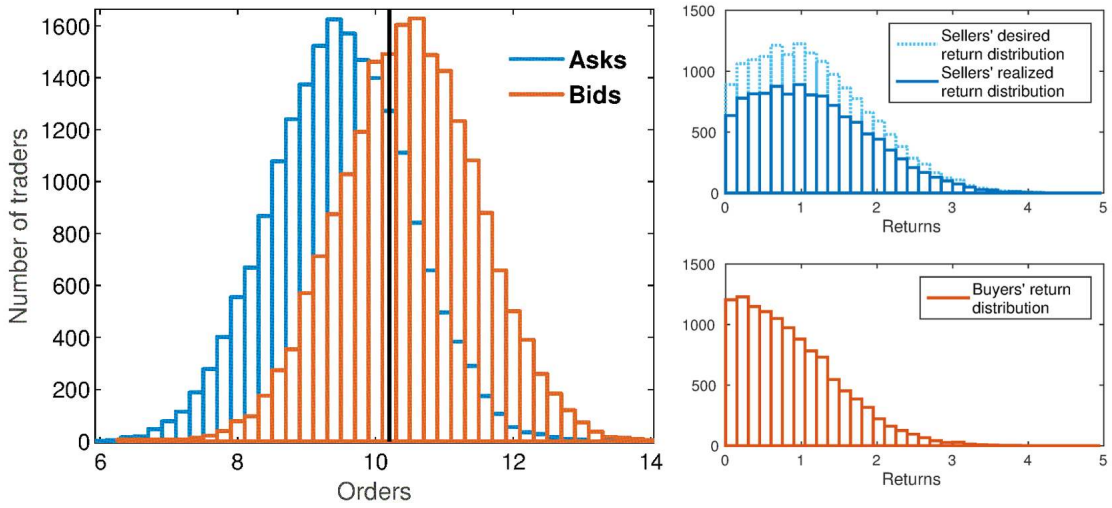


FIGURE 2.1: **Illustration of the market mechanism.** Left: example distributions of orders received in one trading period (orange – orders to buy, blue – orders to sell, black – the trading price for $\theta = 0.8$). Right: example distributions of returns from validated orders at $\theta = 0.8$. In the situation shown, where buyers are in the minority after validation of orders, all buyers find a trading partner (orange). If all sellers could trade they would achieve the "desired" return distribution (light blue). But only a randomly selected fraction finds a trading partner, leading to the "realized" return distribution (dark blue); the other sellers receive a return of zero. The realized sellers' return distribution has the same total area as the buyers' return distribution as both represent the total number of trades.

Fig. 2.1 shows graphically how the trading price is set and how the return distributions look after invalid bids and asks are eliminated. If, as in the example in the figure, the trading price is closer to the average bid ($\theta > 0.5$): only a fraction of the sellers who submitted valid asks gets to trade, but with the higher trading price – so those that do trade receive higher returns. The buyers who submitted valid bids are in a minority compared to the sellers and so determine the number of trades. They can all trade, but receive relatively low returns on account of the high trading price.

[3]Note that traders are not informed about these market biases, nor the market mechanism in general; they only obtain information through the scores they receive.

An example of a discrete time double auction market is the Opening Auction of New York Stock Exchange which is used to determine the opening prices on the market. At the opening auction, once all the orders are submitted, the trade occurs at the single price set by the market that maximises the volume of trades, the equilibrium trading price. In Figure 2.2 we show the demand and supply curves corresponding to the bid and ask

FIGURE 2.2: **Illustration of the market mechanism - equilibrium trading price.** The demand and supply curves, showing the number of orders to buy above (resp. sell below) a certain price. The vertical black line marks the equilibrium trading price, i.e. the price at which demand equals supply, while the arrows show how the trading price changes with $\theta$.

distributions shown in Fig. 2.1. The most efficient resource allocation happens when the demand equal supply - the equilibrium trading price. In a setup like ours where the bids and asks are Gaussian random variables with equal variances ($\sigma_a$=$\sigma_b$) and when the number of buyers is equal to the number of sellers at a given market the equilibrium trading price corresponds to $\theta = 0.5$, i.e. the price is $\pi^{\mathrm{eq}} = (\langle b \rangle + \langle a \rangle)/2$ (marked with black line in Fig. 2.2). In the following sections we will address cases of efficient markets (the trading price is equilibrium trading price, we also call them fair markets), but we also allow possibility that the markets are not efficient and that the trading price deviates. In Fig. 2.2 we note that for $\theta > 0.5$ there is excess of supply, suggesting that not all sellers' needs will be accommodated at that trading price, which we also demonstrated with the desired and realized return distribution in Fig. 2.1.

**Reinforcement Learning Rule.** So far we have described how agents interact at a given market. We next define how they decide *how to trade* (to buy or to sell), and *where to trade* (at which market). Agents trade repeatedly in our model, and they adapt their preferences for the various choices from one trading period to the next. We focus on the case of two markets, though the model can easily be extended to an arbitrary number of markets.

We assume that each agent decides on an action at the beginning of each trading period, only based on his or her past experience. To formalize this we introduce a set of attractions $A_\gamma$ for each player, one for each action $\gamma$: buy at market 1, sell at market 1, buy at market 2, sell at market 2. The attractions will generally differ from player to player, but we suppress this in the notation for now. The attractions are updated after every trading period, $n$, using the following reinforcement rule:

$$A_\gamma(n+1) = \begin{cases} (1-r)A_\gamma(n) + rS_\gamma(n), & \text{if the agent chose action } \gamma \text{ in round } n \\ (1-r)A_\gamma(n), & \text{if the agent chose an action } \delta \neq \gamma \text{ in round } n. \end{cases} \tag{2.2}$$

The quantity $S_\gamma(n)$ is the score gained by taking action $\gamma$ in the $n$-th trading period. The length of the agents' memory is set by $r$: agents weight returns obtained $\Delta n$ time steps ago with exponentially decaying factors $(1-r)^{\Delta n}$, effectively corresponding to a sliding window of length of order $1/r$ for the weighted averaging of past returns.

The update rule above is a special instance of a more general experience-weighted attraction rule [77, 78], which has been shown to be in reasonable agreement with experimental data on human learning in repeated games. Many special cases of this rule are in common use in evolutionary biology and in the game-theoretic literature. One important variant of EWA is a case in which *all* actions are updated with their returns, no matter whether that action was actually taken or not (belief based models [77]). This assumes that an agent can calculate or at least estimate the return (s)he would have obtained from actions $\gamma$ that (s)he did not choose to play [46, 81]. We argue that an agent would not normally have sufficient information to do this in the context of a double auction market: (s)he would need access to the current price, and to the numbers of valid bids and asks

submitted. This is unrealistic, which is why we posit that scores of unplayed actions are updated with an effective payoff of zero. One plausible alternative that does *not* rely on estimation of returns from unplayed actions would be an update rule where the attractions to unplayed actions are forgotten with a different rate (or not forgotten at all); we return to this in Chapter 4.

It only remains to specify how agents choose their actions based on the attractions. This is done in line with the experience-weighted attraction literature [77, 78], simply by converting the attractions to probabilities using the so-called *softmax* or *logit* function. Explicitly, each agent takes action $\gamma$ in trading period $n$ with probability $P(\gamma|\mathbf{A}(n)) = \exp(\beta A_\gamma(n))/\sum_{\gamma'}\exp(\beta A_{\gamma'}(n)) \propto \exp(\beta A_\gamma(n))$, where $\beta$ is the *intensity of choice* [81] and regulates how strongly the agents bias their preferences towards actions with high attractions. For $\beta \to \infty$ the agents choose the option with the highest attraction, while for $\beta \to 0$ they choose randomly with equal probabilities among all options.

One way to interpret $\beta$ is as parameterizing the degree of human rationality, where $\beta \to \infty$ corresponds to the limit of unboundedly rational players who always choose the optimal course of action [82]. Another interpretation is that $1/\beta$ sets a scale of return differences below which traders no longer significantly differentiate between the options available to them. Indeed, if all $A_\gamma(n)$ are within $1/\beta$ of each other then the exponents in the softmax function differ by less than unity and so the resulting probabilities are close to uniform. The existence of such a threshold is not implausible: higher return differences should drive a trader towards optimizing his or her actions more, e.g. by following the historically most rewarding options, while the choice between actions giving nearly the same return will be largely random. The intensity of choice $\beta$ is sometimes denoted $\lambda$ and has also been referred to as *response sensitivity* [28, 77, 78] or *learning sensitivity* [46].

## 2.2 Numerical results

**Emergence of loyalty - return-oriented and volume-oriented traders.** We begin our exploration of the two-market setup defined above with results from numerical simulations (more details in Appendix D). Unless specified otherwise, numerical simulation parameters are as detailed in Table D.1 in Appendix D. All agents start with equal

preferences for all four choices, i.e. $A_\gamma = 0 \; \forall \gamma \in \{\mathcal{B}1, \mathcal{S}1, \mathcal{B}2, \mathcal{S}2\}$ where $\mathcal{B}$ = buy and $\mathcal{S}$ = sell. To aid visualization we project the four-dimensional space of attractions $A_\gamma$ down to two coordinates, the overall attraction to buying as against selling, defined as $\Delta_{\mathcal{BS}} = (A_{\mathcal{B}1} + A_{\mathcal{B}2}) - (A_{\mathcal{S}1} + A_{\mathcal{S}2})$, and the attraction to market 1 as against market 2, $\Delta_{12} = (A_{\mathcal{B}1} + A_{\mathcal{A}1}) - (A_{\mathcal{B}2} + A_{\mathcal{S}2})$. Due to the nonlinearity of the *softmax* function, a single-peaked distribution of attractions with a non-zero spread will, for large enough intensity of choice $\beta$, become a multimodal distribution in the space of preferences. This effect cannot be regarded as genuine segregation. For this reason we will avoid representing agents in the space of their preferences $P_\gamma$, and use the underlying attractions instead.

In Fig. 2.3 (left) we present the steady state attraction distribution for a population of traders with intensity of choice $\beta = 3.45$. The initially narrow, *delta-peaked* distribution of attractions (all initialized at 0) has been broadened due to diffusion arising from the random nature of returns and from the stochasticity of the agents' actions. The steady state shown in the left panel of Fig. 2.3 represents an unsegregated population of traders. While this population does include some traders with moderately strong preferences for one of the actions, preferences remain weak on average. The population as a whole remains homogeneous in the sense that there is no split into discernible groups.

Fig. 2.3 (right) contrasts this scenario with the steady state of a system with exactly the same set of parameters but at the higher intensity of choice $\beta = 7.14$. The population of traders now splits into four groups, with the agents *persistently trading* preferentially at one of the markets and with a preferred buy or sell action. We refer to this state as *segregated*. The markets shown in this example (Fig. 2.3) are biased symmetrically $(\theta_1, \theta_2) = (0.3, 0.7)$: if an agent buys at market 1, or sells at market 2 (actions $\mathcal{B}1$ or $\mathcal{S}2$), and if they manage to trade, they are awarded with a higher score on average than if they were to choose one of the other two actions (cf. Fig. 2.1, where sellers are the group with the higher average return). In this symmetric market setup there are therefore two different kinds of behaviour among the four segregated groups. The agents in two of the groups ($\mathcal{B}1$ and $\mathcal{S}2$) specialize in actions that award them higher average return, we call those traders *"return-oriented"*. We will refer to the agents in the other two groups ($\mathcal{B}2$ or

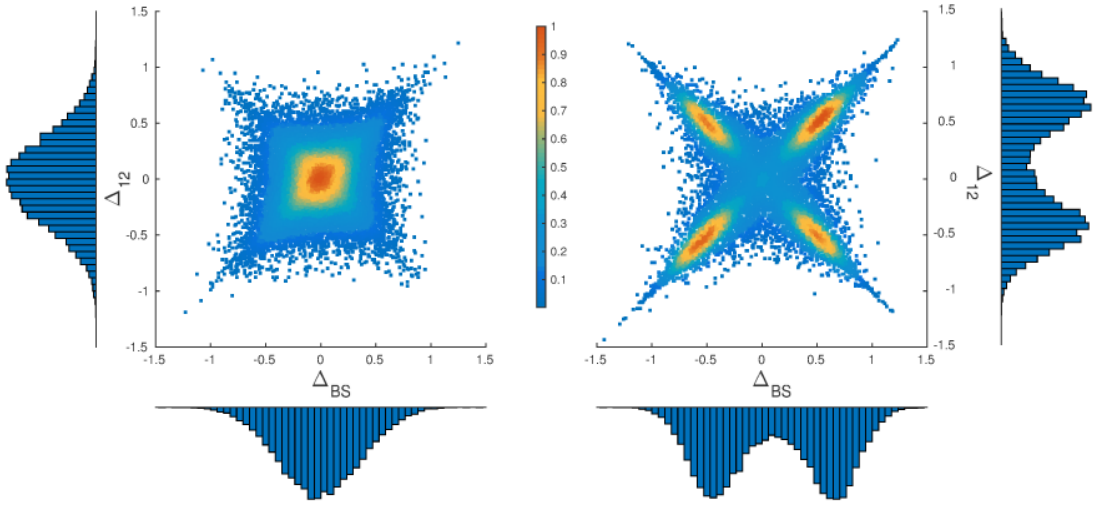


FIGURE 2.3: **Steady states in numerical simulations.** Steady state distributions of attractions for buying vs selling and for market 1 vs 2, respectively, for forgetting rate $r = 0.1$. For low enough intensity of choice (left, $\beta = 3.45$), an unsegregated steady state arises, while higher $\beta$ (right, $\beta = 7.14$) causes traders to segregate into four discernible groups. The histograms along the axes show the marginal distributions of $\Delta_{\mathcal{BS}}$ and $\Delta_{12}$, respectively. From the marginals we note that in the segregated state roughly half of the population specialize in buying (similarly half prefers market 1), although the fractions of buyers (sellers) at different markets are not the same. The data shown are taken from 100 trading periods of 100 independent runs (for more details on numerical simulations and system parameters, see D). The colour scale in the central scatter plots shows the probability density of agents [83].

$\mathcal{S}1$) as *"volume-oriented"* for reasons which we explain shortly. If all traders were return-oriented, they would have no partners to trade as there would be no agents playing $\mathcal{B}2$ or $\mathcal{S}1$. Consequently everyone would receive zero returns. The fact that some traders have developed persistent preferences for placing orders that give them a lower average return (here $\mathcal{B}2$, $\mathcal{S}1$) can thus be interpreted as cooperative, trade-enabling behaviour. Due to the market mechanism, the agents who choose one of $\mathcal{B}2$ or $\mathcal{S}1$ will have their orders rejected as invalid more often (see the group of buyers in Fig. 2.1). However, those whose orders are accepted will form a minority group in the market and will always find a trading partner. Hence, when submitting valid orders, these traders trade more often so we will call them *"volume-oriented"*.

There is a tendency for agents to cluster around the diagonal and anti-diagonal in the

two-dimensional projection shown in Fig. 2.3. Inspection of the underlying attractions $A_\gamma$ shows that this arises because many agents have one large attraction, for their preferred action, while their other attractions are close to zero. For example if a return-oriented agent, say a buyer at market 1, has attractions $\mathbf{A} \approx (A_{\mathcal{B}1}, 0, 0, 0)$, then this projects to the diagonal $\Delta_{\mathcal{BS}} = \Delta_{12} = A_{\mathcal{B}1}$. Similarly a volume-oriented trader who prefers to sell at market 1 is projected to the anti-diagonal $-\Delta_{\mathcal{BS}} = \Delta_{12} = A_{\mathcal{S}1}$ if his/her other three attractions are close to zero. The fact that the attractions of non-preferred actions are often small comes from the fact that, within our reinforcement learning dynamics, agents gradually forget the scores of actions they only use rarely.

To quantify the observed change in the distributions of agent attractions or preferences as we go from unsegregated to segregated states, we measured higher cumulants of the distributions $P(\Delta_{\mathcal{BS}})$ and $P(\Delta_{12})$. Specially we tracked the *Binder cumulant* [84]:

$$B = 1 - \frac{\langle(\Delta - \langle\Delta\rangle)^4\rangle_{P(\Delta)}}{3\langle(\Delta - \langle\Delta\rangle)^2\rangle^2_{P(\Delta)}}, \tag{2.3}$$

as it is a good indicator of segregation because it has different limiting values for unimodal and bimodal distributions. The Binder cumulant takes the value $B = 0$ for a Gaussian distribution, while $B = 2/3$ for a distribution consisting of two equally weighted sharp peaks (in Appendix B we show how Binder cumulant is calculated the two limiting cases).

Figure 2.4 shows values of this Binder cumulant for different intensity of choice, with all other parameters being same as in the previous figures. We note that for low $\beta$, the Binder cumulant of our distributions approaches value characteristic of Gaussian distributions as expected. At the other extreme, in the high $\beta$ regime, the cumulant increases towards the other extreme, Binder cumulant values of a distribution consisting of two sharp peaks with equal weight. The transition between these two regimes is sharper for smaller values of $r$, making it possible to estimate the critical intensity of choice for the onset of segregation.

**Persistence and time correlation.** The above results indicate that segregation is seen above a critical intensity of choice, $\beta > \beta_s$; we defer a discussion of how $\beta_s$ depends on the parameters of the model to the section Analytical description below. One has to bear

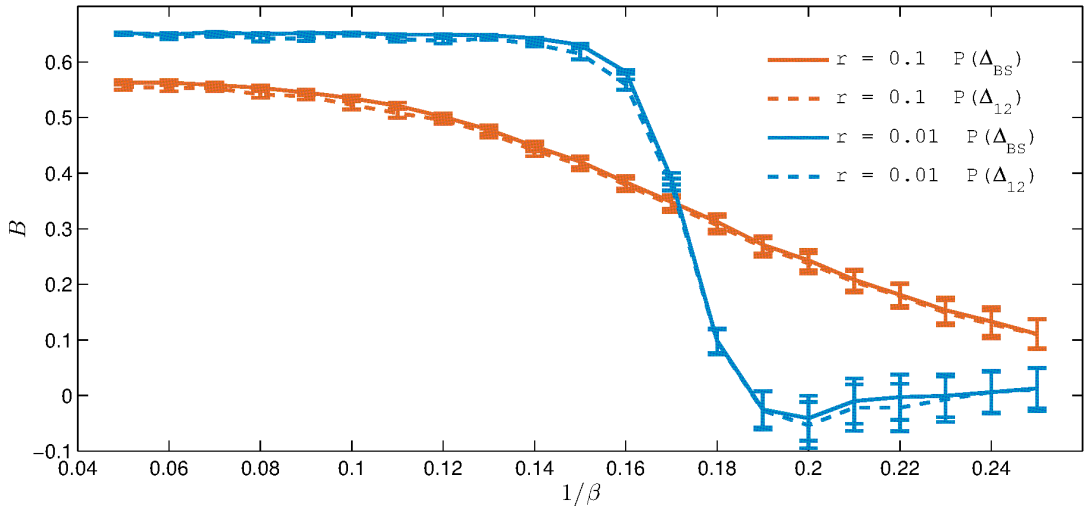


FIGURE 2.4: **Binder cumulant of a simulated system of adaptive agents.** Binder cumulant for $P(\Delta_{BS})$ and $P(\Delta_{12})$ distributions, averaged over last 100 trading periods versus intensity of choice $\beta$ for two different values of the forgetting rate, $r = 0.1$ and $r = 0.01$.

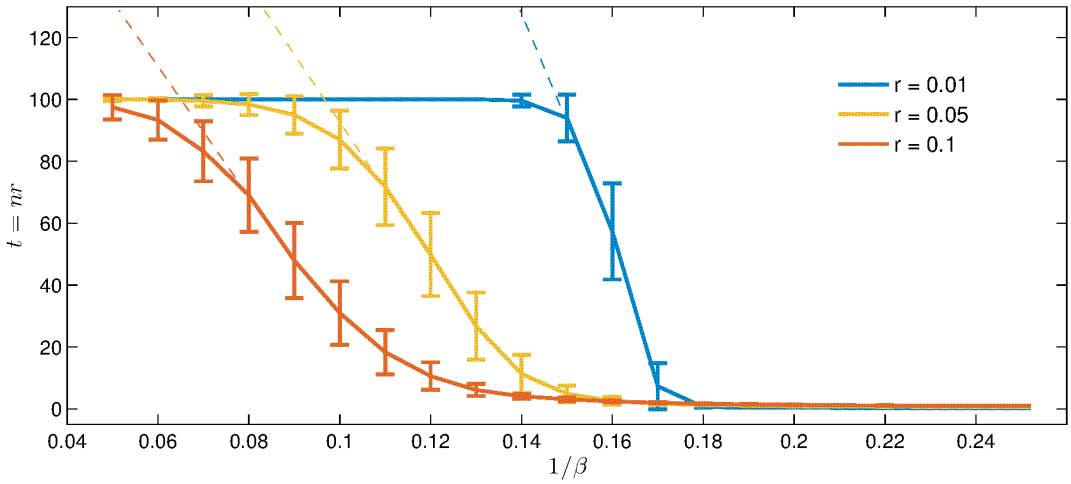


FIGURE 2.5: **Persistence times.** Average time an agent spends in any one of the four preference quadrants, plotted against temperature for different values of the forgetting rate, $r = 0.1$ (blue), $r = 0.05$ (red) and $r = 0.01$ (green). Dashed lines are sketches of how the persistence times would increase further if they were not limited by the length of our simulation runs. Other parameters as defined in the Table D.1.

in mind though that the data shown in Fig. 2.3 represents the state of the system at a given time. It therefore does not tell us whether agents really develop loyalty in the sense that they stay in one of the segregated groups for a long time, or whether they switch frequently between groups. To exclude possibility that distributions in the high $\beta$ regime might be a consequence of some agents' preferences becoming essentially *frozen* after the

first few trades, we investigated to what extent our system is ergodic. Quantitatively, we measured persistence times in one of four quadrants – "prefer buying at market 1" ($\Delta_{\mathcal{BS}} > 0$ and $\Delta_{12} > 0$), "prefer selling at market 1" ($\Delta_{\mathcal{BS}} < 0$ and $\Delta_{12} > 0$), etc.

Figure 2.5 shows the average time an agent spent in any one of these quadrant before leaving it for another quadrant, for various intensity of choice $\beta$. We present these plots for different values of the forgetting rate $r$, and using the rescaled time $t = rn$, where $n$ is the number of trading periods. (The use of $t$ rather than $n$ ensures that the trivial effect on persistence times of agents updating their attractions more slowly at smaller $r$ is removed.) From Figure one sees that at small enough $r$, the onset of segregation is accompanied by a rapid increase in persistence times, showing that in the segregated state agents do indeed remain "loyal" to a given market for long times. On the other hand, we see that when $\beta$ are not too high (i.e. above the levelling off of the small-$r$ curves in Fig. 2.5) then persistence times are short compared to the overall length of our runs, so that the system is ergodic.

Consistent with the intuitive meaning of a segregated state one finds that at high enough intensity of choice $\beta$ the agents develop "loyalty" to a certain market and a choice of buying and selling: their persistence times are much longer than the timescale of the small short-term fluctuations in preferences that every agent experiences. These short-term fluctuations occur on the time scale of the memory-loss, $1/r$. On the other hand the agents are *not* frozen, i.e. the persistence times are finite and the agents change loyalties on longer timescales. Therefore the steady state we observe is well defined rather than a consequence of agent preferences frozen-in from early fluctuations in their trading history.

What emerges from the above discussion is that a key feature of a segregated state is a separation of timescales in the dynamics of the agents. To quantify this further we consider the autocovariance function

$$C_{\gamma\delta}(\tau) = \langle (A_\gamma(t_0+\tau) - A_\gamma(t_0))(A_\delta(t_0+\tau) - A_\delta(t_0)) \rangle_{P(\mathbf{A})}, \tag{2.4}$$

where $\langle \dots \rangle_{P(\mathbf{A})}$ indicates an average over the attractions of players in the population, and over the time $t_0$ in the stationary state. This is a matrix capturing cross-correlations

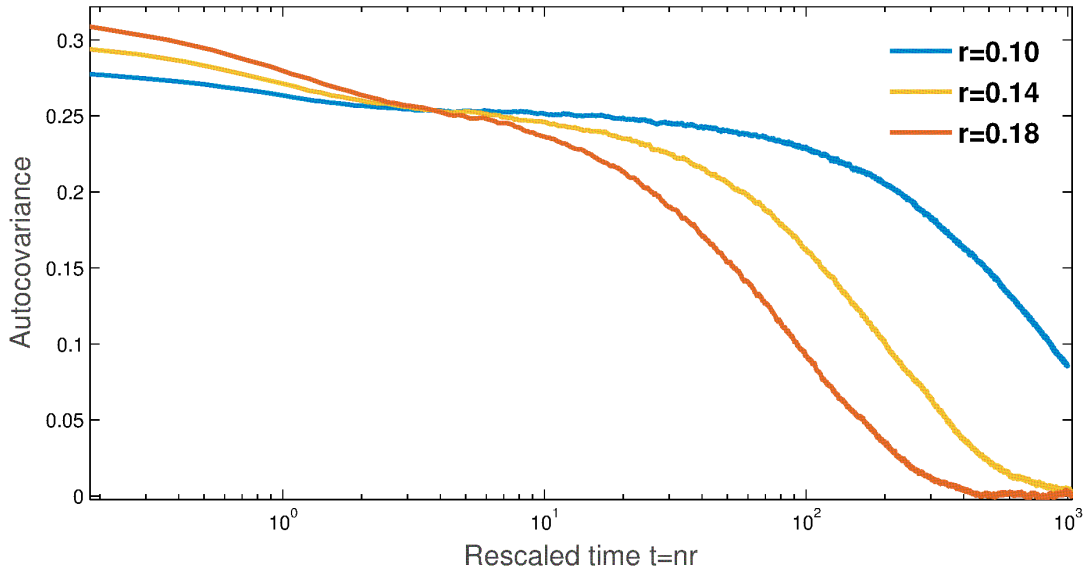


FIGURE 2.6: **Decay of the attraction autocovariance with time.** The intensity of choice $\beta$ and forgetting rate $r$ are different from the standard values in Table D.1: here $\beta = 20$, $r$ as shown in the legend. This is to highlight the separation of timescales in the segregated state. A larger than usual initial number of trading periods was simulated ($\approx 20,000$ trading periods) to ensure the systems reached steady state at such high $\beta$.

in time between the attractions to the various actions an agent can take; here as a summary statistic we look at the trace $C(\tau) \equiv \sum_\gamma C_{\gamma\gamma}(\tau)$, i.e. the sum of the autocovariances. In Fig. 2.6 we show how this autocorrelation function depends on time for various forgetting rates $r$ at fixed $\beta = 20$. We observe two separate decays, which is consistent with the intuition described above: first a fast decay of correlations occurs as an agent moves around one of the peaks of the distribution $P(\mathbf{A})$, caused by randomness in returns at a given market and the fact that the decisions of each agent remain stochastic. This fast decay does not lead to full decorrelation but rather to a plateau in the autocorrelation function: the attractions of an agent stay in the same "loyalty group" (i.e. within the same peak of $P(\mathbf{A})$), and the agent's actions remain correlated. The decay from this plateau defines the slow timescale, and it is a measure of how long agents typically stay in one loyalty group before moving to another peak of $P(\mathbf{A})$.

Because the slow timescale increases very rapidly as $r$ is decreased – the theoretical description below suggests exponential growth with $1/r$ – we show a rather smaller range of $r$ in the figure than elsewhere in the paper. Comparing the curves for different

$r$ we note the increase of the initial value of the autocorrelation function with $r$, which makes sense as the variance of the fluctuations within each peak of $P(\mathbf{A})$ grows roughly proportional to $r$. We also see that the fast time scale is of the order of unity in the rescaled time units, $t = nr$, used in the figure. This reflects the fact that the effective memory of each agent is $1/r$ trading periods.

**Summary and characterisation of segregated state.** Summarizing so far, the existence of a plateau in the autocorrelation function is clear evidence of the segregation of agents into groups that remain loyal over extended periods of time to a certain set of preferences defining a group of agents, while at the same time exhibiting small and much faster fluctuations around these typical preferences. This represents the most intuitive definition of segregation that we can think of. However, the existence of a plateau – quantitatively, a turning point in a plot of autocorrelation versus log time – would not be easy to utilize in practice to detect segretation. This is because already for $r < 0.1$ the amplitude of the initial fast decay becomes so small that it merges into the plateau, while at the same time the slow timescale for switching between loyalty groups outgrows the range of times that can easily be explored computationally. For practical purposes we therefore stick to multimodality of $P(\mathbf{A})$ as our criterion for segregation.

Our simulation results suggest that even our simplified trading system shows rich and interesting behaviour. A more detailed analysis (discussed below) reveals a threshold intensity of choice $\beta_{\mathrm{s}}$ such that for values $\beta > \beta_{\mathrm{s}}$ the system segregates, i.e. the initially homogeneous population of traders splits into groups that persistently choose to trade at a specific market. The pattern of these market loyalties is co-operative, in that some traders – the volume-oriented ones – forego potentially higher returns and instead choose actions that enable trade for everyone. We will see below that this behaviour has clear payback, in giving average returns across all traders that exceed those for the obvious Nash equilibrium. An obvious question that remains open at this point is how robust the observed segregation behaviour is to variation in our model parameters and setup; we defer this issue to the following chapters.

## 2.3 Analytical description

**Fokker-Planck description.** To understand in more detail how segregation arises, and to characterise the nature of the transition to the segregated state, a theoretical analysis of the model dynamics would evidently be useful. Mathematically our model is Markovian. To capture the full dynamics one needs to keep track of the attractions $A^i_\gamma$ to all actions $\gamma \in \{\mathcal{B}1, \mathcal{S}1, \mathcal{B}2, \mathcal{S}2\}$ of all agents $i = 1, \ldots, N$, or equivalently the attraction vectors $\mathbf{A}^i = (A^i_{\mathcal{B}1}, A^i_{\mathcal{S}1}, A^i_{\mathcal{B}2}, A^i_{\mathcal{S}2})$ for all agents. One can write down a master equation for the evolution of the joint distribution of these $4N$ variables. This equation is however difficult to work with and not easily analysed further.

In order to make progress it is useful to realise that the payoff an agent receives when they take a particular action only depends on aggregated quantities, but not on the detailed actions of individual other agents. More specifically the return for a given action is determined by (i) the bid or ask the agent places; (ii) the validity of the bid or ask placed and (iii) whether or not a suitable trading partner is found. All quantities (i)-(iii) are random objects and so the return received for a given action at any one time will be a random variable itself. Properties (ii) and (iii) only depend on the macroscopic statistics of bids and asks placed by the population of traders in its entirety. We now focus on the limit of large (formally infinite) populations, that is we take the limit $N \to \infty$. The distribution of bids and asks submitted in any trading round will then follow Gaussian distributions with mean $\mu_a$ and standard deviation $\sigma_a$ for asks, and analogously for bids ($\mathcal{N}(\mu_b, \sigma_b)$). By definition in our model the returns that flow from these bids or asks are non-negative, implying a truncation at zero of the return distributions. These distributions can then be written as

$$
\begin{aligned}
P(S|m,\mathcal{B}) &= Q_{\mathcal{B}m}T_{\mathcal{B}m}\frac{1}{Q_{\mathcal{B}m}\sigma_b\sqrt{2\pi}}\exp\left(-\frac{(S-\pi_m)^2}{2\sigma_b^2}\right)\theta(S) + \delta(S)(1-Q_{\mathcal{B}m}T_{\mathcal{B}m}),\\
P(S|m,\mathcal{S}) &= \underbrace{Q_{\mathcal{S}m}T_{\mathcal{S}m}}_{\text{agent trades}}\underbrace{\frac{1}{Q_{\mathcal{S}m}\sigma_a\sqrt{2\pi}}\exp\left(-\frac{(S-\pi_m)^2}{2\sigma_a^2}\right)\theta(S)}_{\text{non-negative return}} + \delta(S)\underbrace{(1-Q_{\mathcal{S}m}T_{\mathcal{S}m})}_{\text{agent does not trade}}.
\end{aligned}
\tag{2.5}
$$

The return an agent receives depends on the action $\gamma$ the agent chooses, i.e. on the market, $m$, they trade in, and whether they chose to buy, $\mathcal{B}$, or sell, $\mathcal{S}$. This is reflected in our notation above.

The first term in each of the above expressions describes the case of a non-zero return. This occurs with probability $Q_\gamma T_\gamma$, where $Q_\gamma$ denotes the probability that an agent's order is valid; once validated, it is executed with probability $T_\gamma$, which is the probability of finding a suitable trading partner. If the order is executed an agent receives a return $S$ drawn from a Gaussian distribution, truncated to allow only non-negative payoffs; if the order was invalid, or was valid but not executed, the agent receives $S = 0$. This occurs with probability $1 - Q_\gamma T_\gamma$.

To complete the above description of the single agent dynamics for large $N$ one needs expressions for the market price $\pi_m$ as well as the probabilities $Q_\gamma$ and $T_\gamma$. In the deterministic limit, $N \to \infty$, the expression in Eq. (2.1) reduces to

$$\pi_m = \mu_a + \theta_m(\mu_b - \mu_a),$$

as the means of the bids and asks submitted in any one round become the population means $\mu_b$ and $\mu_a$ by virtue of the law of large numbers.

The probabilities that an order is valid, $Q_\gamma$, are calculated from

$$\begin{aligned} Q_{\mathcal{B}m} &= \frac{1}{\sigma_b\sqrt{2\pi}} \int_{\pi_m}^{\infty} db\, \exp\left(-\frac{(b-\mu_b)^2}{2\sigma_b^2}\right), \\ Q_{\mathcal{S}m} &= \frac{1}{\sigma_a\sqrt{2\pi}} \int_{-\infty}^{\pi_m} da\, \exp\left(-\frac{(a-\mu_a)^2}{2\sigma_a^2}\right). \end{aligned} \tag{2.6}$$

These expressions reflect the requirement for a bid or ask to be on the correct side of the market price, and are based on our assumption of Gaussian bid and ask distributions. The integrals can be carried out in closed form and expressed in terms of error functions as shown in Appendix A.

The trading probabilities $T_\gamma$, finally, can be written as

$$T_{\mathcal{B}m} = \frac{\min\left(\overline{N}_{\mathcal{B}m}, \overline{N}_{\mathcal{S}m}\right)}{\overline{N}_{\mathcal{B}m}}, \qquad T_{\mathcal{S}m} = \frac{\min\left(\overline{N}_{\mathcal{B}m}, \overline{N}_{\mathcal{S}m}\right)}{\overline{N}_{\mathcal{S}m}}, \tag{2.7}$$

where $\overline{N}_\gamma$ is the total number of agents taking an action $\gamma$ and submitting a valid order,

$$\overline{N}_\gamma = NQ_\gamma \langle P(\gamma|\mathbf{A})\rangle \,. \tag{2.8}$$

In this expression $P(\gamma|\mathbf{A}) \propto \exp(\beta A_\gamma)$ is given by the appropriate *softmax* function applied to an agent's vector of attractions $\mathbf{A}$. The average $\langle \dots \rangle$ is over the distribution $P(\mathbf{A}) = \frac{1}{N}\sum_{i=1}^{N} \delta(\mathbf{A} - \mathbf{A^i})$ of attraction vectors across all agents. The expressions (2.7) can be understood as follows: if a trader submits an order that is valid, (s)he will always be able to trade if (s)he is in the minority group, otherwise his/her probability of being able to trade is the ratio of the number of traders in the minority and majority groups.

We can now write an evolution equation for the distribution $P(\mathbf{A})$ of attraction vectors across the population of traders. Writing $P_n(\mathbf{A})$ for the distribution at the end of trading period $n$, we have

$$P_{n+1}(\mathbf{A}') = \int d\mathbf{A}\, K(\mathbf{A}'|\mathbf{A}) P_n(\mathbf{A}), \tag{2.9}$$

with $K(\mathbf{A}'|\mathbf{A})$ a transition kernel that encodes the dynamics of the system. It is of the form

$$K(\mathbf{A}'|\mathbf{A}) = \int dS \sum_\gamma P(S|\gamma) P(\gamma|\mathbf{A}) \delta(\mathbf{A}' - \mathbf{e}_\gamma r S - (1-r)\mathbf{A}), \tag{2.10}$$

where $\mathbf{e}_\gamma$ is a four-dimensional vector with an entry of $1$ for action $\gamma$ and entries $0$ otherwise. The learning rule of Eq. (2.2) is enforced through the delta function. It is worth noting that (2.9) is not a standard linear Chapman-Kolmogorov equation as the right-hand side is nonlinear in the distribution $P_n(\mathbf{A})$. This arises because the kernel $K$ depends on the trading probabilities $T_\gamma$ as given in (2.7), which in turn depend on $P_n(\mathbf{A})$. The nonlinearity arises because we have effectively projected from a description in terms of all $4N$ attractions to one involving only four single-agent attractions.

From our reasoning so far, Eq. (2.9) should constitute an exact description of the model in the limit $N \to \infty$. It can, at least in principle, be solved numerically starting from our chosen initial condition $P_0(\mathbf{A}) = \delta(\mathbf{A})$. The presence of the $\delta$-peaks at zero returns $S = 0$ makes the kernel awkward to deal with numerically, however. We therefore make one further simplification and transform to a Fokker-Planck description. This is

appropriate for small $r$, i.e. agents with long memory. Note to this end that the change in attraction $\mathbf{A}' - \mathbf{A}$ in any one trading period is directly proportional to $r$, see Eq. (2.10). The Kramers-Moyal expansion (see e.g. [85]) of equation (2.9) is of the form

$$P_{n+1}(\mathbf{A}) - P_n(\mathbf{A}) = -r\partial_{\mathbf{A}}\left[\mathbf{M}_1(\mathbf{A})P(\mathbf{A})\right] + \frac{r^2}{2}\partial^2_{\mathbf{A}}\left[\mathbf{M}_2(\mathbf{A})P(\mathbf{A})\right] + \ldots, \tag{2.11}$$

where the scaled jump moments

$$\mathbf{M}_\ell(\mathbf{A}) = \frac{1}{r^\ell}\int d\mathbf{A}'(\mathbf{A}' - \mathbf{A})^\ell K(\mathbf{A}'|\mathbf{A}),$$

are of order $r^0$. The generic $\ell$-th order term on the RHS of equation (2.11) comes with a factor $r^\ell$ so for small $r$ one can proceed by neglecting higher-order terms beyond the first two. Next, it is useful to introduce a re-scaled time $t = rn$. A unit time interval in $t$ then corresponds to $1/r$ trading periods and hence the memory length of the agents. With this replacement, Equation (2.11) reduces to a Fokker-Planck equation in the limit $r \to 0$. Specifically we have in this limit

$$\partial_t P(\mathbf{A}) = -\partial_{\mathbf{A}}\left[\mathbf{M}_1(\mathbf{A})P(\mathbf{A})\right] + \frac{r}{2}\partial^2_{\mathbf{A}}\left[\mathbf{M}_2(\mathbf{A})P(\mathbf{A})\right]. \tag{2.12}$$

As before and to keep the notation compact, we have not written out the various components of the derivatives and jump moments; e.g. $\partial_{\mathbf{A}}[\mathbf{M}_1 P]$ is to be read as $\sum_\gamma \partial_{A_\gamma}[M_{1,\gamma}P]$.

Segregation behaviour can in principle be characterised by studying the steady-state solution of the above Fokker-Planck Equation (2.12). Specifically one would investigate the conditions under which this distribution is multimodal, i.e. has several peaks.

**Iterative procedure for solving the Fokker-Planck equation.** Similar to the kernel $K$, the drift and diffusion coefficients $\mathbf{M}_1$ and $\mathbf{M}_2$ depend on the trading probabilities $T_\gamma$. So finding the steady state requires an iterative approach:

(i) initialize $P(\mathbf{A})$, e.g. with delta peaked distributions, corresponding to agents without preferences;

(ii) calculate the number of traders taking the various actions [Eq. (2.8)] and thus the trading probabilities $T_\gamma$ [Eq. (2.7)];

(iii) find the steady state solution of the Fokker-Planck equation (2.12) for these $T_\gamma$. Steps (ii) and (iii) are then repeated until a self-consistent solution is obtained, i.e. until the $T_\gamma$ no longer change. We note that finding the stationary distribution of the Fokker-Planck equation (step (iii)) is non-trivial in general. This is true particularly because the drift and diffusion coefficients $\mathbf{M}_1$ and $\mathbf{M}_2$ do not define a time-reversible single agent-dynamics, for which determining the steady state would be much simpler (see for example [86]). In the limit of small $r$, where the stationary distribution takes a large deviation form $P(\mathbf{A}) \propto \exp(-f(\mathbf{A})/r)$ analogous to (2.14) below, it can in principle be found by a Freidlin-Wentzel construction [87] but implementing this numerically is still challenging (see e.g. [88]). This is why for analytical work we focus on a slightly simplified model, details of which are given below.

Once we have the steady-state values of the trading probabilities $T_\gamma$, we can also think of the Fokker-Planck equation (2.12) as describing the dynamics of individual agents within a large population with fixed average properties. As we argue that our system is ergodic, the steady state distribution of attractions can then be re-interpreted as the distribution of a single agent's attraction sampled over a long enough time interval. Zeros of the drift velocity $\mathbf{M}_1(\mathbf{A})$ are fixed points of the single agent dynamics, and for small amounts of diffusive noise $r$ the single agent will spend most of its time near (stable) fixed points, causing local maxima of $P(\mathbf{A})$. To detect segregation we therefore look for multiple stable fixed points of the single agent-dynamics in the steady state population.

**Agents with fixed preferences for buying.** As finding the steady state solution of the Fokker-Planck equation even with given trading probabilities is a non-trivial task in the four-dimensional space of attraction vectors $\mathbf{A}$, we proceed with one more simplification to produce a theoretical description directly comparable to simulations. We fix the agents' preferences for buying or selling, i.e. each agent now carries a fixed probability $p_\mathcal{B}$ with which they buy. They sell with probability $1 - p_\mathcal{B}$. This probability may vary from agent to agent, but crucially it remains fixed in time for each trader. Agents thus have a single decision left to make, namely, where to trade.

In the case of two markets the single variable that we then need to track for every agent is the difference or relative attraction $\Delta^i = A_1^i - A_2^i$. This makes a full numerical

analysis possible. The resulting Fokker-Planck equation is one-dimensional and so one can find the steady state solution in closed form, while locating all single agent fixed points can be achieved e.g. by a bisection method. We do find segregation in this way as shown below so the reduced model is useful in its own right, and provides evidence of the robustness of segregation behaviour. Hence we focus on this simplified model in the following, enabling us to compare numerical predictions for nonzero $r$ directly to simulations. Wherever possible we will relate the results back to the original, fully adaptive model.

In the limit of large population size, the analogue of $P(\mathbf{A})$ in the simplified model is the probability distribution $P(\Delta, p_{\mathcal{B}}) = P(\Delta|p_{\mathcal{B}})P(p_{\mathcal{B}})$. The quantity $P(\Delta|p_{\mathcal{B}})$ is the distribution of attraction differences, $\Delta$, among agents with buying preference $p_{\mathcal{B}}$. The distribution over preferences for buying $P(p_{\mathcal{B}})$ is fixed as part of the specification of the model. As a simple case, we investigate a population with $P(p_{\mathcal{B}}) = \frac{1}{2}\delta(p_{\mathcal{B}} - p_{\mathcal{B}}^{(1)}) + \frac{1}{2}\delta(p_{\mathcal{B}} - p_{\mathcal{B}}^{(2)})$, consisting of equal numbers of two types of agents with buying preference $p_{\mathcal{B}} = p_{\mathcal{B}}^{(1)}$ and $p_{\mathcal{B}} = p_{\mathcal{B}}^{(2)}$, respectively. Agent $i$ chooses market 1 with probability $1/[1 + \exp(-\beta\Delta_i)]$ (that we usually denote as $\sigma_\beta(\Delta)$) and independently chooses to buy with probability $p_{\mathcal{B}}^{(1)}$ or $p_{\mathcal{B}}^{(2)}$ depending on his/her type.

As in the case of fully adaptive agents we can formulate the master equation for the process, and derive a Fokker-Planck equation in the limit of small memory-loss rates $r$. We obtain:

$$\partial_t P(\Delta|p_{\mathcal{B}}^{(g)}) = -\partial_\Delta \left[ M_1(\Delta|p_{\mathcal{B}}^{(g)}, T_\gamma) P(\Delta|p_{\mathcal{B}}^{(g)}) \right] + \frac{r}{2}\partial_\Delta^2 \left[ M_2(\Delta|p_{\mathcal{B}}^{(g)}, T_\gamma) P(\Delta|p_{\mathcal{B}}^{(g)}) \right], \quad (2.13)$$

where $g \in \{1, 2\}$ (for type or "group") labels the agent type. The jump moments $M_1$ and $M_2$ couple the two types of agents via the set of trading probabilities $\{T_\gamma\}$. The generic steady state solution of the Fokker-Planck equation (3.8) reads (see for example [85]):

$$P(\Delta|p_{\mathcal{B}}^{(g)}) \propto \frac{1}{M_2(\Delta|p_{\mathcal{B}}^{(g)}, T_\gamma)} \exp\left( \frac{2}{r} \int_0^\Delta d\Delta' \frac{M_1(\Delta'|p_{\mathcal{B}}^{(g)}, T_\gamma)}{M_2(\Delta'|p_{\mathcal{B}}^{(g)}, T_\gamma)} \right). \quad (2.14)$$

As the notation emphasizes, the stationary probability distribution is dependent on the

trading probabilities, and these are themselves function(al)s of the probability distributions $P(\Delta|p_{\mathcal{B}}^{(g)})$, $g = 1, 2$. Accordingly we use the iterative procedure described above to find a solution, repeating steps (ii) and (iii) until the trading probabilities $T_\gamma$ remain stable to an accuracy of $10^{-6}$.

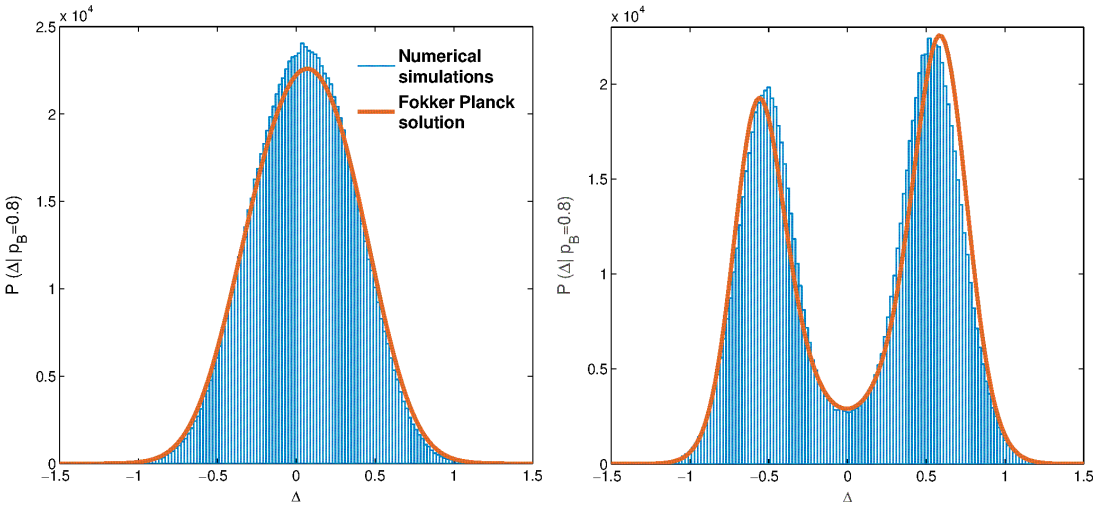


FIGURE 2.7: **Steady states of the reduced model.** The distributions $P(\Delta|p_{\mathcal{B}}^{(1)} = 0.8)$ from simulation and Fokker-Planck theory; the corresponding distributions for the second type of agents $P(\Delta|p_{\mathcal{B}}^{(2)} = 0.2)$ are mirror images with respect to the y-axis. Left: $\beta = 1/0.45$, Right: $\beta = 1/0.15$. Forgetting rate is $r = 0.1$, other system parameters as specified in Table D.1.

Fig. 2.7 compares the steady state distributions $P(\Delta|p_{\mathcal{B}}^{(1)})$ obtained from direct numerical simulations and from the Fokker-Planck theory described above. The buying preferences $(p_{\mathcal{B}}^{(1)}, p_{\mathcal{B}}^{(2)}) = (0.8, 0.2)$ are symmetric about $1/2$ and so we do not show $P(\Delta|p_{\mathcal{B}}^{(2)})$, which would be the mirror image about $\Delta = 0$. The distribution obtained for low $\beta$ (Fig. 2.7 left) shows the behaviour expected for an unsegregated population, with a single-peaked distribution of relative attraction $\Delta$ for each agent type; the mean of the distribution essentially coincides with the fixed point of the single agent dynamics, i.e. the solution of $M_1(\Delta) = 0$.

In the high-$\beta$ regime, the agents of each type segregate into two groups corresponding to the two peaks of the distribution of the attraction differences $\Delta$. As in the case of fully adaptive agents, one group is return-driven, i.e. prefers the market that awards them with higher returns, although they are not always able to trade there. The agents in the

other group are volume-driven; they settle for the market where returns are lower on average but where they can trade more regularly.

The Fokker-Planck theory successfully reproduces the qualitative transition from unsegregated behaviour at low values of the intensity of choice to segregated steady states at higher values of $\beta$. The quantitative agreement with numerical simulations is good, remarkably so given that the latter were obtained for relatively small systems ($N = 200$ agents) and for moderate $r = 0.1$ while we developed the theory for the combined limits of large $N$ and small $r$. The agreement between theory and numerical experiment also suggests that segregation is not a finite-size effect.

**Characterising the phase transition.** To track the change in the shape of the relative attraction distributions from unimodal to bimodal as $\beta$ is changed we again consider the Binder cumulant, $B$. In principle, $B$ is dependent on the type of agent considered, $g$; but in the situations we consider where the two types have distributions of score differences $\Delta$ that are mirror images of each other, this dependence disappears. For numerical simulation data we show $(B^{(1)} + B^{(2)})/2$. For small $r$, where the $\Delta$-distributions become sharp around their peak(s) according to Equation (2.14) we expect for $\beta$ below and above the segregation threshold $\beta_s$ the cumulant will take limiting values discussed previously (Gaussian $B = 0$ in the low $\beta$ and finite $B \approx 2/3$ for equal weighted bimodal distribution). For finite values of the learning rate $r$ this will become a smooth transition between the two limiting values.

In Fig. 2.8 we show the predictions of our Fokker-Planck theory for the Binder cumulant of the reduced model with fixed buy/sell-preferences as a function of $\beta$, and for different values of $r$. These confirm the expectations set out above, with the segregation transition become increasingly sharp as $r$ decreases. The limit $r \to 0$ of the theory can be worked out by a separate procedure (which we address in Chapter 3) and gives a sharp transition at a well-defined segregation threshold $\beta_s$ (for the system presented in Fig. 2.8, $\beta_s = 3.55$). The inset of Fig. 2.8 compares numerical simulations and theory for $r = 0.1$ and again shows very good agreement. We attribute the remaining deviations to finite-size effects and to the fact that simulations necessarily operate at nonzero $r$ while the Fokker-Planck theory is derived in the limit of small $r$. The qualitative behaviour of the

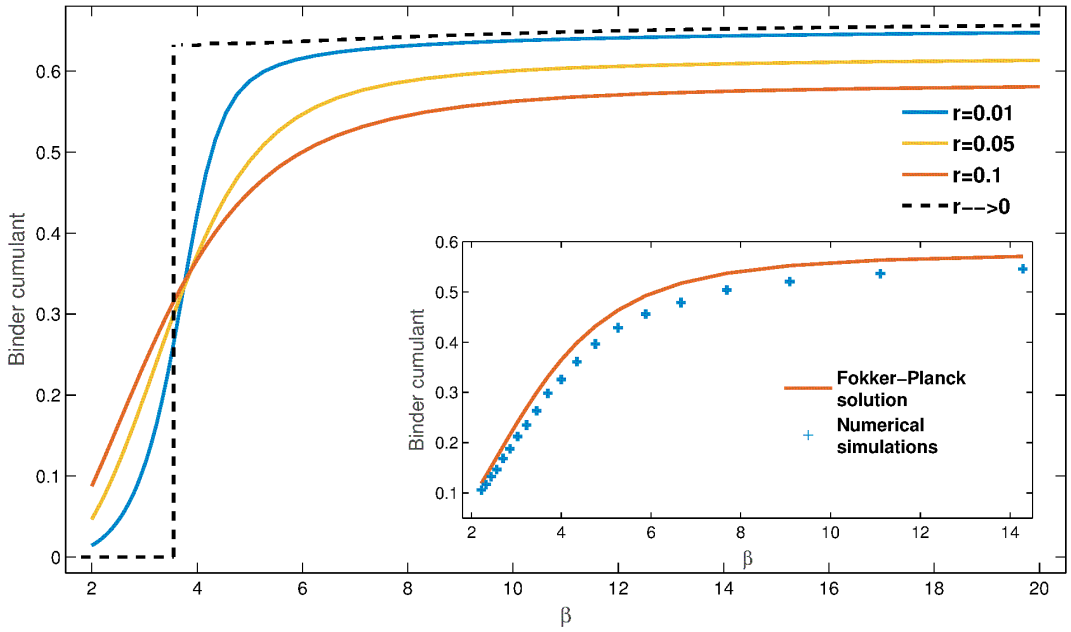


FIGURE 2.8: **Binder cumulant** (as defined in Eq. (2.3)) of the relative attraction distribution for different values of $r$ as shown in the legend (large to small $r$ from bottom to top on the right of the plot, $r \to 0$ values are calculated as explained in Chapter 3 and Appendix B). Inset: Numerical simulations (blue) versus Fokker-Planck theory (orange) for $r = 0.1$. Simulated system size $N = 200$ traders, with $\Delta$ distributions obtained from the last $1/r$ trading periods of 100 independent simulation runs.

Binder cumulant, i.e. a transition between the expected theoretical values for small and large values of $\beta$ that becomes sharper with decreasing $r$, is exactly the same in the fully adaptive model, as we have seen in Fig. 2.4. There are of course quantitative differences; e.g. the threshold value $\beta_s \approx 5.9$ (for $r \to 0$) is somewhat higher.

**Further characterisation of segregation dynamics.** So far we have successfully constructed a mathematical description that reproduces the segregation effects seen in simulations. We now use the theory to look more closely at the emergence of segregation and the properties of the segregated state. To this end we consider average returns across the population of agents. These allow us detect whether segregation brings population-level benefits even though all agents make decisions on a purely individual basis. Given that persistence times are finite, the population-averaged returns also give the long-time average returns for any agent and so they tell us about the benefits of segregation for single agents.

In Fig. 2.9 we plot the average return obtained by agents in the steady state against intensity of choice $\beta$ for populations with different forgetting rates $r$. The data shown are from the Fokker-Planck analysis of the reduced two-strategy model described above. Remarkably, the average return is a non-monotonic function of $\beta$: it has a minimum close to the segregation threshold $\beta_s$, at a level that decreases as $r$ is reduced. The qualitative non-monotonic trend is also found in numerical simulations (see inset). It is harder to detect there as the absolute changes in returns are fairly small, but appears in both the reduced and the fully adaptive model. Related to the observed non-monotonicity, it is important to note two limits - random trading ($\beta \to 0$) and the best past action trading ($\beta \to \infty$). Both will be discussed in more details in the next chapter, but it is worth observing here that over wide range of learning parameters $(r, \beta)$ the population on average earns less when learning how to trade compared to random trading.

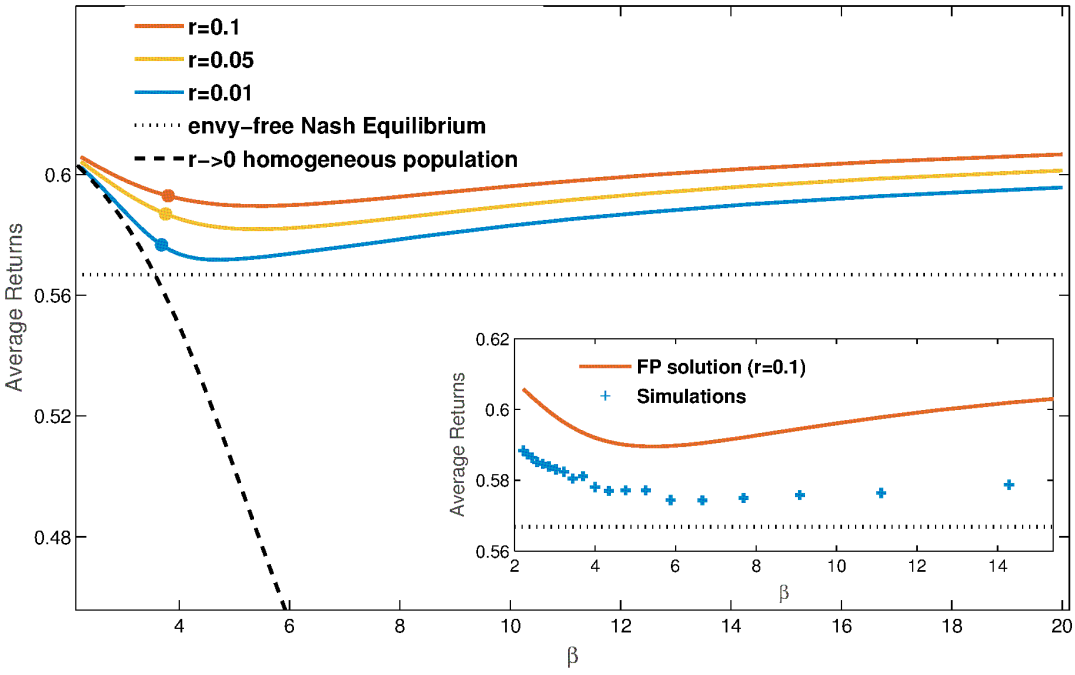


FIGURE 2.9: **Returns.** Average steady state population returns against $\beta$ for different values of $r$ (see legend; $r$ decreases from top to bottom), as predicted by Fokker-Planck theory (circles denote $\beta_s$ for the given value of $r$). Black dashed line: average return of an unsegregated population for $r \to 0$. Horizontal dotted line: envy-free Nash equilibrium (see text). The segregated solution achieves higher returns than either the unsegregated population at the same $\beta$, or the Nash equilibrium. Insert: comparison between numerical simulations and Fokker-Planck theory for $r = 0.1$ and population size $N = 200$.

To put the returns for our segregated steady states into context, we compare them to two benchmark values. The dashed line in Fig. 2.9 indicates the first of these, which is the average return of an unsegregated population (in the limit $r \to 0$ limit, to be discussed in more detail shortly). While this homogeneous population return decreases monotonically with $\beta$, segregation avoids this decrease for intensities of choice $\beta > \beta_s$ and in fact converts it to an increase.

As a second baseline we show in Fig. 2.9 the average return in an envy-free Nash equilibrium. A Nash equilibrium in general is a state in which no agent can increase their payoff by unilaterally changing strategy. In our system, a state would be specified by the probability $p_1^i$ for each agent $i$ to choose market 1 – as the set of actions is {Market 1, Market 2}. The strategy of an agent is defined by $(p_1, 1-p_1)$ – and a Nash equilibrium is reached when no agent $i$ can achieve higher average return by changing $p_1^i$, at fixed strategies of all other players. This still leaves potentially many different Nash equilibria [88] and so we focus on what we will refer to as the *envy-free* Nash equilibrium. This is an equilibrium in which no agent is envious of any other agent's return because they all achieve the same payoff on average over time. This is realized in our system when the average returns for all four distinct actions (buy or sell, at market 1 or 2) are the same. This condition allows us to identify a unique set of trading probabilities and from these the envy-free Nash equilibrium return (see Appendix B). As Fig. 2.9 shows, this is always *lower* than the average return of a segregated population (both in theory and simulations, see the inset). A segregated steady state is thus better in terms of returns than both the homogeneous steady state at the same $\beta$ and the envy-free Nash equilibrium. What is notable here is that the segregated state is not envy-free over short time horizons: an agent in the volume driven group obtains a lower return than one from the return driven group. However, as emphasized above, on very long time scales agents can change their loyalties, i.e. change group, so that in a long-time average all achieve the same return. This again emphasizes the co-operative nature of the segregated state.

**Estimating the segregation threshold $\beta_s$: the $r \to 0$ limit.** We now proceed to study the segregation threshold $\beta_s$ of the intensity of choices and how it depends on the parameters of the model. This is easiest in the limit $r \to 0$ where the segregation transition is sharp,

see Fig. 2.8 above. We first focus on the regime $\beta < \beta_s$, i.e. the unsegregated phase, in which the distributions $P(\Delta|p_{\mathcal{B}}^{(g)})$ will be single-peaked. In the limit $r \to 0$, Equation (2.14) indicates that (i) this peak becomes infinitely sharp, so that the distributions are of the form $P(\Delta|p_{\mathcal{B}}^{(g)}) = \delta(\Delta - \Delta^{(g)})$; and (ii) the location $\Delta^{(g)}$ of the peak for each group of players is determined by the zero-drift condition

$$M_1(\Delta^{(g)}|p_{\mathcal{B}}^{(g)}, T_\gamma) = 0. \tag{2.15}$$

The next step is to solve these two equations for $\Delta^{(1)}$ and $\Delta^{(2)}$, which is the $r \to 0$ analogue of finding the steady state of the FP equation for general $r > 0$. As before one needs to make the solution self-consistent so that the trading probabilities $T_\gamma$ appearing in (2.15) are those calculated from the distributions $P(\Delta|p_{\mathcal{B}}^{(g)}) = \delta(\Delta - \Delta^{(g)})$ themselves. The iterative approach explained above can again be used to find such a self-consistent solution, starting from $(\Delta^{(1)}, \Delta^{(2)}) = (0, 0)$.

We briefly explore the properties of this homogeneous steady state before considering how to detect the onset of segregation. We focus on agent types with symmetric biases toward buying and selling, $p_{\mathcal{B}}^{(1)} = 1 - p_{\mathcal{B}}^{(2)}$. For this choice we find non-zero $(\Delta^{(1)}, \Delta^{(2)})$ even in the limit $\beta \to 0$. This indicates that agents recognize the more rewarding option: agents that are more likely to buy have a preference for the market that is good for buyers, and similarly for sellers. Of course $\beta \to 0$ means that agents nevertheless choose randomly between the markets.

As $\beta$ increases, the relative attractions $(\Delta^{(1)}, \Delta^{(2)})$ become more pronounced, i.e. they move away from zero, and agents start to choose the "better" market more frequently. This is the reason for the decay of the average return in the homogeneous steady state with $\beta$, as shown in Fig. 2.9: as agents of each type increasingly focus on "their" market, buyers congregate in one market and sellers in the other; trading opportunities are reduced and thus the average return (which includes zero returns for trading periods where an agent cannot trade) decreases. The more definitive choices agents make are the consequence of the two effects: (1) the fixed points $(\Delta^{(1)}, \Delta^{(2)})$ increase in absolute value (and they correspond to the difference in the average score an agent receives in the two markets); (2) the increase of $\beta$ makes the choices more definitive. Quantitatively, we find

that (2) is the stronger effect. As the intensity of choice $\beta$ is increased further, we expect a transition to a segregated steady state.

To detect this transition we can follow the general logic explained in the beginning of Analytical Description: a segregated state must have more than one fixed point of the single-agent dynamics. The peak position $\Delta^{(1)}$ is always a fixed point for agent type 1 from Eq. (2.15), and similarly for type 2. To detect the onset of segregation we therefore need to check when *additional* fixed points appear, i.e. additional solutions of the zero-drift condition $M_1(\Delta|p_{\mathcal{B}}^{(g)}, T_\gamma) = 0$. In looking for these alternative fixed points we need to keep the trading probabilities $T_\gamma$ *fixed* at their values calculated for the homogeneous steady state, because we are considering the *single-agent* fixed points. Note that in general one needs to search for alternative fixed points globally, i.e. across all possible $\Delta$. This is because for most parameter settings the new fixed points appear far from $\Delta^{(1)}$ or $\Delta^{(2)}$, respectively, as pairs of stable and unstable fixed points.

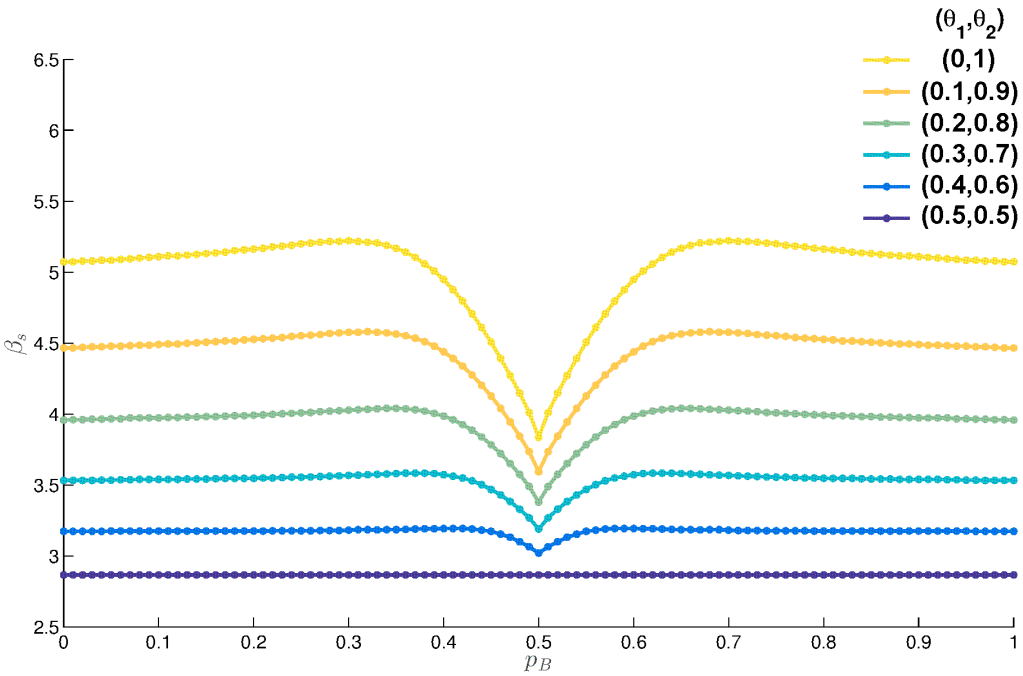


FIGURE 2.10: **Segregation thresholds for different symmetric agent types, at different markets.** Segregation threshold as a function of the first agent type's preference for buying $p_{\mathcal{B}}^{(1)} = p_{\mathcal{B}}$, assuming the other agent type has the opposite preference $p_{\mathcal{B}}^{(2)} = 1 - p_{\mathcal{B}}$. Different sets of symmetric market parameters are compared; non-trivially, the region of segregation is largest when both markets are fair.

In Figs. 2.10 and 2.11 we present the segregation thresholds obtained by the method above, for various parameter settings. In Fig. 2.10 specifically we show how $\beta_s$ changes with $p_B$ for various symmetric markets. One observes that $\beta_s$ does not depend very strongly on the exact preferences for buying of the agents, except for the region of parameters where both agent types have almost even preferences for buying and selling[4]. In contrast, the effect of the market biases follows a simple trend: the region of segregation shrinks as the difference between the two markets increases, suggesting that segregation is not a trivial effect of market biases.

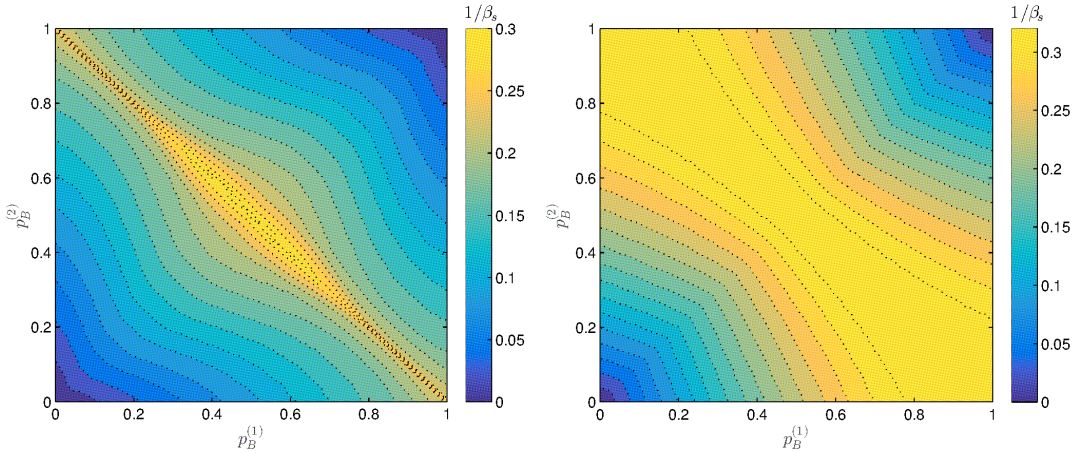


FIGURE 2.11: **Segregation threshold for various agent types.** Contour plots of the segregation threshold $\beta_s$ when preferences for buying $p_B^{(1)}$ and $p_B^{(2)}$ of both agent types are varied independently. Left: symmetric markets $(\theta_1, \theta_2) = (0.3, 0.7)$; Right: two fair markets ($\theta_1 = \theta_2 = 0.5$). Contours are presented in terms of $1/\beta$ for visual clarity.

In Fig. 2.11 we show two contour plots to compare the trends in $\beta_s$ when the two agent types' buying preferences are varied independently, for two different choices of market parameters. On the left is the symmetric markets setup $(\theta_1, \theta_2) = (0.3, 0.7)$ that we have already used several times. From the plot we observe that the segregation threshold $\beta_s$ is lowest when the subgroups are symmetric with respect to buy-sell preferences, i.e. $p_B^{(1)} + p_B^{(2)} = 1$; the variation of $\beta_s$ along that line is presented in Fig. 2.10. We also note that when the two agent types have similar preferences (e.g. both prefer buying over selling) then $\beta_s$ is on average higher than in the case where the types have opposite preferences.

[4]More details on the reasons behind the change in monotonicity in the intermediate $p_B$ region is addressed in Chapter 3.

This qualitative behavior we see also in the case of two fair markets that set the trading price at the equilibrium price, as shown in Fig. 2.11 (right). We do not show similar plots for asymmetrically biased markets; the qualitative behaviour is similar there, but the line of minimal $\beta_s$ is no longer $p_{\mathcal{B}}^{(1)} + p_{\mathcal{B}}^{(2)} = 1$ but $p_{\mathcal{B}}^{(1)} + p_{\mathcal{B}}^{(2)} = c$, where $c$ is a constant that depends on the market parameters.

Finally, we can adapt the above method of calculating the segregation threshold to the original model of fully adaptive agents choosing among all four possible actions (e.g. $\gamma \in \{\mathcal{B}1, \mathcal{S}1, \mathcal{B}2, \mathcal{S}2\}$). Because of the difficulties of finding the steady state solution numerically for finite $r$, this analysis is carried out only in the limit $r \to 0$. Here it is feasible because we only need to find zeros of the drift $\mathbf{M}_1$, rather than solve for a full distribution $P(\mathbf{A})$ that is a stationary solution of the Fokker-Planck equation. As argued before, the first moment ($\mathbf{M}_1$) is a function of the whole distribution, but in the $r \to 0$ limit and for $\beta < \beta_s$ this distribution is a delta distribution, which simplifies the calculation.

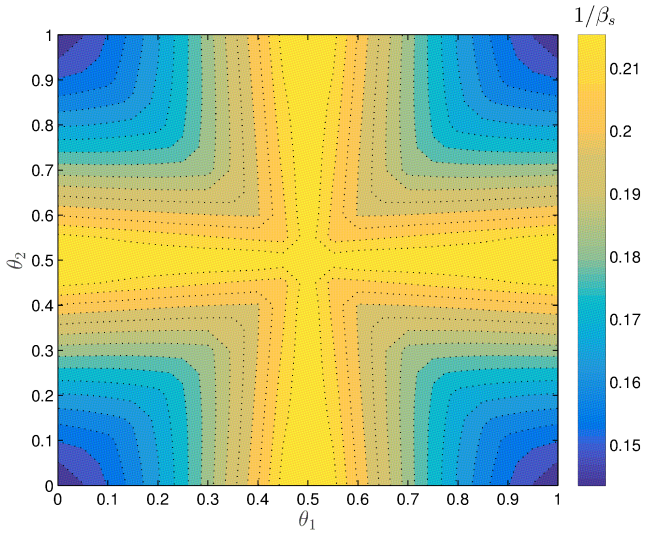


FIGURE 2.12: **Segregation threshold for fully adaptive traders.** Contour plots of the segregation threshold $\beta_s$ in a system of fully adaptive agents, against the market bias parameters $(\theta_1, \theta_2)$. Along the lines where at least one market is fair, $\beta_s$ is lowest so that segregation occurs for the widest possible range of intensities of choice $\beta$.

In Fig. 2.12 we show a contour plot of the segregation threshold against the two market biases. As in Fig. 2.10, for agents with fixed buy-sell preferences, we notice that the segregation threshold $\beta_s$ decreases when the difference in the symmetric market biases decreases; this can be seen specifically by looking at the symmetric markets diagonal of

Figs. 2.12 and 2.10. Additionally in the system of fully adaptive agents we notice that this conclusion extends to the case when at least one market is fair, i.e. segregation then also arises for smaller values of $\beta$. In Fig. 2.12 we note also a four fold symmetry, which we conjecture is a consequence of the fact that agents have more choices: a fully adaptive agent does not have a preferred market initially, so all four action choices are equal. This is not the case for an agent with a fixed preference for buying and selling because returns are buyer/seller-specific. The four fold symmetry in Fig. 2.12 also tells us that the absolute value of $\theta$ is enough to describe the market. This further means that the commonly investigated choice of two symmetric markets is analogous to the case of two identical markets and we note that the segregation threshold is lowest when both markets are fair. This is in agreement with the results of the model with agents with fixed buy-sell preferences, see specifically in Fig. 2.11 where for every choice of $(p_{\mathcal{B}}^{(2)}, p_{\mathcal{B}}^{(2)})$ the segregation threshold $\beta_s$ is smaller when the markets are fair.

**Multiple steady states.** When iteratively finding a self-consistent steady state of the Fokker-Planck equation as discussed around Equation (2.12), we always used as initial condition a distribution of all agents having zero attractions. While the dynamics of the iterative solution is not identical to the real dynamics, this choice was sensible to obtain steady states that match the ones from simulations of the real dynamics as closely as possible. After further analysis we found that in the numerical simulations for small values of $r$ one can obtain two qualitatively different classes of segregated states. To investigate this notion further, we now explore whether there can be more than one self-consistent solution of the Fokker-Planck equation. Such additional solutions could be accessible for example by using our iterative procedure, but starting from other initial conditions.

The simplest way to perform this exploration systematically is to realize that the trading probabilities $T_\gamma$ from Equation (2.7) only depend on the demand-to-supply ratios $D_1$ and $D_2$ at the two markets; we define $D_m$ for each market $m$ as the ratio of the number of buy and sell orders that arrive at the market. Specifying $(D_1, D_2)$ thus tells us all trading probabilities, and hence determines a unique steady state solution of the Fokker-Planck equation. From this steady state solution we can recalculate $D_1$ and $D_2$, and plot in the

$(D_1, D_2)$-plane the two lines where the new and old $D_1$ ($D_2$, respectively) coincide. The intersections of these two lines are then the self-consistent steady states we are after. We find numerically, in the range of parameter values that we have explored, that there is either one such state or there are three.

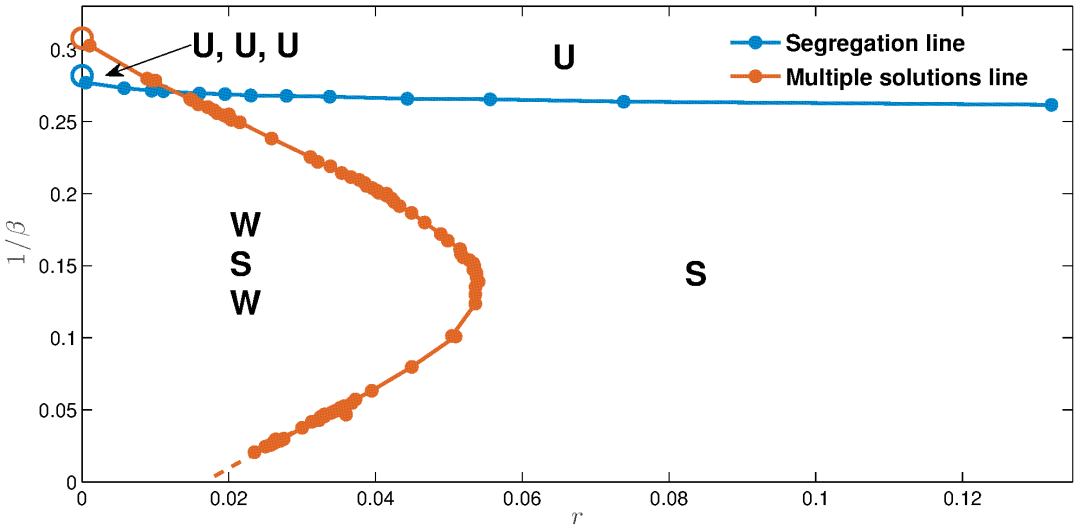


FIGURE 2.13: **Regions of different steady states in the space of parameters $r$ and $\beta$.** Number and nature of the steady state solutions of the Fokker-Planck equations in the $(r, 1/\beta)$-plane (U: unsegregated state, S: strongly segregated state, W: weakly segregated state). Other system parameters are set to their default values (see Table D.1). To the left (small $r$) of the orange line there are three steady state solutions, while to the right there is only one. The blue line separates the region where at least one of the solutions is segregated, i.e. bimodal. Empty circles represent $r \to 0$ endpoints of the two lines, calculated independently.

In Fig. 2.13 we show the resulting phase diagram in the $(r, \beta)$-plane and indicate the number and nature of self-consistent steady state solutions. Where solutions are segregated we differentiate between two possibilities, strong and weak segregation. By strong segregation we mean a solution branch where the two peaks in $P(\Delta|p_{\mathcal{B}})$ remain of comparable height as $r \to 0$. We call a solution branch weakly segregated when one peak weight becomes exponentially small for $r \to 0$, so that the solution effectively reduces to an unsegregated one. In the limit, all agents then typically prefer the same market. The empty circles in the figure are results from a separate analysis of the deterministic ($r \to 0$) theory that we address in Chapter 3, and are consistent with the extrapolation of the results for nonzero $r$. Numerical simulations confirm the existence of all three solution types (U, S, W) in the relevant regions of the phase space, where necessary starting

from appropriately tuned initial conditions, as we also discuss in the following chapter.

The blue line in Fig. 2.13 is the segregation threshold $\beta_s$ discussed previously. It is nearly constant, increasing only very slowly with $r$; this shows that the $\beta_s$ values obtained via the $r \to 0$ analysis will be good estimates also for larger $r$. A second interesting feature of Fig. 2.13 is that there is a threshold value of $r \approx 0.054$ above which the strongly segregated solution is the only possible option, for any $\beta$ large enough for a segregated state to exist at all: this state is then the genuine steady state. Where agents have only moderate memory, with $1/r$ of the order of 10 trading periods, steady states where one market comes to attract most agents thus disappear, and the emergence of persistent market loyalties becomes the norm.

## 2.4 Summary

In this chapter we have developed a stylised model of double auctions and adaptive traders. We considered two variants of the model, one populated with agents who can adaptively tune their preferences for buying and selling along with their preferences for the two markets; in the other model agents have fixed preferences for buying and hence also selling. The two models share our main qualitative result: above a threshold value $\beta_s$ of the intensity of choice $\beta$ the agents segregate, i.e. develop a long lasting loyalty to one action, or one market. The onset of segregation is signalled both in simulations and in the analytical description by the emergence of multiple peaks in the distribution of agent preferences, as summarized e.g. in the Binder cumulant. These peaks are accompanied by long persistence times for the agents to remain within each peak.

In the model with fixed buying preferences we have shown that one can develop an analytical description of segregation to a significant level of detail. We find that even though individual agents do not explicitly try to maximise the well-being of the entire population, the strongly segregated state is in effect cooperative: it is more beneficial for every individual player, and the population as a whole, compared to possible unsegregated and envy-free Nash equilibrium states. The segregated state is neither envy-free – the traders that specialize to what we called volume-driven behaviour have lower returns in the short term than the return-driven ones – nor a Nash equilibrium. In this sense

the segregated state is stabilized by incomplete information, of each agent about the precise returns to be expected from each action and about the average returns achieved by others.

The transition from the homogeneous to the segregated state is caused by increasing the intensity of choice parameter $\beta$. There are two ways of interpreting this. One is that as $\beta$ grows, agents optimize against return differences on smaller and smaller scales $1/\beta$: our results then show that the more stringently agents optimize their behaviour, the higher the likelihood of segregation. Alternatively, as $\beta$ affects the agents' preferences only via products with the attractions, which themselves are proportional to the returns, an increase in $\beta$ has the same effect as an increase in the scale of returns at fixed $\beta$. When the possible returns are small an agent then plays randomly, while if the stakes are high an agent will try to take into account information from previous trades as much as possible. In this interpretation our main result states that there is a critical scale for single transaction returns above which the preferred state of the agent population is the segregated one.

We studied in some detail the dependence of the segregation threshold $\beta_{\mathrm{s}}$ on model parameters. One intriguing finding is that the threshold is generally lowest when the two markets are similar, demonstrating that segregation is not trivially driven by market differences. The precise value of $\beta_{\mathrm{s}}$ is determined by collective behaviour, with agents continually adjusting to trading conditions the population itself creates. This rules out simple intuitive estimates of $\beta_{\mathrm{s}}$. It is reassuring, however, that the quantitative variations in $\beta_{\mathrm{s}}$ are small for the different models we investigated, with values lying in the range $0.1 \ldots 0.3$ across most of the parameter space of our models.

Finally, it is important to discuss simplifications in our analysis and the way they might have affected our main results. We have made a number of assumptions about the bid and the ask distributions. It turns out that when these are relaxed, our main results change only quantitatively but not qualitatively. For example, we have shown all data for the case where the mean bid is greater than the mean ask, which enables more trades at the markets. However, qualitatively identical results are obtained in the opposite case, with the only change being in the specific value of the threshold $\beta_{\mathrm{s}}$. The

specific assumptions we made on the shape of bid/ask distribution can also be relaxed. In fact, within the Fokker-Planck description only the first and the second moment of the truncated bid/ask distribution appear and the precise shape of the distribution is otherwise immaterial (e.g. see more details in Appendix A).

We have also made the simplifying assumption that budget constraints on the agents can be ignored. Above the segregation threshold our results show substantial persistence times for agents in a particular role (e.g. persistent buying, at one of the two markets). While this may be in apparent conflict with budget or stock constraints, it is worth remembering that agents do change their loyalty eventually so they just need a large enough budget to sustain a long period of buying that is then followed by a long period of selling. Also, while persistence times do get exponentially large for very small $r$, our results show (cf. Fig. 2.13) that segregation can occur up to fairly large values of $r$. In this regime persistence times – while longer than in homogeneous states – are only moderately large so that budget constraints should be relatively easy to satisfy. We also note that in Tóth *et al.* [89] the authors show that the well documented persistence in orders of the same sign (i.e. an order to buy tends to be followed by more orders to buy and similar for an order to sell) at the shorter time scales is dominated by a single trader splitting his/her order; also the tendency to buy or sell persistently was shown to be stronger than collective effects such as order herding. Finally, segregation also occurs in models with explicit budget constraints, as we discuss in Chapter 4.

One question that remains, and which is not easy to address in full generality, is whether the emergence of segregation is an intrinsic property of systems with adaptive agents, or a consequence of our specific stylized model. The simplicity of the model itself argues for the former, as we did not need to make exotic assumptions to find segregation. But clearly there is still much to do from here to reach a detailed understanding of segregation in real markets, at a level that can directly influence policies. An initial step in this direction is described in Chapter 4.

# Chapter 3

# The Large Memory Limit

In this chapter, we devote special attention to the segregation in the infinite memory limit (the $r \to 0$ limit). As hinted before this limit is special because only when $r \to 0$ the transition between the unsegregated and segregated state is sharp. But additionally, in this limit, the analysis is simpler which enables us to explain some of the previously reported phenomena - multiple segregated states (Fig. 2.13) and nonmonotonicity of the critical intensity of choice (Fig. 2.10). Also, this analysis will help us to address some new extensions of the model that would not be accessible in the finite $r$ limit - different learning models and three markets, that we discuss those in the next Chapter. We start the large memory limit analysis with small systems - *2 players game* and *4 players game*. These are convenient as we can easily track each trader's adaptation, but still, see some phenomena that we believe are related to segregation - synchronisation at the same market (for $N = 2$) and segregation - pairwise synchronisation (for $N = 4$). After the finite $N$, we proceed with the large population limit and introduce the problem and analyse a *population with homogeneous buying preferences*. Once we develop all the techniques for one such population, we generalise the results to a system with two subpopulations we have analyzed previously.

## 3.1 Finite N

### 3.1.1 2 players - synchronisation

To understand collective effects in trading systems, we train our intuition by looking at a very simple model with only one buyer and one seller. The traders have a choice between

two markets that are symmetrically biased towards one of the players with a higher return. As the system consists only of two agents and two markets, previously introduced segregation in which a population will split into distinctive groups favouring one option is not feasible. However, as a characteristic of the segregated state is long lasting loyalty to a certain option/market, we can investigate whether under some conditions an agent develops strong preference towards one of the markets. To enable the trade, the pair of agents needs to synchronise at a market. Thus, one of the agents will always need to settle for less. An interesting question is under which conditions the pair of agents will prefer to randomly decide who will be a *winner* and the *looser*, and when will the roles become fixed. Thus we will focus on the existence of *synchronization of traders* and investigate parameters for which both agents develop strong preferences for the same market. The two player analysis is largely based on the similar work by Hanaki*et al.* [28] where as a first step in understanding how agents specialise when searching for parking spots, the authors studied if similar dynamics can be observed with only two players.

Our model assumptions are the following:

- Two players: player 1 always buys, player 2 always sells.
- Bids/asks are deterministic, i.e. $\mathcal{N}(\mu_b, 0), \mathcal{N}(\mu_a, 0)$, with $\mu_b - \mu_a = 1$.
- Trading price is as previously $\pi_m = a + \theta_m(b - a)$.
- Market biases are symmetric: $(\theta_1, \theta_{-1}) = (\theta, 1 - \theta)$ where $\theta \in [0, 0.5]$.

We made further simplification to the agent's trading strategy introduced in the previous chapter (where $\sigma > 0$, while now bids and asks are deterministic) to focus only on the synchronisation of the market choices. Preserving stochastic nature of order prices would only correct the average payoff at a market as we need to take into account fraction of meetings at a market when the bid and the ask do not match. When the order prices are deterministic the trading price is as well: $\pi_m = \mu_a + \theta_m(\mu_b - \mu_a) = \mu_a + \theta_m$. Note also that we denote the second market with $-1$ for simpler notation in the following calculations.

As previously, agent's market choosing strategy is driven by its attractions (Eq. 2.2). For each player $i$ we introduce the attraction to trade at market $m$ during the trade $n+1$:

$$A^i_m(n+1) = rS^i_m(n) + (1-r)A^i_m(n) \ ,$$

where $r$ is forgetting rate as before and $S^i_m$ is a return of an agent $i$ at a market $m$, $S^i_m$ is fully determined by the choice of co-player:

$$\begin{aligned} S^i_m(n) &= prob(m^{-i}(n) = m) \begin{cases} \mu_b - \pi_m = 1 - \theta_m, & \text{if agent } i \text{ is a buyer } (i=1) \\ \pi_m - \mu_a = \theta_m, & \text{if agent } i \text{ is a seller } (i=2) \end{cases} \\ &= prob(m^{-i}(n) = m)\Sigma^i_m \ , \end{aligned}$$

where $m^{-i}(n)$ denotes the market of choice of the co-player $-i$ during trade $n$ and $\Sigma$ simplifies the deterministic part of the score depending only on the type of market and agent. Agent's choice of market $m$ is a softmax function with intensity of choice $\beta$ (as introduced in Chapter 2, based on e.g. [28, 29, 77]):

$$P^i_m(n) = \frac{\exp\left(\beta A_m(n)\right)}{\sum_{m'} \exp\left(\beta A'_m(n)\right)} = \frac{1}{1+\exp\left(\beta m \Delta^i(n)\right)} = \sigma_\beta(m\Delta^i(n)) \ ,$$

where we note that important quantity is only attraction difference $\Delta^i = A^i_1 - A^i_{-1}$ and we also simplify notation and use $\sigma_\beta(x)$ to denote sigmoid function we use. Observing that $\Delta^i$ is a quantity of interest for agent's choice of market we proceed with studying its evolution:

$$\begin{aligned} \Delta^i(n+1) &= A^i_1(n+1) - A^i_{-1}(n+1) \\ &= \delta_{m^i(n),1} r S^i_1(n) + (1-r)A^i_1(n) - \left[\delta_{m^i(n),-1} r S^i_{-1}(n) + (1-r)A^i_{-1}(n)\right] \ . \end{aligned}$$

Stochastic variable $\Delta^i(n+1)$ depends on choices of agents during trade $n$ ($m^i(n)$ and $m^{-i}(n)$), which are drawn from the distribution that depends on $\Delta^i(n)$. We consider the limit $r \to 0$, as attraction increments are very small thus system adapts very slowly and

it is reasonable to approximate $\delta_{m^i(n),1}$ by its expected value $\sigma_\beta\left(\Delta^i(n)\right)$. Namely,

$$\Delta^i(n+1) = r\Big[\sigma_\beta\left(\Delta^i(n)\right)\sigma_\beta\left(\Delta^{-i}(n)\right)\Sigma_1^i(n) - \sigma_\beta\left(-\Delta^i(n)\right)\sigma_\beta\left(-\Delta^{-i}(n)\right)\Sigma_{-1}^i(n)\Big] + (1-r)\Delta^i(n)\ ,$$

that can be further simplified into:

$$\frac{\Delta^i(n+1)-\Delta^i(n)}{r} = -\Delta^i(n) + \Big[\sigma_\beta\left(\Delta^i(n)\right)\sigma_\beta\left(\Delta^{-i}(n)\right)\Sigma_1^i(n) - \sigma_\beta\left(-\Delta^i(n)\right)\sigma_\beta\left(-\Delta^{-i}(n)\right)\Sigma_{-1}^i(n)\Big]\ .$$

In the limit of small $r$, we can analyse previous in the continuous time limit, taking $t = nr$ (where a unit time step corresponds to $1/r$ trading periods):

$$\partial_t\Delta^i(t) = -\Delta^i(t) + \Big[\sigma_\beta\left(\Delta^i(t)\right)\sigma_\beta\left(\Delta^{-i}(t)\right)\Sigma_1^i(t) - \sigma_\beta\left(-\Delta^i(t)\right)\sigma_\beta\left(-\Delta^{-i}(t)\right)\Sigma_{-1}^i(t)\Big]\ .$$

A convenient change in variables that simplifies the previous system is $\Delta^1(t) = \xi(t)+\rho(t)$ and $\Delta^{-1}(t) = \xi(t) - \rho(t)$. Applying it, along with some algebraic operations and using market symmetry $\theta_{-1} = 1 - \theta_1$ the previous set of equations becomes:

$$\begin{aligned}\partial_t\xi(t) &= -\xi(t) + \frac{1}{2}\frac{\sinh\left(\beta\xi(t)\right)}{\cosh\left(\beta\xi(t)\right)+\cosh\left(\beta\rho(t)\right)}\ ,\\ \partial_t\rho(t) &= -\rho(t) + \frac{1-2\theta_1}{2}\frac{\cosh\left(\beta\xi(t)\right)}{\cosh\left(\beta\xi(t)\right)+\cosh\left(\beta\rho(t)\right)}\ .\end{aligned} \tag{3.1}$$

The evolution of $\xi$ describes the evolution of the mean agents' attraction differences ($\xi = (\Delta^1 + \Delta^{-1})/2$), while $\rho$ describes their distinction ($\rho = (\Delta^1 - \Delta^{-1})/2$). If previous dynamical equations have a fixed point it needs to satisfy:

$$\begin{aligned}\xi^* &= \frac{1}{2}\frac{\sinh\left(\beta\xi^*\right)}{\cosh\left(\beta\xi^*\right)+\cosh\left(\beta\rho^*\right)}\ ,\\ \rho^* &= \frac{1-2\theta_1}{2}\frac{\cosh\left(\beta\xi^*\right)}{\cosh\left(\beta\xi^*\right)+\cosh\left(\beta\rho^*\right)}\ .\end{aligned} \tag{3.2}$$

The first of these equations is always satisfied if $\xi^* = 0$, and in that case equation for $\rho^*$ has a unique solution whose sign depends on the sign of $(1 - 2\theta_1)$. When market 1 is

favourable towards buyers ($\theta_1 < 0.5$), $\rho^*$ will be positive, which can be interpreted as the solution when buyers and sellers learn which market is good for them, and thus have preferences for the opposite markets (as $\Delta^1$ is in that case positive meaning that player 1, the buyer, prefers market 1 good for buyers). Even though from the perspective of attractions, agents seem to recognize option with higher rewards, this solution is stable only for low intensities of choice where market choice dynamics is random, despite the difference in attractions. The stability of the solution $(\xi^* = 0, \rho^*)$ can be studied through the linearized set of equations (3.1). It can be showed that the fixed point is stable as long as the following criterion is satisfied:

$$\frac{\beta}{2}\frac{1}{1+\cosh(\beta\rho^*)} \leq 1\,. \tag{3.3}$$

Or, using the original variables $\Delta^i(t)$, the solution with $\Delta^{1*} + \Delta^{-1*} = 0$ is stable as long as:

$$\frac{\beta}{2}\frac{1}{1+\cosh(\beta(\Delta^{1*} - \Delta^{-1*})/2)} \leq 1\,. \tag{3.4}$$

The stability condition is exactly the same as the one observed in work of Hanaki *et al.* [28] as the learning dynamics we follow is the same so the two player models differ only in the details of deterministic returns. To demonstrate two different possible states, below and above critical intenisity of choise we show flow diagrams of the equations (3.1) in Figure 3.1. Left figure is for the domain of low choice intensities ($\beta = 2$) where unique fixed point corresponds to the state in which agents are undecided and are picking markets largely at random, though there is a slight recognition of a market that is better for an agent ($\Delta^1 > 0, \Delta^{-1} < 0$). Conversely, for higher intensities of choice ($\beta = 6$) two new fixed points are stable where agent's attraction differences are of the same sign, i.e. they prefer going to the same market.

At first, this is an unusual behaviour: For high intensity of choice, one of the agents decides to settle for less i.e. persistently choose the market where (s)he will be awarded lower scores. However, making this decision, the number of trades happening is maximised. In the low intensity of choice regime, all four states are equally probable:

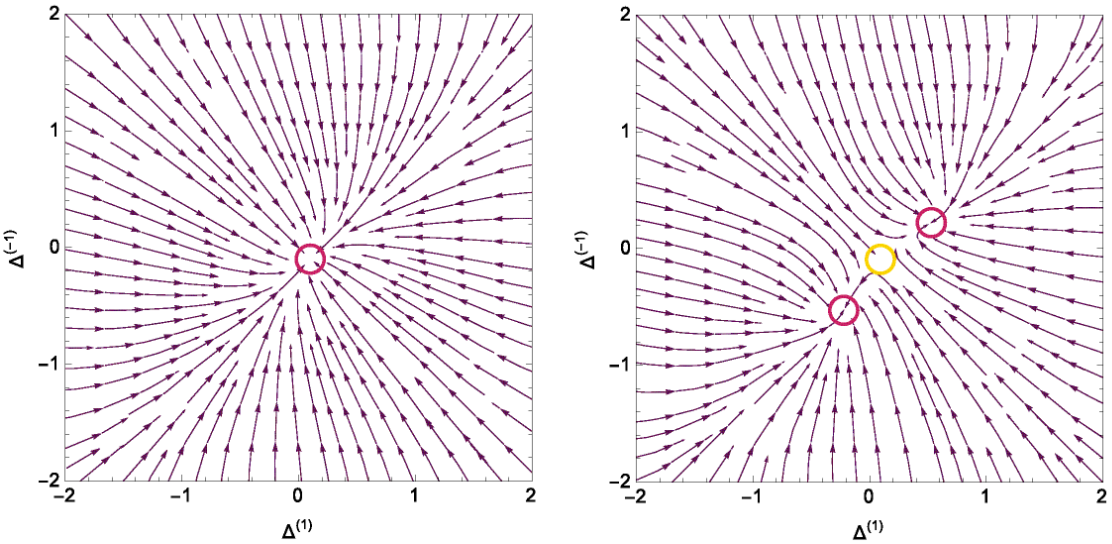


FIGURE 3.1: **2 player-dynamics phase portraits (Eqs. 3.1).** Left: intensity of choice $\beta = 2$, unique fixed point, undecided agents; Right: $\beta = 6$, two new fixed points appear - synchronized states. Market biases used: $\theta = 0.3$. For this set of markets, critical intensity of choice is $\beta_c = 4.16$

$(m^1, m^2) \in \{(1,1),(1,-1),(-1,1),(-1,-1)\}$ while just two of them enable trade. On the other hand, in the high $\beta$ regime, when agents persistently choose one market, they always get to trade, although one of the traders always receive a lower return. Especially, for the market parameters used in Fig. 3.1, $(\theta_1, \theta_2) = (0.3, 0.7)$ an agent who settles for lower score receives persistently score of $0.3$ while for the low $\beta$ expected payoff of both agents is $\frac{1}{4}(\theta_1 + \theta_2) = \frac{1}{4}$, showing that clearly both agents are earning more in the synchronized regime.

Following the condition of stability Eq.(3.3) we can find the domain of parameters $\theta$ and $\beta$ where fixed point associated with indecisive agents becomes unstable, consequently the domain of synchronised solution existence, shown in Figure 3.2. It is important to note that the synchronisation is not only driven by the market difference. This is clear when we note that the same markets ($\theta = 0.5$) synchronisation threshold is the lowest – both agents are happy with synchronising at one of the markets (nobody needs to settle for less). Previously outlined argument (players earn more if synchronised at a single market than if they are randomising between them) is correct only when $\theta > 0.25$. When $\theta$ is low, the greater intensities of choice are needed for synchronisation to occur. Although at high enough $\beta$ the synchronised state will be preferred, agents will not earn

equally. Thus their preferences for the market will differ for every finite $\beta$, i.e. the less satisfied agent will revisit the other market more frequently.

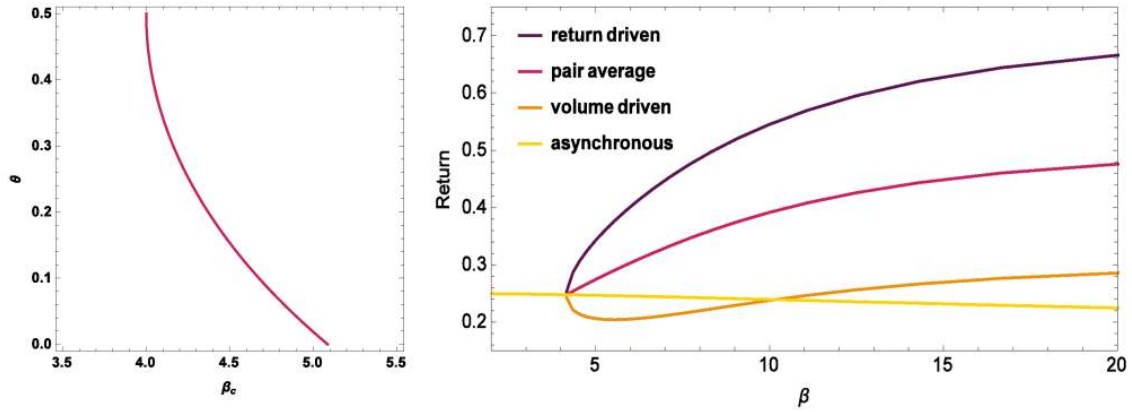


FIGURE 3.2: **2 players $(\theta, \beta)$ phase diagram and returns.** Left: Critical $\beta$ as a function of symmetric market bias $\theta$. Right: Returns for different $\beta$ for market bias $\theta = 0.3$. At the critical ($\beta_s = 4.16$), the return average of the pair is better than staying at the continuation of low $\beta$ fixed point, but one of the agents needs to settle for less.

In the right panel of Figure 3.2 we show how the average agent's returns vary for different $\beta$ for the typical markets ($\theta_1 = 0.3$). We compare the agent's payoffs when they synchronise at one market to the payoff they would receive by choosing markets based on the continuation of the low $\beta$ fixed point, unstable above the critical intensity of choice $\beta_c$. When choosing markets based on low $\beta$ fixed point, agent's returns decrease when $\beta$ is increased. This is due to the mentioned recognition of better market that drives agents to different markets, decreasing trade possibilities and consequently the payoff.

On the other hand, we note large payoff difference between the players when they synchronise at a market. We name an agent who earns more at a market *return driven*, while the agent who decides to settle for lower returns to enable trades we call *volume driven* (the origin of names is more evident in the large trading systems as described in Chapter 2). Large payoff discrepancy is feasible because agents are unaware of the co-player's return, they only keep their own scores and make a decision based on those.

Although no maximisation of the pair average is intended, the synchronised state is such that the overall benefit of the pair overcomes the decrease in returns they would experience if they continued choosing markets as when $\beta$ was low. When $\theta > 0.25$ for high values of $\beta$ both agents benefit from the synchronised state, while when $\theta < 0.25$

the benefits are observed only in the pair average, while the agent who settled for less always earns less than at the asynchronous state. The player who earns more at a market develops a strong preference for it, and even though the other player occasionally tries the other market, (s)he is better off persisting with the desired choice.

Previous results can be generalized to a pair of traders who do not have strict buyer and seller roles but can decide to buy with some probability $p_{\mathcal{B}}$. We continue with a symmetric set up and assume $p^1_{\mathcal{B}} = 1 - p^2_{\mathcal{B}} = p_{\mathcal{B}}$. This way, beside the previous condition, that agents need to be synchronised at a market for a trade to happen, they need to assume opposite roles. As $p_{\mathcal{B}}$ are not taken as adaptive but fixed agent's properties, this only corrects $\Sigma^i_m$ to the following:

$$\Sigma^i_m = p^i_{\mathcal{B}}(1 - p^{-i}_{\mathcal{B}})(1 - \theta_m) + (1 - p^i_{\mathcal{B}})p^{-i}_{\mathcal{B}}\theta_m \,. \tag{3.5}$$

Agent $i$ receives buyer's payoff $1 - \theta_m$ when (s)he assumes role of a buyer (with prob $p_{\mathcal{B}}$) while co-player assumes role of a seller; (s)he can also receives seller's payoff in the opposite configuration. Previous calculation can be then repeated and the following fixed point equations are obtained:

$$\begin{aligned} \xi^* &= \frac{p^2_{\mathcal{B}} + (1 - p_{\mathcal{B}})^2}{2} \frac{\sinh(\beta\xi^*)}{\cosh(\beta\xi^*) + \cosh(\beta\rho^*)} \,, \\ \rho^* &= \frac{(1 - 2\theta_1)(p^2_{\mathcal{B}} - (1 - p_{\mathcal{B}})^2)}{2} \frac{\cosh(\beta\xi^*)}{\cosh(\beta\xi^*) + \cosh(\beta\rho^*)} \,. \end{aligned} \tag{3.6}$$

As before $\xi^* = 0$ and $\rho^* > 0$ are a unique solution pair at low $\beta$ when $p_{\mathcal{B}} > 0.5$ and $\theta < 0.5$, with previous interpretation - player one that more often takes a role of a buyer will prefer a market one while the player two will do the opposite. Similarly, we can find $\beta_c$ above which this fixed point becomes unstable using the following condition:

$$\frac{\beta\left(p^2_{\mathcal{B}} + (1 - p_{\mathcal{B}})^2\right)}{2} \frac{1}{1 + \cosh(\beta\rho^*)} \leq 1 \,.$$

Figure 3.3 shows critical $\beta$ contours above which pair of agents $(p^1_{\mathcal{B}}, p^2_{\mathcal{B}}) = (p_{\mathcal{B}}, 1 - p_{\mathcal{B}})$ prefers to synchronize at one of the markets. We previously observed that the level of attraction to the preferred market might not be the same for the two players, but for high

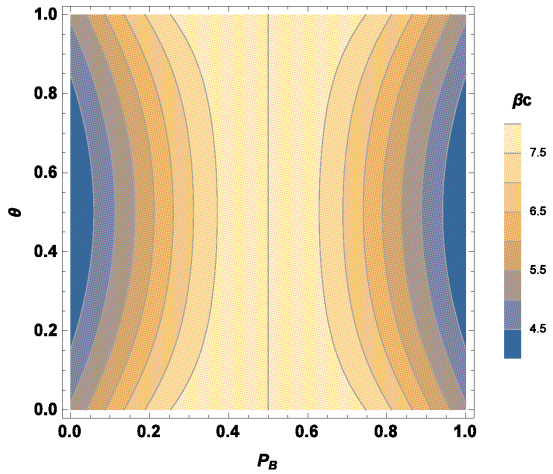


FIGURE 3.3: **2 players synchronisation threshold for system parameters $\theta$ and $p_{\mathcal{B}}$).** Synchronisation threshold is finite for all system parameters and increases with increase agents' similarity.

intensity of choice $\beta$ the new fixed points are such that the two players always prefer the same market. We also note that the region of synchronisation shrinks with increase of $p_{\mathcal{B}}$ which suggests that without strong buy/sell preferences agents need higher intensities of choice to benefit from the synchronized state. This is expected because agents with $p_{\mathcal{B}} = 0.5$ do not have as hight benefit from synchronising at a market – there is still probability of one half that the trade will not occur, as agents need to assume opposite roles at the market for the trade to happen.

### 3.1.2 4 players - onset of segregation

The two player system we have analysed showed already an interesting collective phenomenon – synchronisation at a market to enable more trades although that is not always beneficial for both players individually. To understand more about possible causes of segregation a minimal system where we can expect a similar effect is $N = 4$. A system with four agents is small enough so that we can still easily write down deterministic equations of the evolution of market attractions but large enough for the first signals of segregated states as agents can split across the markets in pairs. To keep analysis simple, we focus on four players who have determined buy/sell roles: two buyers and two sellers, with symmetrically biased markets $\theta_1 = 1 - \theta_{-1} = \theta$. As before, we describe an agent by his/her market attraction difference $\Delta^{g,i}$ whose deterministic equation derivation mostly follows

previously outlined procedure ($g$ index denotes group - buyers or sellers, while index $i$ counts agents in the group as before). The two methods differ in the return calculation at a market of choice because $S_m^{g,i}(n)$ now depends on the configuration of all other players:

$$S_m^{g,i}(n) = \frac{\Sigma_m^g}{2}\delta_{m^{g,-i}(n),m}\left(\delta_{m^{-g,1}(n),m} + \delta_{m^{-g,-1}(n),m}\right) \\ + \Sigma_m^g\left(1 - \delta_{m^{g,-i}(n),m}\right)\left(\delta_{m^{-g,1}(n),m} + \delta_{m^{-g,-1}(n),m} - \delta_{m^{-g,1}(n),m}\delta_{m^{-g,-1}(n),m}\right) ,$$

$\Sigma_m^g$ denotes the deterministic part of the return that is only dependent on the market $m$ and the agent's type $g$, as introduced for two players (see Eq.3.5). With the Kronecker's $\delta$ we ensure other agents are present at the same market $m$ at the trading period $n$. The first term denotes the states where both agents of the same type are at a market $m$ and the return is only half of the possible payoff (as with equal probabilities one of the players will be selected to trade if there is only one trader of the other type). On the other hand, when the second player of the same type is not in the same market, the player receives the return if there's a trader of the opposite group as described by the second term. The deterministic equations are thus:

$$\partial_t \Delta^{g,i}(t) = -\Delta^{g,i}(t) + \sum_{m=-1}^{1} m\sigma_\beta\left(m\Delta^{g,i}(t)\right) S_m^{g,i}(t) ,$$

where values of Kronecker's deltas in $S_m^{g,i}(t)$ are exchanged with their expected values as in the two players derivation. We solve these equations numerically and find that for low intensity of choice $\beta$ there is a unique fixed point whose value depends on $\theta$ denoting preference of buyers to the market good for buyers and similarly for the group of sellers, but as $\beta$ is small players largely choose markets at random. When $\beta$ is increased, two new stable fixed points appear - all four agents synchronise at a single market. These states, as in the two agents systems, ensure population average is higher than the continuation of the low $\beta$ fixed point that leads to asynchronous choices. But, as before one group needs to settle for a lower return. Interestingly, when $\beta$ is increased further, four new stable states appear – the segregated states in which both markets are populated with a pair of traders, one from each group.

In Figure 3.4 we show the two critical $\beta$ lines (the synchronisation and the segregation

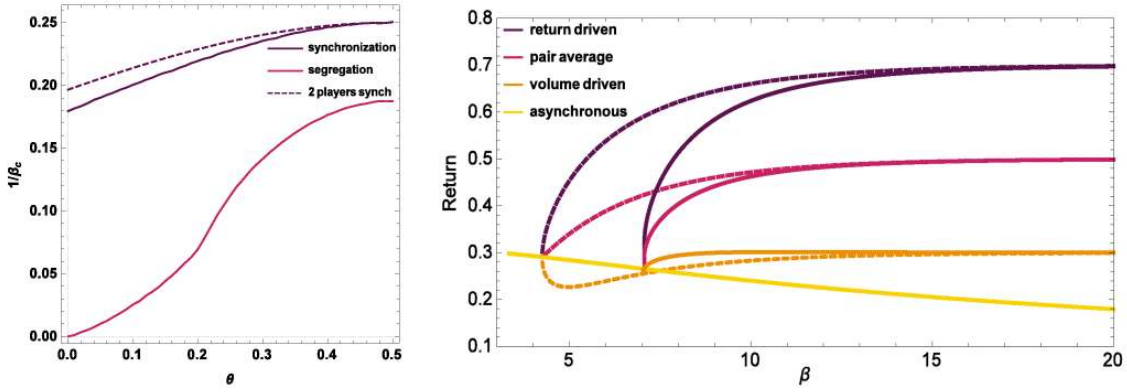


FIGURE 3.4: **System with four agents (two buyers and two sellers): phase diagram and returns.** Left: Phase diagram of possible states for different market parameters $\theta$ and intensities of choice $\beta$: synchronisation at a single market (below the violet line), segregation across two markets (below the purple line). The dashed violet line is synchronisation threshold line for the two agents system for comparison. Right: Returns in different groups as function of intensity of choice $\beta$ when market biases are $(\theta_1, \theta_2) = (0.3, 0.7)$. Dashed lines correspond to synchronised states in which return and volume driven type correspond to whole groups (e.g. buyers choosing market good for buyers). Solid lines are single agent averages in the segregated state when one agent from each group is a return driven (e.g. buyer at market good for buyers) and the other one is volume driven (e.g. seller at the market good for buyers). Yellow line is return of the asynchronous low $\beta$ fixed point.

threshold) for various market configurations and four players with strict buy/sell roles. We included the two player synchronisation line to the plot for the comparison, and we note that the two lines are very close and qualitatively follow the same trend of synchronisation region shrinking when marked difference increases. We note the same tendency with the segregation region, and we note that the segregation region is always smaller than the synchronisation region.

The right panel of Figure 3.4 shows return lines for different intensities of choice $\beta$: dashed lines correspond to synchronised states, while solid lines are averages in the segregated state. We note that in the large $\beta$ limit the population averages corresponding to synchronised and segregated states, are the same. At a state where all agents synchronise at the same market one group earns more (dark violet line) than the other (orange line), but as in the two player game, the population average is higher than at the asynchronized state. In the large $\beta$ limit, everyone is better off in the synchronised state. However, when the segregation occurs the solid dark violet and orange lines denote single player's payoff from both groups while the purple line is the group average (consequently also the

population average). It is interesting that in the large $\beta$ limit the two types of states lead to the same population average but while in one a whole group of agents is earning less, the other does not make the distinction between the groups, but within a group, there are high achievers and low achievers. As there are more states of the segregated type (four: $(m^{1,1}, m^{1,-1}, m^{-1,1}, m^{-1,-1}) \in \{(-1,1,-1,1),(-1,1,1,-1),(1,-1,-1,1),(1,-1,1,-1)\}$) compared to the synchronised type (two), and the difference in the number of states will increase with number of agents in a group $N$, we expect in the large $N$ limit the segregated state to dominate.

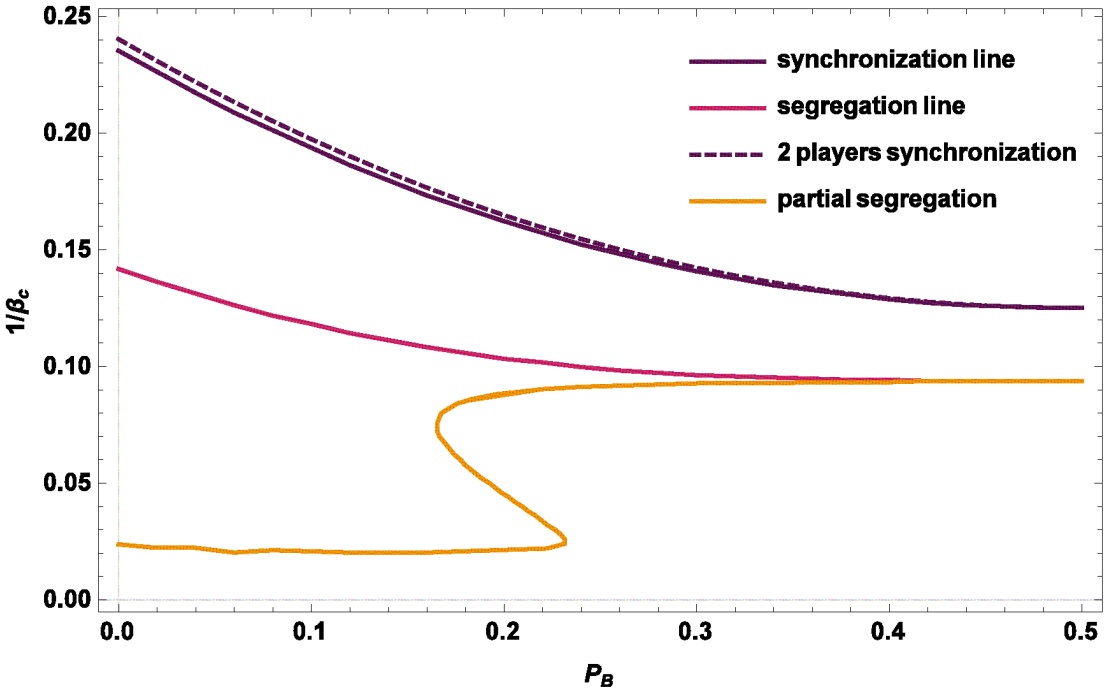


FIGURE 3.5: **Four traders phase diagram when the group buy/sell roles are probabilistic.** We note that both the segregation (purple line) and the synchronization (dark violet line) region shrink when the difference in agent's buy/sell preferences decreases, the trend we have observed in the two player system as well (dashed line). Below the orange line "partially" segregated fixed points exist too - one of the four agents have a preference for the opposite market.

Finally, as when analysing the two players game, we can generalise the results by allowing agents to assume the role of a buyer or a seller with some group dependent probability $p_{\mathcal{B}}^{(g)}$. Using the deterministic part of returns defined in the Eq. (3.5), now function of $p_{\mathcal{B}}^{(g)}$ too, with the same deterministic equations we can investigate how the synchronisation and segregation thresholds depend on groups' properties. In Figure 3.5

we show results for the symmetric markets $(\theta_1, \theta_2) = (0.3, 0.7)$ and symmetric groups $p_{\mathcal{B}}^1 = 1 - p_{\mathcal{B}}^{-1} = p_{\mathcal{B}}$.

As in the system with only two agents, when traders' preferences for buying are similar they do not have as strong incentive to synchronise as players with strict buy/sell roles. The similar trend we observe in the segregation threshold dependence on the preference for buying $p_{\mathcal{B}}$. Interestingly, in the system consisting of four traders we note one more type of fixed points that does not exist in the two-trader-systems: "partially segregated" states. Characteristic of these states is a single agent whose market preference is opposite from the other three players, effectively making only one group segregated. These fixed points appear for high enough $\beta$ for all $p_{\mathcal{B}}$, but in a system with four agents, these states are unstable (proven by methods of linear stability analysis). Their instability in the small systems is probably due to the smaller number of trades. In the large $\beta$ limit of partially segregated fixed point, there is at most one trade per trading period (only one pair will match at a market) while both segregated and synchronised states lead to two trades. As we will see in the following sections, partially segregated states exist in the large population limit too, though in a smaller region of the phase space, where their stability also changes.

## 3.2 Population with a fixed preference for buying $p_{\mathcal{B}}$

Studying systems with a small number of agents we have already encountered rich phenomenology - synchronisation of agents at a single market, pairwise segregation across the markets and even some mixed states where one group segregates, while the other specialises in a single market. We now seek to generalise these already impressive results and investigate possible types of steady states in the large population limit. We start this description with another "toy model", a population with identical preferences for buying $p_{\mathcal{B}}$. The assumption of population homogeneity is a very strong one, but these traders still undergo segregation for a broad range of parameters, while the system is simpler to analyse. Thus it is a useful prelude to analysis of the population consisting of two or more subpopulations of this type. We introduce techniques we will use in the rest of the chapter on this convenient but rich toy model.

We continue the analysis of the system with only two markets, and as in Chapter 2, we use an order parameter per market. We have chosen Demand-To-Supply ratios $D_m$ (ratio of buyers and sellers) as they conveniently translate into the trading probabilities, but other choices are possible, too. Once the order parameters are known, we can easily calculate trading probabilities for buying and selling at both markets:

$$T_{\mathcal{B}m} = \min\left(1, \frac{Q_{\mathcal{S}m}}{Q_{\mathcal{B}m}D_m}\right) \qquad T_{\mathcal{S}m} = \min\left(1, \frac{Q_{\mathcal{B}m}D_m}{Q_{\mathcal{S}m}}\right) . \tag{3.7}$$

When the trading probabilities are known, as introduced in Chapter 2, we can write the Fokker-Planck description of evolution of the attraction difference distribution ($\Delta = A_1 - A_2$, it measures attractiveness of market 1 over market 2):

$$\partial_t P(\Delta|p_{\mathcal{B}}, T_\gamma) = -\partial_\Delta \left[M_1(\Delta|p_{\mathcal{B}}, T_\gamma)P(\Delta|p_{\mathcal{B}}, T_\gamma)\right] + \frac{r}{2}\partial_\Delta^2 \left[M_2(\Delta|p_{\mathcal{B}}, T_\gamma)P(\Delta|p_{\mathcal{B}}, T_\gamma)\right] , \tag{3.8}$$

where the jump moments are function of the order parameters, and as explained in the previous chapter we take a so called adiabatic assumption – we look for the steady states of agent's dynamics, assuming the order parameters are not changing. The drift term is calculated as follows (more details on the derivation and all the explicit functions of market bias parameters, e.g. $Q_\gamma$ or $\langle S_\gamma \rangle$ are in Appendix A):

$$M_1(\Delta|p_{\mathcal{B}}, T_\gamma) = \sum_{m=-1}^{1} \sum_{\tau\in\{\mathcal{B},\mathcal{S}\}} m p_\tau T_{\tau m} \langle S_{\tau m}\rangle \sigma_\beta\left(m\Delta\right) - \Delta , \tag{3.9}$$

where the sum over $\tau$ (trading actions, buy/sell) is used to simplify the equation, under assumption that $p_{\mathcal{S}} = 1 - p_{\mathcal{B}}$. The term $\langle S_\gamma \rangle$ is used to denote agent's return average while playing an action $\gamma$ assuming that there is always an opportunity to trade (note, correction that an agent does not always submit a valid order is taken into account). Similarly, the diffusion term is:

$$M_2(\Delta|p_{\mathcal{B}}, T_\gamma) = \sum_{m=-1}^{1} \sum_{\tau\in\{\mathcal{B},\mathcal{S}\}} \Big[p_\tau T_{\tau m}(\langle S_{\tau m}^2\rangle - 2m\Delta\langle S_{\tau m}\rangle)\Big]\sigma_\beta\left(m\Delta\right) + \Delta^2 . \tag{3.10}$$

The steady state of the system described is (e.g. [90]):

$$P(\Delta|p_{\mathcal{B}}, T_\gamma) \propto \frac{1}{M_2(\Delta|p_{\mathcal{B}}, T_\gamma)} \exp\left(\frac{2}{r}\int_0^{\Delta} d\Delta' \frac{M_1(\Delta'|p_{\mathcal{B}}, T_\gamma)}{M_2(\Delta'|p_{\mathcal{B}}, T_\gamma)}\right) . \tag{3.11}$$

The previous procedure shows that for every pair of market parameters we can find uniquely defined stationary distribution, assuming that the order parameters are not changed. This is insightful if we want to understand states a population might prefer when evolving in a system where order parameters are fixed exogenously. For example, *demand-to-supply* ratio can be unaffected if the population with fixed $p_B$ is just a very small fraction of the trading cohort. Bearing this in mind we can ask – for which *demand-to-supply* ratios will the population prefer a single market, or, when will population split across the markets and more. To answer these questions we will first focus on the $r \to 0$ limit and seek for a condition for segregation in this regime, and later we will see how these results change for the finite $r$.

**Segregation at the $r \to 0$ limit.** Following the line of arguments stated above, for any set of order parameters we can find the steady-state distribution (Eq. 3.11) that can in principle be a bimodal distribution (multimodal when $m > 2$). The bimodality we can check without finding the steady state, by solving $M_1(\Delta|p_{\mathcal{B}}, T_\gamma) = 0$. Every solution $\Delta_i$ corresponds to a peak of a certain weight in the finite $r$ regime. As before we note that the intensity of choice $\beta$ is a control parameter and above a certain threshold, the steady state distribution is bimodal.

In Figure 3.6 we show how the critical intensity of choice depends on market biases $\theta_1, \theta_2$ for different populations "indecisive" ($p_{\mathcal{B}} = 0.5$) and "decisive" buyers ($p_{\mathcal{B}} = 0.8$). We see that for every pair of market biases, above some value of the intensity of choice $\beta$, the moment has multiple zeros which in the case of any finite $r$ results in a bimodal steady state distribution, i.e. segregated state. We note that when agents are indecisive between buying and selling, the region where the segregation occurs is the greatest when markets are identical or symmetrically biased. The decisive buyers' ($p_{\mathcal{B}} = 0.8$) segregation threshold is the lowest when the markets are identical. Note that the change between the two diagrams shown in Figure 3.6 is smooth when $p_{\mathcal{B}}$ is varied.

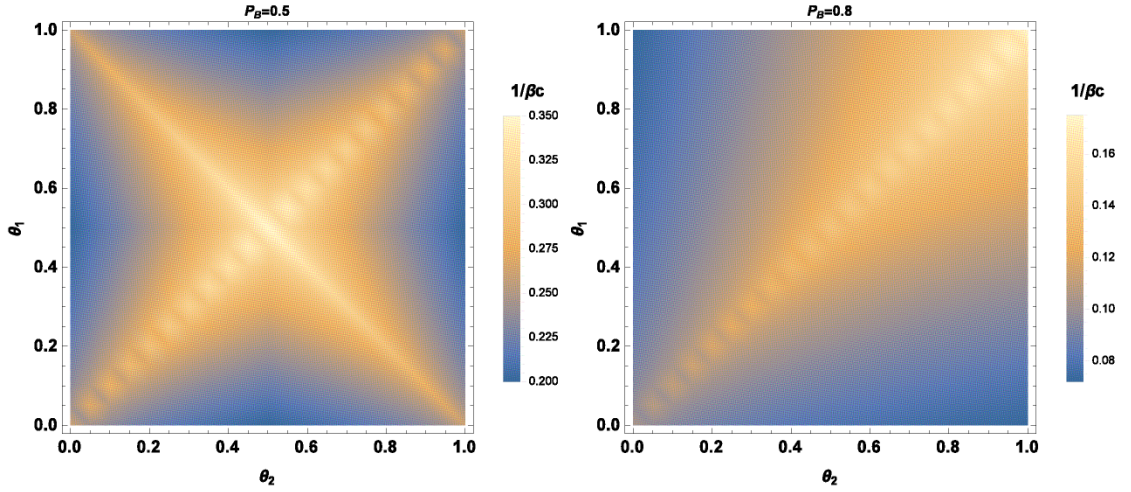


FIGURE 3.6: **Critical intensities of choice as function of market biases.**(left) Indecisive population ($p_{\mathcal{B}} = 0.5$); (right) Population of buyers ($p_{\mathcal{B}} = 0.8$).

Although these results state that the segregation across two markets exists for every pair of market biases, it is not clear from such analysis if these multimodal states have the same properties. To investigate whether the segregation always occurs in the same manner, we show the steady state distributions for two choices of market parameters and then try to generalise the observations. In Fig. 3.7 we show the steady state distributions of traders who are "decisive" buyers ($p_{\mathcal{B}}$) when adapting to two fair markets and two symmetrically biased markets. We intentionally show these steady state distributions for two different values of forgetting rates $r$ as our goal is to investigate the $r \to 0$ limit and although two values are not enough to understand the limit, we can try to observe a trend if it exists. As expected, the peak width decreases with $r$ (from the Eq. (3.11) we see that the peak width is $\approx \sqrt{r}$), but in Figure 3.7(right) we see that the weight ratio depends on $r$, too. The question that remains thus is when the segregated solution exists in the limit $r \to 0$.

To understand if the segregated state exits in the limit $r \to 0$, we assume that in the limit, the steady state is:

$$P(\Delta) = \omega\delta(\Delta - \Delta_1) + (1-\omega)\delta(\Delta - \Delta_2)\ .$$

This is true because the peaks of the multimodal distribution are centred at $M_1(\Delta|p_{\mathcal{B}}) = 0$

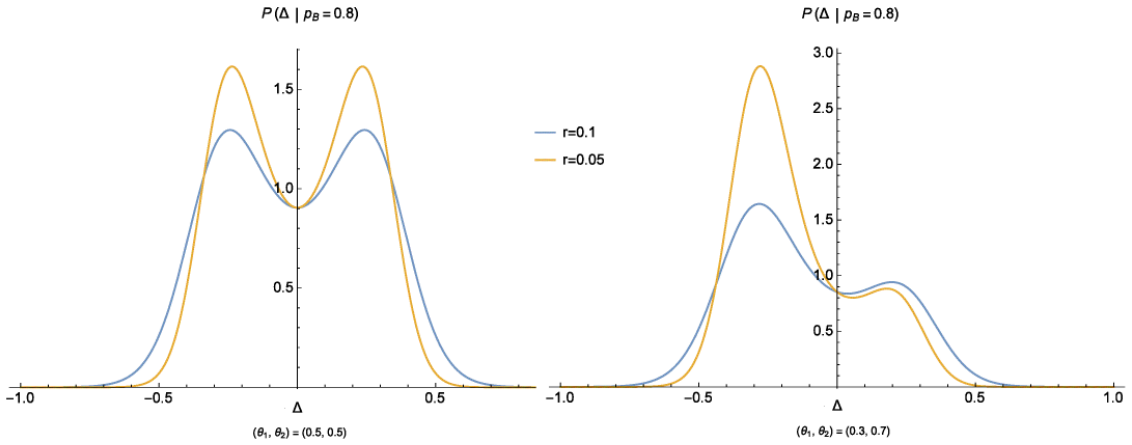


FIGURE 3.7: **Steady state distributions of "decisive" buyers at different markets.** In this figure we compare steady states at $\beta = 20$ for different market set-ups. Left: 2 fair markets - Strongly segregated solution (S); Right: 2 symmetrically biased markets - Weakly segregated solution (W). We also look how forgetting rate $r$ affects the solutions: $r = 0.1$ (blue), $r = 0.05$ (orange). Beside expected peak narrowing when $r$ is decreased, we also see that the weakly segregated solution's peak weight ratio is changed.

here marked $\Delta_i$, while the peak width decreases as $\sqrt{r}$, thus if it exists the segregated steady state is a weighted sum of the delta peaks. Using the steady state distribution Equation (3.11) we can caluculate the peak weight ratio in this limit:

$$\begin{aligned}\frac{\omega}{1-\omega} &= \frac{P(\Delta_1|p_{\mathcal{B}})}{P(\Delta_2|p_{\mathcal{B}})} \\ &= \lim_{r\to 0}\frac{M_2(\Delta_2|p_{\mathcal{B}},T_\gamma)}{M_2(\Delta_1|p_{\mathcal{B}},T_\gamma)}\exp\left(\frac{2}{r}\int_{\Delta_1}^{\Delta_2} d\Delta\frac{M_1(\Delta|p_{\mathcal{B}},T_\gamma)}{M_2(\Delta|p_{\mathcal{B}},T_\gamma)}\right) .\end{aligned} \tag{3.12}$$

This equation explains previous observation: for some solutions the peak weight ratio increases when $r$ is decreased. We realise that when the integral part of the Eq. (3.12) is positive, $\omega \to 1$ as $r \to 0$ and consequently the whole population is centred at $\Delta_1$, i.e. the steady state is unsegregated. Similarly, when the integral factor is negative the steady state is a delta peak centred at $\Delta_2$. From this we see that the peak ratio is finite only when

$$I = \int_{\Delta_1}^{\Delta_2} d\Delta\frac{M_1(\Delta|p_{\mathcal{B}},T_\gamma)}{M_2(\Delta|p_{\mathcal{B}},T_\gamma)} = 0 , \tag{3.13}$$

which is the condition for segregation in the $r \to 0$ limit. Thus at a fixed intensity of choice, for every pair of order parameters $(D_1, D_2)$ we can first find the peak positions

$\Delta_{1,2}$ but we can also calculate $I$ and check if preference to a single market predominates, or there's preference coexistence, thus segregation persists at $r \to 0$. This segregation condition is analogous to the Maxwell construction argument [91] originally applied to find vapour-liquid coexistence curve in the van der Waals model. To distinguish between possible states, we can also introduce a function, analogous to the free energy function in thermodynamics, such that the steady state distribution can be rewritten in the following form:

$$P(\Delta) \propto \exp\left(-\frac{f(\Delta)}{r}\right) .$$

Comparing this to the steady state distribution in the Eq. (3.11) we define $f(\Delta)$ as follows:

$$f(\Delta) = -2\int_0^{\Delta} d\Delta' \frac{M_1(\Delta'|p_{\mathcal{B}}, D_m)}{M_2(\Delta'|p_{\mathcal{B}}, D_m)} .$$

With this notation the condition of segregation in the $r \to 0$ limit reads as $f(\Delta_2) - f(\Delta_1) = 0$. Moreover the steady state classification can now be obtained by analysing the free energy analogue - when the function has a unique minimum the state is unsegregated, it is segregated otherwise. Only when the two minima are equal ($f(\Delta_1) = f(\Delta_2)$) the state is strongly segregated (e.g. shown in the left panel of Figure 3.7) while otherwise the state is weakly segregated (as shown in the right panel of Fig. 3.7). For every finite $r$ the two types of segregated solutions are multimodal distributions, meaning that a finite fraction of population always visits both markets. However, as we have seen in the $r \to 0$ limit only the strongly segregated state will have finte peak weight ratio, thus we call this state strongly segregated opposed to the weakly segregated state which will be a unimodal distribution in the $r \to 0$ limit.

Now that we have a method to find steady states and classify them we return to the space of market order parameters and investigate for which order parameters segregation occurs. In Figure 3.8 we show $r \to 0$ domains of unsegregated (white), weakly segregated (coloured region) and segregated states (solid line, a subset of the weakly segregated domain) at a fixed intensity of choice $1/\beta = 0.12$. We compare again "indecisive" ($p_B = 0.5$) and "decisive" buyers ($p_B = 0.5$) with various market demands, but also different

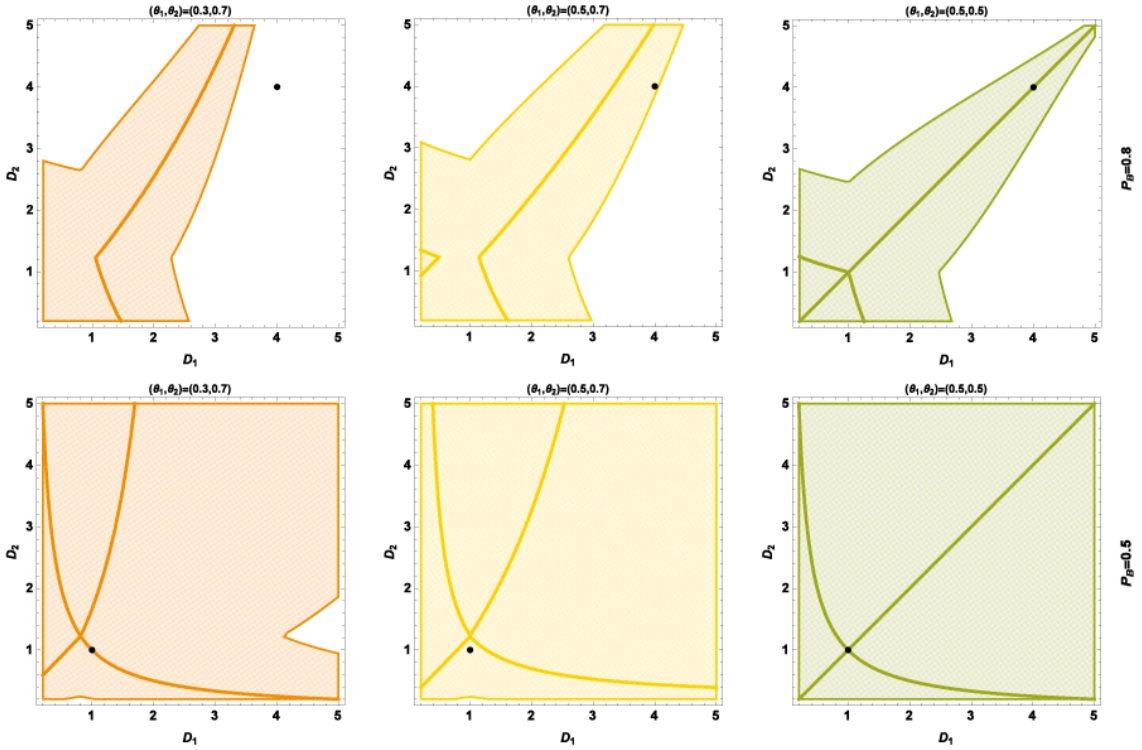


FIGURE 3.8: **Single population steady state types in the space of market order parameters** $(D_1, D_2)$**.** Top: population of buyers ($p_{\mathcal{B}} = 0.8$); Bottom: "indecisive" population ($p_{\mathcal{B}} = 0.5$); Left: symmetrically biased markets $(\theta_1, \theta_2) = (0.3, 0.7)$; Middle: a fair and a biased market $(\theta_1, \theta_2) = (0.5, 0.7)$; Right: two fair markets $(\theta_1, \theta_2) = (0.5, 0.5)$. Coloured regions represent domain of weakly segregated states in the $r \to 0$ limit. Their subsets, domains of strongly segregated states are represented with solid lines. White regions represent order parameters for which steady states are unsegregated.

market setups: (1) two fair markets (equilibrium trading price $\theta_1 = \theta_2 = 0.5$), (2) a fair and a biased market ($(\theta_1, \theta_2) = (0.5, 0.7)$) and (3) two symmetrically biased markets ($(\theta_1, \theta_2) = (0.3, 0.7)$).

We first note that the region of existence of weakly segregated states shrinks when the agents have stronger preferences for buying, the steady state of the indecisive population is a bimodal distribution for almost all presented demand-to-supply ratios. We see that when markets are fair and demand-to-supply is the same, both types of agents prefer to strongly segregate. A rationale for this behaviour might be in the fact that whenever one of the markets is different in terms of its demand or supply the agent will clearly differentiate them and choose a more convenient option. Interestingly, we see that "decisive" buyers segregate in a system of symmetric markets only if at least one of the markets

has higher demand than supply, but notably, the markets are different. Finally, we also note that the "indecisive" buyer perceives the benefit of segregation when markets are symmetric in their demand and supply, i.e. $D_1 \propto 1/D_2$.

It is important to note here again that these segregation conditions are drawn upon the assumption that market order parameters $(D_1, D_2)$ remain fixed over the period of agent's adaptation. As stated before, that is a reasonable assumption if we are interested in understanding e.g. single agent dynamics as his/her own preferences have a negligible effect on overall numbers of buyers and sellers at markets. Having this in mind we see that a single agent prefers settling for a single market for some demand-to-supply ratios, but sometimes (s)he prefers spending long periods of time at one market and then changing the preference to another market. This observation comes from knowing that the steady state distribution we have found in Eq. (3.11) can be interpreted either as a population density or as a single agent distribution of attraction differences over a long time. If we are to think about a large group of agents with preference to buy $p_B$ then the assumption of fixed market order parameters might not be sound, and we need to think about the effects of the group to the order parameters. In this context, we investigate if the segregation is possible if only the population in question is trading at the markets. To rephrase – can the segregated population create market conditions needed for its segregation? This, as we have seen, will usually result in a self-consistent procedure for solving the Fokker-Planck equation (described in Section 2.3), but when the system consists of agents with homogeneous preferences for buying this can be avoided.

**Market conditions.** Here we start by calculating market conditions created by a group of traders with homogeneous preferences for buying $p_B$ if their distribution of market preferences is $P(\Delta)$. Number of buyers/sellers at the market $m$ are:

$$\begin{aligned} N_{\mathcal{B}m} &= p_{\mathcal{B}} \int d\Delta P(\Delta)\sigma_\beta(\Delta) \,, \\ N_{\mathcal{S}m} &= (1-p_{\mathcal{B}}) \int d\Delta P(\Delta)\sigma_\beta(\Delta) \,. \end{aligned} \tag{3.14}$$

From these, we see that the demand-to-supply ratio does not depend on the market preference distribution, but it is completely determined by the input parameter - preference

for buying:

$$D_m = \frac{N_{Bm}}{N_{Sm}} = \frac{p_B N_m}{(1-p_B)N_m} = \frac{p_B}{1-p_B} \,. \tag{3.15}$$

This is true because the population consists of agents of the same type, whose probability of choosing a market $m$ is the same. Consequently, the demand-to-supply ratio is fully determined by $p_B$. In our previously sketched space of market order parameters, this condition corresponds to a single point in the space, marked in black in Figure 3.8. We see that the population of "indecisive" buyers strongly segregates when markets are fair or symmetric (these results extend to $\theta_1 = \theta_2$ or $\theta_1 = 1 - \theta_2$, not only for the market parameters shown in the figure). "Decisive" buyers, on the other hand, strongly segregate only if the markets are equal. In Figure 3.8 we see how the dot of market order parameters created by decisive traders is in the unsegregated domain for the symmetric markets, weakly segregated domain for fair/biased market pair and strongly segregated when both markets are fair.

With these insights, we consider again Fig. 3.6. It shows the existence of the segregation threshold intensity of choice for all market biases (and this critical $\beta$ is obtained as the point when the drift term has multiple solutions). Analysing the types of segregation above $\beta_s$ we now conclude that for the majority of the market biases the steady state is a weakly segregated one. As commented before, for any finite $r$ these states are bimodal distributions in which a finite fraction of the agents is always choosing to settle in a different market, but in the $r \to 0$ limit one market wins, e.g. the distribution of agents is unimodal.

## 3.3 2-subgroup population ($p_{\mathcal{B}}^{(1)}, p_{\mathcal{B}}^{(2)}$)

In the previous section, we showed how for any given pair of market order parameters $(D_1, D_2)$ we can determine the type of steady state of a group of traders with homogeneous preferences for buying $p_{\mathcal{B}}$. We have identified three possible types of steady states: unsegregated state (U), weakly segregated state (W) and strongly segregated state (S). We now generalise the investigation to populations that have more subgroups with fixed

preferences for buying. We demonstrate the procedures in the case of two subgroups, but the principles are general and can be extended further. We denote a steady state of a population consisting of two subgroups with a pair of letters $(X, X), X \in \{U, W, S\}$ indicating the type steady state for the both subgroups. We note that population with two different subgroups can find itself in any of the nine possible states.

When the market order parameters are somehow fixed exogenously, for any given pair $(D_1, D_2)$ we can find domains of different state types as in Figure 3.8 for both subgroups and thus determine what preferred state combination will be the steady state of the population. Just by a quick look at Figure 3.8 we can characterise a steady state of a population consisting of the two subgroups whose solution domains are plotted $(p_{\mathcal{B}}^{(1)}, p_{\mathcal{B}}^{(2)}) = (0.8, 0.5)$. For example, when market order parameters are $(D_1, D_2) = (5, 5)$ (the top right corner of all the diagrams), the population's steady state is $(U, W)$ when markets are symmetrically biased or biased/fair (the left and central diagrams in Fig. 3.8) and $(S, S)$ when both markets are fair (right diagrams in Fig. 3.8). This simple analysis can be extended to any number of subgroups as we treat every one of them independently. However, this only gives us the steady state of such composite population if the market order parameters are fixed exogenously.

More realistically, we want to investigate the steady states of the population that is also the only population trading at different markets, thus defining the market order parameters. In this case, we need to find the steady states self-consistently. We have outlined such procedure for the finite $r$ in Chapter 2 where starting from some initial market order parameters $(D_1, D_2)$ we have been calculating the steady states and updating $(D_1, D_2)$ accordingly until finding a self-consistent pair - order parameters created by the steady state are the ones needed for retrieval of that steady state. Now, instead of looking at the possible order parameter pairs that we can obtain starting from some initial conditions, we want to explore the space of order parameters to find and categorise all the steady states.

In the phase space, we define a locus of points for which one of the order parameters does not change. The intersection of such loci for all the order parameters (in the case of

two markets, only two) gives us all possible steady states. To find the loci, we use the definition of the market order parameters (Eqs. 3.14,3.15) extended to two subpopulations:

$$D_m = \frac{N_{\mathcal{B}}^{(1)} + N_{\mathcal{B}}^{(2)}}{N_{\mathcal{S}}^{(1)} + N_{\mathcal{S}}^{(2)}}$$
$$D_m = \frac{p_{\mathcal{B}}^{(1)} \int d\Delta \sigma_\beta(m\Delta) P(\Delta|p_{\mathcal{B}}^{(1)}) + p_{\mathcal{B}}^{(2)} \int d\Delta \sigma_\beta(m\Delta) P(\Delta|p_{\mathcal{B}}^{(2)})}{(1-p_{\mathcal{B}}^{(1)}) \int d\Delta \sigma_\beta(m\Delta) P(\Delta|p_{\mathcal{B}}^{(1)}) + (1-p_{\mathcal{B}}^{(2)}) \int d\Delta \sigma_\beta(m\Delta) P(\Delta|p_{\mathcal{B}}^{(2)})} \,.$$

For every pair $(D_1, D_2)$ we find steady states $P(\Delta|p_{\mathcal{B}}^{(g)})$ for all subgroups for some small $r$. Using these steady states we find the locus of points for which $D'_m = D_m$. The intersection of such loci will give us the number and market order parameters of all the steady states of the population with small but finite $r$. As we expect the loci to continuously change with $r$, finite but small $r$ gives us a good estimate on the number of solutions and determining in which domain they lie (U, W or S) we can characterise the type of population steady state. In most of what follows we constrain our analysis to symmetric set up of markets (taking symmetric biases $\theta_1 = 1 - \theta_2$) and agents' buying preferences ($p_{\mathcal{B}}^{(1)} = 1 - p_{\mathcal{B}}^{(2)}$). We start this section with examples of transitions of population with "decisive" traders ($(p_{\mathcal{B}}^{(1)}, p_{\mathcal{B}}^{(2)}) = (0.8, 0.2)$) and "indecisive" traders ($(p_{\mathcal{B}}^{(1)}, p_{\mathcal{B}}^{(2)}) = (0.55, 0.45)$) to demonstrate previously described methods. We continue with remarks on algorithmic approaches to find and characterise all the steady states when $p_{\mathcal{B}}$ is continuously varied, and conclude with a phase diagram in the $r \to 0$ limit, where number and type of population's steady states is marked as function of intensity of choice $\beta$ and preference for buying $p_{\mathcal{B}}$.

**"Decisive" traders.** We first analyse the system of agents most commonly discussed in the previous chapter, these are the "decisive" traders $(p_{\mathcal{B}}^{(1)}, p_{\mathcal{B}}^{(2)}) = (0.8, 0.2)$, dubbed this way to distinguish from agents we will discuss later whose preferences for buying/selling are much milder. We continue the investigation on the set of two symmetrically biased markets $(\theta_1, \theta_2) = (0.3, 0.7)$. To illustrate previously described procedure of finding and categorizing population steady states, in Figure 3.9 we show series of diagrams in the space of order parameters $(D_1, D_2)$ for different $\beta$. In each diagram we mark the region of weak segregation and its subset, the strong segregation line, for both

subpopulations (blue for $p_{\mathcal{B}}^{(1)} = 0.8$ and orange for $p_{\mathcal{B}}^{(1)} = 0.2$), while we leave without colouring regions where the unsegregated state exists. On top of this, we add loci where $D'_m = D_m$ for $r = 0.001$. Intersections of the loci give us the population steady states at low but finite $r$. We expect those to move continuously when the $r \to 0$ limit is taken, thus from figures we can read the number and type of solutions and confirm them further by numerical methods in $r \to 0$ limit.

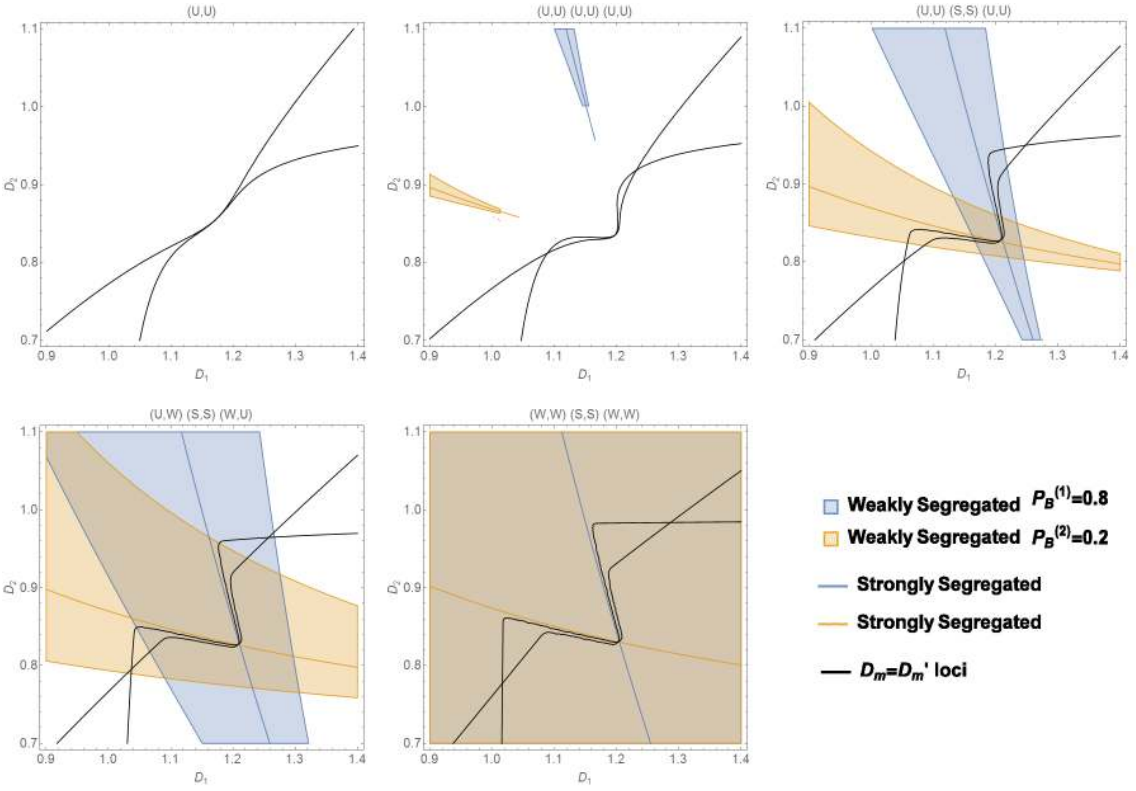


FIGURE 3.9: **Steady states of the decisive population –** $(p_{\mathcal{B}}^{(1)}, p_{\mathcal{B}}^{(2)}) = (0.8, 0.2)$ **– for different** $\beta$ **in the** $r \to 0$ **limit.** Top Row: Left - $1/\beta = 0.31$ (U,U) solution; Middle - $1/\beta = 0.29$ three (U,U) solutions; Right - $1/\beta = 0.265$ (U,U), (S,S), (U,U) solutions. Bottom Row: Left $1/\beta = 0.245$, (U,W), (S,S), (W,U); Right $1/\beta = 0.2$, (W,W), (S,S), (W,W). U - unsegregated; W - weakly segregated; S - strongly segregated steady state.

In the first panel of Figure 3.9, we show the low $\beta$ regime ($\beta = 1/0.31$, just before the transition). We note that at this intensity of choice for all the market order parameters shown both subpopulations' steady states are unsegregated. There is a unique intersection of the $D'_m = D_m$ loci – there is only one population steady state and as it is in the domain of unsegregated solutions for both subpopulations the steady state is $(U, U)$.

The second panel shows just slightly increased intensity of choice ($1/\beta = 0.29$) where

the majority of order parameters are still in the unsegregated domain, but this time, there are three loci intersection, and all three $(U, U)$ states. The steady state which is a continuation of the low $\beta$ solution corresponds to mild preferences between the markets, thought asymmetric - buyers have a slight preference for market one, good for buyers and vice versa as explained in the previous chapter. The other two unsegregated solutions correspond to unimodal distributions, synchronisation at one of the two markets.

Increasing the $\beta$ even further we cross the segregation threshold ($1/\beta_c = 0.28$ for these parameters, as reported before, e.g. Fig. 2.8) and we can see in the third panel, that the continuation of the low $\beta$ steady state is now in the strongly segregated domain of both subpopulations, while previously found two unsegregated solutions remain unchanged. Important to note is that there is an intermediate $\beta$, just above $\beta_c$ when the fixed point is in the domain of weakly segregated solutions, thus the solution is $(W, W)$. That's not clearly visible in this visualisation and we will address the existence of these solutions when we put together all the steady state information in a joint phase diagram.

We note the growth of the weak segregation and strong segregation domains when $\beta$ is increased, thus in the last two diagrams, the two unsegregated solutions $(U, U)$ undergo transitions to $(U, W)$ and finally $(W, W)$ state. Although in the presented plots the initial pitchfork bifurcation from one to tree $(U, U)$ states suggests instability of the middle solution that will later become the segregated state, we should not make stability assumptions based on these diagrams. This is because the analysis presented always takes an assumption that the agent adapts to the fixed demand to supply order parameters. And although with this assumption we can find all the steady states, we can not assess their stability as in the real systems the order parameters are not slowly varied. Once we investigate the phase space and identify all the solutions, we will return to the investigation of dynamics in the finite $N$ systems to see which of these states are favoured by the simulated population.

**"Indecisive" traders.** As opposed to the previously studied agents who are more determined in their buy/sell role, in the next few paragraphs we present different steady states of a population consisting of two not so distinctive subgroups $(p_{\mathcal{B}}^{(1)}, p_{\mathcal{B}}^{(2)}) = (0.55, 0.45)$, keeping all other parameters (e.g. market biases) the same. The choice of subpopulations

with these buy/sell preferences is motivated by observed change in monotonicity of the critical intensity of choice e.g. Figure 2.10. Due to their mild buy/sell preferences we don't expect as strong preferences for markets that are better for buyers/sellers. These traders are not as strongly penalized if only a single subgroup populates a market, as still a large number of trades can be sustained. All this suggests that steady states might be different for the populations consisting of agents with milder buy/sell preferences. As for the previously presented case study population with $p_{\mathcal{B}}^{(1)} = 0.8$ we will show the sequence of steady states for different intensity of choice in the space of market order parameters noting the regions of weak and strong segregation.

FIGURE 3.10: **Steady state of the indecisive traders** $(p_{\mathcal{B}}^{(1)}, p_{\mathcal{B}}^{(2)}) = (0.55, 0.45)$ **for different intensities of choice** $\beta$ **in the large memory limit (**$r \to 0$**).** Top row: Left $1/\beta = 0.31$ the unsegregated state; Middle $1/\beta = 0.295$ unsegreaged $(U, U)$ and four partially segregated states $(U, S)$; Right $1/\beta = 0.28$ weakyly segregated $(W, W)$ and four partially segregated states $(W, S)$. Bottom row: Left $1/\beta = 0.1$ strongly segregated $(S, S)$ and two partially segregated statese $(W, S)$; Right: $1/\beta = 0.05$ strongly segregated $(S, S)$ and two weakly segregated states $(W, W)$. U - unsegregated; W - weakly segregated; S - strongly segregated steady state.

We observe several differences in the transitions compared to the decisive traders,

most notably the number of solutions. Although it is not precisely clear in Figure 3.10, we realise that crossing the segregation threshold (e.g. crossing the cyan line in Fig. 2.10) four new partially segregated states appear. (The central and right panel in the top row, besides the obvious intersection have 4 more solutions – the points where the two loci first meet; the line overlapping segments are spurious finite $r$ effect in this space of representation.)

Partially segregated we label states in which one subpopulation is strongly segregated (thus stay bimodal even at the $r \to 0$) while the other is unsegregated or weakly segregated, as both of these states are unimodal in the $r \to 0$ limit. A similar state we have seen in the systems with four agents where one of the fixed points was such that within one group agents had different market preferences (thus "segregated") while within the other the preference were the same. However, in the small system, this state was an unstable state, which is reasonable because the fourth agent who a had a higher preference for the opposite market had lower chances to trade, thus effectively decreasing the overall number of possible trades for the whole system. In the large population limit one segregated and one unsegregated population still leave many possibilities for trading. This is especially true in the systems with indecisive agents were roughly half of the subgroup would assume the role of buyers and the other half sellers.

When the intensity of choice is increased, the number of solutions is decreased, and one strongly segregated state appear. Only for very high intensities of choice, we note states in which both subgroups are weakly segregated as we have noted in the previously studied system. As in the previous system, we see that for high intensity of choice these two states represent synchronisation at a single market.

### Algorithmic remarks

The method of finding all solution by identifying loci of invariant market order parameters is the best way to exhaust market order parameter space and find all the solutions for the finite $r$. Identifying the position in the different domains we also fully characterize the solution at the finite $r$ and when it is small enough we can assume the type of solution will not change in the $r \to 0$ limit. However, this method is also numerically

very demanding, as for every point in the phase space we need to find a steady state distribution (its normalisation usually takes most of the processing time) and recalculate the corresponding order parameters. It is also the method for finite $r$ and we need to check how these solutions are corrected in the $r \to 0$ limit. To do so, we apply a few numerically less demanding routines described below.

**Population with homogeneous market preferences.** We have seen that for various system parameters population steady states are unimodal in the $r \to 0$ limit ("U" and "W" states). These states represent population with subgroups with homogeneous market preferences. This realisation offers a simple way to find all the states of this type for any system parameter. The demand to supply order parameters are simpler:

$$\begin{aligned} D_m &= \frac{p_{\mathcal{B}}^{(1)} \int d\Delta \sigma_\beta(m\Delta) P(\Delta|p_{\mathcal{B}}^{(1)}) + p_{\mathcal{B}}^{(2)} \int d\Delta \sigma_\beta(m\Delta) P(\Delta|p_{\mathcal{B}}^{(2)})}{(1-p_{\mathcal{B}}^{(1)}) \int d\Delta \sigma_\beta(m\Delta) P(\Delta|p_{\mathcal{B}}^{(1)}) + (1-p_{\mathcal{B}}^{(2)}) \int d\Delta \sigma_\beta(m\Delta) P(\Delta|p_{\mathcal{B}}^{(2)})} \\ &= \frac{p_{\mathcal{B}}^{(1)} \sigma_\beta(m\Delta^{(1)}) + p_{\mathcal{B}}^{(2)} \sigma_\beta(m\Delta^{(2)})}{(1-p_{\mathcal{B}}^{(1)}) \sigma_\beta(m\Delta^{(1)}) + (1-p_{\mathcal{B}}^{(2)}) \sigma_\beta(m\Delta^{(2)})} , \end{aligned} \tag{3.16}$$

where in the second row we have used $\langle \sigma_\beta(\Delta) \rangle = \sigma_\beta(\langle \Delta \rangle)$, a relation that is exact in the $r \to 0$ limit where the steady state distribution is a delta distribution centred at $\Delta^{(g)}$ (the solution of $M_1(\Delta|p_{\mathcal{B}}) = 0$). With this simplification, to identify the peak positions of such distributions, we find zeros of the first jump moment $M_1$ is as defined in Eq. (3.9), but now we are taking into account $D_m$ dependence on the population attraction differences $\Delta^{(g)}$. This means that when searching for the steady state in which both subpopulations of traders have homogeneous market preferences, we need to solve equations for the two populations simultaneously:

$$\begin{aligned} M_1^{(1)}(\Delta^{(1)}|p_{\mathcal{B}}^{(1)}, D_m(\Delta^{(1)}, \Delta^{(2)})) &= 0 , \\ M_1^{(2)}(\Delta^{(2)}|p_{\mathcal{B}}^{(2)}, D_m(\Delta^{(1)}, \Delta^{(2)})) &= 0 . \end{aligned} \tag{3.17}$$

Every solution pair found this way needs to be checked for consistency with our initial assumption - homogeneous market preferences, i.e. market order parameters corresponding to every solution pair need to belong to the unsegregated or weakly segregated

solution domain. For every given fixed point $(\Delta^{(1)*}, \Delta^{(2)*})$ of the Eq. (3.17) we can calculate order parameters $D_m$ Eq. (3.16) and find the "free energy" corresponding to these order parameters. If the free energy minimum (global when it has two) is centred at $\Delta^{(g)*}$ the solution is consistent with initial assumption and we have found a population's steady state. Depending on the signs of $\Delta^*$ we classify these further as either *synchronized* $\Delta^{(1)*}\Delta^{(2)*} > 0$ or *asynchronized* $\Delta^{(1)*}\Delta^{(2)*} < 0$. For any finite intensity of choice $\beta$, a single agent can chose another market even if the state is categorized as synchronized at market 1, but the categorization is exact for the $\beta \to \infty$ limit.

Solving Eqs. (3.17) correspond to some population level optimisation as both order parameters, and population preferences (which are the same for all agents within it) are changing. Had we only solved the equations and assessed the stability of the fixed points by using general linear stability methods (e.g. finding the Jacobian at the fixed point $(\Delta^{(1)*}\Delta^{(2)*})$) we would realize that at the $1/\beta = 0.29$ depicted in the middle panel of the top row in Figure 3.9 corresponds to two stable (synchronized at different markets) and an unstable fixed point (continuation of the low $\beta$ solution). On the other hand, assessing every of these order parameters from single agent's perspective (e.g. finding the free energy) we find that all three solutions are such that the free energy has a unique minimum, i.e. stable. This discrepancy illustrates well the difference between the "population" and "single agent's" approach. In the first, the assumption made is that the population acts as whole trying to find a fixed point optimising the market preferences and trading probabilities. The second approach, of a single agent, makes no assumption on the ability to change global order parameters, but we investigate whether at the global parameters being fixed an agent has an incentive to move or not.

In the second case study, the continuation of the low $\beta$ fixed point is a solution we can consistently find by this method for a wide range of intensities of choice, much wider than when the subpopulations have more pronounced buy/sell preferences. This is due to the previously stated observation that these agents are not penalised when they recognise the market that slightly more awards them, i.e. even if the subpopulations are asynchronized a large number of trades can occur. We also find that the population fixed

point (solution of the 3.17 equations) undergoes first order transition for these parameters which might be a reason for the change in monotonicity of the critical intensity of choice reported in Figure 2.10. Beside the fixed point that is a continuation from the low $\beta$, all new fixed points are inconsistent with the homogeneous population assumption until very high intensities of choice. This is why we need to employ different techniques to find the other solutions presented in Figure 3.10. Only when the intensity of choice is increased further, partially segregated states cease to exist, and solutions consistent with the homogeneous population assumption arise.

**Strongly co-segregated state (S,S).** To find if these states exist we apply a procedure based on Maxwell construction argument outlned for a single subgroup population. For each subpopulation we define a locus in the space of order parameters $(D_1, D_2)$ for which the strong segregation condition Eq.(3.8) is satisfied. If there is an intersection $(D_1^*, D_2^*)$ between the two loci there are market demand-to-supply ratios in which both subpopulations favour strongly segregated state. We finally need to confirm that the two order parameters can be created if only the two segregated subpopulations trade on the markets. If we assume the strongly segregated distributions are of this form:

$$P(\Delta|p_{\mathcal{B}}^{(g)}) = \omega^{(g)}\delta(\Delta - \Delta_1^{(g)}) + (1-\omega^{(g)})\delta(\Delta - \Delta_2^{(g)})$$

and assuming $\Delta_1^{(g)} > 0$, the order parameters that correspond to these distributions are:

$$D_m = \frac{N_{\mathcal{B}m}}{N_{\mathcal{S}m}}$$

$$D_m = \frac{p_{\mathcal{B}}^{(1)}(\omega^{(1)}\sigma_\beta(m\Delta_1^{(1)}) + (1-\omega^{(1)})\sigma_\beta(m\Delta_2^{(1)})) + p_{\mathcal{B}}^{(2)}(\omega^{(2)}\sigma_\beta(m\Delta_1^{(2)}) + (1-\omega^{(2)})\sigma_\beta(m\Delta_2^{(2)}))}{(1-p_{\mathcal{B}}^{(1)})(\omega^{(1)}\sigma_\beta(m\Delta_1^{(1)}) + (1-\omega^{(1)})\sigma_\beta(m\Delta_2^{(1)})) + (1-p_{\mathcal{B}}^{(2)})(\omega^{(2)}\sigma_\beta(m\Delta_1^{(2)}) + (1-\omega^{(2)})\sigma_\beta(m\Delta_2^{(2)}))} \tag{3.18}$$

If there are weights $\omega^{(g)} \in [0,1]$ corresponding to the intersection point $(D_1^*, D_2^*)$ the strongly segregated state exists. These states leave both markets equally active and as we will show in the discussion below, they entail benefits for the population as a whole, not

favouring any of the symmetric subpopulations.

**Partially segregated states.** Finally, we outline a procedure to find a population steady state that is a combination of bimodal (S) and unimodal (U or W) state in the $r \to 0$ limit. A starting point for this search can be obtained by solving two homogeneous population equations (3.17). When one of the subpopulations is consistent with the homogeneous population assumption, while the other is not, we can investigate whether the strongly segregated solution for the other population exists. To find these states, we assume that the subpopulation which is inconsistent with a given homogeneous population solution is in the segregated state. Thus possible order parameters for this state are on the locus as defined by the Maxwell construction. For every pair $(D_1, D_2)$ from the segregated state locus we investigate the "free energy" of the second subpopulation (whether it is unsegregated or weakly segregated). We find the peak position and model it as a unimodal distribution centred at (global) minima. We only need to examine whether by peak weight redistribution of the strongly segregated subpopulation we can retrieve the initial order parameters $(D_1, D_2)$. When this is possible, the partially segregated state exists. In the example we show in Figure 3.10, due to mild buy/sell preferences, when one of the subpopulations is segregated there are two unsegregated options for the second subpopulation - specialisation to any of the two markets.

$(\beta, p_{\mathcal{B}})$ **Phase Diagram.** Observing a variety of possible steady states for different choices of system parameters we realise we need a detailed phase diagram to investigate domains of existence of the previously described states. We also want to examine which of our case studies is a more typical scenario, if there are more atypical situations, etc. We continue the investigation on the symmetric markets $(\theta_1, \theta_2) = (0.3, 0.7)$, but the observations we make are general for symmetric markets. In Figure 3.11 we show phase diagram in the space of intensity of choice $\beta$ and subpopulation preference for buying $p_{\mathcal{B}}$. This diagram is the large population limit version of the diagram shown in Fig. 3.5 where for the system with only four players we have identified regions with states resembling unsegregated indecisive state (low $\beta$), unsegregated synchronised states, segregated and partially segregated states. Phenomenologically, these types of states persist in the large

population limit, but they have additional structure. Thus the new diagram looks more complicated.

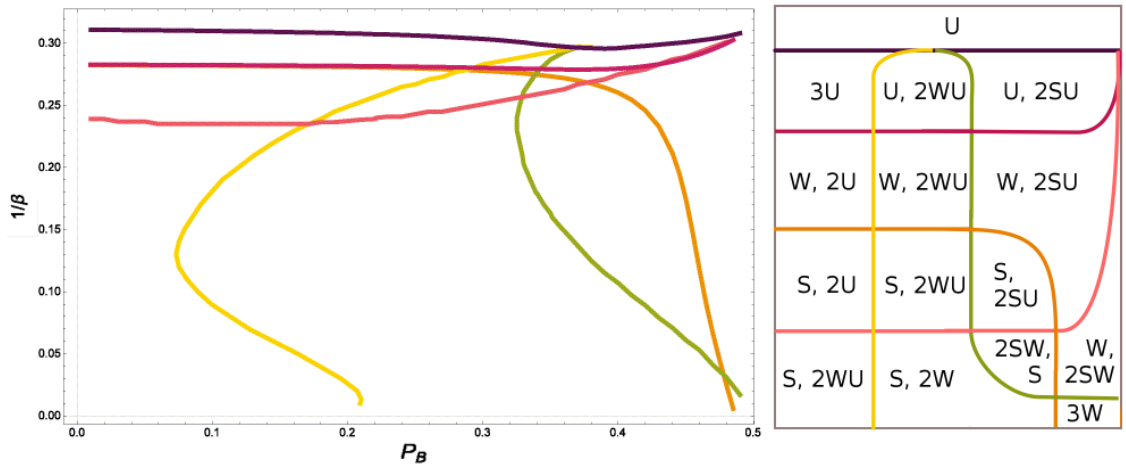


FIGURE 3.11: **Types of steady states of 2 symmetric subpopulation system in $(\beta, p_B)$ space.** Left: Critical lines in the $(\beta, p_B)$ space. Crossing each of the lines changes either number or the type of the steady states. Right: Topologically stretched equivalent diagram to aid phase space understanding. Dark Violet - change in solution multiplicity; Purple and Orange line mark changes in the low $\beta$ fixed point $U \to W$ purple, and $W \to S$ orange; Pink, Yellow and Green mark changes in the other two fixed points, crossing yellow and pink denotes $U \to W$ transition in one of the subpopulation's states, while green demarcates partially segregated states - crossing it one of the subpopulation's states transitions $W \to S$. U - unsegregated; W - weakly segregated; S - strongly segregated steady state.

To help perception and understanding of the diagram, besides the critical lines in the metric $(\beta, p_B)$ space (left panel) we show deformed diagram for clearer visibility and phase notation (the two panels are topologically equivalent). We also simplify the state notation: two subgroups in the same state we denote with only one letter (e.g. (U,U) becomes U); multiple population state which are the same we mark with a number in front (e.g. (U,W) and (W,U) we mark with 2WU). Crossing any line in the phase diagram either changes the number of population solutions or the nature of previously existing states. We note that due to the system's symmetry many of the changes for the two subpopulations happen simultaneously. The dark violet line is the line where the multiplicity of the states changes. This line is an analogue of the same coloured line in the phase diagram (Fig. 3.5) of the system with $N = 4$ players. The region of multiple solutions increased for large $N$, and the monotonicity of the critical intensity of choice $\beta_c$ has changed. While

$\beta_c$ was an increasing function of $p_{\mathcal{B}}$ in the 4-player system, now it is a slowly increasing function only up to some $p_{\mathcal{B}}$ when the monotonicity changes. Dark purple and orange lines mark transitions in the state corresponding to the continuation of the unique low $\beta$ fixed point, while yellow, green and pink line mark changes in the two new fixed points that correspond to "synchronisation" at a single market.

The dark purple line is the line below which the continuation of the low $\beta$ fixed point becomes weakly segregated. This line was reported in Figure 2.10 where we investigated when the segregation happens if the intensity of choice is gradually increased. In such setup, an agent does not have an incentive to deviate from the low $\beta$ fixed point until a possibility for segregation emerges. With the orange line, we mark critical intensities of choice when the same fixed point becomes strongly segregated. We note that for the system of our first case study $p_{\mathcal{B}} = 0.8$ the two lines (dark purple and orange) almost overlap - the region of the weakly segregated indecisive state is very narrow for this choice of parameters and in general for $p_{\mathcal{B}} \leq 0.3$. As previously argued, when preferences for buying/selling are milder the low $\beta$ fixed point corresponding to "recognition" of the good market, although leading to synchronisation remains weakly segregated (thus consistent with homogeneous in the $r \to 0$ limit) in increasing region of $\beta$ when $p_{\mathcal{B}}$ increases.

Other lines (light pink, yellow and green) mark changes in the type of so-called "synchronised" state. Crossing the pink and yellow lines, one of the subpopulations change the state from unsegregated to weakly segregated. Similarly, crossing the green line changes the subpopulation's state from weakly to strongly segregated one. Thus the green line demarcates region to the right of which partially segregated states (bimodal + unimodal distribution at the $r \to 0$ limit) exist. We note that the partially segregated states are not only property of the system with subpopulations with $p_{\mathcal{B}} = 0.55$, but the property is shared within a broader region. We realise that the shape of partial segregation line remained the one we have observed in the small sized system though it expanded. We conjecture that it is due to this region's expansion that the monotonicity of the segregation threshold line changes, as for the system with moderate buy/sell preferences we see that when crossing the dark violet line (an increase of multiplicity) it is the partially segregated states that occur first. Finally, in the small system, we realised

that partially segregated fixed points are unstable. However here we realised that the partially segregated solutions appear in pairs thus it is unlikely that when the two new fixed points appear both of them are unstable. As before, we note that stability needs to be assessed taking into account the simulated dynamics, and we defer the discussion to later sections.

We have identified all the lines presented in Fig. 3.11 by varying smoothly $p_{\mathcal{B}}$ for the fixed intensity of choice and by tracking each of the three solution types we previously discussed - synchronised at market one or two and the continuation of low $\beta$ solution. We do solution tracking as it is numerically faster and more reliable than the finite $r$ procedure (note the noisiness in the two loci in Fig. 3.10). However, when discussing the system with indecisive subpopulations, e.g. Figure 3.10, we noted region of intensity of choice $\beta$ with five steady state solutions.

By returning to the finite $r$ procedure we find partially segregated states and for a fixed moderate $p_{\mathcal{B}}$ we find five solutions. For fixed $\beta_s$ we believe the five solution boundary is defined by the $\max\{p_{\mathcal{B}}^{orange}, p_{\mathcal{B}}^{green}\}$, as our numerical exploration of the greater $p_{\mathcal{B}}$ in the vicinity of these lines always reveal five steady states. We expect that crossing the transition line(s) in the phase diagram should change either number of states or their nature (not both). Consequently, we conjecture that the five solution region line closely follows a combination of the orange and green line (as described before), but that a separate three solution region exist. The three solution region might be too narrow which would explain why we cannot distinguish the two in numerical explorations. We defer further discussion on the five solutions to some future publications. Here, we only explain observed transition sequence that the low $\beta$ solution follows (when the $\beta$ is increased): $UU \rightarrow UU + 4US$ (two symmetric saddle-node bifurcations) $\rightarrow SS + 2VS$ (pitchfork bifurcation on the symmetry line, where also with $V$ denoted an unimodal solution either $U$ of $W$ depending on $p_{\mathcal{B}}$ value).

### Average Population Returns

We have shown in the previous chapter that multiple steady states exist for a range of forgetting rates $r$ not only in the $r \to 0$ limit (see e.g. Fig 2.13, but also in this chapter: Fig. 3.9 where the loci intersections represent $r = 0.001$ solutions). Properties of the strongly segregated states, such as the Binder cumulant and average population returns for finite $r$ were addressed in the previous chapter, while now we address similar properties of the other types of states in both finite $r$ and the $r \to 0$ limit. We will conclude this chapter returning to the finite $N$ numerical simulations to investigate under which circumstances other types of segregated states occur.

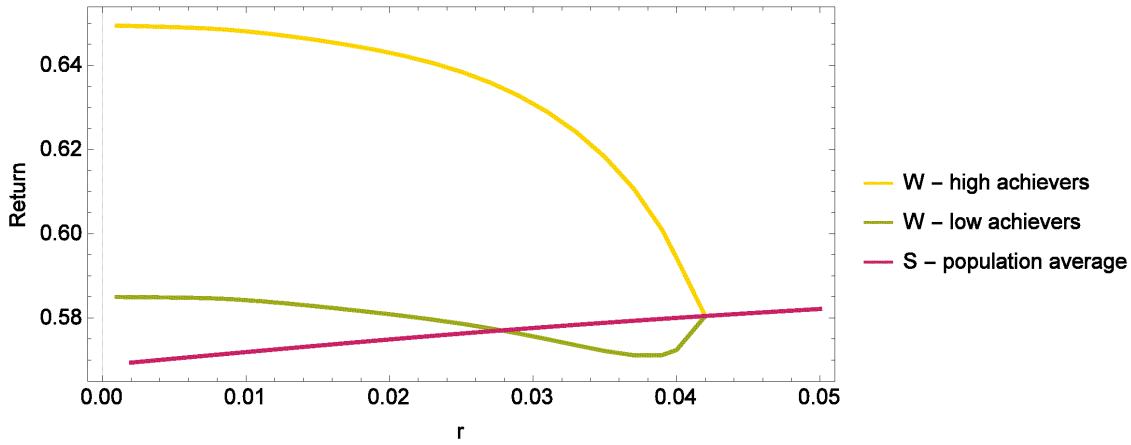


FIGURE 3.12: **Average returns of different steady states as function of forgetting rate $r$.** Intensity of choice $\beta = 5$. We note that average return of the strongly segregated state decays with $r$ thus appearance of weakly segregated states offer a higher population average return. The two subpopulations in the weakly segregated state have different average returns, one always earns more (e.g. buyers at market good for buyers) thus we call them high/low achievers.

In Figure 3.12 we show how average returns change as a function of the forgetting rate $r$ at the fixed intensity of choice $\beta = 5$ (for this set of parameters $\beta = 5 > \beta_s$ for all $r$). Already in Figure 2.9 we have seen that the average population return of the strongly segregated state decreases with $r$ when comparing a few values. Looking at a wider range of $r$ we now note that the strongly segregated state return is a decreasing function. The appearance of another solution type offers higher population average. Two weakly segregated states are symmetric, thus we show results for only one of them. In each weakly segregated state, the majority of both subpopulations develop a strong preference

for the same market. Consequently, there is a subpopulation that is satisfied with the choice, e.g. buyers settling for market good for buyers, we name them high achievers, and a subpopulation that earns less – low achievers. We note that below some forgetting rate even the low achieving traders earn more at the weakly segregated state.

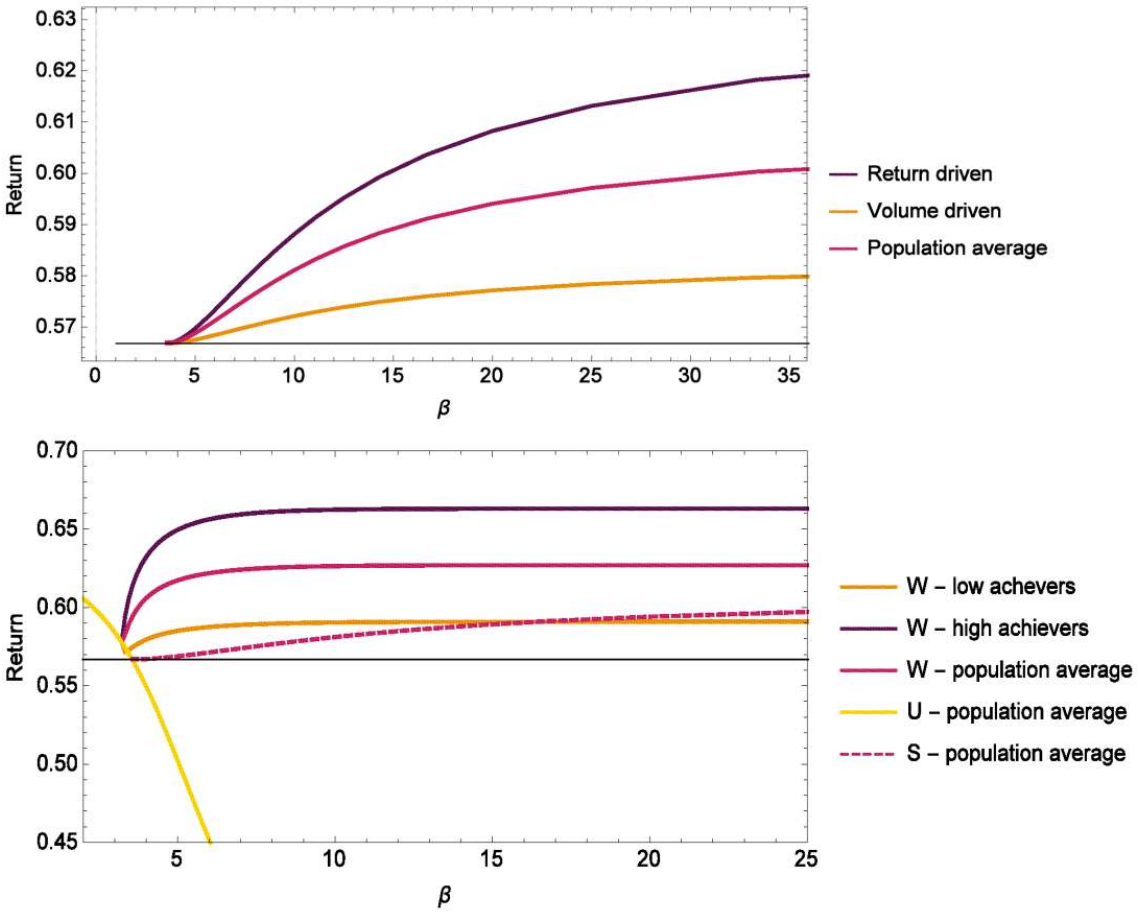


FIGURE 3.13: **Decisive agents' returns for different steady states in the $r \to 0$ limit.** Top: Strongly Segregated state (S) - returns of the segregated subgroups, return driven and volume driven agents compared to the envy free Nash equilibrium (grey line). Bottom: Comparison of different $r \to 0$ states' returns. Unimodal states *synchronisation at a single market* is shown with dark violet (high achieving subpopulation), purple (average) and orange lines (low achieving subpopulation). Its returns are compared against strongly segregated population average (dashed purple) and low $\beta$ unsegregated state's average (yellow).

We now focus on the $r \to 0$ limit. First, in this limit, we can find out more about the strongly segregated state returns as the two groups in the population are now fully specialised into return driven and volume driven traders (i.e. the peaks are well separated). Consequently, we can correctly assess benefits of the segregation for every subgroup. We

kept the same baseline comparison - the envy-free Nash Equilibrium. In the top panel of Figure 3.13, we note that both return driven and volume driven traders earn more than at the envy-free Nash Equilibrium for all $\beta > \beta_s$. Previously we remarked that the population average (also single agent long time average) is higher in the strongly segregated state compared to unsegregated alternatives at finite $r$. Now, we show that both subgroups are better off even at short time scales.

In the bottom panel of Figure 3.13 we investigate the new steady states' returns and compare them to the previously studied ones. In the $r \to 0$ limit, $U$, $UW$ and $W$ states are all the same as in the limit they are all unimodal, delta peaked distributions synchronised at one of the markets. We plot the two subgroups average returns along with the strongly segregated state average and the unsegregated low $\beta$ state average. We note that unimodal states appear at lower $\beta$ (compared to the strongly segregated state), as reported in Fig. 3.9. The returns of the high achieving group and the population average are substantially higher than at the strongly segregated state. However, the population average of the weakly segregated state does not have an interpretation of the single agent's average as it is the case with the strongly segregated state. Once distinguished into the high achievers and low achievers, the two subpopulations always have a different return. Although we can argue that on the level of population average that is a better state, there is no agent who's average return correspond to the population's average.

The average population return in the high $\beta$ limit of the unsegregated state, when all players synchronize at the same market, also corresponds to the average population return when all traders choose random (e.g. $\beta = 0$). This is true because when all traders choose randomly, on average number of agents taking each action is equal, which is also the case when all agents are synchronized at the same market. Intriguingly, this means that when learning is introduced, for small intensities of choice, an agent who takes decisions based on previous history is worse than an agent who plays at random. This is only changed in the large $\beta$ limit of the weakly segregated state where the population average return again reaches the value random trader was obtaining. It is important to note that as opposed to the randomly trading population in the large $\beta$ limit of the weakly segregated state one subpopulation earns more than the other as shown in the lower panel of

Fig. 3.13. As indicated in the same panel, population average in the strongly segregated state does not reach the population average of the randomly trading population. Despite indications that for a given $\beta$ strongly segregated state is the best among the states that do not distinguish between subpopulations in the long run, in terms of average population return this state is outperformed by $\beta = 0$ – the population of traders who do not learn but play at random.

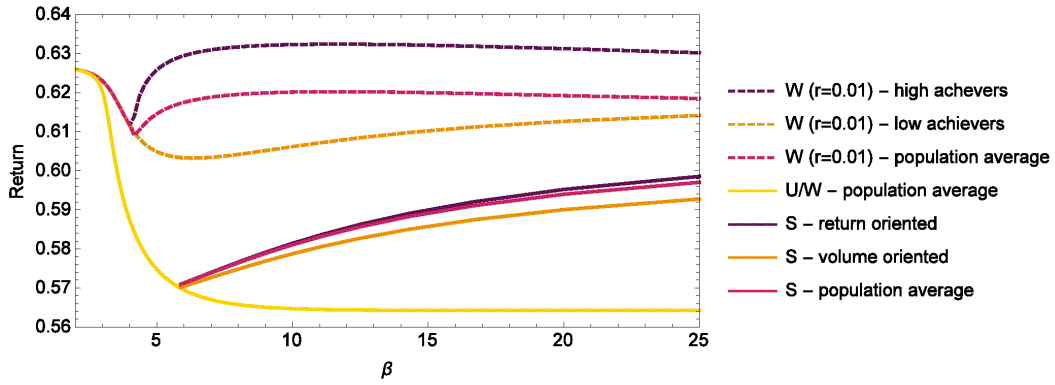


FIGURE 3.14: **Indecisive agents' returns for different steady states** $(p_{\mathcal{B}}^{(1)}, p_{\mathcal{B}}^{(2)}) = (0.55, 0.45)$**.** The dashed lines represent $r = 0.01$ steady state whose limit is a partially segregated state for the $r \to 0$. We compare this state's subgroup's returns with the low $\beta$ state average (that persists population's unsegregated solution for larger intensities of choice) and the strongly segregated state (solid lines).

Finally, we address the returns in the population of indecisive traders $p_{\mathcal{B}} = 0.55$. We omit to plot an analogue of Fig. 3.12, as the qualitative behaviour is identical with one quantitative difference - forgetting rate at which new states appear is lower. This trend is consistently shown across all $\beta$, so the region of multiple segregated states in $(\beta, r)$ space shrinks with $p_{\mathcal{B}}$[1].

Instead, in Figure 3.14 we compare returns of different steady state types as a function of the intensity of choice $\beta$. As previously, one benchmark value is the return of the low $\beta$ fixed points (marked in yellow). Its value quickly decays with the increase of $\beta$ and consistently with previous observation, at some $\beta_s$ the strongly segregated state is a better alternative. We also plot returns of steady states for the $r = 0.01$ as it is a state that

[1]The maximum value of $r$ for which three segregated states exist is $r = 0.002$, compared to $r = 0.0055$ reported for the $p_{\mathcal{B}} = 0.8$

in the $r \to 0$ limit converges to a partially segregated state. We note as previously shown in the phase diagram that the partially segregated states appear first (when $\beta$ is gradually increased). Despite the finite $r$ we expect continuous change to the $r \to 0$ limit, so the finite $r$ can serve as an estimator of the partially segregated state's properties. We note that the average returns in the finite $r$ partially segregated states are much higher than at other states, but also we note that the difference between the two types – high achievers and low achievers decreases with $r$ that is a phenomenology unseen in the "decisive" population.

### 3.3.1 Dynamics

In our initial investigation of the evolution of preferences in the numerically simulated system with a finite number of agents $N$, we focused our attention on high values of the forgetting rate $r$ (e.g. $r = 0.1$ as in Chapter 2). This is because for large $r$ agent's relaxation times are shorter and consequently, we can more easily study patterns in agents' persistence. On the other hand, our analytical investigation of the $r \to 0$ limit showed a variety of possible states above the segregation threshold $\beta_s$ beside the strongly segregated state that was primary focus of the research presented so far. Also in the range of finite $r$, more than one steady state exist (e.g. see the $(r, \beta)$ phase diagram Fig. 2.13), with $r_c$ dependent on system parameters. But so far the forgetting rate we have mostly analysed was in the regime where the strongly segregated state is unique steady state above the $\beta_s$ threshold (e.g. Fig. 2.7 and Figs. 2.8, 2.9). This still leaves the question of existence and stability of other types of states - weakly segregated and partially segregated ones – in numerical simulations of populations with finite $N$ and $r$. Our analysis may suggest that the strongly segregated state becomes unstable when the two weakly segregated states appear, see e.g. Figure 3.9 for $p_{\mathcal{B}} = 0.8$ where in the market order parameter diagram it looks as if the strongly segregated solution undergoes pitchfork bifurcation, leaving the low $\beta$ solution unstable. This might not be the case because when searching for steady states using the Fokker-Planck routine we have made an assumption that the adaptation happens adiabatically, i.e. an agent equilibrate in the fixed market order parameters. This is not true in the simulated system where all agents make simultaneous

market decisions based on his/her past thus adapting to abruptly changing market order parameters. That is why we devote the following section to investigations of the strongly segregated state stability in the numerical simulations.

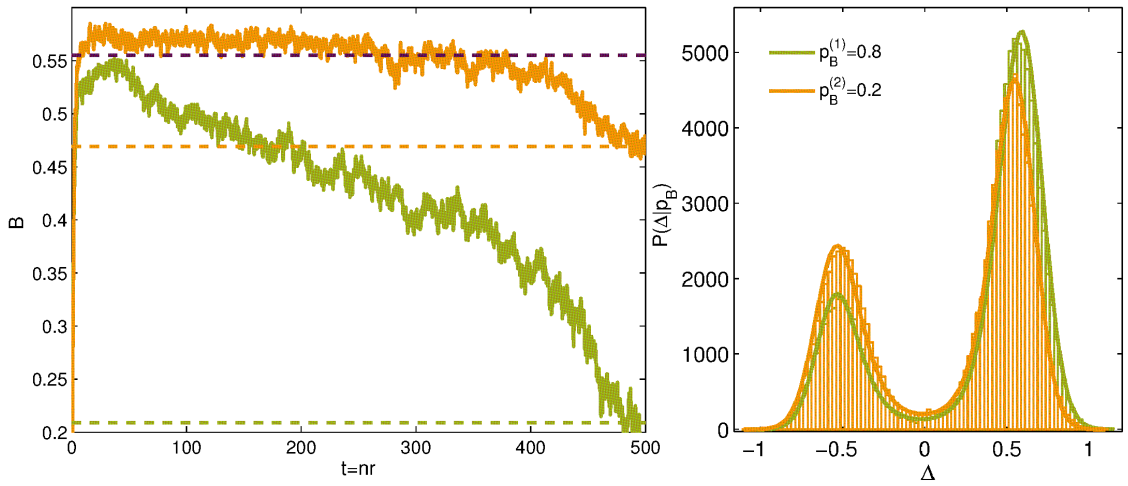


FIGURE 3.15: **Instability of the strongly segregated state and decay to a weakly segregated state.** System parameters: agent's learning $(r, 1/\beta) = (0.05, 0.16)$, preferences for buying $(p_{\mathcal{B}}^{(1)}, p_{\mathcal{B}}^{(2)}) = (0.8, 0.2)$, markets' biases $(\theta_1, \theta_2) = (0.3, 0.7)$, system size $N = 2000$. Left: Evolution of subpopulations' attraction distributions shown with the Binder cumulant time series of a single simulation run - subpopulation of buyers (green), sellers (orange). Dashed lines are theoretical predictions at the strongly segregated state (dark violet) and weakly segregated states (green and orange for the two subpopulations). Right: Weakly segregated steady state distribution of attraction differences from theory (solid line) and simulation (histogram).

In Figure 3.15 we show a single run example of the process of adaptation in a system with $N = 2000$ traders (more details on numerical simulations are in Appendix D). The parameters of agent's learning mechanism are $(r, 1/\beta) = (0.05, 0.16)$, while the buy sell preference and the market parameters are as usually $(p_{\mathcal{B}}^{(1)}, p_{\mathcal{B}}^{(2)}) = (0.8, 0.2)$ and $(\theta_1, \theta_2) = (0.3, 0.7)$. For these parameters the phase diagram presented in Figure 3.11 predicts the existence of tree steady states, two weakly segregated states (with the majority of both subgroups synchronised at the same market, $m = -1$ or $m = 1$) and previously presented strongly segregated state Fig. 2.7. We demonstrate changes in the system with plots of Binder cumulant time series. It is chosen as an observable (defined as in Eq. (2.3) and discussed in more details in Appendix B) because it summarises information about

the distribution's shape and thus helps us track system's evolution over time. In Figure 3.15, beside values of the simulated distribution's Binder cumulants, for the two subpopulations we mark the baseline values from Fokker-Planck analysis for the strongly segregated state (dashed dark violet line) and the weakly segregated states (orange and green dashed lines for the two subpopulations as in the weakly segregated state the distributions are not symmetric). We observe that the system quickly reaches the strongly segregated state (the discrepancy between the expected and observed value can be attributed to the finite $N$). After some time at the symmetrically beneficial strongly segregated state, one of the subpopulations initiates departure to one of the weakly segregated states. We note in Figure 3.15 that the final Binder cumulants of the two subpopulations correspond to the theoretical predictions for the weakly segregated state. On the right panel of the same figure, we show a comparison between the theoretical and simulated distributions of agents' attraction differences. We confirm previously documented good agreement between theory and numerics for the weakly segregated states as well.

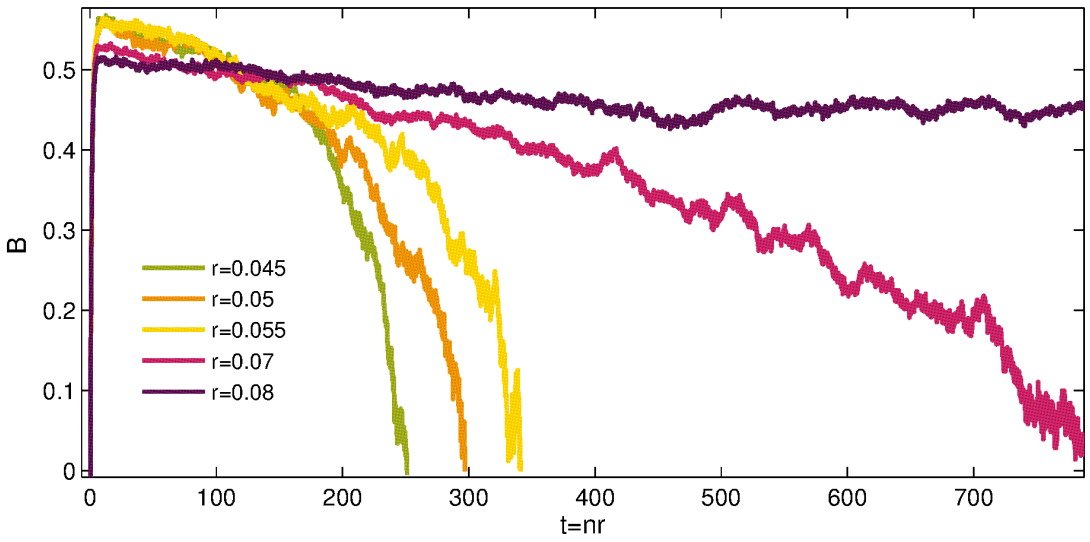


FIGURE 3.16: **Binder cumulant time series for different forgetting rates $r$ at the fixed intensity of choice $1/\beta = 0.15$.** System parameters as previously except for the size $N = 200$. We note strongly segregated state lifetime increases with $r$ corresponding to theoretical prediction that there is a critical $r$ above which the lifetime of the strongly segregated state is infinite. Theoretical prediction obtained in the large $N$ limit suggests $r_c = 0.055$, while numerics suggests a finite $N$ correction to this value.

After initial demonstration of the existence of the weakly segregated states in the finite $N$ simulations, we proceed with more detailed studies of the strongly segregated state's lifetime. We investigate different values of learning parameters $r$ but also system sizes averaged over multiple simulation runs. These experiments show that within the learning parameters region documented in Fig. 2.13 the strongly segregated state is metastable but long-lived.

In Figure 3.16 we show average Binder cumulants for the small system $N = 200$ for different $r$ values and fixed $1/\beta = 0.15$ to investigate the threshold value of $r$ for finite $N$. It is important to note that the noisiness of the Binder cumulant (although it is averaged over multiple runs, here 10 and two subpopulations) is due to the random fluctuations that drive different subpopulations away from the strongly segregated state at a different pace and different strengths. First, we note that for all values of $r$, we observe quick initial convergence to the strongly segregated state which has different Binder cumulant values for different $r$. This has been noted previously, as the distribution width is $r$ dependent, larger $r$ leads to smaller values of Binder cumulants (e.g. Fig. 2.8). We note that the state lifetime is increasing with $r$ that is consistent with previous observation that above some $\beta$ dependent threshold $r$ value, the strongly segregated state is unique, thus having an infinite lifetime. Interestingly, for this $\beta = 1/0.15$, theory predicts threshold $r$ to be $0.055$, but we note the strongly segregated state lifetime is finite even for $r = 0.07$, we do not observe decay from the strongly segregated state only for $r = 0.08$. This should be attributed to the finite $N$ correction to our theory that is derived for the $N \to \infty$. It is important to note that we average the Binder cumulants across multiple runs and over the two subpopulations. Even though we have previously seen that the two subpopulations Binder cumulants converge to different final values in the weakly segregated state and at different pace, the subgroup Binder cumulant at the strongly segregated state is the same and as our goal is to measure when at least one of the subpopulations start converging to another value thus effectively leading to decay of the strongly segregated state, averaging over the two gives us a good estimate of the state's lifetime.

To put the lifetime of the strongly segregated state into a perspective, we compare it with the single agent's relaxation time (right panel of Figure 3.17). We have previously

shown that when the system reaches the strongly segregated state relaxation time of an agent become very long (Fig. 2.6) thus it is interesting to understand whether the state's lifetime is comparable with that a single agent's persistence and also how different system parameters such as size influence it. On the right panel of Figure 3.17, we note that the single agent's relaxation time when $r = 0.05$ is $t = 100$, measured in time steps of agent's memory length $1/r$ (relaxation time is estimated as the time at which correlation decays below $e$ times compared to its initial value). With this information, we observe that the orange line in Figure 3.16, corresponding to the same forgetting rate $r = 0.05$, shows that the state lifetime is larger than the agents' relaxation time. Further as we noted that the state lifetime decays for the smaller $r$, but we also know that the agent's relaxation time increases with $r$, thus in the small $r$ limit we expect the strongly segregated state lifetime to be only the time an agent needs to explore all options, i.e. its relaxation time.

To investigate the effects of the system size in Figure 3.17 we show Binder cumulant time series for different system sizes at the fixed learning parameters $(r, 1/\beta) = (0.05, 0.15)$. We note that increasing the system's size the lifetime of the strongly segregated state increases. On the other hand, single agent's relaxation time showed for the purpose of comparison on the right panel of the same figure is not affected by the system size, as expected. This effectively shows us that in the parameter regions where the weakly segregated state exists, although the strongly segregated state is unstable, a large population will be strongly segregated for a very long time.

In principle, we can also analyse the Fokker-Planck equation by methods of linear stability analysis and determine the state's stability by analysing Jacobian eigenvalues. This procedure is outlined in Appendix E as due to numerical difficulties it does seem to work well only for very low forgetting rate $r$, while we cannot fully reproduce the critical $r$ value with it.

**Initial conditions.** In all of our previous numerical exploration we have always used $P(\Delta|p_{\mathcal{B}}) = \delta(\Delta)$ for the initial conditions, i.e. we assumed agents do not have any initial preferences for the markets, they all start with a blank sheet and adapt based on their

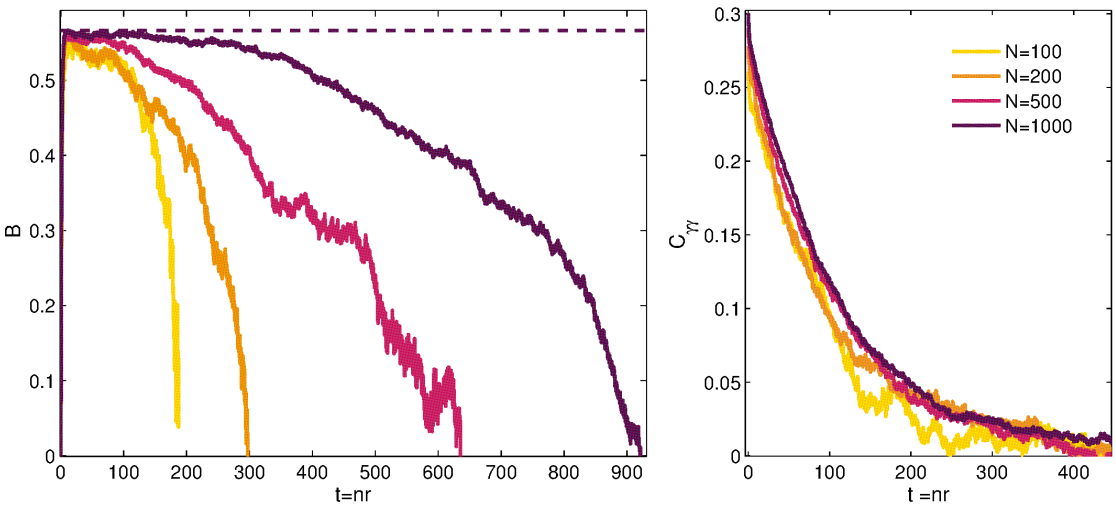


FIGURE 3.17: **Strongly segregated lifetime for different system sizes $N$.** Left: Binder cumulant time series along with the $N \to \infty$ strongly segregated state theoretical prediction (dashed line). Right: Agent's autocovariance function $C = \langle(\Delta^i - \overline{\Delta})(\Delta^i - \overline{\Delta})\rangle_{P(\Delta)}$. As expected single agent's relaxation time (time at which covariance decays $e$ times its original value) is not dependent on system size $N$, though the state lifetime that we can estimate from the left panel increases with $N$.

trials and errors. In general, this is a reasonable starting assumption, and for system parameters where the steady state is unique, the initial conditions do not matter anyway. However, in the parameter region where multiple states exist, our investigation suggests that the strongly segregated state is metastable, and it seems that the neutral initial conditions we have used for simulations lie on a stable direction. This conclusion is backed by the observation that there always exists initial convergence towards the strongly segregated state from which the system departs in the presence of random fluctuations. As these are smaller for large systems, the strongly segregated state, although metastable, persists for a long time, as we have observed in Figure 3.17.

To conclude this analysis, we investigate for which initial conditions the metastable state will be reached. The learning parameters are $(r, 1/\beta) = (0.05, 0.15)$, in the region where we expect existence of three different steady states. We now assume that initial attraction differences are normally distributed in the population, i.e. $P(\Delta|p_{\mathcal{B}}) = \mathcal{N}(\mu, \sigma^2)$ and we vary both the mean $\mu$ and the standard deviation $\sigma$. When $\mu = 0$, we note that independent on the width of the distribution the initial decay to the strongly segregated state always exist and the state lifetime is not affected by initial distribution standard

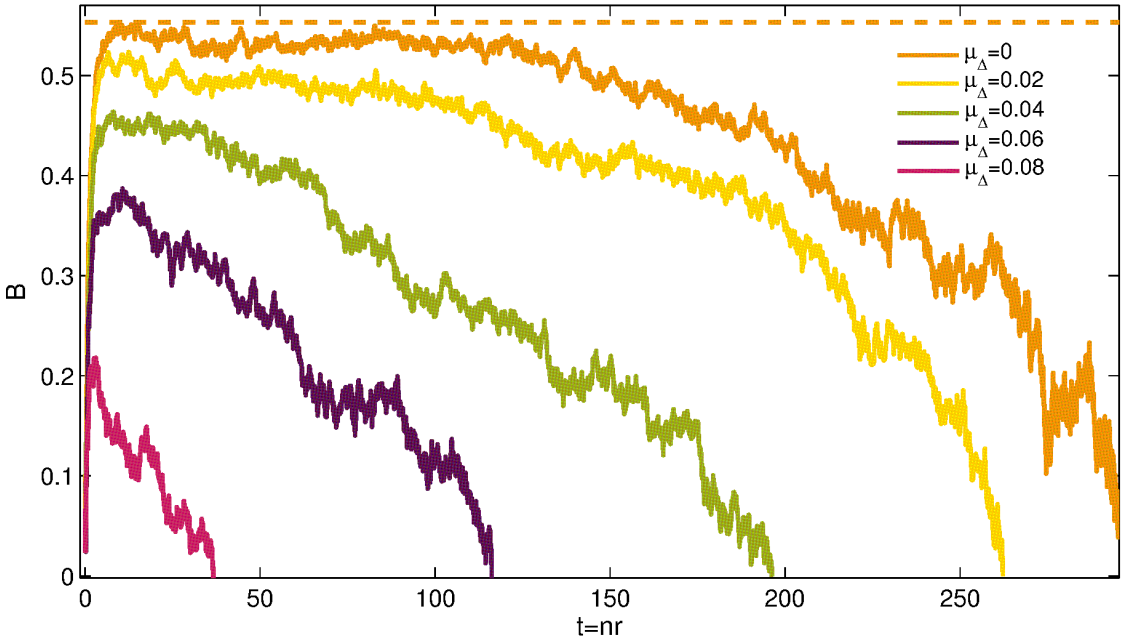


FIGURE 3.18: **Binder cumulant time series for different initial conditions.** Initial market preferences are normally distributed $\mathcal{N}(\mu, 0.1)$. Varying the mean of initial market preference distribution we note that increasing fraction of runs never visits the strongly segregated state and even if it visits it its lifetime is shorter as $\mu$ is increased. Other parameters as usual: $p_{\mathcal{B}} = 0.8$, $\theta = 0.3$, $(r, 1/\beta) = (0.05, 0.15)$

deviation, $\sigma$. We further fix the distribution width with $\sigma = 0.1$ and vary the mean $\mu$ to see if the strongly segregated state will still be reached. We note that already for $\mu = 0.1$ there is no initial convergence to the strongly segregated state. In Figure 3.18 we show how varying $\mu$ below this value affects convergence to the strongly segregated state. First, we observe that for every $\mu > 0$ the maximal value of the Binder cumulant is not theoretical prediction obtained for $\mu = 0$ (up to finite $N$ corrections). This is because we present averaged Binder cumulant time series for different runs and both subpopulations. The fact that these do not reach theoretically predicted maximum tells us that for every $\mu > 0$ some fraction of runs does not visit the strongly segregated state on the way to the stable, weakly segregated, steady state. Similarly, looking at the state lifetime, it seems as if it is shortened as $\mu$ is increased. Part of this effect might have been caused by the Binder cumulant averaging (as many runs do not visit the strongly segregated state but directly transition to the weakly segregated ones characterised by the large negative Binder cumulants), but we also note in individual run inspection that even the states that seemingly reached the strongly segregated states stay there shorter on average. Finally,

when $r > r_c$ the strongly segregated state is unique and independent on $\mu, \sigma$ of the initial conditions it is always reached by the population.

## 3.4 Summary

In this chapter, our aim was to investigate the transition between the unsegregated and segregated state in the long memory limit as only then the transition is sharp. We first studied two traders who learn how to synchronise at a market and maximise their average return despite the fact that one of them will necessarily earn less. We build upon these results by studying a four player system in which beside synchronisation we observe segregation, too. Interestingly, despite different agent types, synchronised and segregated state lead to the same average population return for high intensity of choice $\beta$. In the synchronised state one of the agent types will always earn less, while in the segregated state both types have the same average, but one agent from each group is less satisfied. Thus at the segregated state, there is no apparent "type discrimination". Similar conclusions we draw by analysing returns of the weakly segregated and the strongly segregated state in the large population limit, as in the $r \to 0$ limit the weakly segregated state essentially represents synchronisation at a single market.

Already studying small system sizes, we note that agent's preference for buying $p_{\mathcal{B}}$ is an important system parameter. Beside the dependency of the critical intensity of choice $\beta$ on $p_{\mathcal{B}}$, for $N \geq 4$ we realise that the nature of possible fixed points change when $p_{\mathcal{B}}$ is varied. This realisation is valid also in the $N \to \infty$ limit where we realise plethora of phases in the $(\beta, p_{\mathcal{B}})$ diagram. The diversity of possible steady states is impressive as a very simplified description of markets and traders gives us a variety of possible end states: market coexistence $(S, S)$; a single market dominance $(W, W)$; market indifference $(U, U)$ (e.g. low $\beta$ fixed point); general vs. specialised market (e.g. $(U, S)$ where a single market attracts both subpopulations, while the other is seemingly specialized for only one subpopulation).

We speculate that the change in $\beta_c$ monotonicity reported in Fig. 2.10 might be related to increased region of the partially segregated states. Comparing the same $(\beta, p_{\mathcal{B}})$ phase diagram (Fig. 3.5) for $N = 4$ and the $N \to \infty$ limit, we note that the region of partially

segregated states increased with $N$ and we conjecture these states might be stable for the large populations. In Fig. 2.10 we also noted that the region of changed $\beta_c$ monotonicity increase with increased differentiation between the markets. That might indicate that the region of partially segregated states is even more prominent when markets are extremely biased.

Finally, by methods of numerical simulations, we investigate existence and stability of the other segregated steady states for finite $r$. We once again focus on the commonly studied "decisive" traders because we can observe multiple steady states at the reasonably high $r$ (see e.g. Fig. 2.13). If the agent starts as "blank canvasses" the adaptation always leads to the strongly segregated state first. However, this state is a metastable one and depending on the number of agents its lifetime can be very long, but eventually, the population settles for one of the weakly segregated states. This is true even if the initial conditions are not defined by the Dirac delta distribution, but a Gaussian with zero mean. As soon as the Gaussian mean shows an initial preference to one of the markets, some fraction of runs never visit the strongly segregated state, but directly depart to the weakly segregated one. This is insightful as two markets that enter in a competition to attract on average indifferent traders will always have a period of coexistence (if $r > r_c$ the coexistence, e.g. the strongly segregated state will be indefinite), but if the population is not entirely indifferent monopoly arise much quicker.

In principle, we can do a similar numerical analysis for the system with indecisive traders, aiming to identify partially segregated states in the numerical simulations. What hinders our progress on that end is the observation that the region of multiple segregated states is narrower for these parameters $r_c < 0.002$. This makes the agent's relaxation time very long, and the strongly segregated state is long-lived for all the investigated simulation lengths (we simulated up to 1000000 trading periods with largest $r < r_c$ but there is no departure from the strongly segregated state).

# Chapter 4

# Model Extensions

In the previous chapters, we have introduced and analysed emergence of segregation in a stylised model consisting of two double auction markets and a large number of rudimentary traders. Despite its simplicity, the model showed very rich phenomenology and not only did we reproduce the effects of long-lasting loyalty between traders and markets, but we were able to analyse in great detail why such a state appears and what are its benefits for individual agents and the population. To ensure that results we have obtained are not a mere consequence of an oversimplified trading mechanism and agents' strategies we proceed with the analysis of the model with a few extensions we have developed to test the robustness of our results.

The rest of this chapter is divided into three major parts to address key simplifying assumptions we have made. In the first section of this chapter we return to definitions of the reinforcement learning that drive agent's choice of market and we show that a more general class of the reinforcement learning rules we have used still leads to segregation. Notably, the only case when the steady state is not segregated does not always entail benefits for the population. After the learning extensions, we address systems with more than two markets to show that the full segregation in which agents from every subgroup segregate across all the markets is only a property of the two market setup while when more markets are competing some agents will never develop loyalty for some markets. In the previous chapters we have realised that agent's learning mechanism is the key driver of segregation. Now, we investigate what changes in a well established continuous double auction model if an exact copy of a market is introduced and agents are faced

with the choice. In the third section, we investigate will the segregation persists if realistic features such as budget constraints, more sophisticated trading strategies and the continuous double auction markets are introduced.

## 4.1 Reinforcement learning

In Chapter 2 when we introduced agent's choosing strategy we have argued that agent's choices of actions are based on attractions - scores accumulated by taking certain actions in the past. The form of attraction update rule we have used can be rewritten in the following way (using the notation as in [77]):

$$A^i_\gamma(n+1) = (1-r)A^i_\gamma(n) + rI(a^i(n),\gamma)S^i_\gamma \,,$$

where $a^i(t)$ represents an action agent $i$ have taken at the time $t$, while with $\gamma$ as before we denote possible actions, e.g. $\gamma \in B1, S1, B2, S2$ when we study two markets and agents with adaptive buy/sell preferences. We have also used $I(x,y)$ as indicator function, equal to one when $x = y$, zero otherwise (for the same purposes in the earlier chapters we have used Kronecker's delta - $\delta_{xy}$, while here we use the indicator function for consistency with the EWA literature).

This form of attraction update is commonly known as reinforcement learning based on averaged not accumulated scores (accumulated attractions are a variant where there's no $r$ in front of the second term) and it has been used in various games before, see for example [92] or [93]. It is also a special form of the Experience Weighted Attraction learning [77, 78] which is a unifying method aiming to join two historically divided routes of modelling discrete choices - reinforcement learning and belief based models. The first make an assumption that actions are "reinforced" by their past scores and in general an agent who uses reinforcement learning does not have information on other players scores nor strategies but base his/her action only on past trials. On the other hand, in the belief based models, the assumption is made that an agent kept track of other players actions and based on that information makes estimates on the possible scores for every action taken. That way an agent can update attractions to every action at a given time step, the

one played by an actual score and all the others based on fictitious score - a score (s)he would receive had (s)he played that action [46, 81].

In evolutionary dynamics, when attractions to possible actions are calculated it is usually assumed that the agent can estimate the score (s)he would receive had (s)he taken every action. This might be a reasonable assumption if an agent is choosing between going to a resource one or resource two where both of these are large enough so agent's satisfaction will not be dependent on other players' choices. We have argued that within the trading setup an agent does not have sufficient information to make estimates about the scores (s)he would receive had (s)he played other actions. This is because for the score estimate an agent needs the order price (s)he would have made, but also the trading price and fractions of agents whose orders were valid to assess the trading probabilities. Although one might argue that the first two could be estimated based on the agent's attraction data, the last one can not, so we do not consider fictitious scores. Nevertheless, whether the attractions of unplayed actions should be forgotten when not played is a question worth pursuing, and we present a simple model to interpolate between the model studied so far (where everything is forgotten with the same rate) and a case where unplayed actions are not forgotten.

Let us assume that attractions are updated in the following manner:

$$A_\gamma(n+1) = \begin{cases} rS_\gamma(n) + (1-r)A_\gamma(n), & \text{if agent played action } \gamma \\ (1-\alpha r)A_\gamma(n), & \text{if agent played action } \delta, \delta \neq \gamma \end{cases} \tag{4.1}$$

$\alpha$ is a parameter we introduced to interpolate the forgetting rate of unplayed actions between the two extremes - $\alpha = 0$ - *an agent does not forget scores of the other actions*, and $\alpha = 1$, *everything is forgotten with the same rate*, which is the system we have studied so far. If rewritten this update rule reads as:

$$A^i_\gamma(n+1) = (1-r)A^i_\gamma(n) + r\left(I(a^i(n),\gamma)S^i_\gamma + (1 - I(a^i(n),\gamma)(1-\alpha)A^i_\gamma(n)\right) ,$$

This effectively means that instead of fictitious score, unplayed actions are updated with a fraction of the last attraction which is essentially averaged score received playing that

action in the past $1/r$ rounds. We note that in the extreme $\alpha = 0$ an attraction to unplayed action is updated with the average score received playing that action in the past, while in the $\alpha = 1$ extreme attractions are effectively updated with score of zero.

Following the same procedure as for the initial attraction update rule, we can write the master equation and the corresponding Fokker-Plack equation. To solve the Fokker-Planck equation in the general case is a nontrivial task, but to find the segregation threshold, as before we can only analyse the first jump moment and its zeros. As introduced in Chapters 2 and 3, in the $r \to 0$ limit, we can focus on solutions of the homogeneous population equations, and at the corresponding market order parameters, find the distribution peak positions as solutions of the first jump moment. The first jump moment for this system reads as[1]:

$$\mathbf{M_1}(\mathbf{A}) = \sum_{\gamma} (\mathbf{e}_\gamma T_\gamma \overline{S}_\gamma - (1-\alpha)\mathbf{A}) P(\gamma|\mathbf{A}) - \alpha \mathbf{A} \,. \tag{4.2}$$

We note that when $\alpha = 0$ the Eq. (4.2) has a unique fixed point for every $\beta$ if the market order parameters (and consequently the trading probabilities) are fixed. Whenever the attractions to the unplayed actions are not forgotten (effectively we assume infinite memory for unplayed actions $\alpha = 0$) the steady state distribution is unimodal, i.e. segregation does not occur. For the general value of $\alpha$ we show in Figure 4.1 how the threshold intensity of choice $\beta_s$ is affected by different update rule and we note that only in the case $\alpha = 0$ segregated steady state does not exist.

In Figure 4.1 we plot the inverse intensity of choice for visual simplicity (as values of $1/\beta_s$ are bounded). The main plot shows $1/\beta_s$ as a function of $\alpha$ in the linear axis plot from which it is not clear what is the limiting value of $\beta_s$ when $\alpha$ approaches zero. As we do not assume $\beta_s$ to be a discontinuous function of $\alpha$ and we have already seen that $1/\beta_s = 0$ when $\alpha = 0$, in the insert of Fig. 4.1 we show $1/\beta_s$ as function of $-1/\log(\alpha)$. In that plot we see clearer convergence to 0 indicating $\alpha \propto \exp(-\beta)$ confirming our previous constatation that for $\alpha = 0$ there is no finite intensity of choice threshold. Interestingly, we note that $\beta_s$ is non-monotonic function of $\alpha$, but the reasons behind the minima for the value $\alpha \approx 0.45$ are not yet understood.

[1] More details are in Appendix A.

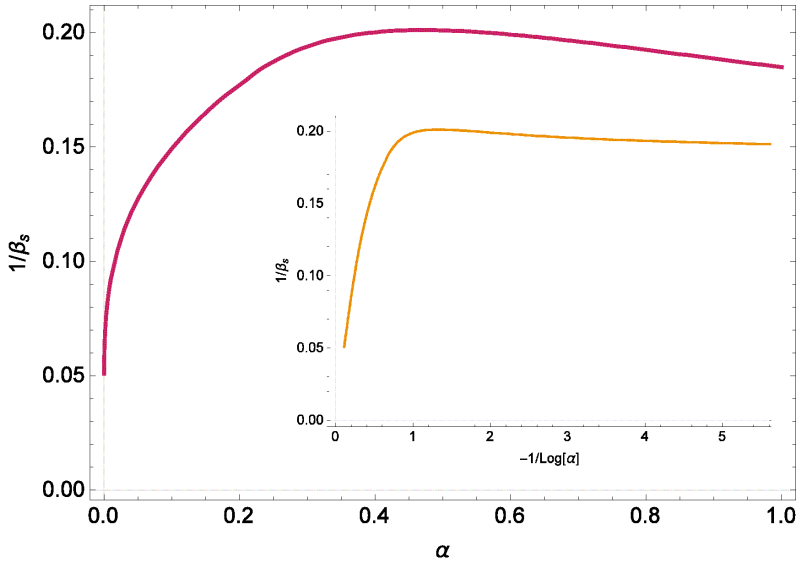


FIGURE 4.1: **Effect of $\alpha$ on the segregation threshold $\beta_s$ in population with adaptive buy/sell preferences.** In the linear axis plot it is not clear if the $\beta_s$ diverges at $\alpha = 0$ which is why we add the insert with $-1/Log(\alpha)$ as an axis (see the text for more details).

The same analysis we can perform for the population consisting of two subgroups with fixed buy/sell preferences $(p_{\mathcal{B}}^{(1)}, p_{\mathcal{B}}^{(2)})$. When $\alpha \neq 1$, the analysis can not be simplified to a unique attraction difference parameter $\Delta^{(g)} = A_1^{(g)} - A_{-1}^{(g)}$, but we need to describe each subgroup with attractions to both markets $\mathbf{A^g} = (A_1^{(g)}, A_{-1}^{(g)})$. We can write an explicit form for the first jump moment $\mathbf{M_1^{(g)}}$:

$$\mathbf{M_1}(\mathbf{A}^{(g)}|p_{\mathcal{B}}^{(g)}) = \sum_{m=-1}^{1} \left( \mathbf{e}_m \sum_{\tau \in \{\mathcal{B},\mathcal{S}\}} \left[ p_\tau^{(g)} T_{\tau m} \overline{S}_{\tau m} \right] - (1-\alpha)\mathbf{A}^{(g)} \right) \sigma_\beta(m\Delta^{(g)}) - \alpha \mathbf{A}^{(g)}. \tag{4.3}$$

In these equations, as for the populations of adaptive buy/sell agents, we see that for $\alpha = 0$ (when agents do not update scores of for the actions not taken at the particular time step), the solution of $\mathbf{M_1}^{(g)}(\mathbf{A}^{(g)}) = 0$ is unique, thus there is no critical intensity of choice. However, for all other $\alpha$ values, i.e. when we assume that agents can not have an extremely long memory of the unplayed actions, we see that there is a critical value of the intensity of choice above which segregation again emerges, as shown in Figure 4.2. Agents buy/sell preferences are as usual $(p_{\mathcal{B}}^{(1)}, p_{\mathcal{B}}^{(2)}) = (0.8, 0.2)$ with market biases $\theta_1 = 1 - \theta_2 = 0.3$. As for the population of adaptive buy/sell agents we plot the

inverse intensity of choice as function of $\alpha$, but also as a function of $-1/\log(\alpha)$, following the same argument.

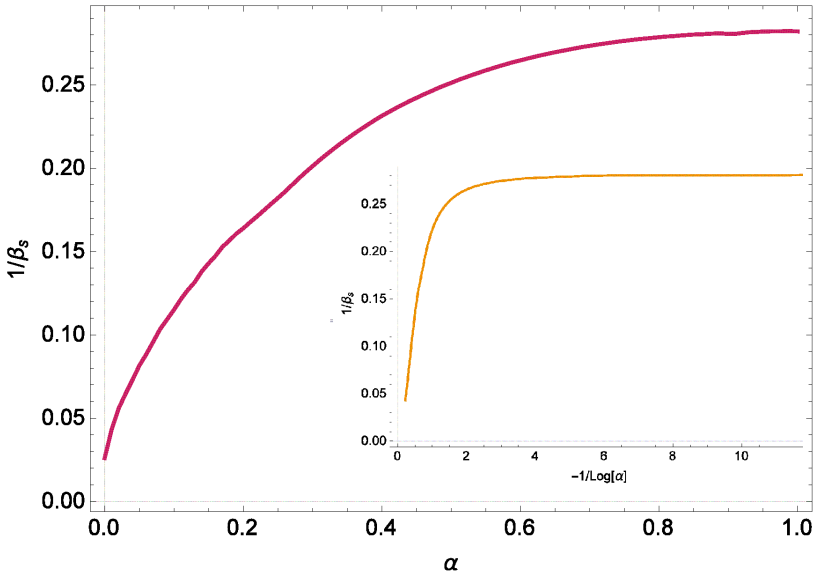


FIGURE 4.2: **Effect of $\alpha$ on the segregation threshold $\beta_s$ in population with fixed buy/sell preferences $pB^{(1)} = 0.8$, $pB^{(2)} = 0.2$.** The insert shows that $\alpha \propto \exp(-\beta)$ as discussed in the main text.

A tentative explanation why the segregation ceases to exist for $\alpha = 0$ is the following: whenever $\alpha$ is finite, there is a finite period necessary for an agent to forget about their failures and successes at the other markets, this forces an agent to explore those options again which makes agents who were return driven to exchange roles with volume driven agents (and vice versa), effectively enabling the segregated state and allowing both groups to receive a higher long-term average return. On the other hand, when $\alpha = 0$, all agents have good information about all available options and thus no incentive to settle for lower returns. In what follows we explore the average returns an agent receives in this unsegregated state. Solving the deterministic equation stated previously (Eq. 4.3), we can find the position of the delta peaked distribution which is a steady state solution in the $r \to 0$ limit. This gives us an opportunity to investigate possible benefits this unsegregated solution might bring to the population of traders. In Figure 4.3 we plot average population returns of this state at different intensities of choice and compare it with returns of the strongly segregated state and the $\alpha = 1$ unsegregated state.

We compare these returns with the two states discussed previously - unsegregated

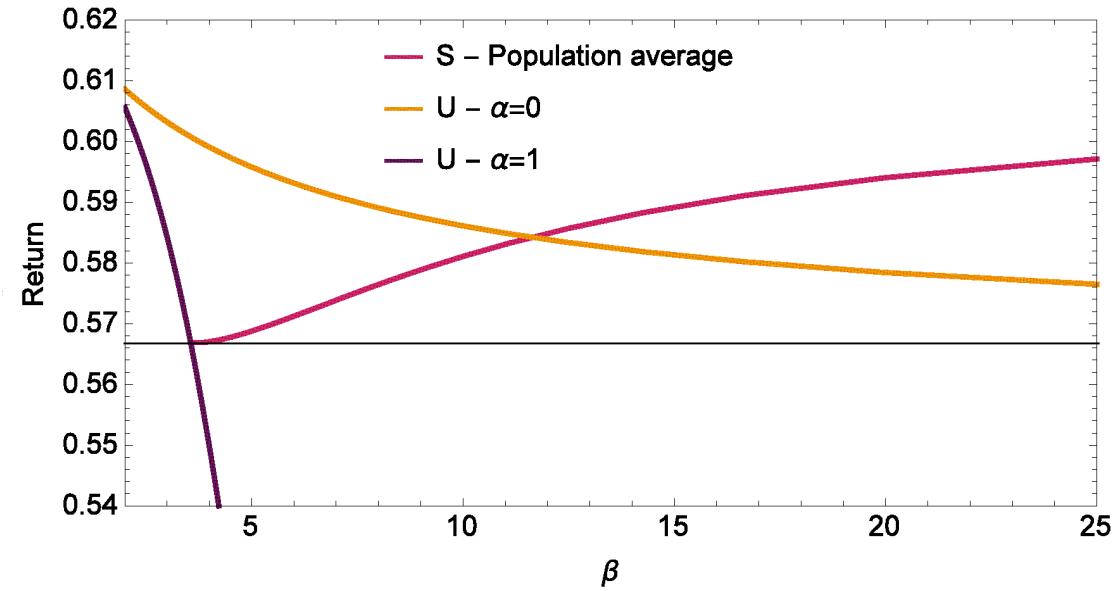


FIGURE 4.3: **Return of the unsegregated state $\alpha = 0$ against intensity of choice $\beta$.** We show average population return of the population consisting of decisive traders $(p_{\mathcal{B}}^{(1)}, p_{\mathcal{B}}^{(2)}) = (0.8, 0.2)$ who don't forget attractions of unplayed actions ($\alpha = 0$). We compare these returns against typically studied $\alpha = 1$ strongly segregated state and low $\beta$ unsegregated state.

low $\beta$ state and the strongly segregated states, both at $\alpha = 1$. All the returns are compared against the baseline introduced in Chapter 2, the envy-free Nash equilibrium (discussed in more detail in Appendix C).

Interestingly, both unsegregated states are envy-free and enable the population to have a higher return compared to envy free Nash equilibrium, at least in some ranges of intensity of choice. On the other hand, we can think of the strongly segregated state as envy-full in the short terms, but in the long term average, all agents are the same. Analysing Figure 4.3, we realise that for a wide region of intensities of choice having an option not to update attractions of unplayed actions raises average returns. Even above the critical intensity of choice $\beta_s$ for $\alpha = 1$, where the segregation allowed the population to earn more compared to its unsegregated counterpart, if an agent keeps unplayed attractions unchanged (s)he earns more without assuming the role of a volume or return driven agent. However, at some even higher intensities of choice, the $\alpha = 0$ unsegregated state return average drops below the return of the strongly segregated state. This is because the unsegregated $\alpha = 0$ state converges to the envy-free Nash Equilibrium (see e.g. [88]), which as previously shown is worse than the strongly segregated state.

Interestingly, at the high intensities of choice, choosing to temporarily settle for lower returns enables better returns for an agent and the population as a whole compared to all other states that maximise returns keeping all individual returns equal.

Finally, besides the choice of attraction updating mechanism, when setting up an action choosing strategy we have chosen to use softmax or logit function to translate attractions into probabilities of taking an action $\gamma$. Although some authors use power or probit functions as well, use of logit function was documented under risk and uncertainty but also in choosing brands (see e.g. [77, 94, 95]). As argued by Camerer and Ho [77], this choice should be ultimately driven by empirical findings, and they show that the logit function fits the empirical data equally well [96, 97] or better [98] than the probit function.

## 4.2 Multiple markets

The original model of double auction markets and traders can in principle be extended to any number of markets, as we have noted in Chapter 2. However, for most of the thesis we have focused on analysis of the two market system for its simplicity and analytical tractability, but in the following section we outline results we obtain for the system with three market and traders with fixed buy/sell preferences and make an argument about the possible steady states for the general number of markets $M$. This is of particular interest in analysing possible steady states of a more realistic system that consist of more than two competing markets. The key questions are related to the possible numbers of coexisting markets – as we have summarised in the Introduction, some authors argue that competing double auctions can coexist due to the negative network effect [44], while others argue that the coexistence is possible only if the markets have distinctive pricing policies [36]. As we have seen in the previous chapters, strongly segregated states exist for various market and population parameters and these are the states that guarantee market coexistence as opposed to the weakly segregated states in which one of the markets predominates. In this section we want to explore possibilities of coexistence for more than two markets.

To proceed with analysis we first realize our previously outlined procedure is still an adequate description as the system is still Markovian and accordingly the master equation (Eq. 2.9), as introduced in Chapter 2 is still an exact and complete description of the evolution of agents in the limit of infinite population $N$ and large memory $1/r$. We note that for the description of a population with fixed buy/sell preferences, we seek for a steady state distribution $P(\mathbf{A}|p_{\mathcal{B}})$ where $\mathbf{A}$ is a $M$-dimensional vector. When a number of markets is $M > 2$, changing to attraction differences will not simplify the problem as much as in the case of two markets when the problem became one dimensional. When we study more than two markets the distribution is multivariate, though we can introduce attraction differences and seek for the solution in the space of $M - 1$ variables.

The dimensionality of the problem (as before for the adaptive population case) makes finding the steady state a non-trivial task, even if we introduce approximate Fokker-Planck equation in the small $r$ limit. Although we can't easily find the steady state solution for the finite $r$, we can address the problem in the $r \to 0$ limit, as introduced in Chapter 3 and evaluate the onset of segregation. We do this by analysing the first jump moment $\mathbf{M_1}(\mathbf{A})$ defined as follows:

$$\mathbf{M_1}(\mathbf{A}^{(g)}) = \sum_{m=1}^{M} \mathbf{e}_m \sum_{\tau \in \{\mathcal{B},s\}} p_\tau^{(g)} T_{m\tau}\left(\mathbf{A}^{(g)}, \mathbf{A}^{(-g)}\right) S_{m\tau} \frac{\exp\left(\beta A_m^{(g)}\right)}{\sum_{m'=1}^{M} \exp\left(\beta A_{m'}^{(g)}\right)} - \mathbf{A}^{(g)}, \quad (4.4)$$

where we preserved previous notation, but explicitly stated dependence of trading probabilities $T_\gamma$ on both studied subpopulation $(g)$ and the other one.

As before, when analysing the single agent's steady state, we will search for zeros of the first jump moment assuming the market order parameters fixed (thus the trading probabilities are not dependent on $\mathbf{A}$). To control for the changes in order parameters, we follow the algorithmic procedure outlined in Chapter 2. We start by assuming that the subpopulations have homogeneous preferences for the markets (i.e. $P(\mathbf{A}^{(g)}|p_{\mathcal{B}}^{(g)})$ is delta peaked distribution), which is the expected solution in the low $\beta$ limit, when the steady state is unsegregated. With this assumption, market order parameters are simplified, and we can proceed by solving the Eqs. (4.4) for the two subpopulations simultaneously. At any fixed point solution $(\mathbf{A}^{(1)*}, \mathbf{A}^{(2)*})$ we evaluate the order parameters $D_m$ and check if

the single agent's dynamics is consistent with the homogeneous population assumption (e.g. we solve $M_1^{(g)}(\mathbf{A}|D_m) = 0$ expecting only one zero, coinciding with $A^*$). At an intensity of choice where we find that the single agent's dynamics has multiple zeros when evaluated at the homogeneous population market order parameters, we declare a segregated steady state.

In Figure 4.4 we show line of critical intensity of choice of the previously studied system $(p_{\mathcal{B}}^{(1)}, p_{\mathcal{B}}^{(2)}, \theta_1, \theta_2) = (0.2, 0.8, 0.3, 0.7)$ to which a third market is added and its bias $\theta_3$ is varied. We note that addition of the third market independent of its bias shrinks the segregation region (segregation threshold without the third market is shown with dashed line).

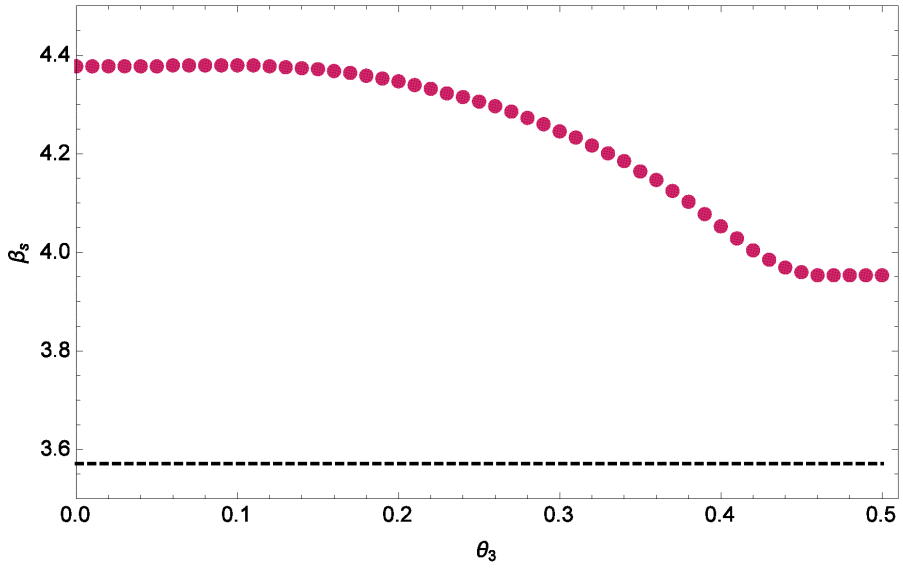


FIGURE 4.4: **Segregation threshold $\beta_s$ as a function of the third market bias,** where other parameters are those of a typically studied system $(p_{\mathcal{B}}^{(1)}, p_{\mathcal{B}}^{(2)}, \theta_1, \theta_2) = (0.2, 0.8, 0.3, 0.7)$. The dashed black line shows segregation threshold of the two market system.

Without a solution of the Fokker-Planck equation, we cannot introduce a "free energy" analogue and thus can not distinguish between a weakly or strongly segregated state above the noted threshold. To gain an insight into possible types of segregation (and analogously outcomes of market competition), we analyse the steady states obtained in numerical simulations for different values of the forgetting rate $r$. Motivated by our previous analysis, we expect to see changes in the peak weights when $r$ is decreased and we expect the peak weight ratio to remain of the order one for the strongly segregated state

and to diverge for the weakly segregated state (as we demonstrated in Chapter 3 in the case of single subpopulation).

In the following figures, we show steady states of the simulated systems for different choices of the third market bias at the intensity of choice $\beta = 5$ (segregated for any choice of $\theta_3$ as shown in Fig. 4.4). The distributions are shown in a two-dimensional projection $(\Delta^i_{12}, \Delta^i_{13}) = (A^i_1 - A^i_2, A^i_1 - A^i_3)$ for visually clearer representation. Overall preference for the market one is in the top right quadrant, preference for market two is on the on the negative part of the "x" axis, while the preference for market three is on the negative part of the "y" axis.

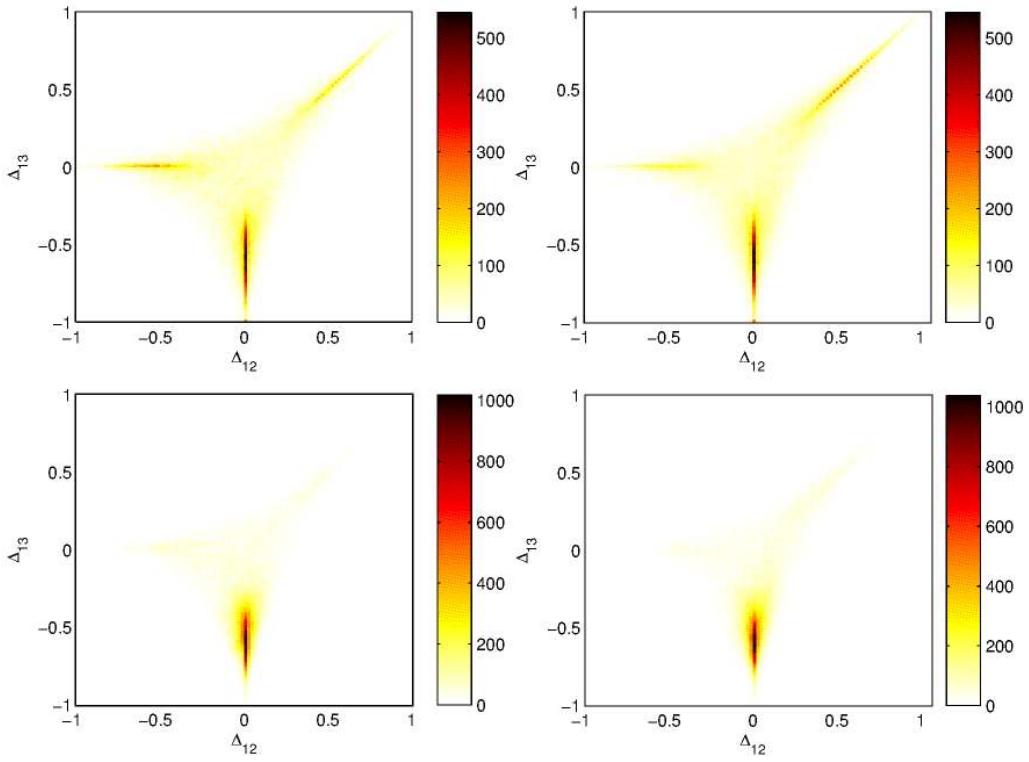


FIGURE 4.5: **Simulated steady states of a system with two symmetrically biased and a fair market.** Left: $P(\mathbf{A}|p_{\mathcal{B}} = 0.2)$; Right: $P(\mathbf{A}|p_{\mathcal{B}} = 0.8)$; Top: $r = 0.1$; Bottom: $r = 0.05$. Note that as $r$ is decreased peak at the third market dominates, suggesting this is a weakly segregated state.

We explore three different systems with the commonly used symmetric system with the third market: (1) fair ($\theta_3 = 0.5$), (2) biased, but same as one of the symmetric markets ($\theta_3 = 0.7$) and (3) more biased than the two already present markets ($\theta_3 = 0.9$). Intriguingly, simulations suggest that in all three different systems in the small $r$ limit only a subset of markets will remain populated. In Figure 4.5 we show the steady states when

the third market is "fair". We compare the two steady states obtained for forgetting rates $r = 0.1$ and $r = 0.05$. For the greater $r$ both subpopulations split into three groups, the majority chooses the fair market, but the segregation among the two symmetric markets resembles the one we have observed in the two market scenario - e.g. sellers prefer market good for them $\theta_2 = 0.7$ (the subpopulation $p_{\mathcal{B}}^{(1)} = 0.2$ is shown on the left, note beside the peak at the third market, the peak at the second market is more populated) and similar for buyers. However, when $r$ is decreased the majority of both subpopulations prefer the fair market (see bottom panels of Figure 4.5 where the other two peaks weights decayed). This suggests the steady state is a weakly segregated one - in the $r \to 0$ limit the distribution will be unimodal centred at $\Delta_{12} \approx 0$ and $\Delta_{13} < 0$ (everyone prefers market three).

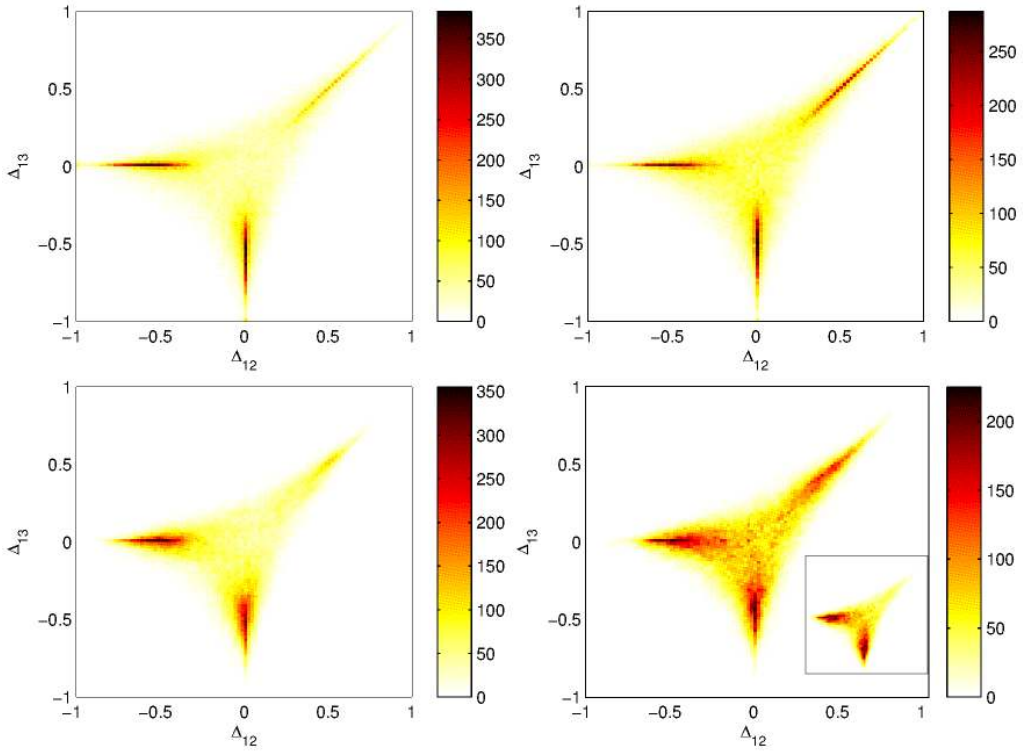


FIGURE 4.6: **Simulated steady states of a system with three markets** $(\theta_1, \theta_2, \theta_3) = (0.3, 0.7, 0.7)$**.** Left: $P(\mathbf{A}|p_{\mathcal{B}} = 0.2)$; Right: $P(\mathbf{A}|p_{\mathcal{B}} = 0.8)$; Top: $r = 0.1$; Bottom: $r = 0.05$; Insert: $r = 0.03$. When $r$ is decreased the peak weight at the first market (only one good for buyers) decreases.

When no fair market exists, two of the three markets, being biased towards the same subpopulation, break the symmetry and we note that the steady state distribution becomes unimodal, peaked at the fairer of the two markets (e.g. in the system $(\theta_1, \theta_2, \theta_3) =$

$(0.3, 0.7, 0.9)$ as $r$ is decreased the increasing peak weight is at the second market). Especially, when the two markets are the same $(\theta_1, \theta_2, \theta_3) = (0.3, 0.7, 0.7)$, the results suggest that the steady state distribution is bimodal - both markets favouring sellers will attract traders, see Figure 4.6. The subpopulation for which that is not the preferred market bias (buyers, in this case, shown in the right panels) will prefer a state with three peaks even at the lower $r$ when the population of sellers already mostly settled for the two markets. That is why in the insert (bottom right) we show simulated steady state for even lower value of the forgetting rate $r = 0.03$ where we note that the buyers choose to align with the preference of sellers and trade mostly at markets two and three.

More generally, our numerical exploration suggests that in the system with three different markets (with no symmetries), at the steady state the population will settle for only one market (the one closest to the fair market) thus only the weakly segregated states will exist. Motivated by the observations from two market systems, where we have seen that when both markets are fair, the equal weight strong segregation exist (see e.g. Fig. 3.7), we investigate if the same is true in a system with three fair markets. In Figure 4.7 we show steady state distributions of the two subpopulations when faced the choice between three fair markets. We note that even for relatively small $r = 0.05$ all three peaks are equal weighted suggesting that in this case even in the $r \to 0$ limit the population will persist segregated across all three markets.

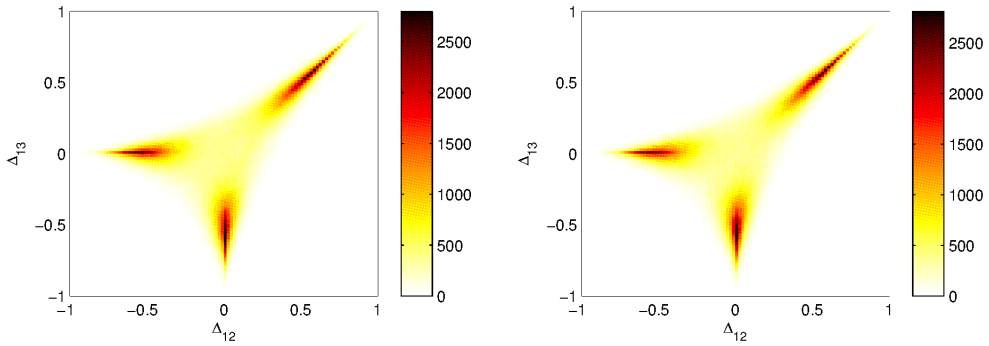


FIGURE 4.7: **Simulated steady states of a system with three fair markets.** Left: $P(\mathbf{A}|p_{\mathcal{B}} = 0.2)$; Right: $P(\mathbf{A}|p_{\mathcal{B}} = 0.8)$. When all markets are fair the steady state is a multimodal distribution with equal weights at all three markets. The forgetting rate is $r = 0.05$.

In these examples, we have seen two types of weakly segregated states, the ones that

we conjecture will become unimodal distributions in the $r \to 0$ limit ($\theta_3 = 0.5$) and the ones that suggest equal weighted coexistence of the two markets in the same limit ($\theta_3 = \theta_2 = 0.7$). We have also seen an example of a full segregation (finite weights at all three peaks) but only when the three markets are identical. This provokes a question of the maximal number of segregated groups for the general number of markets $M$ - when is it possible that both subpopulations segregate across all markets as we have seen in the systems with $M = 2$ markets?

We address this questions making a simple counting argument regarding necessary variables to describe segregated population under given market constraints. In the following argument, we make an assumption that even for the $M > 2$ there is segregation threshold $\beta_s$ above which the first moment has multiple zeros (low $\beta$ - market indifference and at most $M$ zeros corresponding to a strong preference for one of the markets). Even if the drift term has that many zeros, it is not clear if all subpopulations of agents will develop loyalty groups for all the markets.

To describe a subgroup that is segregated across $M$ markets, in the $r \to 0$ limit, we need $M$ delta peaks and their corresponding weights. The peak positions we can obtain by solving the $\mathbf{M_1}(\mathbf{A}^{(g)}|p_{\mathcal{B}}^{(g)}) = 0$, but without the Fokker-Planck solution, we can not obtain the peak weights. We can, however, make a general argument about how many non-zero peak weights can exist for the general number of subpopulations $G$ and markets $M$. As before, we assume the general shape of the steady state distribution:

$$P^{(g)}(\mathbf{A}) = \sum_{m=1}^{M} \omega_m^{(g)} \delta(\mathbf{A} - \mathbf{A}_m^{(g)}).$$

Thus, each of the subpopulations is described by peak weights $\omega_1^{(g)}, \ldots, \omega_M^{(g)}$ that satisfy the normalization condition $\sum_{m=1}^{M} \omega_m^{(g)} = 1$, thus without any symmetry imposed we have $M-1$ variables per subpopulation. On the other hand, for each market we define an order parameter $D_m$, thus the system of equations we need to solve to find a segregated solution is:

$$\mathcal{F}_m(\omega_1^{(1)}, \omega_2^{(1)}, \ldots, \omega_M^{(1)}, \ldots, \omega_M^{(G)}) = D_m \ ,$$

where $\mathcal{F}_m$ denotes the relation between the peak weights and market order parameters, for the two subpopulations and two markets it is explicitly written in Eq. 3.18. Without symmetries, when all the equations and variables are independent, this system of $M$ equations and $G(M-1)$ variables has a unique solution only when the number of equations is equal to the number of variables, i.e. $M = G(M-1)$. This equation has an integer solution pair only when both number of market $M$ and subpopulations $G$ is equal to two, $(G, M) = (2, 2)$. For example, our previously studied population that consists of 2 subpopulations would require $2(M-1)$ weights for full segregation across $M$ markets. The solution of $2(M-1) = M$ is only previously studied the case of $M = 2$ markets.

We can also assume that not all subpopulations will segregate across all markets. Let us suppose there are $M$ markets and two subpopulations, each of them segregating into $\eta^{(g)}$ subgroups, thus system of equations to determine weights is determined when $\eta^{(1)} + \eta^{(2)} - 2 = M$. This shows that if one subpopulation divides into $M$ loyalty groups, consequently the second subpopulation will segregate only across two markets (but also other combinations satisfying $\eta^{(1)} + \eta^{(2)} = M + 2$ are possible). Similarly, for the general number of subpopulations, previous equation reads as $\eta^{(1)} + \eta^{(2)} + \cdots + \eta^{(G)} - G = M$ suggesting that if one subpopulation develops loyalties to all $M$ markets, total number of subgroups of the other $G-1$ subpopulation needs to equal $G$, consequently giving one bimodal and $G-2$ unimodal steady state distributions.

Interestingly, this shows that when all the markets coexist (which we enforce by assuming that at least one subpopulation has loyalty groups for every market), not all markets will be visited by all traders[2]. As some markets will have only a subset of the subpopulations loyal to them, it will appear as if the markets targeted only a subset of the population although no such intention is implemented. This observation is based on previously stated assumption that we discuss peaks centred at attractions to only one market. In principle, we can also think about a possibility that some of the subpopulations that have only one or two peaks remain undetermined between different market options.

[2]For any finite $\beta$ this is not entirely correct as traders will always have a probability to visit the markets to which they are not "loyal", but the statement was meant to stress that not all markets will have loyal visitors from all the subpopulations

This brief counting argument states that in the $r \to 0$ limit at most $G + M$ loyalty groups can coexist. In the three market scenario with two subpopulations, this is at most five loyalty groups, although the three fair market setup showed coexistence of six loyalty groups. We believe this is because our argument is constructed under the assumption of independent variables and equations which in the case of equal markets and symmetric subgroups can not be true.

Similar counting argument can be made for the population of adaptive agents who, having the adaptive preference for buying, need $2M - 1$ weigh parameter description. With only $M$ order parameters, in the general nonsymmetric setup, the system can be fully segregated only for $M = 1$ (emergence of buyer/seller specialisation). On the contrary, in the previous chapter we have seen four distinctive peaks in the steady state distribution obtained in simulations. Again, we believe the reason for that lies in the symmetry of the system, as not all equations will be independent. As in the case of the population with fixed buy sell preferences, we can see how many loyalty groups there can exist when $M$ markets compete in the system.

We make an assumption that whenever a part of population specialises in selling at a market (i.e. $\omega_{m\mathcal{S}} > 0$), there needs to be a part of the population that specialises in buying at the same market $\omega_{m\mathcal{B}} > 0$. We believe this is a reasonable assumption given that single sided specialisation will always lead to low scores as there will not be enough trading opportunities. If we note with $\mathcal{M}$ number of active markets (those for which a part of subpopulation specialised, i.e. $\omega_{m\mathcal{T}} > 0$), determining the weights is possible when $2\mathcal{M} - 1 = M$. Intriguingly, this gives us an argument that in a competition of $M$ markets in a population of adaptive traders only $\mathcal{M} = \frac{M+1}{2}$ of markets will coexist in a steady state.

Without the assumption on specialisation to buying/selling the number of constraints $M$ together with the normalisation constraint tells us that a population of adaptive agents can have at most $M+1$ peaks. This tells us that at least at one market the traders specialise in buyers and sellers (2 peaks) and the other $M-1$ peaks could either represent indecisive agents at different $M - 1$ markets, or each new specialisation to specific roles cause one less active market in the steady state.

It is remarkable how this simple argument gives a variety of new conjectures for the systems with multiple markets. With the argument, we obtained a minimal number of loyalty groups, and we have seen that only roughly a half of markets can coexist when the population is with adaptive buy/sell preferences, while in the population consisting of a subpopulation with fixed buy/sell preferences, all markets can in principle coexist. In that case, we also note that markets will unwittingly reach a state where only a subset of the population will persistently visit them. We propose further ideas to investigate these interesting results in the last chapter.

## 4.3 Toth and Scalas model of continuous double auctions

Our previous investigation has shown that the parameters of agent's reinforcement learning are the key control parameters that distinguish between different steady states. We show that the threshold intensity of choice for the segregated state exist for various market/population parameters and only if the memory of the unplayed actions is infinite the segregation will cease the exist, but that will not always lead to better returns of individual agents, nor entire population. However, these conclusions are based on a model of two double auction markets and large number of traders, that relies on various simplifying assumptions: (1) markets operate in discrete time with a global trading price mechanism; (2) agents are modelled as zero intelligence with respect to their trading strategy, i.e. the order prices are random; (3) agents do not have budget constraints; (4) agents do not possess any information, other than their own history they use to choose between the markets.

In this section, our goal is to investigate whether the segregation might exist if these simplifying assumptions are relaxed. We do this by focusing on an already existing model of continuous double auction market developed by Toth and Scalas [99, 100] to investigate benefits of information. We take this model and upgrade it to examine if by implementing only the main segregation driver (the choice of market is based on the reinforcement learning) will lead to segregation. We start by explaining the original model and existing variations; we then introduce our extensions and present main results. We

conclude addressing the original question of information benefits with preliminary results in the two market system.

**Original model and adaptations.** We consider a system of market and traders introduced by Tóth and Scalas [99, 100]. The market model is a continuous double auction with an open limit order book (list of orders to buy or sell at a given price). Mechanism of continuous double auctions is utilized in many real stock exchanges, e.g. New York Stock Exchange, currency exchange markets (but also extensively researched [33, 67, 71, 75]), and the main difference compared to our previous model is that traders can submit their bids and asks in continuous time, when they can either trade immediately or their order will be stored in the limit order book.

In the simulated system each trading period consists of an open call, during which every trader submits an order to populate the limit order book, followed by rounds during which a random trader is selected to inspect the limit order book and then decides whether to execute an already existing order (market order) or to submit a new one (limit order). This decision process is governed by a fundamentalist trading strategy as follows. To be able to investigate effects of different information levels, the authors define an underlying dividend process that determines the value of stock to be paid to every stockholder at the end of the trading period:

$$D(n) = |D(n-1) + \epsilon| \,,$$

where initial value of the dividend is $D(0) = 0.2$, while $\epsilon$ is normally distributed random variable with mean zero and standard deviation $\sigma = 0.1$.

Different traders have a different number of future dividend values accessible to them, starting from no information (thus, close to our Zero Intelligence Traders) to information about L future dividend values. (In previous studies L ranged from 2 to 9 [99, 101, 102]; we use L = 4, giving a total of five different types of agents including the uninformed ones). Based on their knowledge of future dividends, agents evaluate their stock

holding using a dividend discount model, e.g. Gordon's growth model [103]:

$$pv_j(n) = \frac{D_{n+j-1}}{(1+r_e)^{j-2} r_e} + \sum_{i=n}^{n+j-2} \frac{D_i}{(1+r_e)^{i-n}} ,$$

where $r_e$ is the risk adjusted interest rate ($r_e = 0.005$ as in previous works), $j$ is the information level of the agent while $n$ denotes the trading period as previously. Using this formula an agent implicitly assumes that the dividend value stays the same below his/her horizon. Based on the private value ($pv$) an agent decides whether to buy (when the best ask is lower than his/her private value), sell (when the best bid is higher than the private value) or submit a new order[3]. The details of the trading strategy are the same as in [99, 100], where the pseudo codes are also given; generally and unless mentioned otherwise, we follow exactly the existing model.

We previously simulated the trading periods as only the open call followed by the global price setting after which the buyers and sellers are matched, and the market is cleared. The continuous double auction mechanism enables more trades as many orders that would be deemed invalid in our previous market model will now remain in the limit order book and possibly be executed during the trading period. At the end of the trading period in this model, too, we clear the limit order book[4].

The uninformed trader of the model differs from the Zero Intelligence trader we have described and modelled previously, (s)he has information about the latest trading price, but it is uninformed about the dividend values. The uninformed trader's private value is a normally distributed random variable centred at the most recent trading price, while the rest of the trading strategy is as for the informed traders.

Finally, Toth and Scalas's agents have budget constraints. Everyone starts with equal endowments in terms of a number of stocks and available cash: in the original studies each agent had 40 shares and the equivalent value in cash to start with, same endowments were used in experiments, but other authors used also greater wealth constraints and showed no phenomenological difference [104]. As we look at much longer simulations,

[3] When selected to inspect the limit order book, an agent does not have information about their previously submitted order, e.g. can not recognise it and can in principle trade execute it if it is satisfactory at the moment.

[4] In the original work [99, 100], the authors state there is no difference between the two scenarios – all orders are preserved or cleared at the end of every trading period.

of 100 to 1000 trading periods as opposed to 10–30, we increase the initial wealth to 100 shares plus the equivalent value in cash to avoid agents running out of possessions.

This market mechanism release all of our simplifying assumptions, the trading mechanism resembles more realistic ones (agents discover the price rather than obey one fixed by the market globally), the agents have budget constraints, and the information driven trading strategies. To this system, we now add the second identical market. When confronted with the choice of markets, beside the trading strategy agents need a market choosing strategy which we will assume is independent on their trading strategy, but only driven by reinforcement learning, as before.

To implement the reinforcement rule, we need to define the scores in each trade $S_m$. Because of the existence of a limit order book, it is necessary to differentiate between the Aggressor (the trader who executes an order from the limit order book) and the Quoter (the trader whose order was waiting in the limit order book) in assigning scores. When the Aggressor executes an order from the book, (s)he accepts the price listed; thus the trading price is the Quoter bidding/asking value. If we assume that the scores are assigned as previously (as the difference between asked and executed price value) the quoters will always receive $S_m = 0$. To avoid that we introduce the quoter's returns in the following way:

$$S(n) = \begin{cases} \pi(n-1) - \pi(n), \text{ for buy orders} \\ \pi(n) - \pi(n-1), \text{ for sell orders} \end{cases}$$

assuming that the buyers will value price decrease while sellers will value price increase. On the other hand, the aggressor's returns are as before, related to his/her private value and the trading price: $S(n) = pv(n) - \pi(n)$ if the agent buys (as (s)he values the stock more) and $S(t) = \pi(t) - pv(t)$ if the agent sells (as s/he believes the stock is worth less). The attractions to the markets are updated as defined in the Eq. (4.1) for $\alpha = 1$, while the probability of choosing market $m$ is as previously a logit/softmax function $p_m \propto \exp(\beta A_m)$.

We ran large systems ($N = 2000$ as opposed to $N = 100$ in the original works) and looked at $N$ rounds per the trading period so that on average every trader is chosen

once to observe the order book and make a trading decision. This decision was taken to make the resemblance to our original model as close as possible, where a trader has at most one trade per the trading period. We also assume that every time an agent is chosen to make an action (either during the open call or the rounds during the trading period), (s)he consults its choosing strategy and only when the market is chosen the limit order book is consulted to decide on the trading action. As agents are chosen randomly to try to trade, the same agent can in principle be chosen to trade several times during a trading period. We assume that during a single trading period agent always uses the same choosing strategy, despite the fact that (s)he might have attempted to trade several times and consequently updated attractions.

**Simulation resuslts** We first analyse a system that is the most similar to our model - a population consisting of only uninformed traders. As noted, these traders are already improved compared to the ZI traders analysed so far; they have a knowledge of the latest trading price, and they have budget constraints. We simulate a system of $N = 2000$ of uninformed traders with two identical continuous double auctions markets and show the steady state results in Figure 4.8. The steady state distribution is a distribution at the end of 20 independent runs each lasting $200$ trading periods. Variable number of trading periods was simulated and for analysed values of $r$ we did not note departure from the strongly segregated state, thus we didn't run very long simulations (as before initial transient to the segregated state is very quick)[5].

Intriguingly, we note that despite the budget constraints and different trading mechanism, the segregation still emerges. In the right panel of Figure 4.8 we show Binder cumulant values for different intensities of choice that show same trend as in originally analysed model - the steady state for low $\beta$ is a Gaussian distribution (characterised by $B = 0$), while the high $\beta$ steady state is a bimodal distribution[6], e.g. segregated state.

We should stress that this system is very close to the equilibrium price setting ($\theta = 0.5$) we have used previously. This observation is supported by experiments of Gode and

[5] As previously, the observable we use to follow the changes in the system over time is the Binder cumulant, and we note quick initial convergence, within order $1/r$ trading periods and small fluctuations thereafter.

[6] $B \approx 0.5$, which is a finite $r$ correction to a distribution consisting of two equally weighted delta peaks with $B = 2/3$.

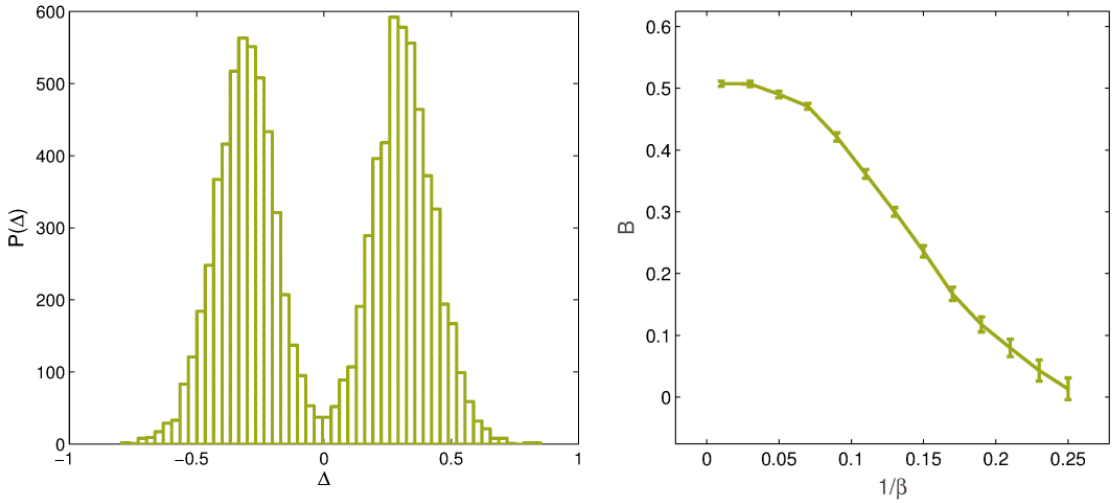


FIGURE 4.8: **Segregation of uninformed traders in the Toth model.** Left: Steady state distribution of uninformed traders with the forgetting rate $r = 0.05$ and intensity of choice $\beta = 5$. Right: Binder cumulant of the steady state distribution for different values of intensity of choice $\beta$ while $r = 0.05$.

Sunder [76] that show that random bidding agents in the continuous double auction retrieve the equilibrium trading price. Additionally, authors of the paper [105] argue that this is because of Marshallian price dynamics where extreme crossing orders are executed in alternating order until the equilibrium price is reached. See e.g. bids and asks in Fig. 2.1, but now all agents start with a Gaussian bids/asks centred around the same initial price (initially it is communicated to everyone that the stock value is $40$, thus in previous parameters $\mu_a = \mu_b$). The first trader who observes the bids and asks will be happy to execute either the highest bid or the smallest ask (as his price will still be in the vicinity of the mean of the Gaussian), as both of those will lead to large returns. Let's assume (s)he executes the bid; that means that the next trader's private value will be very large (random variable centred at past largest bid) so the lowest ask will be the most satisfactory, etc. This dynamics repeats until all the valid orders (in our previous notation) are traded and afterwards the traders either submit new orders or trade at prices close to the equilibrium trading price. That is why this system is the closest to our previously studied system with $\mu_a = \mu_b$ and two equal, fair markets. The steady state and the Binder cumulant values for different $\beta$ confirm this similarity.

Continuing the analysis of the Toth model, in Figure 4.9 we show the analogue of

Fig. 4.8 for a system with five subpopulations – from just analysed uninformed ones to those who know the future four dividend values. Remarkably we still observe qualitatively the same behaviour. In the left panel, we observe the bimodal steady state, with a half of population developing loyalty for both markets. In the right panel, we see a noisier variant of the plot we have observed before, but a tentative explanation is the following. Given that all the subpopulations have different private value, means of their Gaussian distributions are non-overlapping so the overall score distribution will not be just a simple truncated Gaussian distribution as previously. This will have its impact on attraction distribution and obviously on the Binder cumulants. Additionally, given that there is now a big influence of the dividend time series, the numerical runs should probably be averaged over many more independent runs. However, up to possible improvement of numerical results, the qualitative implications are clear already – even with more sophisticated trading strategies, agents still prefer to segregate, i.e. to trade at same markets for long periods of time before changing their loyalty.

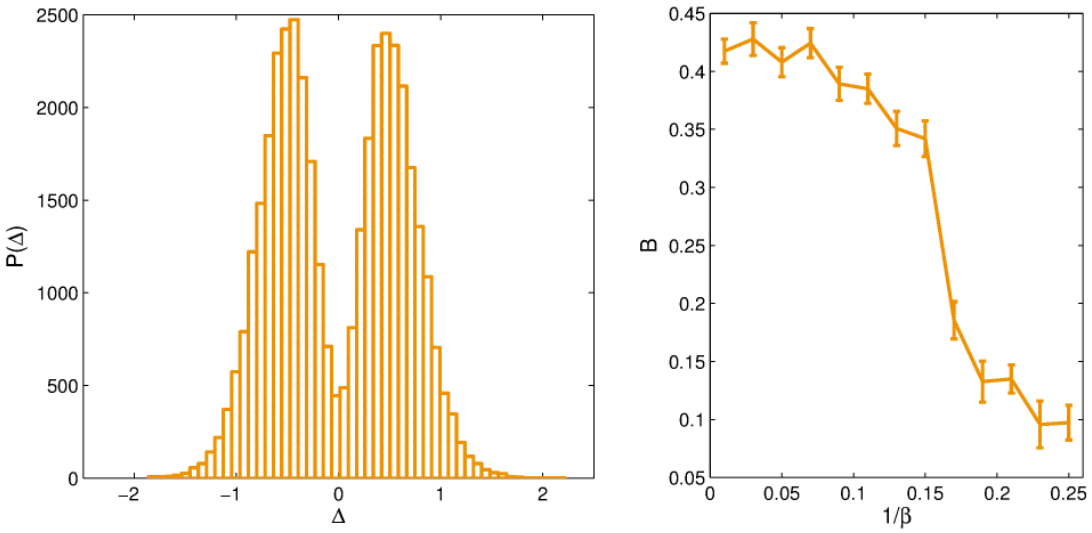


FIGURE 4.9: **Segregation of informed traders in the Toth model.** Left: Steady state distribution of informed traders with the forgetting rate $r = 0.05$ and intensity of choice $\beta = 20$. Right: Binder cumulant of the steady state distribution for different values of intensity of choice $\beta$ while $r = 0.05$. The population consists of $400$ traders of each information level $L = 0$ to $L = 4$. We do not note different steady states of the subpopulations with different information levels that is why the overall attraction distribution is shown.

Finally, we comment the original problem the Toth model was addressing. Namely,

Huber and Kirchler [101, 106] run several experiments where participants were trying to trade at a continuous double auction markets and were given different future dividends. The authors showed, contrary to previously believed, that the more information is not always the better. It was noted that the wealth does not grow monotonically with information, instead a "J curve" of wealth was reported. Only the most informed traders were able to outperform the market, while below average informed traders were worse off then the uninformed traders. Although the experiment participants were given the Gordon formula next to their information, it was not clear what drove this phenomenon in those experiments which is why Toth *et al.* [99, 100] developed a numerical model to help them reproduce the phenomena. Following the experiments, numerical simulations confirmed

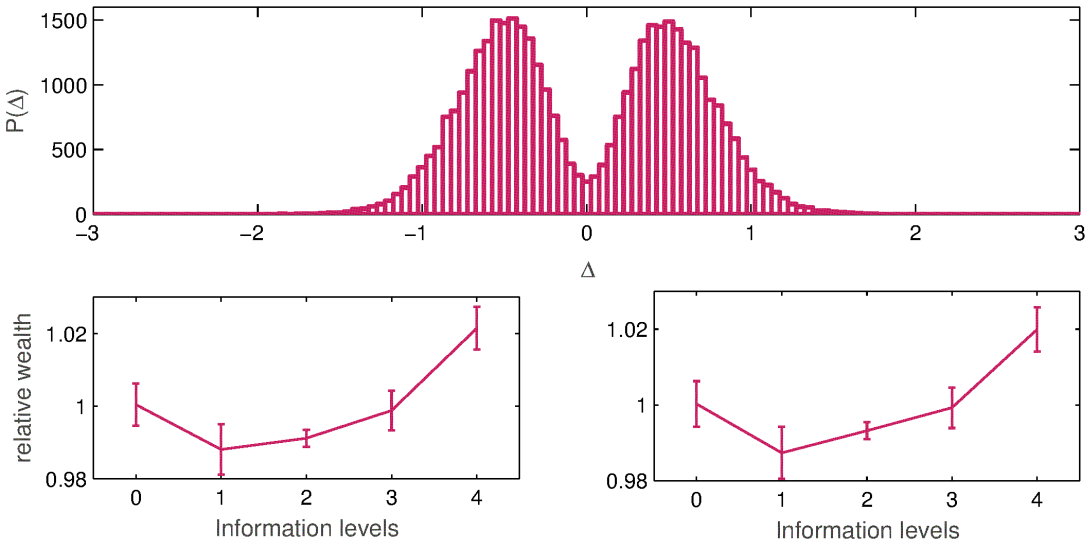


FIGURE 4.10: **Steady state distribution and wealth averages for different information levels at different markets.** Top: Steady state distribution of a 2000-traders population with five different information levels (uninformed, plus up to four future dividends) with learning parameters $r = 0.05$ and $\beta = 20$; Bottom: Average relative wealth for agents of each group is presented. We note that despite segregation into two distinguishable groups based on market preferences, the J curve in agents' wealth persists.

these effects in various scenarios, with different information cost functions [107] (fixed or linear information pricing preserves "J curve", but quadratic does not), noise [107] (exponential noise damages the structure, but fixed or linear do not affect the finding more than spreading the wealth distributions for each level). Other studies looked at the different distribution of informed traders (original study assumes a uniform distribution

of agents with different information level), both power law ( the majority of traders are uninformed or poorly informed) and normally distributed information levels within the population still lead to the "J curve" [102]. However, Kalimullina *et al.* [104] report that there is a critical frequency threshold of uninformed traders above which the effect disappears.

None of the studies investigated whether the effect persists when agents are given a choice of markets. If the agents with low information levels are exploited by the highly informed agents, so that they can outperform the market, it is unclear whether the agents with low information levels will still prefer to trade with informed agents if such choice exists. To investigate whether there is additional information structure in the segregated subgroups in Figure 4.10, beside already shown steady state, we show the relative wealth of agents with different information level who have preferences for the different markets. Intriguingly, we note that among agents of both markets, the same wealth distribution structure persists, showing that the reinforcement mechanism that leads the population to segregation did not perturb the information structures. We also note that there is no statistically significant difference in the number of agents of each information group in their preference for the market one or two. Probable reason for the persistence of "J curve" might be in the fact that agents do not base their market choice on their relative wealth, but still on their perceived scores, and as in our simplified model, with segregation they just might maximise their trading possibilities and thus perceived scores. On the other hand, if agents posses information about their relative wealth in the market (whether they are below or above average), the influence on the "J curve" phenomena might be different. As this is beyond the scope of this thesis, we discuss it in the last chapter, together with some more ideas on how to extend this model and investigate the phenomena.

## 4.4 Summary

The goal of this chapter was to investigate the robustness of the segregation phenomena by relaxing some of the simplifying assumptions and obtain a deeper understanding of the driving forces behind the segregation. We aimed to understand if the segregation

is only a mere consequence of the oversimplified model we have introduced, or beside its analytical tractability it provides fundamental insights. The results of the last section reassured us, as even in the more realistic double auction markets, with agents who have budget constraints and more sophisticated trading strategy, the segregation still occurs. This leads us to conclude that the key enabler of segregation is the reinforcement learning. This on its own is an interesting result as the reinforcement rule is although simple, a widely used one.

We discussed the learning rule in the first section and realised that only if agents are allowed not to update attractions to the unplayed actions (that effectively means updating them with the average return from the previous $1/r$ trades) the segregation is diminished. Additionally, we study this new unsegregated state and realise that for a wide range of intensities of choice it is better for the population (as compared to previously studied unsegregated state and strongly segregated one), but at high intensities of choice, segregation offers more benefits. This is mainly because the $\alpha = 0$ state in the high $\beta$ limit leads to the Nash Equilibrium that, as we already discussed, does not outperform strongly segregated state.

Finally, in this chapter, we also studied systems with multiple markets and realised that market coexistence is not always possible. For example, when agents are adaptive already for $M > 1$ when no symmetries are imposed our simple counting argument suggests that some of the markets will lose the competition. In a population with fixed buy/sell preferences, we note that full market coexistence leads to seemingly specialised markets, not all subpopulation visit all the markets. This is not a consequence of a market's targeting toward some subset of the population, but, as subpopulations will develop loyalty to only some markets, it will necessarily appear as if the market become specialised.

# Chapter 5

# Evolutionary Auctions

Competition for resources in biological context bears a resemblance to auction mechanisms, many agents compete but only a few (or only one) get the reward. Contrary to the well-studied auction models in the economy, a reasonable assumption in this context is that everybody (not only the winner) pays their bid, e.g. time/energy invested to endure a conflict or foraging food. Here we look at dynamics of the k-player all-pay auctions searching for the states evolution might favour. We analyse these systems with an associated birth-death process governed by agent's strategy success in the repeated interactions modelled as k-player all-pay auctions. Intriguingly, when more than one reward is available in competition, the specialisation arise. In the following chapter, we investigate under which conditions that happens (e.g. how many players interact, how large the second reward needs to be, etc.) and whether such states are stable.

## 5.1 Introduction

Pioneering works of Maynard Smith & Price [56] recognise that some animal conflicts resemble auctions. They introduce the game *War of attrition*, modelling non-violent interaction, an endurance contest between two individuals. The players' strategies are the times they are willing to spend in the contest; the longest enduring player will take the reward, and costs are evaluated based on the conflict duration, i.e. second player's endurance time. This game is a biological formalisation of the second-price sealed bid auction or Vickrey auction [108] in economic theory, with a single difference - not only the winner will pay the cost of enduring the competition.

In an evolutionary context, Haigh & Rose [59] generalise two player conflicts that could be modelled by auction theory and coin the phrase *evolutionary auctions*. They study variety of games smoothly varied from Scotch auctions, in which all participants pay their own bid (e.g. tree growth competition, where every player has an energy investment, but only the tallest tree wins the reward - most of the sunlight) to the other extreme, War of attrition in which the winner pays the co-player's bid. Early studies focused on the static description of the games, namely the evolutionary stable strategies (ESS - a strategy such that if employed by the population as a whole is resistant under a small number of invading mutant strategies, see [56] and Appendix G). Haigh & Rose showed that evolutionary auctions have a mixed strategy (a probability distribution over the domain of available actions, in the case of War of Attrition times $t$) ESS, except for the Scotch auction [58].

Evolutionary stable strategies for the War of Attrition game were found for the generalised number of players (see e.g. Bishop & Cannings [109], Haigh & Cannings [110] and more recently Chatterjee *et al.* [111]). A general number of participants in the Scotch auction was studied by Chatterjee *et al.* [111], and it was shown that the evolutionary stable strategy exists whenever the number of participants is greater than two. Chatterjee *et al.* also introduced convenient names for the two types of evolutionary auctions that we will use in this chapter - *all-pay biological auctions*, short APA, $k$ participant extension of Scotch auctions and *second-price all-pay biological auction*, SAPA, $k$ participant generalisation of the War of attrition game.

As previous authors noted [59, 111] evolutionary auctions with $k$ participants, represent a simple model for a variety of interactions in biological context, from competition for resources, e.g. treescape growth to maximise access to the sunshine, evolution of male traits that increase their sexual attractiveness (tail [112], ornaments [113]) but also their dominance over other males (weapon size [114]) to territory contests [115]. This motivates us to contribute to an investigation of the evolutionary dynamics of these games.

As opposed to other games studied to the great extents such as prisoner's dilemma or hawk-dove game, the evolutionary auction games have continuous strategy space, that makes them a convenient evolutionary model for various phenotypic features in the

living world, but also makes their analysis slightly more difficult.

Games with discrete strategy space are widely studied using evolutionary dynamics. From a set of microscopic rules, a birth-death process, macroscopic description is usually derived, in the form of replicator equation (and stochastic replicator equation, but also replicator-mutator equation, see e.g. Bladon *et al.* [116]). We also know that if it exists, an evolutionary stable strategy (ESS) is an asymptotically stable fixed point of the replicator dynamics (see e.g. Taylor & Jonker [117], Hofbauer & Schuster & Sigmund [118], Zeeman [119]). The reverse is not true, thus an interesting question is the stability of the mixed strategy fixed points in the parameter regions where an ESS does not exist, e.g. 2-player APA game.

The works of Chatterjee *et al.* [111] and Reiter *et al.* [55] suggest that an evolutionary dynamics of the APA and SAPA games studied in the form of the Fisher-Wright evolution converge to the ESS distributions. This motivated us to develop a theoretical framework analogous to the one previously known for the games with discrete strategy space. Similarly to the works of Taylor *et al.* [63] and Traulsen *et al.* [61, 62], we study frequency dependent Moran model – a birth-death process driven by the fitness obtained by repeated interactions described by the evolutionary auction games.

In the continuous strategy space, this work is motivated by Rogers *et al.* [64] who studied the evolution of continuously distributed phenomenological traits and effects of demographic noise to spontaneous speciation. Our work is a continuation in the same direction, formalising the methodology for the $k$ player evolutionary auctions with continuous strategies. This framework enables us to develop the replicator equation and confirms that the fixed points of this population dynamics corresponds to the evolutionary stable strategies. Furthermore, we can study the effects of demographic noise analysing the stochastic replicator equation and consequently analysing existence of cycles reported by Chatterjee *et al.* [111].

Finally, it is important to note that we will study population dynamics in the continuous time as Traulsen *et al.* [61, 62] did, rather than the discrete time dynamics of the Fisher-Wright type whose results are reported in Chatterjee *et al.* [111]. It has been shown that in the large population limit the diffusion approximation of the Fisher-Wright model

holds and the replicator and the stochastic replicator equation can be derived, see for example Chalub *et al.* [120]. These equations are equivalent to the replicator equations that can be derived from the continuous time Moran process up to time rescaling, i.e. Moran model is twice as fast as the analogue Fisher-Wright model [121–123].

## 5.2 Evolutionary dynamics for games with continuous strategy space

In this section, we develop a formalism for studying evolutionary dynamics of games with continuous strategy space. The goal is to derive the macroscopic replicator-like equation starting from the microscopic dynamics, a birth-death process governed by the fitness obtained by repeatedly playing a game. Having this description, we will be able to find the fixed points of the dynamics and analyse their stability, but also how the finite size effects (diffusion approximation) lead to deviation from the replicator limit. This has already been done for the games with discrete strategy space [61, 62]. In the space of continuous phenotypic traits, Rogers *et al.* [64] derive macroscopic stochastic dynamics for the co-evolution of species. Our works build upon these with an application to games with continuous strategy space such as all-pay auctions biological auctions, as introduced [55, 111] based on previous works [60, 110] and others.

We start with a population of $N$ individuals, each of which can play a pure strategy $s$, a real number corresponding to a waiting time in a conflict (like in the war of attrition game) or energy investment (foraging resources) or bidding value in the economic context. We assume well-mixed population with random interactions. In such a set up the state of the population at any given time is fully described by $n(s)$, a number of players of each type $s$:

$$n(s) = \sum_{i=1}^{N} \delta(s - s_i).$$

We can also introduce a density:

$$\psi(s) = \frac{1}{N}\sum_{i=1}^{N}\delta(s - s_i)\,, \tag{5.1}$$

as in the case of games with discrete strategy space, $\Psi$ can be interpreted as a mixed strategy of a single player, or the strategy density distribution in the population of individuals playing a pure strategy (e.g. population playing a pure strategy always bid $s^*$ is represented as $\psi(s) = \delta(s - s^*)$).

We look at the frequency-dependent generalized Moran process in which an individual is randomly selected for reproduction with probability proportional to its fitness. The identical offspring then replaces an individual that is randomly selected to die, keeping the population size constant. We consider this dynamics in a continuous time. We consider general form of transition rates without mutations defined as follows:

$$R_{s_1\to s_2}(\mathbf{n}) = N\frac{n(s_1)}{N}\frac{n(s_2)}{N}g(\pi(s_1),\pi(s_2)). \tag{5.2}$$

The factor $\frac{n(s_1)}{N}\frac{n(s_2)}{N}$ broadly represents rate with which an individual of the type $s_1$ meets an individual of the type $s_2$, while the factor $g(\pi(s_1),\pi(s_2))$ encodes selection pressure to replace less successful with a more successful strategy. Many choices exists in the literature (see e.g. Bladon *et al.* [116]), we restrict ourselves to the so-called local process [61] defined by:

$$g(\pi(s_1),\pi(s_2)) = \frac{1}{2}\left(1 + \frac{\pi(s_2) - \pi(s_1)}{\Delta\pi_{max}}\right), \tag{5.3}$$

where the $\Delta\pi_{max}$ represents the maximal difference between any two strategy's fitness and thus normalize the transition rates. The overall pre-factor N in the transition rates $R$ is there to ensure that the rate with which the event of the type $s_1 \to s_2$ occurs in the system in a state $n$ is proportional to the number of individuals in the population. The typical time between events scales as 1/N, while a unit of time corresponds to an $\mathcal{O}(N)$ number of events, so the time is measured on the level of generations. We will also use $T_{s_1\to s_2}(n) = R_{s_1\to s_2}(n)/N$. The quantity $\pi(s)$ is a fitness function fully defined by the

game or another type of interaction we might consider. In the general case, we might assume that the interaction includes $k$ individuals so, the most general form of $\pi$ is:

$$\pi(s) = \int ds_1 ... ds_{k-1} a(s, s_1, ... s_{k-1}) \psi(s_1) ... \psi(s_{k-1}), \tag{5.4}$$

where $a$ encodes the interaction (game or another type of k-player interaction). In the case of two-player game with a discrete number of strategies, $a$ is a payoff matrix, but in the general case, it is a payoff a player playing strategy $s$ gets when confronted with $k-1$ players taking actions $s_1 \cdots s_{k-1}$.

### 5.2.1 Functional system-size expansion

To follow the evolution of a population in the previously described process the quantity of interest is the functional $P$ on the space of functions $\psi$ and it is the evolution of $P(\psi, t)$ that we want to understand. Similarly to the formalism for games with discrete strategy space [61–63], we derive the master equation that describes the evolution of $P(\psi, t)$ and its diffusion limit, the Fokker-Planck equation. We introduce creation/annihilation operators (see for example van Kampen [90]) that correspond to a single birth/death events:

$$\hat{E}^{\pm}_{s'} P[\psi] = P\left[\psi \pm \frac{1}{N}\delta_{s'}\right],$$

where $\delta_{s'}(s) = \delta(s - s')$, i.e.

$$\left(\psi + \frac{1}{N}\delta_{s'}\right)(s) = \psi(s) + \frac{1}{N}\delta(s - s').$$

The functional master equation describing the previously introduced evolutionary dynamics is:

$$\partial_t P[\psi] = \int ds ds' \left(\hat{E}^{-}_{s} \hat{E}_{s'} - 1\right) \left\{R_{s \to s'}[\psi] P[\psi]\right\}, \tag{5.5}$$

where the transition rates are introduced as before $R_{s\to s'}[\psi] = N\psi(s)\psi(s')g(\pi(s),\pi(s'))$. We use the following expansion (a functional variant of the Kramers-Moyal expansion [90]):

$$\begin{aligned}\hat{E}_s^{\pm}Q[\psi] &= Q\left[\psi \pm \frac{1}{N}\delta_s\right] \\ &= Q[\psi] \pm \frac{1}{N}\frac{\delta}{\delta\psi(s)}Q[\psi] + \frac{1}{2N^2}\frac{\delta^2}{\delta\psi(s)^2}Q[\psi] + \mathcal{O}(N^{-3}),\end{aligned}$$

where $\delta/\delta\psi$ denotes functional differentiation. Master equation then becomes the functional Fokker-Planck equation:

$$\begin{aligned}\partial_t P[\psi] = &-\int dsds'\frac{\delta}{\delta\psi(s)}\left\{\mathcal{A}[\Psi,s,s']P[\Psi]\right\} \\ &+\frac{1}{2N}\int dsds'\frac{\delta}{\delta\Psi(s)}\frac{\delta}{\delta\Psi(s')}\left\{\mathcal{B}[\Psi,s,s']P[\Psi]\right\} + \mathcal{O}(N^{-3}),\end{aligned} \tag{5.6}$$

where $\mathcal{A}$ is the drift term:

$$\mathcal{A}[\Psi,s,s'] = \frac{R_{s\to s'}[\Psi] - R_{s'\to s}[\Psi]}{N},$$

and $\mathcal{B}$ is the diffusion term:

$$\mathcal{B}[\Psi,s,s'] = \frac{R_{s\to s'}[\Psi] + R_{s'\to s}[\Psi]}{N}.$$

We can also write a stochastic equation that corresponds to the Fokker-Placnk Eq. (5.6) (where we already simplified the drift term by explicitly writing transition rates $R_{s\to s'}[\Psi]$):

$$\partial_t\psi(s) = \psi(s)\int ds'\psi(s)[g(\pi(s'),\pi(s)) - g(\pi(s),\pi(s'))] + \frac{1}{\sqrt{N}}\eta(s,t).$$

Accordingly, the noise covariance is given by:

$$\begin{aligned}\langle\eta(s,t)\eta(s',t')\rangle = \delta(t-t')\Big[\delta(s-s')\int ds''\Big(&\psi(s)\psi(s'')[g(\pi(s''),\pi(s)) + g(\pi(s),\pi(s''))]\Big) \\ &- \psi(s)\psi(s')(g(\pi(s),\pi(s')) + g(\pi(s'),\pi(s))\Big].\end{aligned}$$

We can further simplify these equations using the expression for $g$ (Eq. 5.3) which leads to a stochastic replicator equation:

$$\partial_t \psi(s) = \frac{\psi(s)}{\Delta\pi_{max}}\Big(\pi(s) - \pi\Big) + \frac{1}{\sqrt{N}}\eta(s,t), \tag{5.7}$$

with noise covariance matrix:

$$\langle \eta(s,t)\eta(s',t')\rangle = \delta(t-t')\Big[\delta(s-s')\psi(s) - \psi(s)\psi(s')\Big], \tag{5.8}$$

where we also used the following property of the pairwise comparison rule $g(a,b) + g(b,a) = 1$ and $\pi$ is used to denote the average fitness $\pi = \int ds\pi(s)\psi(s)$. The stochastic replicator equation given by the Eqs. (5.7) was not previously derived for the games with continuous strategy space, while we demonstrated that following an analogous path from the birth-death process, a macroscopic equation can be derived. The existence of such a dynamical equation gives us a possibility to study steady states of the evolutionary dynamics in games such as evolutionary auctions. We can also analyse fixed point stability by methods of linear noise analysis, but also effects of finite population size that we demonstrate in the following sections.

### 5.2.2 Replicator limit

In this section, we study evolutionary auctions in the replicator limit (i.e. the limit of large populations $N \to \infty$). In this limit, the stochasticity in the Eq. (5.7) can be neglected, and we focus only on the deterministic equation and study the fixed points of the dynamics:

$$\partial_t \psi(s) = \frac{\psi(s)}{\Delta\pi_{max}}\Big(\pi(s) - \pi\Big).$$

Specially we study dynamics of evolutionary auctions whose evolutionary stable strategies were studied previously [55, 56, 59, 109, 111]: (1) APA - all-pay biological auction (generalisation of the scotch auction); (2) APA with two rewards; (3) SAPA - second-price all-pay biological auction (generalization of the war of attrition).

**All-pay auctions (APA).** In APA games we study $k$ players competing for a single reward $V$. Every player has a strategy $s \in [0, V]$, a player with the highest strategy wins the reward $V$, but everyone pays the cost of playing the strategy $s$. Examples of these types of interactions in natural world include competition for resources (e.g. $s$ can correspond to the energy a tree invests in growing a tall scape to reach the reward - sunlight) and evolution of ornament and weapon traits in males to attract females or defend territory. There is a cost associated with producing and bearing a larger weapon, such as horn, but it might lead to rewards without battle as often its purpose is to demonstrate the power rather than to practice it [124].

Strategy space is continuous and bounded by the reward value (i.e. $s \in [0, V]$) as investing more than the reward $V$ would lead to negative fitness[1]. The payoff function for $k$ players - the fitness a player bidding $s$ receives, assuming that other $k-1$ players bid $s_1, s_2, ...s_{k-1}$) is:

$$a_{APA}(s, s_1, ...s_{k-1}) = \begin{cases} V - s, & \prod_{i=1}^{k-1} \theta(s - s_i) = 1 \\ \frac{V}{m} - s, & \sum_{i=1}^{k-1} \delta_{s,s_i} = m - 1 \neq 0 \wedge \prod_{i=1, s_i \neq s}^{k-1} \theta(s - s_i) = 1 \\ -s, & \prod_{i=1}^{k-1} \theta(s - s_i) = 0 \end{cases} \tag{5.9}$$

where $\theta(x)$ is the Heaviside step function ($\theta(x) = 1, \forall x > 0$ and $\theta(x) = 0, \forall x < 0$). The middle term in the payoff function represents the reward splitting which takes place when the highest bid is not unique and the reward is divided among the winners. In case of continuous strategy space, this can be neglected as the set of such events has measure 0, so the payoff function can be simplified to:

$$a_{APA}(s, s_1, ...s_{k-1}) = V \prod_{i=1}^{k-1} \theta(s - s_i) - s.$$

[1]Bidding values that lead to negative returns even when the reward is obtained, i.e. $s > V$ is not considered, as not playing, i.e. $s = 0$ is allowed in the game, so an agent should always favour nonegative return.

When taking an action $s$, the expected fitness in a population where every agent plays the same strategy $\psi(s)$ is:

$$\begin{aligned}\pi_{APA}(s) &= \int ds_1...ds_{k-1} a_{APA}(s, s_1, ..s_{k-1})\psi(s_1)...\psi(s_{k-1}) \\ &= \int ds_1...ds_{k-1}(V\prod_{i=1}^{k-1}\theta(s-s_i)-s)\psi(s_1)...\psi(s_{k-1}) \\ &= V(\int_0^s ds'\psi(s'))^{k-1} - s \\ &= V\phi^{k-1}(s) - s. \end{aligned} \tag{5.10}$$

Where $\phi(s)$ is $\phi(s) = \int_0^s ds'\psi(s')$. Interpretation of this fitness is clear - only if $k-1$ players invest lower amounts of energy, a player with strategy $s$ wins the reward V, while (s)he pays own investment $s$ in any case. To find a non-trivial fixed point[2] we require $\pi(s) = c, c = const$ for all $s$ where $\psi(s) > 0$[3]. Consequently $\phi(s)$ is:

$$\phi(s) = \left(\frac{c+s}{V}\right)^{\frac{1}{k-1}}. \tag{5.11}$$

Using the normalisation condition (i.e. $\phi(V) = 1$) we obtain $c = 0$. Interestingly, at the fixed point fitness for playing any pure strategy $s$ is 0, and consequently any player receives the fitness (s)he would receive even if (s)he was not playing the game. The fixed point distribution of strategies is:

$$\psi(s) = \frac{1}{(k-1)V}\left(\frac{s}{V}\right)^{\frac{2-k}{k-1}}. \tag{5.12}$$

These are the mixed strategy solutions previously reported by Chatterjee *et al.* [120] and specially for $k = 2$ where the distribution is uniform $\psi(s) = 1/V$ by Haigh and Rose [59]. In Figure 5.1 we show fixed point distributions of the replicator dynamics for different number of game participants $k$. We note that the fixed point of the replicator dynamics are the evolutionary stable strategies (ESS) previously reported in [111] and [59] when

[2] Any pure strategy, i.e. $\psi(s) = \delta(s - S^*)$ would be a solution of the replicator equation, as $\psi(s) = 0, \forall s \neq S^*$, while for $S^*$ fitness related to it is equal to the population average. However, we denote this fixed point as trivial and search for the nontrivial (mixed), defined on the full domain $s \in [0, V]$.

[3] This is because in that case, also the population average fitness is constant $\pi = \int ds\pi(s)\psi(s) = c$ and we note that for the fixed point distribution defined on the whole domain the replicator equation will lead to $\partial_t\psi(s) = 0$,$\forall s \in [0, V]$.

FIGURE 5.1: **Fixed point mixed strategy distributions of evolutionary auction games with different number of players $k$.** Left: all-pay biological auctions (APA); Right: Second-price all-pay biological auctions (SAPA). The reward value is $V = 1$, note domain of APA games is $[0, V]$, while the strategy domain of SAPA games is $[0, \infty)$, only the $[0, V]$ interval is shown for comparison with APA games.

$k > 2$. This is is because $\pi(s) = const, \forall s$ is a necessary condition for an ESS, although not sufficient (see e.g. Bishop-Canings theorem [60]). This tells us that introduced dynamics, fitness dependent birth-death process, has a unique mixed strategy fixed point that is also an ESS, except for the $k = 2$ as proved previously [59, 111]. The all-pay biological auction with 2 players will be additionally discussed in further sections as there are various dynamical features that distinguish this game from the others.

**Second highest bid all-pay auctions (SAPA).** These games are a $k$ player extension of the famous War of attrition game [56, 57, 109, 110] ($k = 2$) that model animal conflict - whoever waits for longer wins but pays only in time spent in the game, i.e. the second highest bid. As before, we introduce generalised fitness function and find the fixed point of the Eq. (5.7). The payoff function for the Second Price all-pay Auctions is:

$$a(s, s_1, ...s_{k-1}) = \begin{cases} V - \max(s_1, ...s_{k-1}), & \prod_{i=1}^{k-1} \theta(s - s_i) = 1 \\ \frac{V}{m} - s, & \sum_{i=1}^{k-1} \delta_{s,s_i} = m - 1 \neq 0 \wedge \prod_{i=1, s_i \neq s}^{k-1} \theta(s - s_i) = 1 \\ -s, & \prod_{i=1}^{k-1} \theta(s - s_i) = 0 \end{cases} \tag{5.13}$$

that as before we can simplify to:

$$a_{SAPA}(s, s_1, ...s_{k-1}) = (V + s - \max(s_1, ...s_{k-1})) \prod_{i=1}^{k-1} \theta(s - s_i) - s,$$

neglecting reward-splitting terms as argued previously. We see that it differs from the APA payoff function in the maximum term to account for the second highest bid that is the cost the winner pays. We proceed to calculate the average payoff of a strategy $s$:

$$\begin{aligned}
\pi_{SAPA}(s) &= \int ds_1...ds_{k-1} \left( (V + s - \max(s_1, ...s_{k-1})) \prod_{i=1}^{k-1} \theta(s - s_i) - s \right) \psi(s_1)...\psi(s_{k-1}) \\
&= (V + s)\phi^{k-1}(s) - \int ds_1...ds_{k-1} \max(s_1, ...s_{k-1}) \prod_{i=1}^{k-1} \theta(s - s_i)\psi(s_1)...\psi(s_{k-1}) - s \\
&= (V + s)\phi^{k-1}(s) - (k-1) \int ds_1...ds_{k-1} s_1 \theta(s - s_1) \prod_{i=2}^{k-1} \theta(s_1 - s_i)\psi(s_1)...\psi(s_{k-1}) - s \\
&= (V + s)\phi^{k-1}(s) - (k-1) \int_0^s ds' s' \psi(s')\phi^{k-2}(s') - s \\
&= (V + s)\phi^{k-1}(s) - s - (k-1)\Big(s\frac{\phi^{k-1}(s)}{k-1} - \frac{\int_0^s ds'\phi^{k-1}(s')}{k-1}\Big) \\
&= V\phi^{k-1}(s) - s + \int_0^s ds'\phi^{k-1}(s'). \qquad (5.14)
\end{aligned}$$

We can note that the last term in the fitness is a correction to the APA game due to the fact that the winner does not pay his/her bid but the second highest one. Requiring again that the $\pi(s) = const$ for all $s$ for which $\psi(s) > 0$, we obtain the cumulative distribution $\phi(s)$ and the fixed point distribution $\psi(s)$:

$$\begin{aligned}
\phi(s) &= \Big(1 - \exp(-\frac{s}{V})\Big)^{\frac{1}{k-1}}, \\
\psi(s) &= \frac{1}{V(k-1)} \Big(1 - \exp(-\frac{s}{V})\Big)^{\frac{2-k}{k-1}} \exp(-\frac{s}{V}).
\end{aligned}$$

These fixed points are previously reported evolutionary stable strategies, and for the 2-player game we retrieve famous Maynard Smith & Price's result [56] - the evolutionary stable strategy of the War of attrition game: $\psi(s) = \frac{1}{V}\exp(-s/V)$. SAPA game has a mixed strategy ESS for all $k$ which is why we expect to find that the fixed points are

asymptotically stable. In Figure 5.1 we show these fixed point mixed strategy distributions next to the corresponding strategies of APA games. Note that we only plot a part of the SAPA fixed point distributions as these are defined on $[0, \infty)$ domain.

Specially, when the strategy space is not $s \in [0, \infty)$ but there is a maximal bidding value $A$, Bishop and Cannings [109] prove that the mixed strategy distribution is an ESS only if the maximal strategy is attainable, i.e if the domain is $s \in [0, A]$. They also prove that the ESS distribution is not a continuous function but there is a gap in the strategy support - playing the highest strategy is always beneficial, so there will always be a delta peak at $s = A$, however bidding slightly below will lead to worse results which is why these strategies are avoided. We demonstrate this by finding the fixed point of the SAPA game in the domain $[0, A]$ in Appendix I and realize that the strategies that are less than the reward value $V$ smaller than the highest bidding value $A$ are not played by the population at the fixed point, i.e. the fixed point distribution is previously found continuous distribution on $[0, A - V]$ with a delta peak at $s = A$ that takes care of the normalization. Interestingly, when $A = V + \epsilon$ ($\epsilon$ being any small positive number) that leads to the specialised population, a fraction of population bids $s = 0$ effectively not playing, while the other group bids $s = V$, we discuss this in more detail in Appendix I.

**All-pay auctions with multiple rewards.** Although already early works of Maynard Smith& Price [56, 57] and Haigh & Rose [59] pointed out that many animal interactions have the structure of the auctions, recent works added an important extension when auctions are applied in ecological context - multiple rewards [55]. In previously described metaphor of growing trees competing for the sunshine or large flowers attracting insects, it is difficult to argue that the player with the second highest strategy is left without any reward, similarly the third, etc.

Accordingly, we follow the game extension suggested by Reiter *et al.* [55] and study the all-pay biological auction with $r$ rewards available, we assume $r \leq k$ and the following order $V_1 \geq V_2 \geq \cdots \geq V_r$. As in the single reward case, when the space of available strategies is continuous we can neglect reward splitting, i.e. the probability of non-unique highest bid is zero. In analogy with previously studied games, the fitness of

an individual playing strategy $s$ is:

$$\pi(s) = \sum_{i=1}^{r} V_i \binom{k-1}{i-1} (1-\phi(s))^{i-1} \phi^{k-i}(s) - s,$$

i.e. the player receives reward $V_i$ if $i-1$ players were playing higher strategy - invested more, (with probability $(1-\phi(s))$) while other $k-i$ players invested less (with prob $\phi(s)$). We also need to take into account selection of $i-1$ higher bidders out of $k-1$ available players, thus binomial coefficient.

To find the interior fixed point of the replicator dynamics, again we find $\psi(s)$ from $\pi(s) = const$ for all $s$ in the support of $\psi(s)$. Enforcing conditions on $\phi$ to ensure it is a properly defined cumulative distribution (i.e. $\phi(0) = 0$ and $\phi(V_1) = 1$) we find that $\pi(s) = 0$ for all $s$, i.e. at the fixed point average fitness of any pure strategy against the population is zero. Finally, we note that $\phi(s)$ is a root of the $k-1$-th order polynomial that does not have a closed form expression but we can find solutions numerically. As reported by Reiter *et al.* [55] we realize that for some values of rewards and $k > 2$ participants in the auctions the fixed point mixed strategies differ drastically from the single reward game. Specially, we note that the distributions become bimodal - population splits into low bidders and high bidders for $k > 3$ participants in an auction. To analyse this further we focus the rest of multiple reward APA analysis to the simplest case – only two rewards. This game already offers variety of interesting fixed points, while still being simpler to analyse. We assume $V_1 = V$ and $V_2 = \alpha V$, thus the fitness when playing $s$ becomes:

$$\begin{aligned}\pi(s) &= V\phi^{k-1}(s) + \alpha V(k-1)(1-\phi(s))\phi^{k-2}(s) - s \\ &= V(1-\alpha(k-1))\phi^{k-1}(s) + \alpha V(k-1)\phi^{k-2}(s) - s.\end{aligned}$$

In line with our main question of specialization (segregation-like phenomenna), we are interested to find for which game parameters, i.e. pairs of $(k, \alpha)$, fixed point distribution $\psi(s) = \dfrac{d\phi(s)}{ds}$ becomes bimodal. To be a bimodal distribution, $\psi(s)$ has to have an interior minimum, i.e. $\psi'(s_m) = 0$ and $\psi''(s_m) > 0$. Starting from the relation $\pi(s) = 0$ and its

derivatives, we obtain:

$$\phi(s_m) = \frac{(3-k)\alpha}{1-(k-1)\alpha}.$$

As long as $\phi(s_m) \in (0,1)$, there is unique $s_m$ and the distribution is bimodal, and this requirement gives us relation between $\alpha$ and $k$ that enables specialization. As our numerical exploration already showed us that fixed points of $k = 3$ are always unimodal, monotonically decreasing for $\alpha < 0.5$, constant for $\alpha = 0.5$ and increasing for $\alpha > 0.5$, we look only at $k > 3$:

$$\frac{(3-k)\alpha}{1-(k-1)\alpha} > 0 \iff \alpha > \frac{1}{k-1}$$
$$\frac{(3-k)\alpha}{1-(k-1)\alpha} < 1 \iff \alpha > \frac{1}{2}.$$

As the second constraint is stronger for all $k > 3$ we realize that the critical reward ratio is independent of $k$ - when the second reward is higher than a half of the first reward the population fixed point includes a fraction of high bidders.

In Figure 5.2 we show fixed point distributions for $k \geq 3$ and $\alpha = 1$. We note that for all $k > 3$ the fixed point distributions are bimodal, but we also note that the fraction of high bidders decreases with $k$. To quantify this observation in the right panel of Figure 5.2, we plot the fraction of players at the $s = V$ peak (if $s_m$ is the minimum of $\psi(s)$, fraction of high bidders is $1-\phi(s_m)$) as a function of $\alpha$ for various $k$. We note that with an increase of game participants $k$ fraction of high bidders decreases as a number of rewards become small compared to the group size making the game effectively comparable to a single reward game with a large number of participants.

Finally, Reiter *et al.* [55] proved that for $k = 3$ the evolutionary stable state exists only when $\alpha < 0.5$, corresponding to the region of reward ratios when the fixed point distribution is a monotonically decreasing function (as for $\alpha = 0$). This is interesting because in the 3-player game the population does not undergo specialisation, but for $\alpha > 0.5$ the distribution is an increasing function, with a majority of the population making big energy investments (for $\alpha = 0.5$ the distribution is uniform). This prompts the question whether the bimodal fixed point distributions we find for $k > 3$ and $\alpha > 0.5$

FIGURE 5.2: **Fixed point distributions for the APA evolutionary game with two rewards and variable number of players $k$.** Left: Fixed point distributions for $\alpha = 1$; Right: Fraction of players at the high bidding peak as function of reward ratio $\alpha$. Circles in the right panel show $\alpha_c$ above which the bimodal fixed point distribution is not an evolutionary stable strategy.

are evolutionary stable strategies (they are nevertheless unique interior fixed points of the evolutionary dynamics we have introduced). Following the procedure outlined by Chatterjee *et al.* [111] and Reiter *et al.* [55], based on general formalism introduced by Maynard Smith [57], we prove that for $k > 3$ the bimodal fixed point distribution are evolutionary stable but only in some regime of $\alpha$ with $\alpha_c$ increasing with $k$. In Figure 5.2 with coloured circles in the right panel we mark $\alpha_c$ above which an ESS does not exist (details of numerical calculations are in Appendix G). As the mixed strategy fixed point, we have found is unique and defined for all $\alpha$, we will address in the following sections whether some of its properties change for $\alpha > \alpha_c$.

We note that in the replicator limit, we retrieve previously reported evolutionary stable strategies for the single reward games. Based on the previous results [117–119] we expect that the fixed points we have found are asymptotically stable. However, the APA game with two players is known not to have an evolutionary stable strategy. Thus it is curious to investigate its stability under the evolutionary dynamics that we have introduced. Similarly, we have extended the results of Reiter *et al.* [55] in the domain of two reward games and proved that when a number of players is greater than three bimodal

distributions (specialised populations) are evolutionary stable, but only in part of the domain of reward ratios. As the mixed strategy fixed point is unique for all the reward rations, we ask if there is an associated loss of stability under the evolutionary dynamics once the strategy stops being an evolutionary stable one. As previously remarked, the relation between stability and the ESS is not equivalent, i.e. an ESS is an asymptotically stable fixed point, but the converse is not true.

Similarly as in chapters that preceded, our foremost interests are in the states that are selected by an adaptive population in a dynamical process (previously it was adaptive learning, while now it is natural selection). We compare our results with the states found by static analysis (such as the Nash equilibrium or the evolutionary stable strategies) as those are known to have remarkable properties, but our goal is to investigate which states the population selects and if those might even be better (e.g. strongly segregated state vs. envy-free Nash equilibrium). That is why we investigate the stability of the fixed points, rather than focus on the evolutionary stable strategies. We utilise methods of linear stability, but also we investigate effects of finite population. We will analyse if the stochasticity that the finite population brings (demographic noise) might induce cycles that were reported by Chatterjee *et al.* [111].

#### Linear Noise Approximation

Previously, we have found unique mixed strategy fixed point distributions for various evolutionary auction games, to know something about their stability would evidently be useful. Specially, in some cases previous results reported that the fixed points are the evolutionary stable strategies, so their asymptotic stability should be expected [117–119]. In some other cases e.g. 2 player APA game, there is no evolutionary stable strategy so it would be interesting if we can understand stability of the fixed point we have found. To answer these questions we use methods of linear stability. Starting from the replicator

equation (5.7):

$$\begin{aligned}\dot{\psi}(s) &= \frac{\psi(s)}{\Delta\pi_{max}}\left(\pi(s) - \int ds'\pi(s')\psi(s')\right) \\ &= \frac{\psi(s)}{\Delta\pi_{max}}\left(\int ds_1...ds_{k-1}a(s,s_1,..s_{k-1})\psi(s_1)...\psi(s_{k-1})\right. \\ &\left. - \int ds'ds_1...ds_{k-1}a(s',s_1,..s_{k-1})\psi(s')\psi(s_1)...\psi(s_{k-1})\right),\end{aligned} \tag{5.15}$$

we perform functional linearisation around the fixed point $\psi^*(s)$. When $\psi(s)$ is in the vicinity of the fixed point (i.e. $\psi^*(s) + \delta\psi(s)$) and keeping only the terms linear in $\delta\psi(s)$ the following equation is obtained:

$$\partial_t\delta\psi(s) = \int ds' J(s,s')\delta\psi(s'),$$

where the functional Jacobian for the fixed point of the replicator equation is:

$$J(s,s') = \frac{\psi^*(s)}{\Delta\pi_{max}}\Big((k-1)M(s,s') - \pi^*(s') - (k-1)\int drM(r,s')\psi^*(r)\Big). \tag{5.16}$$

With $*$ we denote all the evaluations at the fixed point of the replicator Equation (5.7), while the $\Delta\pi_{max}$ is the maximal difference between the payoffs of players with different bidding strategies which is equal to $V$. We also note that for the evolutionary auction games we have proved the fitness at the fixed point is zero ($\pi^*(s) = 0$). To simplify the equation in the Jacobian we have introduced $M(s,s')$:

$$M(s,s') = \int ds_2...ds_{k-1}a(s,s',s_2,...s_{k-1})\psi^*(s_2)...\psi^*(s_{k-1}),$$

it is an effective two player payoff function in the k-player game, i.e. $M$ denotes payoff a player playing $s$ obtains against $s'$ averaged over the remaining $k-2$ agents.

In the most general case, for a specific game, we can calculate $M(s,s')$ and consequently the integral operator $J(s,s')$ and sometimes its spectra will be known in the most general case. We leave explicit forms of these operators for Appendix F where we also prove that for APA games with $k = 2$ players there is only a single eigenvalue – zero, whose corresponding eigenfunction is a constant (as also the fixed point distribution is,

i.e. $\psi(s) = 1/V$). For the general $k$ evolutionary auction game the spectrum of the continuous operator is not easily attainable, so we only leave our preliminary results in the supplementary material.

Another route we can take analysing the stability of the previously found fixed points is to look at the system with discrete strategies where the spectra could be numerically analysed. When the spectra of the operator is not easily analysed in the continuous case, instead of discretizing the continuous operator (5.16) and analysing the spectra of a matrix obtained that way, we propose to reintroduce the problem in the discrete strategy set up and observe how the results behave when the discretization becomes finer to help us conjecture something about the fixed point stability in the continuous strategy space. We propose this approach as a potentially more careful way to analyse the spectra (it is known that the discretisation of continuous operators sometimes leads to spurious spectral results, see e.g. section 5.4 of Wing [125]). For a small number of available discrete strategies $L$, we will note that the discrete problem is clearly different from the discretised continuous problem, but we expect these differences to decay as $L$ increases.

## 5.3 Evolutionary auctions with discrete strategy space

In this section, we address the dynamics of the biological all-pay auctions when the bidding strategies are available only in the discrete steps. We consider this simplification as the discrete strategy space is easily accessible in numerical simulations and the linear noise analysis becomes numerically accessible. Additionally, numerical results of evolutionary dynamics in discrete strategy space reported by Chatterjee *et al.* [111] showed interesting dynamical features - ESS present only as a long time average and an existence of cycles. To reproduce and study these effects closely we will reintroduce the problem of k-player evolutionary auctions in the system with discrete strategy space.

We will assume that the strategy space is discretized with steps $\Delta$, i.e. strategy $S_i$ correspond to bidding the value $i\Delta$, with $i = 1 \dots L$ spanning strategy space equidistantly. Previously it has been shown (e.g. Traulsen *et al.* [61]) how from the generalized Moran

process the stochastic replicator equation can be derived, we thus only state it below:

$$\dot{\psi}_i = \frac{\psi_i}{\Delta\pi_{max}}\Big(\pi_i - \pi\Big) + \frac{1}{\sqrt{N}}\eta_i(t), \tag{5.17}$$

with the following noise covariance matrix:

$$\langle \eta_i(t)\eta_j(t)\rangle = \delta(t-t')\Big(\delta_{ij}\psi_i - \psi_i\psi_j\Big).$$

Here it is worth noting that the stochastic replicator equation itself is not different from the discretized Eq. (5.7). What makes the following analysis different from the discretized version of the previous results is encoded in the payoff $\pi_i$ and comes from the treatment of situations when the highest bidding strategy is not unique. As we argued when the space of strategies is continuous the probability of such events is 0, but that is not the case when the strategy space is discrete. Below we show and discuss the fitness associated with playing a strategy $S_i$ in evolutionary auction games. The fitness of an individual playing strategy $S_i$ in the All-Pay Auction is:

$$\pi_i^{APA} = \sum_{m=1}^{k} \frac{V}{m}\binom{k-1}{m-1}\psi_i^{m-1}\left(\sum_{j=1}^{i-1}\psi_j\right)^{k-m} - S_i. \tag{5.18}$$

In the Eq. (5.18), all the terms for $m \geq 2$ are payoff contributions in situations of non-unique highest bid when the reward is only partially obtained, either by randomly selecting a winner that earns the whole reward $V$ or all the winners receiving an equal part of the reward. Specially, playing the lowest strategy $S_1$ leads to the reward only if all other $k-1$ players do the same, i.e. $\pi_1 = (V/k)\psi_1^{k-1} - S_1$. On the other hand, we can introduce a game in the space of discrete strategies that will lead to the same fitness and fixed point as the discretized Eq. (5.12) in the following way - nobody wins the reward if the highest strategy is not unique. Some details on this game we discuss in Appendix H, but if APA game is used as a metaphor for previously described biological interactions, we believe splitting the reward is a more reasonable assumption. We also extend the

fitness to the two reward APA game:

$$\pi_i^{2APA} = V\left(\sum_{j=1}^{i-1}\psi_j\right)^{k-1} + \sum_{m=2}^{k}\frac{V(1+\alpha)}{m}\binom{k-1}{m-1}\psi_i^{m-1}\left(\sum_{j=1}^{i-1}\psi_j\right)^{k-m} + (k-1)\left(1-\sum_{j=1}^{i}\psi_j\right)\sum_{m=1}^{k-1}\frac{V\alpha}{m}\binom{k-2}{m-1}\psi_i^{m-1}\left(\sum_{j=1}^{i-1}\psi_j\right)^{k-1-m} - S_i, \quad (5.19)$$

where we assumed as before that the second reward is $\alpha$ times smaller than the first one ($\alpha \in [0,1]$). Here we also introduce non-unique highest bidding strategy corrections (the second and third term): (1) if the highest strategy is not unique, players split both rewards; (2) if the second highest strategy is not unique players split the second reward.

Similarly, the fitness when playing the strategy $S_i$ in the SAPA game is:

$$\pi_i^{SAPA} = (V+S_i)\left(\sum_{j=1}^{i-1}\psi_j\right)^{k-1} + \sum_{m=2}^{k}\frac{V}{m}\binom{k-1}{m-1}\psi_i^{m-1}\left(\sum_{j=1}^{i-1}\psi_j\right)^{k-m} - \sum_{j=1}^{i-1}S_j\left(\Big(\sum_{l=1}^{j}\psi_l\Big)^{k-1} - \Big(\sum_{l=1}^{j-1}\psi_l\Big)^{k-1}\right) - S_i. \quad (5.20)$$

It is worth noting that whenever the highest bid is not unique there is no difference between APA and SAPA games as in both cases the reward will be split and everyone will pay their own bid. However, when in the SAPA game the highest bid is unique the payment is smaller, described by the second to last term in Eq. (5.20). As argued before, the domain of APA game strategies is $S \in [0, V]$, while for the SAPA games $S \in [0, \infty)$ and consequently when discretising SAPA games beside the strategy density we need to decide the cut off. The set up of the game with the discrete strategy space enables us to study more directly fixed points of the dynamics, their stability and the possible existence of the noise induced cycles. Following the same line of arguments as in the continuous space of strategies we can introduce a Jacobian of the system in the following way:

$$J_{ij} = \frac{\psi_i^*}{\Delta\pi_{max}}(k-1)\left(M_{ij} - \sum_{l=1}^{L}\psi_l^* M_{lj}\right), \quad (5.21)$$

where as before $M_{ij}$ is an effective payoff matrix for two players $i$ and $j$ in the field of $k-2$

players (explicit form for $M_{ij}$ of all evolutionary auction games are in Appendix H). At this stage we can analyse the spectra of the Jacobian matrix and based on its eigenvalues we can say more about the fixed point's stability, these we will present in the following sections for the APA and SAPA games.

Previously, we only focused on the replicator limit where we assume infinite population size and consequently that all the fitnesses can be well estimated and the dynamics follow the replicator equation. In the case of finite populations, due to the random nature of the microscopic interaction, the dynamics follows stochastic replicator equations (5.17). For populations of a finite size, we would like to investigate the effects of the noise. When many strategies are available, it is not improbable that some number of eigenvalues will be complex numbers. In the limit of infinite population, these eigenvalues would correspond to spiralling trajectories towards the fixed point, i.e. damped oscillations. However, in the finite system regime, persistent random fluctuations drive the system away from the fixed point. Sometimes, the combination of these two effects results in a coherently maintained cyclic patterns [116, 126]. To look for the existence of these effects, we take a Fourier transform of the stochastic replicator equation and from there we derive the noise induced power spectra (the method is also described here [116, 126]). In the linear noise approximation the stochastic replicator equation can be approximated to:

$$\partial_t \psi_i = \sum_j J_{ij}\psi_j + \eta_i. \tag{5.22}$$

The Fourier transform of this equation in the matrix form is:

$$(i\omega \mathbf{I} - \mathbf{J})\tilde{\psi} = \tilde{\eta}.$$

Finally, the power spectra that we can measure in the numerical simulations as well as analytically is:

$$\mathbf{P}(\omega) = \langle \tilde{\psi}^T \tilde{\psi} \rangle = (i\omega \mathbf{I} - \mathbf{J})^{-1} \langle \eta^T \eta \rangle \left(-i\omega \mathbf{I} - \mathbf{J}^T\right)^{-1}. \tag{5.23}$$

We can either look at the oscillations in the number of agents playing the same strategy $S_i$ and that corresponds to the $\mathbf{P}(\omega)_{ii}$, but often it is useful to look at the overall noise effects on all the strategies together i.e. $P(\omega) = Tr[\mathbf{P}(\omega)]$. We will look for amplification induced by the demographic noise that we should be able to detect as peaks in the power spectra at positive frequencies. In the following sections, we show how this analysis can be implemented in the case of specific games All-Pay Auctions (APA) and Second highest bid All-Pay Auctions (SAPA).

### 5.3.1 All-pay biological auctions APA

In this section, we present the results of evolutionary dynamics of a population playing APA game with discrete strategies. We initially only analyse the games with more than two players ($k > 2$) previously reported to have an evolutionary stable strategy and address the dynamics of 2-player game at the end of the section. We start our investigation with games with only a few available strategies followed by a general finite $L$ number of strategies and finish with conjectures about the $L \to \infty$ limit.

**Small number of available strategies.** Firstly, we analyse *3-player* games with $L = 3, 4$ available strategies because of simplicity and instructiveness of these games where the evolution of the population is still easy to follow in a simplex. The dynamics of such a system can be described by a small set of stochastic replicator equations, introduced previously. Using the replicator limit approximation (i.e. just the first term on the right side of Eq. (5.17)) we find the fixed point of the dynamics (the fitness is described by Eq. (5.18) for $k = 3$).

In Figure 5.3, we show results of a game with 3 available strategies, e.g. tree levels of energy investments in a competition. We show the vector field of the corresponding replicator equations together with a single realisation of a numerically simulated birth-death process. We note that the numerically simulated population dynamics converges to the analytically predicted fixed point. In the phase portrait, we only present the first part of the trajectory, the initial convergence to the fixed point, while the further dynamics we depict with a single time series of the number of players bidding the lowest value in the top panel of the same Figure 5.3. Analysing the vector field we realise that the

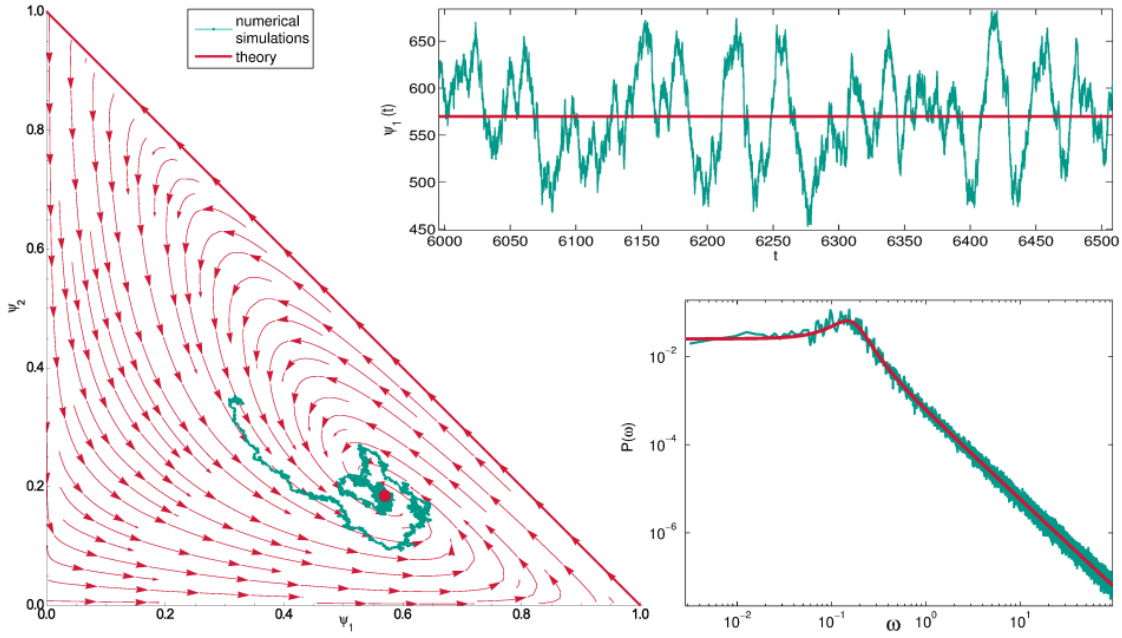


FIGURE 5.3: **3-player All-Pay Auction with 3 available strategies.** Bottom left: Phase portrait of the corresponding replicator equations (pink) with a single realisation of the simulated birth-death process of $N = 1000$ players (cyan). Top: Time series of the number of players playing $S_1$, we note noisy oscillations around the fixed point of the deterministic limit, pink line correspond to the fixed point present in the Bottom left panel. Bottom right: Power spectra of the numerically simulated system (cyan) and analytical prediction (pink), both showing a resonant frequency $\omega_r \approx 0.145$ corresponding to the oscillations of a period $\approx 43$ generations.

fixed point is a stable focus. We confirm this by analysing eigenvalues of the Jacobian that in this case has 2 complex conjugated eigenvalues with negative real part (besides the trivial zero eigenvalue). Thus, there is a chance for an oscillatory behaviour induced by the demographic noise.

The time series we present suggests a noisy oscillatory behaviour around the expected number of players calculated in the replicator limit, but to characterise the dynamics further, we employ previously described power spectra analysis. In the bottom right panel of Figure 5.3, we compare the power spectra $P(\omega)$ obtained both numerically (cyan) and analytically (pink) and realise that there is a resonant frequency that corresponds to the noisy cyclic behaviour documented in the top panel. We note that there is a peak in the power spectra at the frequency $\omega \approx 0.145$ corresponding roughly to the oscillations with the period of $43$ generations which also qualitatively agree with the observation that can be made based on the time series plot.

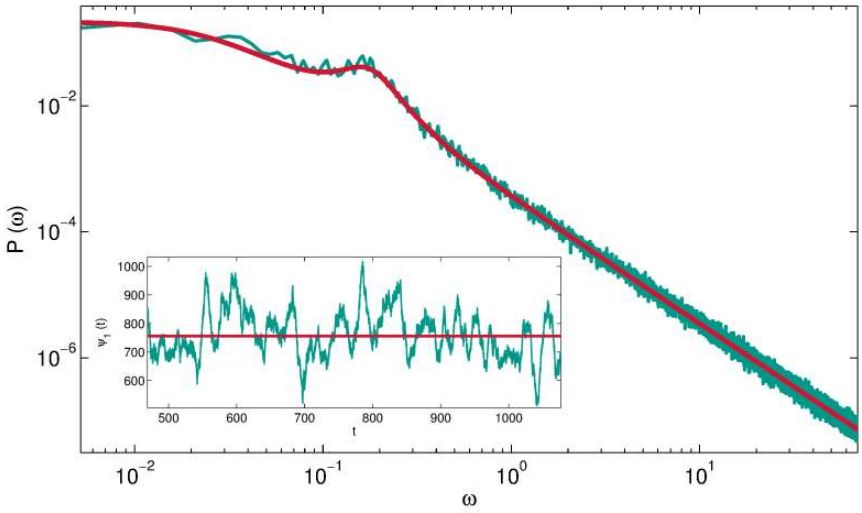


FIGURE 5.4: **3-player All-Pay Auction with 4 available strategies.** We note the existence of resonant frequency with roughly the same value as in the case of 4 strategy game. However, existence of additional strategy adds a stable direction making the oscillations less prominent, as we also illustrate by the insert with a time series of number of players playing strategy $S_1$.

Good correspondence between the theoretical and numerical power spectra motivates us to explore further this phenomena even for the parameter values that would be more difficult to simulate (systems with large number of strategies $L$ require large number of players as we need to keep number of agents per strategy reasonably high for the stochastic replicator equation to be applicable).

It is worth noting that when the strategy space is finite, some of its properties are affected by the parity of the number of available strategies $L$, but we expect that the difference to disappear as $L$ increases leading to a unique continuous limit, as we will argue below. The parity of $L$ affects the number of real eigenvalues of the Jacobian. Beside the 0 eigenvalue, Jacobian of the system does not have additional real eigenvalues when $L$ is odd, while it has an additional real eigenvalue when $L$ is even. This results in a qualitative difference between the power spectra for the even and odd number of strategies - in the case of the even number of strategies, there is no global maximum. We present this in the case of the 3-player APA game with $L = 4$ available strategies in Figure 5.4. We note that the value of $P(\omega)$ is greater for small $\omega$, as expected, while the relative position and the amplitude of the peak stayed in a similar position as they are determined by the complex eigenvalues that have similar amplitudes in both cases.

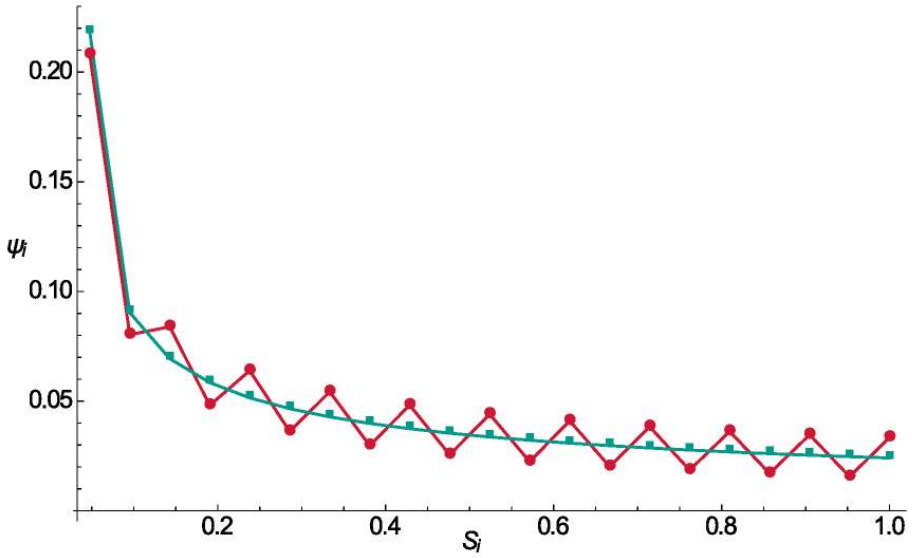


FIGURE 5.5: **Fixed point distribution of the 3-player All-Pay Auction game with $L = 21$ strategies in the unit interval (V=1).** Cyan: Discretized fixed point distribution obtained in the game with continuous strategies; Pink: Fixed point distribution of the game with discrete strategies. We note that the fixed point of the discrete strategy game is not a monotonic function as its continuous strategy counterpart.

**General number of strategies L.** Before proceeding to discuss stability results and the existence of cycles for a general number of discrete strategies $L$, we note that there is the structural difference between the fixed point mixed strategy of the discrete strategy game and the continuous strategy game. As we have seen, the continuous game has a fixed point that is a strictly decreasing function (except for the $k = 2$ which will be discussed separately). On the other hand, the fixed point distribution of the discrete game is not monotonic but has a zig-zag structure. As an example of the difference between the fixed point distributions, we show the results for the 3-player all-pay auction with $L = 21$ strategies. We also, observe the zig-zag structure of the distribution in the numerical simulations when they are run without mutations[4]. In Appendix H we show how this difference emerges out of the corrected fitness function.

In the All-Pay Auction games with a small number of strategies we have seen the

[4]When running simulations with a large number of strategies, to ensure that all the strategies will persist in the fixed point we usually introduce a small mutation rate, this, however, seem to smoothen the zig-zag structure. However, the deviation between the discretized distribution and fixed point of the game with discrete strategies is already clear with small number of strategies $L = 3$ presented earlier, though the difference decreases with increase in $L$.

noise-induced cycles in Figs. 5.3 and 5.4, and we have shown that the theory and simulations agree both at the level of fixed point prediction and the existence and quantitative properties of the cycles. Here we proceed with the analysis to understand how these phenomena depend on the density of the strategy space (or equivalently number of strategies $L$ as all the strategies are confined to the $[0, V]$ interval) and the number of players participating in the game $k$. We will present the results always for the same parity of strategy number (L odd) for the sake of plot clarity, while in Appendix H we show how the two differ for finite $L$.

We continue the analysis of the 3-player games. As before we solve the replicator equation in the deterministic limit (Eq.5.17), evaluate the Jacobian at the fixed point (Eq.5.21) and finally find the power spectra (Eq.5.23). We note that for all $L$ beside the trivial zero eigenvalue all eigenvalues have negative real parts, i.e. the fixed points are stable focuses. In Figure 5.6 we show power spectra for a different number of strategies $L = 5 \dots 101$. As indicated before, the number of peaks in power spectra increases with $L$, as the number of complex conjugated pairs of eigenvalues is $(L-1)/2$. We also note that beside the increase in the number of resonant frequencies, their relative amplitude decreases as $L$ increases. Additionally, we see that small period cycles disappear when $L$ is increased, note specially the peak at the greatest value of $\omega$. We see that in the high $\omega$ regime, as $L$ is increased the power spectra tends to $\omega^{-2}$ behaviour (Brownian noise spectra). Looking at the plateau value in the low $\omega$ regime, we can see that its value quickly increases when $L$ is increased leading us to conjecture that in the $L \to \infty$ and $\omega \to 0$ $P(\omega)$ diverges. It is not clear whether in such a spectra there is more structure, or it is fully described by $\omega^{-2}$. Another reason for the conjecture in the $L \to \infty$ limit lies in the spectral theory of compact operators. Namely, when defined in the continuous space, the Jacobian is a compact operator and as such has discrete spectra with zero as the accumulation point [127], leading to $P(\omega)$ divergence as $\omega \to 0$.

Chatterjee *et al.* [111] report cyclic behaviour for the 3-player All-Pay Auction with 21 strategies. The cycles were observed in a numerical evolutionary dynamics of the Fisher-Wright type, but as we mentioned before and was documented elsewhere [120–123], in the limit of large populations Moran birth-death process and the Fisher-Wright evolution

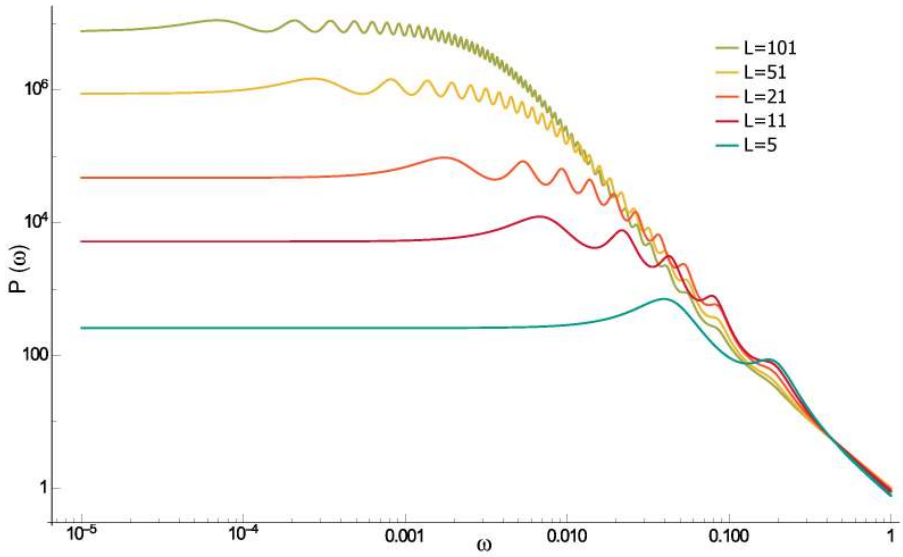


FIGURE 5.6: **Power Spectra in 3-player APA game with variable number of strategies.** The number of resonant frequencies (peaks in the power spectra) increases with number of available strategies, but the amplitude of some nose induced cycles decays with $L$, note specially amplitudes of the peaks at the largest $\omega$.

lead to the same Fokker-Planck equation or stochastic replicator equation, thus the power spectra presented in Figure 5.6 in orange should describe observed cycles. Based on the snapshots of the evolution provided in the paper, we believe that the second smallest $\omega$ correspond to the reported cycles.

**How the number of players competing in an auction influence the fixed point stability?** When we analysed All-Pay Auction games with continuous strategies, we have seen that the fixed point distribution becomes sharply peaked at $S = 0$ when $k$ is increased. However, it is not clear whether that distribution is more stable than the broader distributions for smaller numbers of participants in an auction. Here we try to answer this question in the case of fixed number of strategies.

We repeat our analysis for the $L = 21$ strategies $S_i \in [0, V]$, looking for the fixed points distributions and their stability and power spectra. The Jacobian analysis shows that the mixed strategy fixed points are as before unique, stable focuses. If we analyse only the shape of the Jacobian spectra, we would not see any major difference between these different games. However, if we investigate whether there are noise induced cycles and how their existence depends on the number of participants in an auction, the results

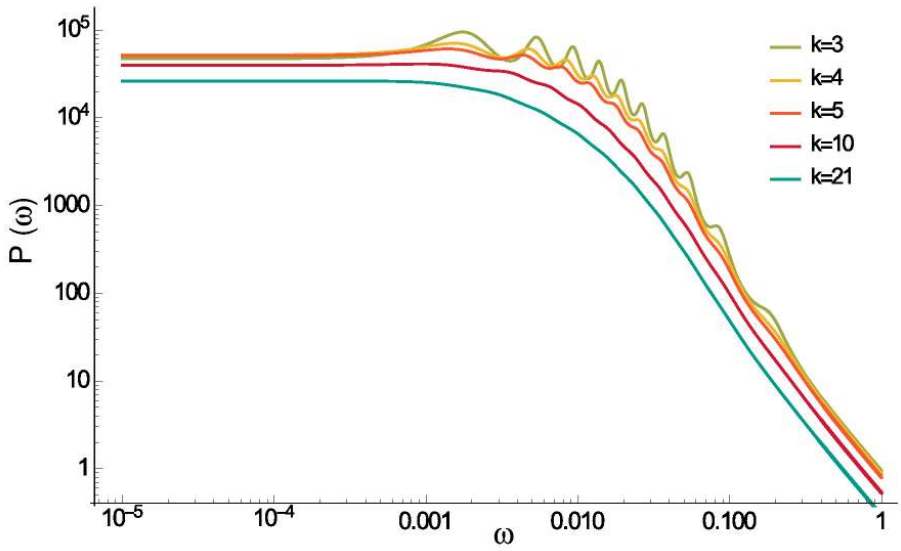


FIGURE 5.7: **Power Spectra in a k-player APA game with $L = 21$ different strategies.** Here we investigate how the number and amplitude of resonant frequencies of the noise induced cycles depend on the number of game players. We note that with increased number of players the fixed point becomes more stable against demographic noise.

are different. In Figure 5.7 we show power spectra for games with $k = 3, 4, 5, 10, 21$ participants, we note that as a number of players is increased the amplitudes of the noise-induced cycles decrease. Already for $k > 5$, it is hard to argue that there are any noise-induced cycles at all. Consequently, the greater number of participants in an auction makes the deterministic fixed point more robust and the finite population effects such as noise induce cycles to appear only when the number of participants in an auction is small.

**2-player APA games.** As reported previously, this game is special because it does not have an evolutionary stable strategy [59, 111]. Additionally, we have proven that when the strategy space is continuous, the stability of unique non-trivial fixed point (the uniform distribution) can not be assessed by methods of linear stability, i.e. the Jacobian does not have non-zero eigenvalues. Here we investigate whether these results change when the game is analysed in the discrete strategy set up.

Interestingly, the fixed point distribution depends on the parity of $L$ the total number of available strategies. When the odd number of strategies is available, the fixed point

distribution is uniform, i.e. the reward splitting did not affect the fixed point distribution as for the $k > 2$ APA games. On the contrary, when the even number of strategies is available, there is a family of fixed point distributions (for details see Appendix H), one of which is the uniform distribution. When we evaluate the Jacobian at the uniform distribution, we realise it is an antisymmetric operator ($J(s, s') = -J(s', s)$, also called skew-symmetric). These operators have only imaginary eigenvalues (complex conjugated pairs, see for example Robert [128]). Consequently, the Jacobian has one or two zeros (depending on parity, two zeros for $L$ even), but all the eigenvalues have zero real parts, and thus their stability can not be assessed by methods of linear stability. The second zero eigenvalue when $L$ is even corresponds to direction of changes in the distribution within the family of consistent fixed point distributions as defined in Appendix H.

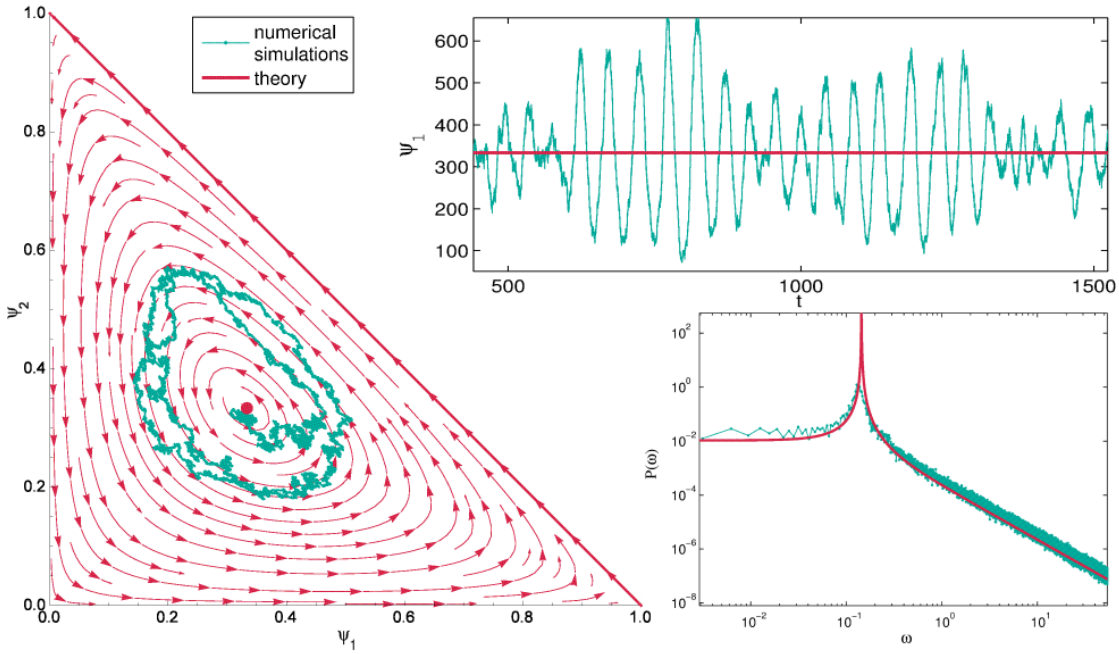


FIGURE 5.8: **2-player APA game with 3 available strategies.** Left: Phase portrait of the corresponding replicator equations (pink) with a single simulated trajectory (cyan); Top right: Number of agents playing the lowest available strategy time evolution from simulation (cyan) and deterministic fixed point expectation (pink); Bottom right: Power spectra obtain analytically (pink) and numerically (cyan) both showing existence of a resonant frequency (at $\omega \approx 0.14$) as demonstarted by a single time series in the Top right panel.

Similarly to 3-player APA game, in Figure 5.8 we show phase portrait of the replicator equations for the 2-player APA game with 3 available strategies with a single simulated

trajectory (details of numerical simulations in Appendix D). As expected from the linear noise analysis (e.g. eigenvalues are imaginary) we note cycles in the phase portrait corresponding to the population's replicator equations. Consequently, when a finite population evolves according to the fitnesses of this game, there is no pressure to return to the fixed point when the random fluctuations drive the system away. This is why these systems are always simulated with small mutation rate to maximise survival time of all the strategy types. Furthermore, when $L$ is even, there is an additional zero eigenvalue, i.e. there is a direction along which the system only diffuses in the finite $N$ regime. Even though this case is particular and it cannot be assessed by linear analysis method, we note that the agreement between the theoretical and simulated data is very good, and the power spectra analysis correctly identifies the period of oscillations for the simulated finite size system.

We realise that except for the case of 2-player APA games where the cycles always exist for the finite number of strategies, the fixed point of the $k$-player game is stable against demographic noise effects as long as the number of available strategies is large. Additionally, for the small number of available discrete bidding strategies, increased number of participants in the game offers stabilisation against the noise induced cycles.

### 5.3.2 All-pay auctions with 2 rewards

We now investigate if the introduction of the second reward changes the fixed point distribution and its stability in the APA game with a finite number of bidding strategies. For these games, spectral analysis of Jacobian of the continuous game is non-trivial (this case is made more difficult by the absence of an explicit formula for the fixed point distribution), so we rely on numerical methods in analysing the spectra of the game with discrete strategy space. When strategies are continuous, we have seen that for $k > 3$ and $\alpha > 0.5$ the fixed point distribution is bimodal. Especially, it is also an evolutionary stable strategy as long as $\alpha < \alpha_c$ where $\alpha_c$ is dependent on a number of players $k$ (as shown in Fig. 5.2 with more details in Appendix G). As the fixed point distribution of the evolutionary dynamics exists for any $\alpha \in [0, 1]$ we want to use numerically accessible

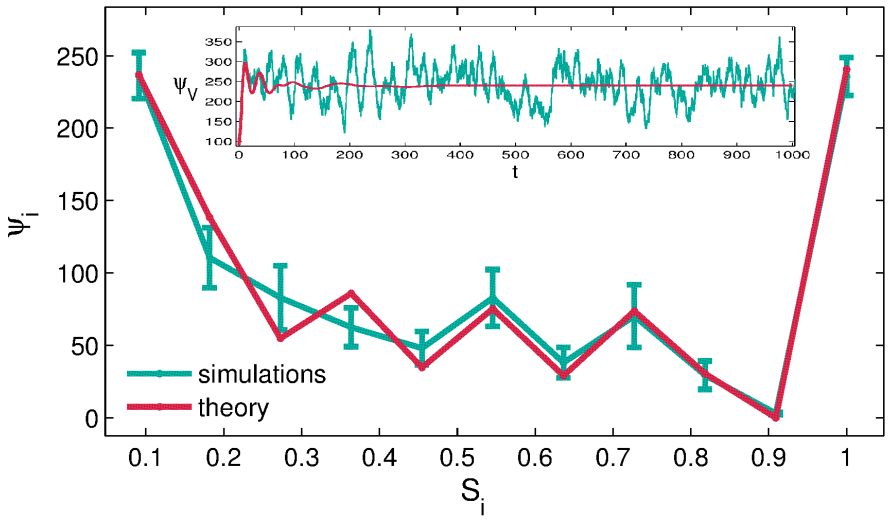


FIGURE 5.9: **Fixed point distribution of the 5-player APA game with two equal rewards.** We compare the fixed-point distribution of a numerically simulated system with $N = 1000$ players who have $L = 11$ bidding strategies (cyan) to the theoretical prediction (pink). The insert shows a time series of number of players bidding the highest value $V$ and compare it with the numerically integrated solution of the replicator equation.

discrete strategy space to analyse whether the fixed point distribution stability changes as $\alpha$ is increased.

Firstly, we consider if the fixed point distributions change when the reward splitting corrections are introduced. As we have seen in Eq. (5.19) there are two reward splitting contributions when the highest bid is not unique, and both rewards are divided among the highest bidders, but there's also a possibility that only the second reward is divided. Based on the experience with single reward game, we expect these payoff corrections to have an effect on the monotonicity of the fixed point distribution. If these expectations are correct, we may ask a question whether $V_1/V_2 = \alpha = 0.5$ is still the critical reward ratio above which the specialisation occurs and the fraction of high bidders increases.

In Figure 5.9 we show an example of a fixed point distribution for a 5-player game with $L = 11$ bidding strategies and two equal rewards. We note that the fixed point distribution is again a nonmonotonic function with a zig-zag structure. We show that the zig-zag structure persists in the numerical simulations although they are run with small mutation rate to ensure the existence of all strategies (we believe the combined effect of mutations and finite population size are responsible for the difference between theoretical prediction and simulated results for the low bidding strategies).

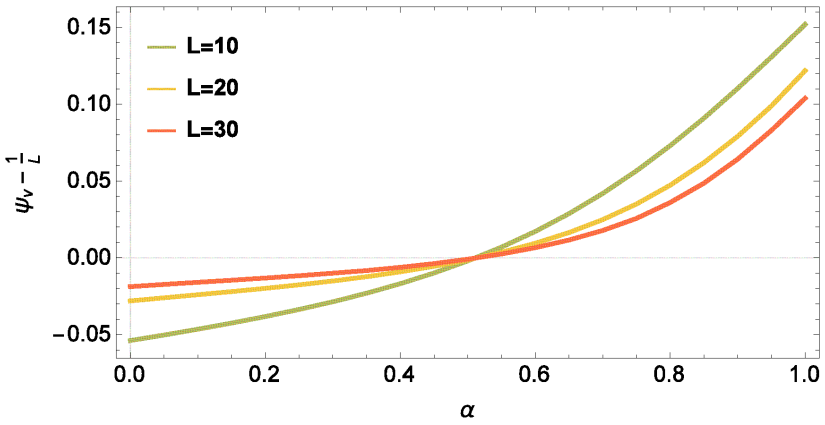


FIGURE 5.10: **Fraction of players bidding the highest value ($s = V$) as function of $\alpha$ in the 5-player APA game with two rewards.** To compare fraction of agents bidding the highest value for different $L = 10, 20, 30$ we plot $\psi_V - 1/L$. Fraction of agents bidding $V$ becomes higher than random for $\alpha = 0.5$ for all compared $L$.

The non-monotonicity of the fixed point distribution makes it slightly more difficult to estimate the bimodality condition when the strategy space is discrete, but as we can observe in Fig. 5.9 there is clearly a large fraction of agents bidding the highest value. To address specialisation in the discrete strategy space, we investigate how the fraction of population bidding the highest value $S = V$ changes when $\alpha$ is varied between single reward and two equal rewards extremes. In Figure 5.10 we show a fraction of agents bidding $V$ in the 5-player APA game. To enable comparison between systems with a different number of strategies $L$ we look at a fraction of bidders relative to $1/L$, the fraction of players who would bid $S = V$ had they make the choice at random. We note that games with tree different sizes of strategy space all show increase in high bidders compared to the uniform distribution as $\alpha > 0.5$. The observation that this increase in high bidders is independent of $L$, i.e. all different $L$ curves intersect at $\alpha = 0.5$ suggests that it is also the bimodality condition for finite strategy space.

What about the fixed point's stability, especially when the specialisation within the population occurs? To answer this question we derive Jacobian matrix evaluated at the fixed point and as before analyse its spectra. As for the APA games with the single reward, the fixed point distribution we have discussed is a stable focus. For some values of $\alpha$ close to 1, the Jacobian's spectra have a second zero eigenvalue, but this is due to the absence of players playing second highest strategy in the fixed point strategy (see e.g.

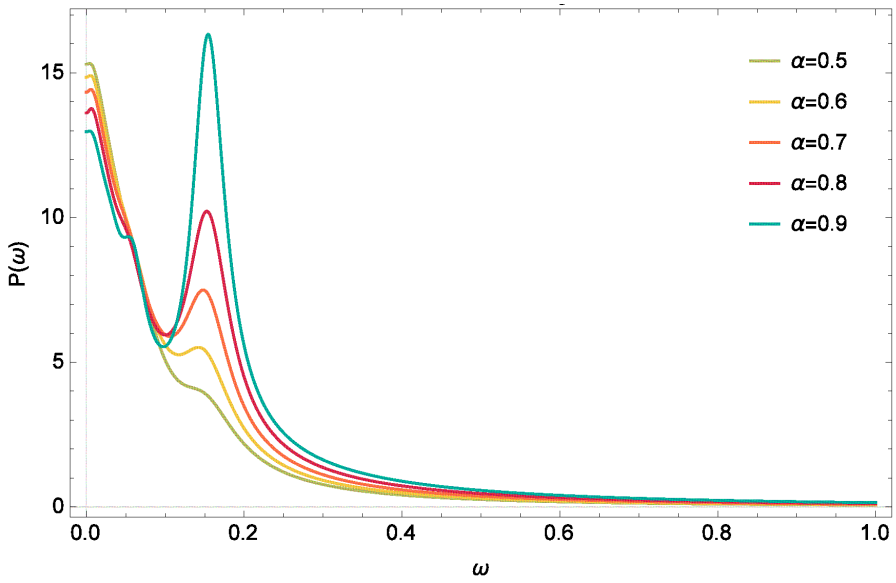


FIGURE 5.11: **Effect of $\alpha$ on the power spectra in the 4-player 2 rewards APA game with $L = 20$ strategies.** Critical $\alpha$ above which there is no evolutionary stable strategy for this set of parameters is $\alpha = 0.6$, we note increase in the amplitude of noise-induced cycles gradually across $\alpha$.

Fig 5.9). Having not observed difference in stability of the fixed point as a function of $\alpha$ by mere analysis of Jacobian eigenvalues, we investigate whether the effects of demographic noise are somehow correlated with $\alpha$ and other system's parameters.

In Figure 5.11 we show power spectra corresponding to the fraction of highest bidding agents for different values of reward ratios $\alpha$. We note that mildly pronounced peak that exists even for $\alpha < 0.5$ becomes a global maximum for large values of $\alpha$. Especially we note that the higher the $\alpha$, the greater the amplitude of the noise-induced cycles. This trend does not continue for $\alpha = 1$ where the peak height is close to the one for $\alpha = 0.8$, but we omit plotting it for clarity of the range presented. We show analysis of the oscillations in the fraction of agents bidding the highest value $V$ because the effects of demographic noise seem to be the most pronounced on this strategy, but we see the same effects of $\alpha$ increased even if we look at the trace of the power spectra we have analysed in the single reward game. It is interesting that we do not note a different behaviour as a function of $\alpha_c$ (above which the ESS does not exist, for the 4-players game shown in Figure 5.11 it is $\alpha_c = 0.6$), rather the effect of demographic noise becomes stronger with $\alpha$ gradually.

Finally as when analysing the single reward APA game, we investigate how the number of available strategies $L$ and a number of players participating in the game $k$ affect the

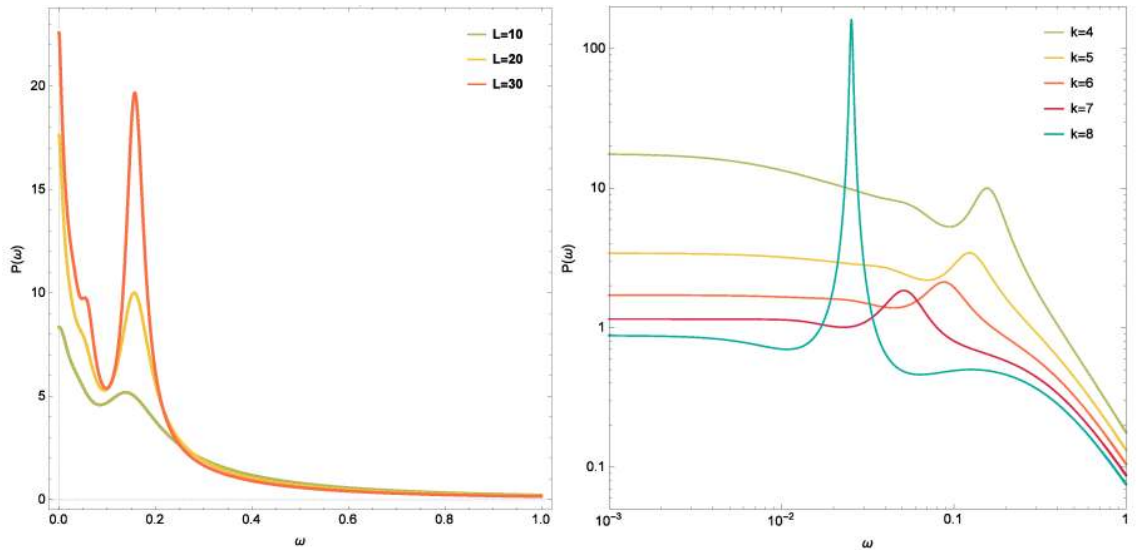


FIGURE 5.12: **Power spectra of APA game with 2 equal rewards.** Left: 4-player game with variable number of strategies in the $s \in [0, V]$ domain; Right: Various k-player games with $L = 20$ available strategies. Both panels show power spectra of the fluctuations of the highest bidding strategy $S_L$ as the effect on those strategies is the strongest.

fixed point's stability. To our surprise, two reward game is again substantially different from its single reward counterpart.

In Figure 5.12 we show power spectra analysis of the APA game with two equal rewards ($\alpha = 1$) with a varied number of available strategies (left in a 4-player game) and a varied number of players (right, while the number of available strategies is $L = 20$). As we can observe the strategy space refinement increases the amplitude of the noise-induced oscillation while the frequency stays unchanged. Similarly, increased number of game participants promotes cycles. We see that as $k$ is increased the peak becomes global maxima (when $k > 4$) and its amplitude keeps increasing. There is also a shift in the resonant frequency, i.e. the cycles' period increases. We realise that introducing the second reward in the APA game adds more instability. The fixed point distribution becomes more interesting as the specialisation in the population occurs, but the population also becomes more sensitive to demographic noise. Even more intriguing is the fact that a large number of available strategies $L$ and increased number of game participants $k$ that stabilised the fixed point in the single reward case (decreasing the amplitude of the noise-induced cycles) have an opposite effect when the second reward is introduced.

### 5.3.3 Second price all-pay auctions

Finally, we look how the SAPA game dynamics is changed when the strategies are discrete. Due to extensive study of the generalised War of Attrition game, the existence of evolutionarily stable strategy has been proven for all $k$ in both continuous and discrete strategy space (see e.g. [109–111]). Specially, Bishop and Cannings [109] note that when the strategy space is constrained from above it is important if the maximum bid is attainable, i.e. if strategy domain is $s \in [0, A)$ there is no evolutionary stable strategy (both when bids are continuous or discrete). We here briefly show that our simulated dynamics converges well to the theoretical predictions even for relatively small populations and a small number of strategies ($N = 1000$, $L = 21$). In Figure 5.13 we show the fixed point of the dynamics (corresponding to the evolutionary stable strategy previously found) obtained in the simulated population evolution and numerical integration of the replicator equations. Contrary to the APA game, we note no (or very small) deviations from the distribution monotonicity and in general the fixed point distributions of the SAPA game are well described by the discretized fixed points of the continuous game fixed point.

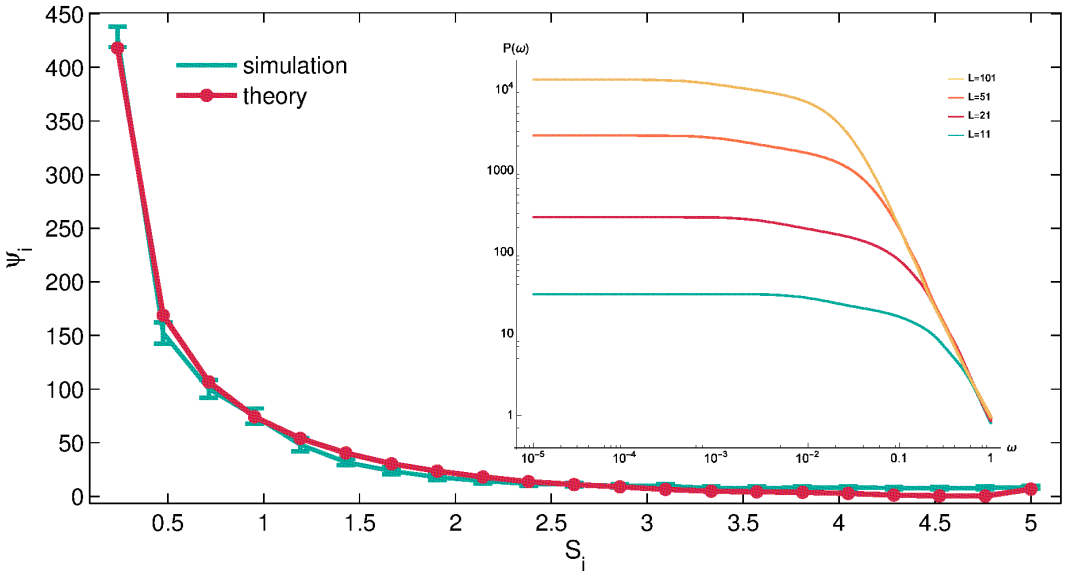


FIGURE 5.13: **3-player SAPA auction with discrete strategies from the $[0, 5V]$ domain**. Fixed point distribution of the 3 player SAPA game as predicted by the replicator equations in the discrete strategy space with $L = 21$ and as obtained by numerically simulated evolution of 1000 agents. The insert shows power spectra for different number of available strategies for the same 3-player SAPA game on $[0, 5V]$ domain.

Beside the number of bidding strategy, the question of strategy cut off is an important one in modelling SAPA game. As proven by Bishop and Cannings [109] and extended in Appendix I, when the domain is bounded, there is always a delta peak at the maximum available bid, but also there is a gap in the strategy distribution, i.e. some fraction of high bidding strategies just below the maximum one are always less favourable than bidding the highest one, so they are not played in the evolutionary stable state. We address the question of a gap in the strategy space in Appendix I for the continuous strategy space, but the rationale for its existence is valid here as well, and it is confirmed by our numerical investigation. Analysing the spectra of Jacobian, we realise that all the eigenvalues have non-postitive real parts with an increasing number of zeros when the strategy space is refined. Refinement of strategy space leads to more discrete strategies being offered from the region of strategies that are not in the support of the fixed point. Thus the frequency of agents playing them is 0 at the fixed point, consequently, more eigenvalues are zero. These 0 eigenvalues thus do not tell us anything new about the dynamics of the system. However, simulating the system with large cut-off values means that even if the strategy space was unbounded probability of playing strategies from the gap range would be very small (due to fast exponential decay of the fixed point distribution), thus the difference between the unbounded and the bounded strategy domain fixed point becomes small.

Knowing that the fixed point distribution is a stable focus, we once more look for the effects of demographic noise. In the insert of Figure 5.13 we show the power spectra for various number of strategies $L$ keeping the cut off fixed. We do not note pronounced peaks in the spectra, and similar as for the APA games we note that the plateau level in the small $\omega$ regime increases. Although as discussed the different cut off might induce a slightly different fixed point distribution, i.e. with a more pronounced peak at the highest bidding value, the power spectra do not show more structure in those cases either. Thus we can conclude that the SAPA games are more resistant to the effects of finite population size.

## 5.4 Summary

In this chapter, we derived a macroscopic, replicator equation starting from an associated birth-death process in a population of agents who interact via games with continuous strategy spaces. The method has been known for games with discrete strategy space, and it is now extended to include an understanding of evolutionary dynamics of phenotypic and other continuous features. We applied the method to evolutionary auction games, and we note that the fixed points of the introduced dynamics are the previously reported evolutionary stable strategies (when such exist).

Particularly interesting is the all-pay auction game when more than one reward is offered in the competition, as in that case, we note that the population specialise. We realise that whenever the second reward is at least a half of the first reward value, and the number of participants in an auction is greater than three, the evolutionary dynamics leads to a bimodal fixed point distribution. Some agents specialise in bidding low (as in the single reward case), but a fraction of agents also bids high values. The portion of high bidders increases with $\alpha$, but as it might be expected decreases with $k$ (as the game effectively becomes more similar to the single reward game). As opposed to the segregated state we have studied in the context of double auctions and where we noted that different population subgroups earn a different average score, the evolutionary dynamics leads to the fixed point such that both subgroups have zero fitness on average. However, it is interesting to note that a population needs to specialise into low bidders and high bidders to make equal fitness possible. We also prove that not all bimodal fixed point distributions are evolutionary stable strategies – they are evolutionary stable strategy only when the reward ratio is lower than some $k$-dependent threshold, i.e. $\alpha = V_2/V_1 < \alpha_c(k)$.

With the evolutionary dynamics, not only did we identify one microscopic mechanism that leads to the previously found evolutionary stable strategies, but now we can also study the stability of the already determined fixed points. As stability assessment is not trivial in the continuous strategy space, instead of discretising distributions and operators obtained for continuous strategy space, we suggest a more cautious route – to reintroduce the problem in the discrete strategy space and analyse how the properties change when the strategy space is refined. We realise that fixed point distributions are

stable focuses, independent on evolutionary stability, except for the 2-player APA game. This game was known not to have an evolutionary stable strategy, while now we showed that it does not have eigenvalues with non-zero real part. Besides the stability of the fixed point in the replicator limit (the infinite population size) we also assessed finite system size corrections and investigated possibility of the noise induced cycles. We realise that those are properties of the all-pay auctions (APA) games whereas the second-price all-pay auctions show remarkable stability despite the system size. We note that the cycles induced by the demographic noise decay in intensity when either the number of participants or number of available strategies is increased, in the single reward game. While when the two rewards are offered the cycles, especially in the number of risk-taking players are even more pronounced with increased $L$ or $k$. We also realise that the cycles are not related to the loss of evolutionary stability (e.g. there's no difference in cyclic behaviour before and after $\alpha_c$), but rather they seem to be linked with the bimodality (e.g. their effects become more pronounced when $\alpha > 0.5$).

# Chapter 6

# Concluding Remarks

## 6.1 Summary of results

This thesis addresses the question of the possible emergence of spontaneous segregation in a population of adaptive agents. The introduction contains an overview of empirically and numerically observed segregation-like phenomena in the socio-economic and ecological context that motivated the research. Being always a composition of various aspects and intricate agents and interactions, examining and studying directly these realistic models is not straightforward and not always informative. That is why, to test the hypothesis that the segregation can emerge spontaneously, a stylised model of a population of adaptive agents who choose between two double auction markets is devised. The model, together with reproduced segregation effects is presented in Chapter 2. When the two markets are fair, e.g. equilibrium price-setting markets, the emergence of four distinctive groups (agents specialised in buying and selling at different markets) is noted. Specialisation into buyers and sellers is justifiable as that way maximisation of trading opportunities is achieved. However, segregation between the markets can be explained entropically - synchronisation at the same market will lead everyone to the same return, but the number of different states where the population is divided among the markets is much greater making the segregated state more probable. More intriguing and overall more analysed in this thesis is the case of symmetrically biased markets, where we realise that the segregation is a collective effort to maximise the number of trades and returns. The population specialise into return-driven and volume-driven agents, who stay in a role for extended periods of time and in this way everyone achieves higher returns

compared to alternative states. We realise that the segregation is signalled by time scale separation – short decorrelation time within a single loyalty group (described by agent's memory length) and a long time until the full decorrelation, i.e. changing the loyalty group. The modelled population was also described analytically, and the remarkable level of agreement between theory and simulation motivated further theoretical research into causes and benefits of segregation.

We have identified the reinforcement learning as the key driver of segregation. In particular, for all system parameters, we find finite values of the intensity of choice $\beta$ above which the segregation occurs. Having in mind that one way to interpret $\beta$ is a scale of possible returns (e.g. keeping $\beta$ fixed we can achieve the same effect by increasing the average of return distribution) suggests that one possible way to suppress or promote segregation can be achieved by regulating returns per transaction, e.g. not allowing orders higher than some value. Agent's memory is another control parameter as depending on its value, above the segregation threshold we distinguish between strongly segregated states – market coexistence, and weakly segregated states – single market dominance.

In Chapter 3 the analytical description of the model is continued in the large memory limit. The small systems with two and four agents are analysed, as in their long-run adaptation we can also identify synchronisation and segregation. Agents' preferences for buying are noted as a major system parameter that distinguishes between different types of steady states above the threshold intensity of choice. With this realisation, we returned to the large systems and in the space of intensities of choice and buy/sell preferences we identified a variety of steady states for a population consisting of two subpopulations. Finally, we returned to numerical simulations to test the stability of different segregated states and concluded that populations with large memory limit prefer weakly segregated states, in the long run, i.e. one market acquire the majority of shares. Intriguingly, it is the agents' learning parameters that determine the possibility of market coexistence vs. market monopoly, but the larger the system is, the longer the lifetime of the strongly segregated state (a.k.a market coexistence) – even though single market dominance would be preferred, the time necessary to reach monopoly might not be reachable.

To test the robustness of the findings presented in Chapters 2 and 3, in Chapter 4 we

discuss how the simplifying assumptions we have initially taken can be relaxed. We first address possible extensions to the reinforcement learning, the key driver of segregation. We realise that for an extended range of learning rules the segregation phenomena persists. In a single exception, when an agent does not forget scores of unplayed actions, or effectively update his/her attractions by the past attraction (which is an average score in the last $1/r$ periods), the segregation cease to exist. We investigate this state more carefully and conclude that for a broad range of intensities of choice the strongly segregated state still ensures higher returns for a single agent and the population overall.

Further, we introduce more than two markets in the system and observe that *full segregation*, e.g. when all subpopulations develop loyalty groups for all the markets, is not typical for systems with more markets. Instead, many systems are such that only a subset of markets persists in the competition, or not all agent types visit all the markets. Finally, we show that the segregation persists even when more realistic features are implemented – budget constraints, fundamentalist trading strategies, continuous double auctions with open limit order books. This strengthens our observation that the segregation is a consequence of agent's adaptation rather than simplified rules and markets we have initially used.

In the end, we have considered a different type of auctions (single sided evolutionary auctions) and agents (adaptation not based on learning but the natural selection). When agents compete in an evolutionary auction with multiple rewards, an effect similar to segregation occurs – some agents specialise into bidding low, while others are bidding high, ensuring this way that the average fitness in the population is equal. We build on existing works by developing macroscopic dynamics of the replicator type starting from a microscopic birth-death process. With the evolutionary dynamics, we reproduce previously obtained evolutionary stable strategies but also investigate stochastic effects present in the finite populations, especially occurrence of cycles. We note that the Second price all-pay auctions (SAPA) offers more stability, i.e. the fixed points of the dynamics (that are also evolutionary stable strategies) are stable focuses and robust under the finite size stochasticity. On the contrary, in populations interacting via All-pay auctions (APA), we note noise-induced cycles, both in single and multiple reward case.

## 6.2 Future work

The research presented in this thesis was initiated by an observation of segregation phenomena in real (e.g. market segmentation reported in [38, 41]) and *in silico* (CAT [33–35]) financial systems. Upon construction of a minimal model to reproduce the phenomena under controlled conditions of numerical simulations, we identified an agent's reinforcement learning as the key driver of segregation. Although the reinforcement rule we have used is fairly generic – it has been used in other studies, confirmed empirically and experimentally tested [28, 29, 46, 77, 78, 95] – the existing body of work does not offer clear demarcation between different existing update mechanisms, nor about learning parameter variability across games and within a population. As this question is ultimately answered by empirical and experimental studies, we would like to encourage more research into this field. The work of Cheung *et al.* [129] draws on evidence from Behavioural Game Theory and suggests that values of $\beta$ are consistent across games but increase in more informative environments. The authors argue that a parameter closely analogous to $r$ also increases with the trustworthiness of information in the system. Bearing in mind the results shown in Fig. 2.13, where for large $r$ and large $\beta$ the only steady state is the segregated one, this suggests that more informative environments, or ones where information is more trustworthy because e.g. of stability over long timescales, might naturally lead to segregated states. It would be exciting to study this effect explicitly in a suitably extended model, or possibly in experiments with market games.

Another direction worth investigating would be a persistence of segregation in systems where agents are allowed to abstain from a trade. Related to the Minority Game, an extension with agents who can choose to be inactive - the grand canonical game - was also studied and the phase transitions in the game persist. It is precisely the introduction of *speculators* (agents who can decide whether to participate in the game – they play only if will lead to higher return than some threshold $\epsilon$) that enabled investigation of market stylised facts in the game [25, 130]. Critical parameters in such a setup were a fraction of *producers* - agents who can't abstain from the game, but also the threshold gain $\epsilon$. It is not entirely clear how such an extension might change segregation. The threshold $\epsilon$ should be treated as a permanent attraction to abstain, and if it is small enough compared to the

possible returns in any of the markets its effect should not be felt. However, when the state is segregated while changing, the loyalty agent's attractions usually pass through a vicinity of the zero attraction state. Thus, even if $\epsilon$ is small for high enough intensity of choice, there would be a chance for long inactive periods. Especially, this might be expected if the forgetting was imposed on attractions while an agent is inactive.

There is clearly also scope for capturing more complex trading strategies in models like ours, something we have postponed as we were motivated by the simplicity of high-frequency trading algorithms and more broadly by the aim to develop a baseline model on which further extensions could be built. Our initial steps in this direction, presented in Chapter 4, show that the results are robust against the introduction of more sophisticated trading strategies, e.g. fundamentalists with different information levels. In Section 4.3, we have used the Toth model due to its simplicity yet numerical and experimental studies, but we did not expect that its original phenomenology – the "J curve" in the wealth against information level data - will persist across the two markets. Naively, one might expect that the segregation is correlated with the traders' level of information. As remarked in Section 4.3, the absence of such correlation is due to the fact that each agent chooses among markets based only on his/her score and the notion of earning less than the market is not known to them. This leaves an interesting question for further studies – will the "J curve" persist if agents base their market choices on the information about their wealth related to the other players. More broadly, it is an interesting question how the observed phenomenon depends on the properties of the dividend process.

Further directions for investigation might include agents with heterogeneous learning parameters, a feature that will clearly be present in markets that are used both by individual investors and e.g. large funds. An initial step toward these investigations was taken in the following study [88] where it was shown that even if agents have different forgetting rates, the segregation persists.

We could also consider adaptive markets, after all as in the original CAT games; in reality, market specialists aim to increase market share and profit. It is not entirely clear if the competition between the markets would suppress or promote segregation. When discussing systems with multiple markets, we addressed a question of market competition

in a very general way as the segregated state corresponds to market coexistence, while weakly segregated and unsegregated but synchronised states correspond to a single market dominance. In the analysed system markets do not have the intention to compete, but we have realised that even unwillingly some steady states correspond to the more balanced market share division. In this domain it would be especially interesting to build upon the findings of Shi *et al.* [36] that with a slightly different trading strategies[1] and using the evolutionary dynamics shows that the monopoly always emerges (e.g. one market wins) if the market fee charging strategies are the same type[2]. Based on our results it is possible to argue that the market fee-charging strategy of the profit type (e.g. market charges agents only if they manage to trade requiring a fraction of their earning) would still allow for the existence of the segregated steady state, as that would only affect the return distribution. Interestingly, the coexistence of markets with same profit charging strategies was not observed in studies by Shi *et al.* [36], while our results leave that possibility as long as agent's learning parameters are in the domain where only a single strongly segregated steady state exist. We might argue that the profit charging strategy will only affect the return distribution, not necessarily existence of segregation (as we note in previous chapters, the only requirement on the return distributions is a finite mean and variance), but it is not clear how the market strategies would adapt in such a system and whether that adaptation could affect otherwise possible segregation. On the other hand, if there is a fixed participation fee, it might lead to negative scores for agents when they do not manage to trade, and consequently, this could affect the segregated phenomena. This is because there would be a clear difference between not trying to trade and not succeeding to trade. In this case, the possibility of abstaining would make more sense and could result in a fraction of inactive traders.

As we have only scratched the surface of the segregation related phenomena in an ecological context, we envision a few directions for possible investigations and extensions

[1] The authors [36] use *ray bidding strategies* – buyers/sellers have a private value and a parameter so that they can bid truthfully or "shade" their private value, meaning that agents bid a fraction of their private value, or ask for a multiple of their private value.

[2] Authors report market coexistence only in the case when one market charges profit fee while the other charges fixed participation fee [36].

of our results. The most general question we seek to address is related to the generalization of the results we have observed. Namely, under the specific buyer-seller interaction via market, we have seen that populations of buyers and sellers specialise and develop preferences for one of the two markets. The interaction we have studied is a relevant one in the context of the financial exchange. However, it is not clear how much of these observations are general and extend beyond the financial model. Suppose a member of a group needs to decide about one of the possible resources (s)he can utilise. Further, we assume the agent's fitness when exploiting a resource is a function of the total number of other users who try to utilise the same resource. The question we are interested in answering is related to the generic fitness function that leads to segregation within a population. This relates back to the positive and negative size effects, e.g. it is unclear whether segregation requires the fitness function to be such that an agent receives higher fitness when more agents are already there (e.g. a resource that requires collaborative effort for exploitation), or such that an agent receives higher fitness if (s)he is in minority (e.g. a scarce resource), or as in the double auctions, agent prefers high number of agents of different type, but small number of agents of his type (e.g. plant-pollinator interaction, where the pollinator's fitness increases with number of available plants, but decreases with number of pollinators in competition).

Our initial efforts to answer these questions start again simple. We consider two populations choosing between two available resources. First, we inspect the fitness functions of a very general type, based on the logistic growth [131]:

$$f_m^{(g)} = r_m^{(g)}(1 - \frac{N_m}{K_m}) \, ,$$

i.e. an individual has a population dependent and resource dependent fitness – $r_m^{(g)}$, but the fraction of it (s)he will be able to obtain will depend on the total number of other agents trying to exploit the same resource $N_m$ and the carrying capacity of that resource $K_m$. Interestingly, even this very simple fitness function where $r$ and $K$ are taken to be the same across populations and resources lead to specialisation if we still model agent's adaptation by reinforcement learning, i.e. attraction to the resource is updated by these

returns. However, in this context, it is probably more meaningful to abandon the reinforcement learning and consider natural selection, e.g. adaptation described by evolutionary dynamics and investigate how that might affect the possibility of segregation.

Finally, the evolutionary auctions, we introduced in Chapter 5, are anticipated as a model of interactions between animals. Particularly, some of the example interactions include competitions of males for a reward – a female. In that context, it is not enough to consider a contest between males whose bidding strategies (e.g. ornament traits) are adapting via natural selection, but assuming that the reward values are not changing. This raises a question – can we model an All-pay biological auction where the reward values are adaptive as well. The initial idea is to consider a simple reward updating mechanism based on their actualisation, e.g. if the purpose of the high reward trait is to select the highest bidding individuals, but it regularly selects one that bids far below the reward value, then it is not necessary for the reward to be as high (e.g. reward fitness is $V - \max bid$). We conceive a study with a pool of rewards whose values are updated between the generations at the same time when the bidding strategies are updated. For example in the setting of the Fisher-Wright type with discrete generations, we noted that previous authors [55, 111] studied $N$ agents participating in $N$ evolutionary auctions during a single generation. We find it curious to think if the fixed point distribution of bidding strategies might change if along with $N$ bidding agents there are also $N$ adaptive rewards. It is not entirely clear if the distribution of rewards, in the long run, aligns with the distribution of bids and that is something we believe worth investigating, even more so in the multiple reward case when the distribution of bids is bimodal. More sensible way to address reward adaptation is to consider a population of females next to the population of males but to construct a minimal model of sexual reproduction using which we can consider how the reward and bid traits evolve in a population. One goal of such a model would be to investigate the emergence of assortative mating (pattern in mating that deviates from random mating, usually denoting a preference for mating between individuals with similar traits, see e.g. [132]).

With suggestions to extend our results in the direction of ecological systems, by no means, we wish to simply relabel results applicable in one field and claim their relevance

in another. We do not intend to make a dubious ecological assumption for the sake of convenient mathematical exercise. However, we recognise that even the main results in this thesis are obtained with minimal assumptions to allow more generality and analytical tractability, but hoping that some of the insights will be valid in the vast field of their intended application. Still aiming to validate the results against more specific market/trader mechanisms and finally experimentally test, the first simplified mathematical model was a necessity. In a similar vein, our simplifying assumptions in the ecological modelling, being general enough but still offering insights in a fascinating segregation-like phenomenon, prompted us to think that with a sensible ecological adjusting they might be relevant in the wider community.

# Appendix A

# Details of the Fokker-Planck description

In this appendix we provide explicit functions necessary for the Fokker-Planck description of models discussed in Chapter 2. As previously explained, the return distributions for the choice of market $m$ and a trading action $\mathcal{B}$ or $\mathcal{S}$ are:

$$P(S|m,\mathcal{B}) = Q_{\mathcal{B}m}T_{\mathcal{B}m}\frac{1}{Q_{\mathcal{B}m}\sigma_b\sqrt{2\pi}}\exp\left(-\frac{(S-\pi_m)^2}{2\sigma_b^2}\right)\theta(S) + \delta(S)(1-Q_{\mathcal{B}m}T_{\mathcal{B}m}),$$

$$P(S|m,\mathcal{S}) = \underbrace{Q_{\mathcal{S}m}T_{\mathcal{S}m}}_{\text{agent trades}}\underbrace{\frac{1}{Q_{\mathcal{S}m}\sigma_a\sqrt{2\pi}}\exp\left(-\frac{(S-\pi_m)^2}{2\sigma_a^2}\right)\theta(S)}_{\text{non-negative return}} + \delta(S)\underbrace{(1-Q_{\mathcal{S}m}T_{\mathcal{S}m})}_{\text{agent does not trade}}.$$

These functions describe the returns for all the analytical models we use. With the only difference that when agents have fixed buy sell preferences, their return is only market dependent, so:

$$P(S|m) = p_{\mathcal{B}}P(S|m,\mathcal{B}) + (1-p_{\mathcal{B}})P(S|m,\mathcal{S}).$$

We first derive explicit formulas for the market related functions $Q_\gamma$ - probability of a valid order, and the moment of the return distributions (the truncated Gaussian part, the return of a validated order with existing pair for trade). The probabilities that an order is

valid, $Q_\gamma$, are calculated from:

$$Q_{\mathcal{B}m} = \frac{1}{\sigma_b\sqrt{2\pi}} \int_{\pi_m}^{\infty} db \, \exp\left(-\frac{(b-\mu_b)^2}{2\sigma_b^2}\right),$$
$$Q_{\mathcal{S}m} = \frac{1}{\sigma_a\sqrt{2\pi}} \int_{-\infty}^{\pi_m} da \, \exp\left(-\frac{(a-\mu_a)^2}{2\sigma_a^2}\right).$$

The two integrals are related to the error function, so the order validity can be stated in the following form:

$$Q_{\mathcal{B}m} = \frac{1}{2}\left(1 + \mathrm{erf}\left(\frac{\mu_b - \pi_m}{\sigma_b\sqrt{2}}\right)\right) = \frac{1}{2}\left(1 + \mathrm{erf}\left(\frac{(\mu_b - \mu_a)(1-\theta_m)}{\sigma_b\sqrt{2}}\right)\right),$$
$$Q_{\mathcal{S}m} = \frac{1}{2}\left(1 + \mathrm{erf}\left(\frac{\pi_m - \mu_a}{\sigma_a\sqrt{2}}\right)\right) = \frac{1}{2}\left(1 + \mathrm{erf}\left(\frac{(\mu_b - \mu_a)\theta_m}{\sigma_a\sqrt{2}}\right)\right).$$

where in the second equalities we used the fact that in the $N \to \infty$ limit trading price can be expressed in terms of input means of bids and asks $\pi_m = \mu_a + \theta_m(\mu_b - \mu_a)$. Usually, we have used $\sigma_a = \sigma_b = \sigma$ and $\mu_b - \mu_a = \sigma$ so that the previous expressions are only functions of the market biases $\theta_m$. For the drift and diffusion term $\langle S_{\mathcal{T}m}\rangle$ and $\langle S^2_{\mathcal{T}m}\rangle$ are also needed, thus we calculate them below:

$$\begin{aligned}
\langle S_{\mathcal{B}m}\rangle &= \frac{1}{\sigma_b\sqrt{2\pi}} \int_0^{\infty} dS S \exp\left(-\frac{(S-(\mu_b-\pi_m))^2}{2\sigma_b^2}\right) \\
&= \frac{\sigma_b}{\sqrt{2\pi}} \exp\left(-\frac{(\mu_b-\pi_m)^2}{2\sigma_b^2}\right) + \frac{\mu_b - \pi_m}{2}\left(1 + \mathrm{erf}\left(\frac{\mu_b-\pi_m}{\sigma_b\sqrt{2}}\right)\right), \\
\langle S_{\mathcal{S}m}\rangle &= \frac{1}{\sigma_a\sqrt{2\pi}} \int_0^{\infty} dS S \exp\left(-\frac{(S-(\pi_m-\mu_a))^2}{2\sigma_a^2}\right) \\
&= \frac{\sigma_a}{\sqrt{2\pi}} \exp\left(-\frac{(\pi_m-\mu_a)^2}{2\sigma_a^2}\right) + \frac{\pi_m - \mu_a}{2}\left(1 + \mathrm{erf}\left(\frac{\pi_m-\mu_a}{\sigma_a\sqrt{2}}\right)\right).
\end{aligned}$$

These can again be further simplified when the expression for $\pi_m$ in the $N \to \infty$ limit is introduced and our typical values for variance and means of bids and asks are used, but we leave the expressions in the most general form. The second moments of the returns

$\langle S^2_{\mathcal{T}m}\rangle$ are:

$$\begin{aligned}
\langle S^2_{\mathcal{B}m}\rangle &= \frac{1}{\sigma_b\sqrt{2\pi}}\int_0^\infty dS S^2 \exp\left(-\frac{(S-(\mu_b-\pi_m))^2}{2\sigma_b^2}\right)\\
&= \frac{\sigma_b(\mu_b-\pi_m)}{\sqrt{2\pi}}\exp\left(-\frac{(\mu_b-\pi_m)^2}{2\sigma_b^2}\right)+\frac{(\mu_b-\pi_m)^2+\sigma_b^2}{2}\left(1+\mathrm{erf}\left(\frac{\mu_b-\pi_m}{\sigma_b\sqrt{2}}\right)\right),\\
\langle S^2_{\mathcal{S}m}\rangle &= \frac{1}{\sigma_a\sqrt{2\pi}}\int_0^\infty dS S^2 \exp\left(-\frac{(S-(\pi_m-\mu_a))^2}{2\sigma_a^2}\right)\\
&= \frac{\sigma_a(\pi_m-\mu_a)}{\sqrt{2\pi}}\exp\left(-\frac{(\pi_m-\mu_a)^2}{2\sigma_a^2}\right)+\frac{(\pi_m-\mu_a)^2+\sigma_a^2}{2}\left(1+\mathrm{erf}\left(\frac{\pi_m-\mu_a}{\sigma_a\sqrt{2}}\right)\right).
\end{aligned}$$

We proceed with calculation of the drift and the diffusion terms for different models previously introduced. The $l$-th jump moment is:

$$\mathbf{M}_\ell(\mathbf{A}) = \frac{1}{r^\ell}\int d\mathbf{A}'(\mathbf{A}'-\mathbf{A})^\ell K(\mathbf{A}'|\mathbf{A}).$$

As the kernel is model dependent, what follows is grouped in subsections devoted to different models we have used in the thesis.

## Adaptive agents

As introduced in Chapter 2 the transition kernel for the fully adaptive model is:

$$K(\mathbf{A}'|\mathbf{A}) = \int dS \sum_\gamma P(S|\gamma)P(\gamma|\mathbf{A})\delta(\mathbf{A}'-\mathbf{e}_\gamma rS-(1-r)\mathbf{A}). \tag{A.1}$$

Accordingly the drift term is:

$$\begin{aligned}
\mathbf{M}_1(\mathbf{A}) &= \frac{1}{r}\int d\mathbf{A}'(\mathbf{A}'-\mathbf{A})K(\mathbf{A}'|\mathbf{A})\\
&= \int dS\sum_\gamma (S\mathbf{e}_\gamma-\mathbf{A})P(S|\gamma)P(\gamma|\mathbf{A})\\
&= \sum_\gamma T_\gamma\langle S_\gamma\rangle\mathbf{e}_\gamma P(\gamma|\mathbf{A})-\mathbf{A}\,,
\end{aligned}$$

while the $\beta$ component of the diffusion term is:

$$\begin{aligned} M_{2\beta}(\mathbf{A}) &= \int dS \sum_{\gamma} (S\delta_{\gamma\beta} - A_\beta)^2 P(S|\gamma) P(\gamma|\mathbf{A}) \\ &= \int dS \sum_{\gamma} (S^2\delta_{\gamma\beta} - 2SA_\beta\delta_{\gamma\beta} + A_\beta^2) P(S|\gamma) P(\gamma|\mathbf{A}) \\ &= \sum_{\gamma} (T_\gamma \langle S_\gamma^2\rangle \delta_{\gamma\beta} - 2T_\gamma \langle S_\gamma\rangle \delta_{\gamma\beta} A_\beta + A_\beta^2) P(\gamma|\mathbf{A}), \\ \mathbf{M}_2(\mathbf{A}) &= \sum_{\gamma} T_\gamma (\langle S_\gamma^2\rangle - 2\langle S_\gamma\rangle A_\gamma) \mathbf{e}_\gamma P(\gamma|\mathbf{A}) + \mathbf{A}^2. \end{aligned}$$

For the reinforcement learning rule we have introduced in Chapter 4, the delta function term in the kernel changes into $\delta(\mathbf{A}' - \mathbf{e}_\gamma r(S + (\alpha - 1)A_\gamma) - (1 - \alpha r)\mathbf{A})$ (to enforce the new update rule), and accordingly new jump moments are:

$$\begin{aligned} \mathbf{M}_1(\mathbf{A}) &= \int dS \sum_{\gamma} ((S - (1-\alpha)A_\gamma)\mathbf{e}_\gamma - \alpha\mathbf{A}) P(S|\gamma) P(\gamma|\mathbf{A}) \\ &= \sum_{\gamma} (T_\gamma \langle S_\gamma\rangle \mathbf{e}_\gamma - (1-\alpha)\mathbf{A}) P(\gamma|\mathbf{A}) - \alpha\mathbf{A}. \end{aligned}$$

## Agents with fixed preferences for buying $p_{\mathcal{B}}$

In the Chapter 2 we have also introduced the population of agents with fixed buy-sell preference whose only choice is market. When all unplayed actions are forgotten with the same rate $r$ and agents choose between two markets, we realized that we need a single parameter per agent - difference between attractions to different markets $\Delta = A_1 - A_2$. The transition kernel between two states $\Delta$ and $\Delta'$ of an agent with a preference for buying $p_{\mathcal{B}}$ is:

$$K(\Delta'|\Delta, p_{\mathcal{B}}) = \int dS \sum_{m=-1}^{1} \left[P(S|\mathcal{B}, m)p_{\mathcal{B}} + P(S|\mathcal{S}, m)(1 - p_{\mathcal{B}})\right] P(m|\Delta)\delta(\Delta' - mrS - (1-r)\Delta). \tag{A.2}$$

Corresponding drift term is calculated as follows:

$$\begin{aligned} M_1(\Delta, p_{\mathcal{B}}) &= \frac{1}{r}\int d\Delta'(\Delta'-\Delta)K(\Delta'|\Delta, p_{\mathcal{B}}) \\ &= \int dS \sum_{m=-1}^{1} (mS-\Delta)\left[p_{\mathcal{B}}P(S|m,\mathcal{B}) + (1-p_{\mathcal{B}})P(S|m,\mathcal{S})\right] p_m(\Delta) \\ &= \sum_{m=-1}^{1} m\left[p_{\mathcal{B}}T_{\mathcal{B}m}\langle S_{\mathcal{B}m}\rangle + (1-p_{\mathcal{B}})T_{\mathcal{S}m}\langle S_{\mathcal{S}m}\rangle\right]\sigma_\beta\left(m\Delta\right) - \Delta. \end{aligned}$$

Similarly, the diffusion term is:

$$\begin{aligned} M_2(\Delta, p_{\mathcal{B}}) &= \frac{1}{r^2}\int d\Delta'(\Delta'-\Delta)^2 K(\Delta'|\Delta, p_{\mathcal{B}}) \\ &= \int dS \sum_{m=-1}^{1} (mS-\Delta)^2\left[p_{\mathcal{B}}P(S|m,\mathcal{B}) + (1-p_{\mathcal{B}})P(S|m,\mathcal{S})\right] p_m(\Delta) \\ &= \int dS \sum_{m=-1}^{1} (m^2S^2 - 2mS\Delta + \Delta^2)\left[p_{\mathcal{B}}P(S|m,\mathcal{B}) + (1-p_{\mathcal{B}})P(S|m,\mathcal{S})\right] p_m(\Delta) \\ &= \sum_{m=-1}^{1}\Bigg\{\Big[p_{\mathcal{B}}T_{\mathcal{B}m}(\langle S^2_{\mathcal{B}m}\rangle - 2m\Delta\langle S_{\mathcal{B}m}\rangle) \\ &+ (1-p_{\mathcal{B}})T_{\mathcal{S}m}(\langle S^2_{\mathcal{S}m}\rangle - 2m\Delta\langle S_{\mathcal{S}m}\rangle)\Big]\sigma_\beta\left(m\Delta\right)\Bigg\} + \Delta^2. \end{aligned}$$

# Appendix B

# Binder cumulant

In this Appendix we provide details on the Binder cumulant. Namely, we mentioned the threshold values $B = 0$ (Gaussian distribution) and $B = 2/3$ (equal weighted sum of two delta peaks), while below we derive the Binder cumulant for the generic weighted sum of two delta peaks that appears more frequently in the $r \to 0$ limit.

As defined previously, the Binder cumulant is:

$$B = 1 - \frac{\langle (x - \langle x \rangle)^4 \rangle_{P(x)}}{3 \langle (x - \langle x \rangle)^2 \rangle^2_{P(x)}}.$$

Let's denote the two peaked distribution in the following way:

$$P(x) = \omega \delta(x - x_1) + (1 - \omega)\delta(x - x_2).$$

The mean of the distribution is:

$$\langle x \rangle = \omega x_1 + (1 - \omega) x_2.$$

The n-th central moment is:

$$\begin{aligned}
\langle (x - \langle x \rangle)^n \rangle_{P(x)} = & \\
&= \int dx (\omega(x - x_1) + (1 - \omega)(x - x_2))^n P(x) \\
&= \int dx \sum_{k=0}^{n} \binom{n}{k} (\omega(x - x_1))^k \left((1 - \omega)(x - x_2)\right)^{n-k} P(\omega) \\
&= \omega(1 - \omega)^n (x_1 - x_2)^n + (1 - \omega)\omega^n (x_2 - x_1)^n.
\end{aligned}$$

All other terms in the binomial expansions given that they have a term $(x - x_1)(x - x_2)$ lead to zero when averaged with $P(x)$. Especially, the second central moment is:

$$\begin{aligned}\langle (x - \langle x \rangle)^2 \rangle_{P(x)} &= \omega(1-\omega)^2(x_1 - x_2)^2 + (1-\omega)\omega^2(x_2 - x_1)^2 \\ &= \omega(1-\omega)(x_1 - x_2)^2,\end{aligned}$$

while the fourth is:

$$\begin{aligned}\langle (x - \langle x \rangle)^4 \rangle_{P(x)} &= \omega(1-\omega)^4(x_1 - x_2)^4 + (1-\omega)\omega^4(x_2 - x_1)^4 \\ &= \omega(1-\omega)\left(\omega^3 + (1-\omega)^3\right)(x_1 - x_2)^4.\end{aligned}$$

Consequently, the Binder cumulant is:

$$B = 1 - \frac{1 - 3\omega + 3\omega^2}{3\omega(1-\omega)} = 2 - \frac{1}{3\omega(1-\omega)},$$

that leads to $B = 2/3$ for $\omega = 1/2$ as stated before. In Figure 2.8 we show Binder cumulants for the strongly segregated states for different $\beta$ where $\omega$ is not half where we have used previously derived formula.

Similarly, below we calculate the central moments of Gaussian distribution and its associated Binder cumulant. The n-th central moment is:

$$\begin{aligned}\langle (x - \mu)^n \rangle &= \frac{1}{\sqrt{2\pi\sigma^2}} \int_{-\infty}^{\infty} dx (x - \mu)^n \exp\left(-\frac{(x-\mu)^2}{2\sigma^2}\right) \\ &= \frac{1}{\sqrt{2\pi}} \sigma^n \int_{-\infty}^{\infty} du u^n \exp\left(-\frac{u^2}{2}\right).\end{aligned}$$

For $n$ odd the moment $\langle (x-\mu)^n \rangle$ is zero as the odd function is integrated on the symmetric domain. Accordingly, even moments are:

$$\begin{aligned}
&\langle (x-\mu)^n \rangle = \\
&= \frac{2}{\sqrt{2\pi}} \sigma^n \int_0^\infty dt \frac{1}{\sqrt{2t}} (\sqrt{2t})^n \exp(-t) \\
&= \frac{\sigma^n 2^{n/2}}{\sqrt{\pi}} \int_0^\infty dt t^{n/2-1/2} \exp(-t) \\
&= \frac{\sigma^n 2^{n/2}}{\sqrt{\pi}} \Gamma\left(\frac{n+1}{2}\right).
\end{aligned}$$

Especially, the second moment:

$$\langle (x-\mu)^2 \rangle = \frac{2\sigma^2}{\sqrt{\pi}} \frac{\sqrt{\pi}}{2} = \sigma^2,$$

where we used properties of Gamma funtion $\Gamma(n+1) = n\Gamma(n)$ and $\Gamma(1/2) = \sqrt{\pi}$. Similarly the fourth central moment is:

$$\langle (x-\mu)^2 \rangle = \frac{4\sigma^4}{\sqrt{\pi}} \frac{3\sqrt{\pi}}{4} = 3\sigma^4,$$

Finally, the Binder cumulant of the Gaussian distribution is:

$$B = 1 - \frac{3\sigma^4}{3(\sigma^2)^2} = 0.$$

# Appendix C

# Envy-free Nash Equilibrium

Many interactions between agents can be formulated in terms of games. A game in a broad sense is defined by a list of actions that can be taken by players and scores assigned to all combinations of actions. In this setup agent's strategy is a prescription describing how actions are to be taken, e.g. a probability vector assigning probability with which any of the action is taken. When an interaction is defined in this way, Nash equilibrium can be defined as a set of strategies played by each player such that no player can increase his/her score by unilaterally changing his/her strategy.

Populations with a large number of agents with complicated interactions, could in principle have many Nash equilibria. For example, in the choice of market interaction we described, when all agents synchronise at a single market, there is no incentive for an individual player to change his/her preference, thus that state represents a Nash equilibrium. In the thesis, we focus on another type of Nash equilibrium, the one at which everyone earns the same (as opposed to synchronization at a single market where if markets are biased and subpopulations have buy/sell roles there would be score discrepancy) - *envy-free* Nash equilibrium. For example in a simple game Battle of sexes, where a female and a male player have only two actions - to go to a ballet or a football match (where the female prefers ballet, while the male prefers football, but both prefer to be together), there are three Nash equilibria. Two of them are envious - going to the ballet or the match are Nash equilibria as being at that state none of the players would benefit by going to the different choice alone, but at the venue one of the players is always happier. However, there is also a third Nash equilibrium, the mixed strategy where players decide between the ballet and the match randomly so, in the long run, they are both equally happy. The

similar state we can define for the two subpopulations choosing between two markets – if on average all choices lead to same return no one has the incentive to deviate, and everyone earns the same.

The goal is to search if there is such a division between markets in two subpopulations that would lead to equal payoff at both markets. We denote with:
$f_1^{(1)}$ - fraction of agents with $p_{\mathcal{B}}^{(1)}$ who trade at market 1,
$f_1^{(2)}$ - fraction of agents with $p_{\mathcal{B}}^{(2)}$ who trade at market 1.
Average numbers of valid bids/asks ($\mathcal{T} \in \{\mathcal{B}, \mathcal{S}\}$) at market $m$ is therefore:

$$\overline{N}_{\mathcal{T}m} = Q_{\mathcal{T}m}(p_{\mathcal{T}}^{(1)} f_m^{(1)} + p_{\mathcal{T}}^{(2)} f_m^{(2)}).$$

While the trading probabilities are calculated as usually:

$$T_{\mathcal{B}m} = \min\left(1, \frac{\overline{N}_{\mathcal{S}m}}{\overline{N}_{\mathcal{B}m}}\right), \qquad T_{\mathcal{S}m} = \min\left(1, \frac{\overline{N}_{\mathcal{B}m}}{\overline{N}_{\mathcal{S}m}}\right).$$

Following previous definition, it is clear that at least one of the trading probabilities at market $m$ needs to be equal to 1. The condition of an envy-free Nash equilibrium is the following:

$$\begin{gathered} S_1^{(i)} = S_2^{(i)}, \\ p_{\mathcal{B}}^{(i)} T_{\mathcal{B}1}\langle S_{\mathcal{B}1}\rangle + (1 - p_{\mathcal{B}}^{(i)}) T_{\mathcal{S}1}\langle S_{\mathcal{S}1}\rangle = p_{\mathcal{B}}^{(i)} T_{\mathcal{B}2}\langle S_{\mathcal{B}2}\rangle + (1 - p_{\mathcal{B}}^{(i)}) T_{\mathcal{S}2}\langle S_{\mathcal{S}2}\rangle, \end{gathered} \tag{C.1}$$

i.e. an agent with preference for buying $p_{\mathcal{B}}^{(i)}$ does not perceive the difference between trading at market 1 or 2. If there is such a pair of $f_1^{(1)}, f_1^{(2)}$ to provide that the equality C.1 holds, than that is indeed a Nash Equilibrium because an agent does not benefit from unilaterally changing his strategy profile. This equilibrium is an envy-free one, as both groups are equally satisfied. For more details on the Nash equilibrium for this game and its link to our dynamical model see Nicole et al. [88]. For the Nash equilibrium lines we have ploted in the thesis earlier we also proved as stated below that the average return value is not $p_{\mathcal{B}}$ dependent as long as the system is symmetric. We do so by rewritting the

condition C.1 in the following form:

$$p_{\mathcal{B}}^{(1)}(T_{\mathcal{B}1}\langle S_{\mathcal{B}1}\rangle - T_{\mathcal{B}2}\langle S_{\mathcal{B}2}\rangle) + (1-p_{\mathcal{B}}^{(1)})(T_{\mathcal{S}1}\langle S_{\mathcal{S}1}\rangle - T_{\mathcal{S}2}\langle S_{\mathcal{S}2}\rangle) = 0,$$
$$p_{\mathcal{B}}^{(2)}(T_{\mathcal{B}1}\langle S_{\mathcal{B}1}\rangle - T_{\mathcal{B}2}\langle S_{\mathcal{B}2}\rangle) + (1-p_{\mathcal{B}}^{(2)})(T_{\mathcal{S}1}\langle S_{\mathcal{S}1}\rangle - T_{\mathcal{S}2}\langle S_{\mathcal{S}2}\rangle) = 0.$$

Although $T_\gamma$ depends on the value of $p_{\mathcal{B}}$ (as $p_{\mathcal{B}}$ will influence $f$ and thus $T_\gamma$), for specific choice of $p_{\mathcal{B}}^{(1)}, p_{\mathcal{B}}^{(2)}$ we can ask if previous condition has solution in terms of $\Delta_{\mathcal{T}} = T_{\mathcal{T}1}\langle S_{\mathcal{T}1}\rangle - T_{\mathcal{T}2}\langle S_{\mathcal{T}2}\rangle$ (these are difference in buyer's/seller's returns at two markets $\Delta_{\mathcal{B}}/\Delta_{\mathcal{S}}$). Using this notation, the NE condition becomes:

$$p_{\mathcal{B}}^{(1)}\Delta_B + (1-p_{\mathcal{B}}^{(1)})\Delta_S = 0,$$
$$p_{\mathcal{B}}^{(2)}\Delta_B + (1-p_{\mathcal{B}}^{(2)})\Delta_S = 0.$$

These equations have unique solution $(\Delta_B, \Delta_S) = (0,0)$ whenever $p_{\mathcal{B}}^{(1)} \neq p_{\mathcal{B}}^{(2)}$. The solution $(\Delta_B, \Delta_S) = (0,0)$ translates our NE condition into:

$$T_{\mathcal{B}1}\langle S_{\mathcal{B}1}\rangle = T_{\mathcal{B}2}\langle S_{\mathcal{B}2}\rangle,$$
$$T_{\mathcal{S}1}\langle S_{\mathcal{S}1}\rangle = T_{\mathcal{S}2}\langle S_{\mathcal{S}2}\rangle.$$

When markets are symmetric, condition $\theta_1 = 1-\theta_2$ the following average returns (as proven in Appendix A) are equal:

$$\langle S_{\mathcal{B}1}\rangle = \langle S_{\mathcal{S}2}\rangle \text{ and } \langle S_{\mathcal{S}1}\rangle = \langle S_{\mathcal{B}2}\rangle.$$

Under the symmetry condition depending on the order between the two returns (either $\langle S_{\mathcal{B}1}\rangle > \langle S_{\mathcal{B}2}\rangle$ or the other way around), the trading probabilities are fixed. If for example $\langle S_{\mathcal{B}1}\rangle > \langle S_{\mathcal{B}2}\rangle$ that leads to $T_{\mathcal{B}2} = T_{\mathcal{S}1} = 1$ and $T_{\mathcal{B}1} = T_{\mathcal{S}2} = \langle S_{\mathcal{B}2}\rangle/\langle S_{\mathcal{B}1}\rangle$.

Finally, in the case of the symmetric markets, we observe:

$$\begin{aligned} T_{\mathcal{B}1}\langle S_{\mathcal{B}1}\rangle &= T_{\mathcal{S}2}\langle S_{\mathcal{B}1}\rangle \text{ as we shown in previous argument} \\ &= T_{\mathcal{S}2}\langle S_{\mathcal{S}2}\rangle \text{ market symmetry} \\ &= T_{\mathcal{S}1}\langle S_{\mathcal{S}1}\rangle \text{ NE condition} \end{aligned}$$

Thus in the case of symmetric markets $S^*$ – average return obtained at Nash equilibrium is:

$$\begin{aligned} S^* &= p_{\mathcal{B}}^{(1)} T_{\mathcal{B}1}\langle S_{\mathcal{B}1}\rangle + (1 - p_{\mathcal{B}}^{(1)}) T_{\mathcal{S}1}\langle S_{\mathcal{S}1}\rangle \\ &= T_{\mathcal{B}1}\langle S_{\mathcal{B}1}\rangle = T_{\mathcal{S}1}\langle S_{\mathcal{S}1}\rangle = \langle S_{\mathcal{S}1}\rangle. \end{aligned}$$

which in the case of symmetric markets is equal to the lower of the two possible average market returns. Remarkably, we have shown that as long as markets and subpopulations are symmetric, the average return obtained by an agent at the Nash equilibrium is not dependent on the subpopulation buy/sell preferences $p_{\mathcal{B}}$. This result holds for general choice of $(p_{\mathcal{B}}^{(1)}, p_{\mathcal{B}}^{(2)})$ provided that they are not equal and that there exists pair $(f_1^{(1)}, f_1^{(2)})$ such that the trading probabilities are as calculated before.

# Appendix D

# Numerical simulations

In this appendix, we provide details of numerical simulations used for the results presented in the thesis. The comments and instructions are organised in three different sections to follow three different models we analysed.

### Discrete double auctions

In Chapters 2, 3 and 4 we presented results of the numerically simulated adaptation of agents who choose between two or more discrete time double auctions. The defining parameters of the system are summarised in Table D.1 with their explanations and the standard values that are used in the main text unless otherwise specified. The pseudo code of the simulated system is shown in the Algorithm 1. The algorithm addresses agents with adaptive buy/sell preferences, but the agents with fixed preferences are simulated similarly (one more set of input parameters, $p_{\mathcal{B}}^{(g)}$ and the $chooseAction$ step of the algorithm is independent of $\beta$).

We usually initialised numerical simulations with zero attractions (e.g. $A_\gamma = 0\ \forall\gamma \in \{\mathcal{B}1, \mathcal{S}1, \mathcal{B}2, \mathcal{S}2\}$ and $A_{1,2}^{(g)} = 0$), but in Chapter 3 we also address normally distributed attractions. The time required to reach a steady state was highly dependent on the chosen parameters (longer for low $r$ and high $\beta$). Initial convergence to the strongly segregated state is usually within 10-100 memory lengths ($1/r$). However, the agent's relaxation times become very long (see Fig. 2.6) in the segregated regime so the simulation length is decided by confirming stability and relaxation times by probe runs and then automatized so that the simulation lasts at least couple of times longer than the agent's relaxation time.

**System definition in terms of parameters**

| *Parameter* | *Description* | *Typical Value* |
|---|---|---|
| $M$ | Number of markets | 2 |
| $(\theta_1, \theta_2)$ | Market biases - usually symmetric, $\theta_1 = 1 - \theta_2$ | $(0.3, 0.7)$ |
| $N$ | Number of traders | 200 |
| $(\mu_a, \sigma_a)$ | Mean and standard deviation of the ask distribution | $(9.5, 1)$ |
| $(\mu_b, \sigma_b)$ | Mean and standard deviation of the bid distribution | $(10.5, 1)$ |
| $r$ | Forgetting rate; range $r \in [0, 1]$ | $r = 0.1$ |
| $\alpha$ | Forgetting rate of unplayed actions; range $\alpha \in [0, 1]$ | $\alpha = 1$ |
| $\beta$ | Intensity of choice; simulation range $\beta \in [1, 50]$ | – |
| $(p_{\mathcal{B}}^{(1)}, p_{\mathcal{B}}^{(2)})$ | Preferences for buying of the two subpopulations | (0.8,0.2) |

TABLE D.1: **List of parameters defining the system; unless otherwise stated, the typical values are used.**

To be sure that the system reached the steady state we measured average returns, attractions and higher cumulants of the attraction distributions; when the averages of these observables became independent of time, we assumed stationarity and started collecting the data for the analysis. Statistics presented in the thesis are gathered for each parameter setting from 100 independent runs (in Chapter 2, while 20 in the following chapters) of the stochastic dynamics. Time averages are usually taken over $10/r$ trading periods at the end of each simulation run.

**Algorithm 1:** Discrete double auctions

**Data:** $\mathcal{A}$,$\beta$,$r$,$N$,$M$,$SimLen$
**Result:** Attraction $\mathcal{A}$ time series.
**begin**
  Initialize agent's attractions $\mathbf{A} = \left(A^i_{m\tau}\right)^{i=1\ldots N}_{m=1\ldots M \tau\in\{\mathcal{B},\mathcal{S}\}} \longleftarrow \mathcal{A}$
  **for** *n=1* **to** *SimLen* **do**
    **for** *i=1* **to** $N$ **do**
      $m_i = chooseMarket(\mathbf{A}^i, \beta)$ agent's choice of market
      $\tau_i = chooseAction(\mathbf{A}^i, \beta)$ agent's choice of buy/sell action
      $AppendToMarketOrderList(i, \tau_i, m_i)$
    **for** *m=1* **to** $M$ **do**
      $a_m = mean(MarketOrderList(\mathcal{S}, m))$ average bid at market $m$
      $b_m = mean(MarketOrderList(\mathcal{B}, m))$ average ask at market $m$
      $\pi_m = a_m + \theta_m(b_m - a_m)$ trading price at market m
      $\mathbf{S} \longleftarrow RemoveInvalidBids(MarketOrderList(\mathcal{B}, m), \pi_m)$
      $\mathbf{S} \longleftarrow RemoveInvalidAsks(MarketOrderList(\mathcal{S}, m), \pi_m)$
      $\mathbf{S} \longleftarrow Trade(MarketOrderList(:, m), \pi_m)$
    $\mathbf{A} = (1 - r)\mathbf{A} + r\mathbf{S}$
    print $\mathbf{A}$

### Continuous double auctions

In Chapter 4 we analysed a more detailed market mechanism – continuous double auctions with an open limit order book and adaptive traders with fundamentalist trading strategies. There we closely follow algorithmic suggestions of previous authors (e.g. in the Toth et al. [99] there are strategy and simulation codes). At this moment we discuss the list of parameters, especially the ones we have changed compared to the original model.

**Continuous double auction parameters**

| *Parameter* | *Description* | *Typical Value* |
|---|---|---|
| $M$ | Number of markets | 2 |
| $R$ | Number of rounds within a trading period | $N$ |
| $\pi$ | Initial trading price | 40 |
| $N$ | Number of traders | 2000 |
| $r$ | Forgetting rate; range $r \in [0, 1]$ | $r = 0.1$ |
| $\beta$ | Intensity of choice; simulation range $\beta \in [1, 50]$ | – |
| $n_s$ | Initial stock endowment of an agent (previously 40) | 100 |
| $c$ | Initial cash endowment of an agent $n_s\pi$ | 4000 |

TABLE D.2: **List of parameters defining the system; unless otherwise stated, the typical values are used.**

The dividend process is simulated using the same parameters as in the original model $D_0 = 0.2$ while $\epsilon \in \mathcal{N}(0, 0.01)$. To allow more time for agent's learning and adaptation our simulation lasts longer than in previous works (e.g. 30 trading periods [99, 100]) between 10 and 100 memory lengths (e.g. 100 to 1000 trading periods for the typically used $r = 0.1$). As in the discrete auction model we track the Binder cumulant and similar macroscopic quantities to assess stability in the attraction distributions. We also increase the number of agents as opposed to previous models that usually studied systems with only one representative agent from each group. In a system with 10 types of agents, previous authors would usually consider the trading period which lasts 100 rounds. As we look at larger populations e.g. $N = 2000$ traders, the trading period lasts $N$ rounds so that each trader has on average one chance to be in the role of aggressor.

As in the original model we track agent's wealth that is changed at the end of each trading period (the dividend is paid for all stocks an agent possesses and the risk-free interest rate $r = 0.1$ is paid on cash) although the market choosing strategies are not

based on this information.

### Evolutionary auctions

Finally in Chapter 5 we look at the evolutionary auctions. As opposed to previous works we do not simulate agents perpetually participating in the game. Instead, we make an assumption that the population is large and well mixed so knowing the total number of agents with any available strategy we can calculate all the fitnesses $\pi_i$ and accordingly the transition rates. Thus we simulate the continuous time adaptation based on Gillespie algorithm [133]. As the evolution is in continuous time and at each instance of time (of variable length) a single agent is updated, to measure time in generations we always simulate $TN$ time steps (where $T$ is desired simulation time). The analytical framework, especially the power spectra analysis suggests that majority of dynamically interesting events should happen within periods of 100 generations (see e.g. peak frequencies in Figs. 5.6, 5.11). Similarly, the initial convergence to the steady state can be calculated and used as an estimator of the necessary simulation time.

A large number of discrete strategies, require large populations for comparison with our analysis, thus large $L$ needs very long simulation times so for most of our simulation work we focused on up to 20 different strategies. Additionally, when a large number of strategies is available but the population is not too large we introduce small mutation rates $u = 0.005$ to ensure the presence of all strategy types in the population.

# Appendix E

# Linear stability analysis of the Fokker-Planck equation

In Chapter 2 and Appendix A we have introduced the Fokker-Planck description for the adaptation of a system with traders with fixed buy-sell preferences. We noted in a restricted region of the space of agent's learning parameters (high $\beta$ and low $r$), there are three steady state solutions of the Fokker-Planck equation (see e.g. Figure 2.13). Further, in Chapter 4 we realise that in that region of parameters the simulated system converges to one of the two new solutions we named weakly segregated states. In this appendix, we introduce the linear stability analysis method for the Fokker-Planck equation using which we should in principle be able to understand the state's stability. Unfortunately, numerical implementation of the description below provides us with spurious results, but we still provide the description for the interested reader who might be able to utilise it properly.

In the previous chapters we have realised that with an order parameter per market, the Fokker-Planck equations for different subpopulations decouple and we can find the steady states of the system. We have used market Demand to Supply ratio as an order parameter as it has a clear interpretation and it conveniently translates into trading probabilities. In a system with two subpopulations and two markets, fractions of players at the market one for both subpopulations can also be used as order parameters as they easily translate into demand to supply ratios. For the simplicity of the following analysis, we use $f^{(1)}, f^{(2)}$, the population averages of the preferences for the market one, as order

parameters:

$$f^{(1)}(t) = \int \sigma_\beta(x) P^{(1)}(x,t|p_{\mathcal{B}}^{(1)})dx,$$
$$f^{(2)}(t) = \int \sigma_\beta(x) P^{(2)}(x,t|p_{\mathcal{B}}^{(2)})dx,$$

where $x$ stands for $\Delta^{(g)}$ in previous notation, introduced to simplify the notation below. Additionally instead of $P(x,t|p_B^{(g)})$ only $P^{(g)}(x,t)$ will be used. The average preferences for the market one $f^{(g)}$ translate into previously used demand to supply ratios in the following way:

$$D_1 = \frac{p_{\mathcal{B}}^{(1)} f^{(1)} + p_{\mathcal{B}}^{(2)} f^{(2)}}{(1-p_{\mathcal{B}}^{(1)}) f^{(1)} + (1-p_{\mathcal{B}}^{(2)}) f^{(2)}},$$
$$D_2 = \frac{f^{(1)} p_{\mathcal{B}}^{(1)} + f^{(2)} p_{\mathcal{B}}^{(2)}}{f^{(1)}(1-p_{\mathcal{B}}^{(1)}) + f^{(2)}(1-p_{\mathcal{B}}^{(2)})}.$$

The coupled Fokker-Planck equations for the two subpopulations are as previously (with a slightly simplified notation):

$$\partial_t P^{(1)}(x,t) = -\partial_x(M_1^{(1)}(x,f_1,f_2)P^{(1)}(x,t)) + \frac{r}{2}\partial_x^2(M_2^{(1)}(x,f_1,f_2)P^{(1)}(x,t)),$$
$$\partial_t P^{(2)}(x,t) = -\partial_x(M_1^{(2)}(x,f_1,f_2)P^{(2)}(x,t)) + \frac{r}{2}\partial_x^2(M_2^{(2)}(x,f_1,f_2)P^{(2)}(x,t)).$$

The jump moments, when expressed in terms of new order parameters are:

$$M_1^{(g)}(x,f_1,f_2) = \sum_{m\in\{-1,1\}} \sum_{\tau\in\{\mathcal{B},\mathcal{S}\}} m\sigma_\beta(mx) p_\tau^{(g)} T_{m\tau}(f^{(1)},f^{(2)}) \langle S_{m\tau}\rangle - x$$
$$M_2^{(g)}(x,f_1,f_2) = \sum_{m\in\{-1,1\}} \sum_{\tau\in\{\mathcal{B},\mathcal{S}\}} \sigma_\beta(mx) p_\tau^{(g)} T_{m\tau}(f^{(1)},f^{(2)}) (\langle S_{m\tau}^2\rangle - 2mx\langle S_{m\tau}\rangle) + x^2$$

where the notation is as before: $m$ for the choice of market (with $m=-1$ denoting the second market); $\tau \in \{\mathcal{B},\mathcal{S}\}$ for the choice of trade, buy or sell; $p_{\mathcal{S}}^{(g)} = 1 - p_{\mathcal{B}}^{(g)}$. Trading probabilities that contain the dependence on the order parameters $f^{(1)}, f^{(2)}$ can be written

in the following way:

$$T_{m=1,\tau}(f^{(1)}, f^{(2)}) = \frac{\min\left(\sum_g p_{\mathcal{B}}^{(g)} f^{(g)}, \sum_g p_{\mathcal{S}}^{(g)} f^{(g)}\right)}{\sum_g p_{\tau}^{(g)} f^{(g)}},$$
$$T_{m=-1,\tau}(f^{(1)}, f^{(2)}) = \frac{\min\left(\sum_g p_{\mathcal{B}}^{(g)} (1-f^{(g)}), \sum_g p_{\mathcal{S}}^{(g)} (1-f^{(g)})\right)}{\sum_g p_{\tau}^{(g)} (1-f^{(g)})}.$$

To investigate stability of segregated solutions, we linearise the Fokker-Planck equations around the steady state solution we have previously found:

$$P^{(g)}(x,t) = P_{ss}^{(g)}(x) + \delta P^{(g)}(x,t).$$

The linearised Fokker-Planck equation, keeping only the terms linear in $\delta P^{(g)}(x,t)$ is:

$$\begin{aligned}
&\partial_t \left(P_{ss}^{(g)}(x) + \delta P^{(g)}(x,t)\right) = \\
&= -\partial_x \left(M_1^{(g)}(x, f^{(1)}, f^{(2)})(P_{ss}^{(g)}(x) + \delta P^{(g)}(x,t))\right) \\
&+ \frac{r}{2}\partial_x^2 \left(M_2^{(g)}(x, f^{(1)}, f^{(2)})(P_{ss}^{(g)}(x) + \delta P^{(g)}(x,t))\right) \\
&= -\partial_x \left(M_{1ss}^{(g)} P_{ss}^{(g)}(x)\right) - \partial_x \left(M_{1ss}^{(g)} \delta P^{(g)}(x,t)\right) \\
&- \partial_x \left((\partial_{f^{(1)}} M_1^{(g)})_{ss} P_{ss}^{(g)}(x)\right) \delta f^{(1)} - \partial_x \left((\partial_{f^{(2)}} M_1^{(g)})_{ss} P_{ss}^{(g)}(x)\right) \delta f^{(2)} \\
&+ \frac{r}{2}\partial_x^2 \left(M_{2ss}^{(g)} P_{ss}^{(g)}(x)\right) + \frac{r}{2}\partial_x^2 \left(M_{2ss}^{(g)} \delta P^{(g)}(x,t)\right) \\
&+ \frac{r}{2}\partial_x^2 \left((\partial_{f^{(1)}} M_2^{(g)})_{ss} P_{ss}^{(g)}(x)\right) \delta f^{(1)} + \frac{r}{2}\partial_x^2 \left((\partial_{f^{(2)}} M_2^{(g)})_{ss} P_{ss}^{(g)}(x)\right) \delta f^{(2)},
\end{aligned}$$

where $\delta f^{(g)}$ is defined as:

$$\delta f^{(g)} = \int dx \sigma_\beta(x) \delta P^{(g)}(x,t).$$

With subscript $ss$ we denote all the evaluations at the steady state. When we cancel the terms corresponding to the Fokker-Planck at the steady state, the time evolution of the

variation from the steady state becomes:

$$\begin{aligned}\partial_t\Big(\delta P^{(g)}(x,t)\Big) &= L_{FP}^{(g)}\delta P^{(g)}(x,t)\\ &+\Big(-\partial_x\Big((\partial_{f^{(1)}}M_1^{(g)})_{ss}P_{ss}^{(g)}(x)\Big)+\frac{r}{2}\partial_x^2\Big((\partial_{f^{(1)}}M_2^{(g)})_{ss}P_{ss}^{(g)}(x)\Big)\Big)\,\delta f^{(1)}\\ &+\Big(-\partial_x\Big((\partial_{f^{(2)}}M_1^{(g)})_{ss}P_{ss}^{(g)}(x)\Big)+\frac{r}{2}\partial_x^2\Big((\partial_{f^{(2)}}M_2^{(g)})_{ss}P_{ss}^{(g)}(x)\Big)\Big)\,\delta f^{(2)},\end{aligned}$$

where $L_{FP}^{(g)}$ represents the Fokker-Planck operator evaluated at the steady state order parameters. Previous two equations for the subpopulations can be summarized in the following way:

$$\partial_t\begin{pmatrix}\delta P^{(1)}(x,t)\\ \delta P^{(2)}(x,t)\end{pmatrix}=\begin{pmatrix}L_{FP}^{(1)}+L_{11} & L_{12}\\ L_{21} & L_{FP}^{(2)}+L_{22}\end{pmatrix}\begin{pmatrix}\delta P^{(1)}(x,t)\\ \delta P^{(2)}(x,t)\end{pmatrix}$$

where $L_{ij}$ is introduced to shorten the following notation:

$$L_{ij}[P(x')]=\Big(-\partial_x\Big((\partial_{f^{(j)}}M_1^{(i)})_{ss}P_{ss}^{(i)}(x)\Big)+\frac{r}{2}\partial_x^2\Big((\partial_{f^{(j)}}M_2^{(i)})_{ss}P_{ss}^{(i)}(x)\Big)\Big)\int dx'\sigma_\beta(x')P(x').$$

**Stability analysis.** The procedure for assessing segregated state stability is the following:

1. Self-consistently solve Fokker-Planck equations for the two subpopulations, iterating in the space of order parameters until these are stable $\rightarrow P_{ss}^{(1)}(x), P_{ss}^{(2)}(x), f_{ss}^{(1)}, f_{ss}^{(2)}$.
2. Construct $L_{FP}^{(g)}$ and $L_{ij}$ and the effective operator accordingly.
3. Find eigenvalues of the effective operator.

Zero eigenvalues of the effective operator should retrieve the steady states corresponding to order parameters used on input (there are two zeros, one for each subpopulation, though the eigenvectors might be a linear combination of the steady state distributions). Other eigenvalues should tell us more about the state's stability and based on numerical evidence acquired so far, we expect the weakly segregated state to have all eigenvalues with negative real parts (i.e. stable) while the strongly segregated states should have a positive real eigenvalue too (i.e. marginally stable). Our numerical implementation of

the previously described procedure is consistent with our expectation only for very small values of forgetting rate $r$. When $r$ is increased, but still below the critical threshold (so there are still three solutions based on which we can construct the effective operators), the procedure does not differentiate between the solutions, i.e. all eigenvalues are negative. Given that the method seems to retrieve our intuition for small $r$ we believe there is a numerical mistake whose effect is reduced at small $r$ (possibly it is in terms that are multiplied with $r$), but we were not able to identify it so far.

# Appendix F

# Linear noise analysis for evolutionary auction games

In this Appendix we provide further details on the linear noise analysis for the evolutionary games, with the proof that 2-player APA games do not have a non-zero eigenvalues.

**Jacobian** In this section we show derivation of functional Jacobian, check its basic properties, and when possible analyse its spectra. We derive functional Jacobian starting from the Replicator equation F.1, we perform functional linearisation around the fixed point $\psi^*(s)$:

$$\begin{aligned}\dot{\psi}(s) &= \frac{\psi(s)}{\Delta\pi_{max}}\left(\pi(s) - \int ds'\pi(s')\psi(s')\right)\\ &= \frac{\psi(s)}{\Delta\pi_{max}}\left(\int ds_1...ds_{k-1}a(s,s_1,..s_{k-1})\psi(s_1)...\psi(s_{k-1})\right.\\ &\left. - \int ds'ds_1...ds_{k-1}a(s',s_1,..s_{k-1})\psi(s')\psi(s_1)...\psi(s_{k-1})\right). \end{aligned} \tag{F.1}$$

When $\psi(s)$ is rewritten as $\psi^*(s) + \delta\psi(s)$ keeping only the terms linear in $\delta\psi(s)$ the following equation is obtained:

$$\begin{aligned}\delta\dot{\psi}(s) = \frac{\psi^*(s)}{\Delta\pi_{max}}\Bigg((k-1)\int ds_1...ds_{k-1}a(s,s_1,...s_{k-1})\delta\psi(s_1)\psi^*(s_2)...\psi^*(s_{k-1})\\ - \int ds'ds_1...ds_{k-1}a(s',s_1,...s_{k-1})\Big(\delta\psi(s')\psi^*(s_1)...\psi^*(s_{k-1})\\ - (k-1)\psi^*(s')\delta\psi(s_1)\psi^*(s_2)...\psi^*(s_{k-1})\Big)\Bigg).\end{aligned}$$

Where with $*$ we denote all the evaluations at the fixed point of the replicator equation F.1, while the $\Delta\pi_{max}$ is the maximal difference between the payoffs of players with different biding strategies which is equal to $V$. In previous we also used the fact that the payoff function is symmetric in the second to last argument, e.g. $a(s, s_1, s_2, ...s_{k-1}) = a(s, \mathcal{P}(s_1, s_2, ...s_{k-1}))$, where $\mathcal{P}$ denote permutation. As noted in Chapter 5, we have introduced effective two player payoff function:

$$M(s, s') = \int ds_2...ds_{k-1} a(s, s', s_2, ...s_{k-1})\psi^*(s_2)...\psi^*(s_{k-1}),$$

to simplify the notation, accordingly:

$$\begin{aligned}\partial_t \delta\psi(s) &= (k-1)\frac{\psi^*(s)}{\Delta\pi_{max}}\Bigg(\int ds_1 \delta\psi(s_1)M(s, s_1) - \frac{1}{k-1}\int ds_1\delta\psi(s_1)\pi^*(s_1) \\ &\quad - \int ds' ds_1 \psi^*(s')\delta\psi(s_1)M(s', s_1)\Bigg) \\ &= (k-1)\frac{\psi^*(s)}{\Delta\pi_{max}}\int ds'\delta\psi(s')\Bigg(M(s, s') - \frac{1}{k-1}\pi^*(s') - \int dr M(r, s')\psi^*(r)\Bigg).\end{aligned}$$

The Jacobian for the fixed point of the replicator equation is then:

$$J(s, s') = (k-1)\frac{\psi^*(s)}{\Delta\pi_{max}}\Big(M(s, s') - \int dr M(r, s')\psi^*(r)\Big), \tag{F.2}$$

where we used $\pi^*(s) = 0$ at the fixed point as shown in the main text. We proceed with calculations of two player effective payoff functions $M$ for different games.

$$\begin{aligned}M_{APA}(s, s') &= \int_0^V ds_2...ds_{k-1} a_{APA}(s, s', s_2, ...s_{k-1})\psi^*(s_2)...\psi^*(s_{k-1}) \\ &= \int_0^V ds_2...ds_{k-1}\Big(V\prod_{i=2}^{k-1}\theta(s - s_i)\theta(s - s') - s\Big)\psi^*(s_2)...\psi^*(s_{k-1}) \\ &= V\theta(s - s')\Big(\int_0^s dr\psi^*(r)\Big)^{k-2} - s\Big(\int_0^V dr\psi^*(r)\Big)^{k-2} \\ &= V\theta(s - s')\phi^{k-2}(s) - s.\end{aligned}$$

For $k = 2$ this simplifies to $V\theta(s - s') - s$, i.e. the payoff function $a(s, s')$ as expected. Similarly the effective 2-player payoff of the SAPA game is:

$$
\begin{aligned}
&M_{SAPA}(s, s') = \\
&= \int ds_2 ... ds_{k-1} a_{SAPA}(s, s', s_2, ...s_{k-1})\psi^*(s_2)...\psi^*(s_{k-1}) \\
&= \int ds_2 ... ds_{k-1} \Big( (V + s - \max(s', s_2 ... s_{k-1}))\theta(s - s') \prod_{i=2}^{k-1} \theta(s - s_i) - s \Big) \psi^*(s_2)...\psi^*(s_{k-1}) \\
&= \theta(s - s') \Big( (V + s)\phi^{k-2}(s) \\
&- \int ds_2 ... ds_{k-1} \max(s', s_2 ... s_{k-1}) \prod_{i=2}^{k-1} \theta(s - s_i)\psi^*(s_2)...\psi^*(s_{k-1}) \Big) - s \\
&= \theta(s - s') \left( (V + s)\phi^{k-2}(s) - s'\phi^{k-2}(s') - (k - 2) \int_0^s ds_2 s_2 \phi^{k-3}(s_2)\psi(s_2) \right) - s \\
&= \theta(s - s') \left( (V + s)\phi^{k-2}(s) - s'\phi^{k-2}(s') - (k - 2) \Big( s\frac{\phi^{k-2}(s)}{k - 2} - \frac{\int_0^s dr \phi^{k-2}(r)}{k - 2} \Big) \right) - s \\
&= \theta(s - s') \left( V\phi^{k-2}(s) - s'\phi^{k-2}(s') + \int_0^s dr \phi^{k-2}(r) \right) - s.
\end{aligned}
$$

To find $M(s, s')$ for the two reward APA, we use the interpretation of $M$ as effective two player payoff rather than averaging $a(s, s', s_1 \dots s_{k-2})$.

$$
M_{2APA}(s, s') = \begin{cases} V\phi^{k-2}(s) + \alpha V(k - 2)(1 - \phi(s))\phi^{k-3}(s) - s, & s > s' \\ \frac{(1+\alpha)V}{2}\phi^{k-2}(s) + \frac{\alpha V}{2}(k - 2)(1 - \phi(s))\phi^{k-3}(s) - s, & s = s' \\ \alpha V\phi^{k-2}(s), & s < s' \end{cases}
$$

**Spectra of k-player APA jacobian.** The right eigenvalue problem is:

$$
\begin{aligned}
&\int ds' J(s, s')U(s') = \lambda U(s) \\
&\int ds' \frac{\psi^*(s)}{\Delta\pi_{max}} \Big( (k - 1)M(s, s') - \pi^*(s') - (k - 1) \int dr M(r, s')\psi^*(r) \Big) U(s') = \lambda U(s) \\
&(k - 1)\psi^*(s) \int ds' \Big( M(s, s') - \int dr M(r, s')\psi^*(r) \Big) U(s'),
\end{aligned}
$$

where in the last line we have fixed $V = 1$ and realized $\Delta\pi_{max} = V$, similarly we used previous result that $\pi(s) = 0$ at the fixed point. We know that there is at least one solution

$\lambda = 0$ and $U(s) = \psi^*(s)$:

$$\int ds' J(s,s')\psi^*(s') = \\ = (k-1)\psi^*(s)\int ds'\Big(M(s,s') - \int drM(r,s')\psi^*(r)\Big)\psi^*(s') \\ = (k-1)\psi^*(s)\Big(\int ds' M(s,s')\psi^*(s') - \int ds'\int drM(r,s')\psi^*(r)\psi^*(s')\Big),$$

we realize that the first term in the bracket is $\pi(s)$ while the second is an average population payoff $\pi$, evaluated at the fixed point these two terms are equal, thus $\psi^*$ is right eigenfunction of 0 eigenvalue. Below we instead search for non zero eigenvalues if they exist to try to say something about the fixed point stability. For the jacobian we also need to find $\int_0^1 drM_{APA}(r,s')$:

$$\begin{aligned}\int_0^1 drM(r,s')\psi^*(r) &= \int_0^1 dr\left(\theta(r-s')\phi^{k-2}(r) - r\right)\psi^*(r) \\ &= \left(\int_{s'}^1 dr\phi^{k-2}(r)\psi^*(r) - \int_0^1 drr\psi^*(r)\right) \\ &= \left(\frac{1}{k-1}\Big(1-\phi^{k-1}(s')\Big) - \frac{1}{k}\right) \\ &= \frac{1}{k-1}\left(-\phi^{k-1}(s') + \frac{1}{k}\right).\end{aligned}$$

In previous we used:

$$\langle s\rangle = \int_0^V dss\psi^*(s) = \frac{V}{k}.$$

Returning to the eigenvalue problem:

$$\psi(s)\int_0^1 ds'U(s')\left((k-1)\theta(s-s')\phi(s)^{k-2} - (k-1)s + \phi(s')^{k-1} - \frac{1}{k}\right) = \\ \psi(s)\left((k-1)\phi(s)^{k-2}\int_0^s ds'U(s') + \int_0^1 ds'\phi(s')^{k-1}U(s') - (\frac{1}{k} + (k-1)s)\int_0^1 ds'U(s')\right),$$

defining $V(s) = \int_0^s ds' U(s')$ and noting the following constants (that will be selfconsistently calculated later):

$$\int_0^1 ds' U(s') = A,$$
$$\int_0^1 ds' \phi(s')^{k-1} U(s') = B,$$

previous eigenvalue equation becomes:

$$\psi(s)\left((k-1)\phi(s)^{k-2}V(s) + B - \left(\frac{1}{k} + (k-1)s\right)A\right) = \lambda \frac{dV(s)}{ds}.$$

We now realize this differential equation can be solved by the integrating factor method, as it can be rewritten in the following way:

$$\frac{dV(s)}{ds} - \frac{k-1}{\lambda}\psi(s)\phi(s)^{k-2}V(s) = \frac{\psi(s)}{\lambda}\left(B - \frac{A}{k} - (k-1)As\right)$$
$$\frac{dV(s)}{ds} + g(s)V(s) = h(s),$$

where we have divided everything with $\lambda$ as our goal is to find if there is any eigenvalue $\lambda \neq 0$. The solution can be written in this form (see, e.g. [134]):

$$V(s) = \frac{\int ds \mu(s) h(s) + C}{\mu(s)} \text{ where the integrating factor } \mu \text{ is}$$
$$\mu(s) = \exp\left(\int ds g(s)\right).$$

Let us first calculate the integrating factor:

$$\mu(s) = \exp\left(-\frac{k-1}{\lambda}\int ds \psi(s)\phi(s)^{k-2}\right)$$
$$= \exp\left(-\frac{1}{\lambda}\phi^{k-1}(s)\right) = \exp\left(-\frac{s}{\lambda}\right),$$

where we used the fact that $\frac{d\phi}{ds} = \psi(s)$ and the explicit form of $\phi(s) = s^{1/(k-1)}$ for APA auctions with $V = 1$. To obtain the full solution we still need to calculate $\int ds\mu(s)h(s)$:

$$\int ds \exp(-\frac{s}{\lambda}) \left( \frac{B - \frac{A}{k}}{\lambda}\psi(s) - \frac{(k-1)A}{\lambda} s\psi(s) \right) = \int ds \exp(-\frac{s}{\lambda}) \left( \frac{B - \frac{A}{k}}{\lambda(k-1)} s^{\frac{2-k}{k-1}} - \frac{A}{\lambda} s^{\frac{1}{k-1}} \right).$$

The two integrals in $s$ can be cast in the form of incomplete Gamma function, defined as $\gamma(\alpha, x) = \int_0^x dt \exp(-t)t^{\alpha-1}$ (see e.g. Polyanin et al. [135]). However, carrying out calculations to determine constants $A$ and $B$ was not entirely successful, so we carry out the rest of the calculation for the **special case** $k = 2$. This case is also of particular interest as the fixed point found, constant $\psi(s) = 1/V$ is not an evolutionary stable strategy. The previous integral becomes simpler in this case:

$$\begin{aligned}\int ds\mu(s)h(s) &= \int ds \exp(-\frac{s}{\lambda}) \left( \frac{B - \frac{A}{2}}{\lambda} - \frac{A}{\lambda} s \right) \\ &= \frac{B - \frac{A}{2}}{\lambda} \left( -\lambda \exp(-\frac{s}{\lambda}) \right) - \frac{A}{\lambda} \left( -\lambda(s+\lambda) \exp(-\frac{s}{\lambda}) \right) \\ &= \exp(-s/\lambda) \left( -B + \frac{A}{2} + A(s+\lambda) \right).\end{aligned}$$

Consequently, the solution $V(s)$ is:

$$\begin{aligned}V(s) &= \frac{\exp(-s/\lambda) \left( -B + \frac{A}{2} + A(s+\lambda) \right) + C}{\exp(-s/\lambda)} \\ &= -B + \frac{A}{2} + A(s+\lambda) + C\exp(s/\lambda),\end{aligned}$$

while $U(s)$ is:

$$U(s) = \frac{dV(s)}{ds} = A + \frac{C}{\lambda}\exp(s/\lambda).$$

Finally we need to determine constants A and C to fulfil our initial simplification:

$$A = \int_0^1 ds' U(s') = A + C(\exp(1/\lambda) - 1).$$

From this constraint it follows that $C = 0$ which as a consequence has $U(s) = const$. Remembering that $\psi(s) = const$ for $k = 2$ and having in mind $\int ds' J(s, s')\psi(s') = 0$ it follows that there are no non zero eigenvalues of the $k = 2$ APA Jacobian.

# Appendix G

# Evolutionary stable strategies in two reward APA games

In this Appendix we address the question of evolutionary stable strategies for $k > 3$ two reward APA games. Reiter et al. [55] proved that 2-player game does not have an evolutionary stable strategy, while 3-player game has one but only when $\alpha < 0.5$, i.e. in the case when the distribution is monotonically decreasing as for $\alpha = 0$. Games with $k > 3$ players were particularly impressive as associated fixed points and also mixed strategy candidates for evolutionary stable strategies are bimodal for $\alpha > 0.5$, thus it is intriguing to investigate whether such specialised populations could be evolutionary stable. The condition we need to check is introduced by Maynard Smith[57], and it is stated below. We will keep the same notation Reiter et al.[55] used for the sake of clarity – e.g. $E(I,(I^{k-2},J^1))$ represents fitness of strategy $I$ (that can be mixed or pure strategy) when playing against $k-2$ players who play the same strategy and one player who plays strategy $J$ (denoting strategy of possible intruder).

1. $E(I,(I^{k-1},J^0)) \geq E(J,(I^{k-1},J^0))$
2. If $E(I,(I^{k-1},J^0)) = E(J,(I^{k-1},J^0))$ then $E(I,(I^{k-2},J)) > E(J,(I^{k-2},J))$

if $I$ satisfies previous conditions for all $J$ marking pure strategy from the strategy domain, then $I$ is an evolutionary stable strategy.

We check if the two conditions hold for $I$, the fixed point mixed strategy we have derived from $\pi(s) = 0$. Note $I$ is just a notation for $\psi(s)$ which as we stated previously need to satisfy the following (with $\phi(s) = \int_0^s ds'\psi(s')$): $(1-(k-1)\alpha)\phi^{k-1}(s) + (k-$

$1)\alpha\phi^{k-1}(s) = s$. Below are important payoff calculations necessary to investigate ESS condition.

- $E(J,(I^{k-1},J^0))$ corresponds to the $\pi(s)$ in our previous notation, it is a fitness of any pure strategy when confronted with $k-1$ players who play mixed strategy $\psi$. We know that for $\psi^*$ this fitness is zero.

- Similarly, $E(I,(I^{k-1},J^0))$ corresponds to the $\pi$ in our previous notation. It is a payoff of a player who plays a mixed strategy $\psi$, thus it is $\int ds\pi(s)\psi(s)$ which is also zero at the fixed point.

- These two results show that the (2) condition should be checked, i.e. as this condition holds $E(I,(I^{k-1},J^0)) = E(J,(I^{k-1},J^0))$ we need to see for which $\alpha$ the second condition will hold $E(I,(I^{k-2},J)) > E(J,(I^{k-2},J))$ and thus prove $\psi$ is invasion resistant.

- $E(J,(I^{k-2},J))$ corresponds to the following payoff:

$$\int ds_1 \dots ds_{k-2} a(s,s,s_1,\dots s_{k-2})\psi(s_1)\dots\psi(s_{k-1}).$$

  We realize that rewards will always be split and we can distinguish between two scenarios - when s is the highest strategy, thus both $V$ and $\alpha V$ are divided, or one of $k-2$ other players is a winner and the second reward is split. In previously introduced notation this corresponds to $M(s,s)$.

$$E(J,(I^{k-2},J)) = \frac{1+\alpha}{2}\phi^{k-2}(s) + (k-2)\frac{\alpha}{2}(1-\phi(s))\phi^{k-3}(s) - s$$

- Finally, $E(I,(I^{k-2},J))$ corresponds to the $\int drM(r,s)\psi(r)$ and we calculate it below:

$$\begin{aligned}E(I,(I^{k-2},J)) &= \int_0^1 dr\psi(r)\Big(\theta(r-s)\left(\phi^{k-2}(r)+\alpha(k-2)(\phi^{k-3}(r)-\phi^{k-2}(r))\right)\\ &\quad+\theta(s-r)\alpha\phi^{k-2}(r)-r\Big)\\ &= \frac{1-\phi^{k-1}(s)}{k-1}+\alpha(k-2)\left(\frac{1-\phi^{k-2}(s)}{k-2}-\frac{1-\phi^{k-1}(s)}{k-1}\right)\\ &\quad+\alpha\frac{\phi^{k-1}(s)}{k-1}-\frac{1+\alpha}{k}\end{aligned}$$

  Where in finding the last term $\int drr\psi(r)$, we have used a relation coming from the $E(I,(I^{k-1}))=0$. From one side, we can realize that the expected reward for any of the $k$ pariticipants is $(1+\alpha)/k$ as every of $k$ participants have equal chance of winning first or second reward given they all play the same mixed strategy. The cost, on the other hand is $\int drr\psi(r)$, knowing that the difference between the two is zero, we can calculate that the average bidding strategy is $(1+\alpha)/k$.

Introducing a function $f(s,\alpha,k)=E(I,(I^{k-2},J^1))-E(J,(I^{k-2},J^1))$, after some algebraic manipulation and using mixed strategy relation on $\phi$ we have previously derived we obtain:

$$f(s,\alpha,k)=s\frac{k-2}{k-1}+\frac{1+\alpha}{k(k-1)}+\frac{(k-3)\alpha-1}{2}\phi^{k-2}(s)-\frac{(k-2)\alpha}{2}\phi^{k-3}(s)$$

Now, using numerical solutions for $\phi(s)$, we can find $\alpha$ and $k$ for which $f(s,\alpha,k)>0$ for all $s\in[0,1]$. In Figure G.1 we show contour plots of the function $f$ for $k=3$ and $k=4$ from which we see that 3-player game does not have an evolutionary stable strategy for $\alpha>0.5$ (as $f$ is negative), while the 4-player game does not have an ESS for $\alpha>0.6$. In the same Figure we also show how $\alpha_c$ depends on $k$. It is important to note that although an evolutionary stable strategy does not exist for all $\alpha$ there is a stable fixed point for all $\alpha$ (as discussed in Chapter 5) while here we showed that there is an evolutionary stable bimodal distribution for some range of $\alpha$ for every $k>3$.

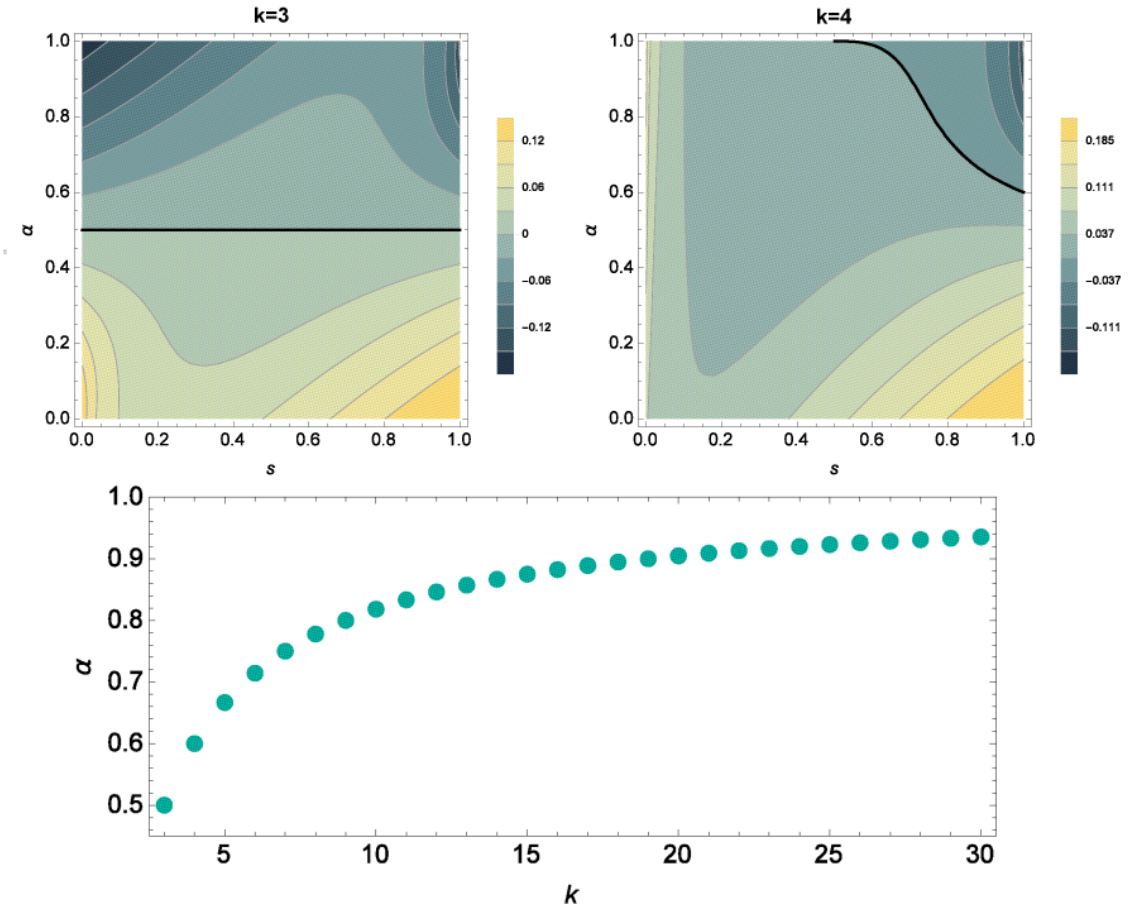


FIGURE G.1: **Existence of the Evolutionary Stable Strategy.** Top panels show contours of the $f(s, \alpha, k)$ for $k = 3$ (left) and $k = 4$ (right) demonstrating that the sign of the function becomes negative for some $s \in [0, V]$ when $\alpha = 0.5$ for $k = 3$ and $\alpha = 0.6$ for $k = 4$, marking the inexistence of ESS for $\alpha$ greater than those values. (Black line in both contour plots marks $f(s, \alpha, k) = 0$ contour.) Bottom panel shows $\alpha_c$ dependence on $k$, for $\alpha < \alpha_c$ there exist unique evolutionary stable strategy.

# Appendix H

# Discrete evolutionary auction games

This Appendix has further details on the discrete evolutionary auction games. Firstly we address the difference between the fixed point in the discretized and discrete game, illustrating it with an example of 3-player APA games with 3 available strategies. We then show that there is no such difference in the 2-player APA games. We proceed with explicit two player effective payoff matrices for all games $M_{ij}$ (necessary for the spectral data shown in Chapter 5). Finally, we address a discrete game that will lead to same fixed points as the discretized one.

### APA discrete strategy Fixed point mixed strategy

In this section we address the zig-zag structure of the mixed strategy fixed point in the all-pay auction with discrete number of bidding strategies. As argued in Chapter 5, there is a different fitness associated with playing a bidding strategy $s_i$ when it is a bid from the continuous or discrete range. The difference comes from the treatment of the non unique winning bids which in the discrete strategy set up have non zero probability of occurrence. The two payoff functions are listed below for the $k$ player auction. It is assumed that in the continuous case strategy $s_i \in [0, V]$ while in the discrete case $s_i = iV/L$:

$$\pi_i = V \left( \int_0^{s_i} ds \psi(s) \right)^{k-1} - s_i$$

As argued before, setting $\pi_i = const$ leads to the solution $\phi(s) = (s/V)^{1/(k-1)}$ and the discrete strategy corresponding to this solution is thus:

$$\psi_i = \phi(s_i) - \phi(s_{i-1})$$

On the other hand, the payoff in the discrete strategy game is:

$$\pi_i = V\left(\sum_j^{i-1}\psi_j\right)^{k-1} + \sum_{m=2}^{k}\frac{V}{m}\binom{k-1}{m-1}\psi_i^{m-1}\left(\sum_j^{i-1}\psi_j\right)^{k-m} - s_i$$

In a special case $k = 2$ these two methods lead to the same $\psi_i = const$ strategy, below is derivation of that result from the discrete game side:

$$\pi_i = V(\sum_{j=1}^{i-1}\psi_j) + \frac{V}{2}\psi_i - s_i = c$$

From these equation we find:

$$\psi_i = \begin{cases} \frac{2}{V}(s_1 + c), & i = 2l+1 \\ -\frac{2c}{V}, & i = 2l \end{cases}$$

where we used the fact that $s_i = iV/L$. Using the constraing $\sum_{i=1}^{L}\psi_i = 1$ for $L$ odd we obtain $c = -\frac{V}{2L}$. Using this constant in the previous formula we obtain $\psi_i = 1/L$, for all $i$. However, when $L$ is even the $\sum_{i=1}^{L}\psi_i = 1$ condition is satisfied for any $c$ (though we note that be needs to be $-V/L \leq c \leq 0$ for $\psi_i$ to be greater or equal to zero). This means that for $L$ even there is a family of distributions that are the fixed point of the replicator equation. The uniform distribution we obtain for $L$ odd is one of the solutions, but also a family of zig-zag distributions. As these different distributions lead to different average fitness $c$, we note that it is maximised for $c = 0$ when only the odd bidding strategies are played.

For $k > 2$ the discretized continuous fixed point is not any more equivalent to the fixed point in the discrete game. This is due to the fact that in the discrete game $\psi_i$ is a non trivial $k-1$st root which we illustrate below in a simple example for 3 player auction.

The discretized fixed point of cont. game leads to the mixed strategy:

$$\psi_1 = \sqrt{\frac{s_1}{V}}$$
$$\psi_i = \sqrt{\frac{s_i}{V}} - \sqrt{\frac{s_{i-1}}{V}}$$

On the other hand, the fixed point of the discrete game with $L = 3$ strategies (solving $\pi_i = c, \forall i \in \{1, 2, 3\}$:

$$\psi_1 = \sqrt{\frac{3(c + s_1)}{V}}$$
$$\psi_2 = -\frac{3}{2}\psi_1 \left(1 - \sqrt{1 - \frac{4}{3}(1 - \frac{c + s_2}{V})}\right)$$
$$\psi_3 = \frac{3}{2}\left(1 - \sqrt{1 - \frac{4}{3}(1 + \frac{c + s_3}{V})}\right)$$

We find that $c \neq 0$ when strategy number is finite, but we note that its absolute value decays to zero in the $L \to 0$ limit. We observe that the three $\psi$ values reported can not be matched with the discretized solution despite the freedom of varying $c$ (note for example to set $\psi_1$ equal we need $c = -2s_1/3$ which would lead to undefined $\psi_2$). This example illustrates the difference in fixed point distributions coming from the reward splitting contributions.

**Effective 2 player payoff matrices for the games with discrete strategies.** Here we present effective 2 player payoff matrices ($M_{ij}$) for the (S)APA games with discrete strategies. We write again the fitness for playing a pure strategy $s$ for every game for the comparison. As it will be clear below, when $i > j$ (as then $S_i > S_j$), $M_{ij}$ is a fitness of the player $i$ in the $k - 1$ game, as the second player can at most play the role in the SAPA game if (s)he is the second highest bidder thus cost of player $i$ is $S_j$. If $i = j$ $M_{ij}$ becomes the fitness of the player $i$ in a $k - 1$ game with the reward value always being split in $m + 1$ pieces (for $m \in \{1, \ldots, k - 1\}$). Finally when $i < j$, the player $i$ can not win and $M_{ij}$ is the cost of playing the game - $S_i$, except in the two reward APA when the player $i$

might still receive the second reward.

$$\pi_i^{APA} = \sum_{m=1}^{k} \frac{V}{m} \binom{k-1}{m-1} \psi_i^{m-1} \left( \sum_{j=1}^{i-1} \psi_j \right)^{k-m} - S_i \tag{H.1}$$

$$M_{ij}^{APA} = \begin{cases} \sum_{m=1}^{k-1} \frac{V}{m} \binom{k-2}{m-1} \psi_i^{m-1} \left( \sum_{j=1}^{i-1} \psi_j \right)^{k-1-m} - S_i, & i > j \\ \sum_{m=1}^{k-1} \frac{V}{m+1} \binom{k-2}{m-1} \psi_i^{m-1} \left( \sum_{j=1}^{i-1} \psi_j \right)^{k-1-m} - S_i, & i = j \\ -s_i, & i < j \end{cases}$$

$$\begin{aligned} \pi_i^{SAPA} =& (V + S_i) \left( \sum_{j=1}^{i-1} \psi_j \right)^{k-1} + \sum_{m=2}^{k} \frac{V}{m} \binom{k-1}{m-1} \psi_i^{m-1} \left( \sum_{j=1}^{i-1} \psi_j \right)^{k-m} \\ & - \sum_{j=1}^{i-1} S_j \left( \Big( \sum_{l=1}^{j} \psi_l \Big)^{k-1} - \Big( \sum_{l=1}^{j-1} \psi_l \Big)^{k-1} \right) - S_i \end{aligned} \tag{H.2}$$

$$M_{ij}^{SAPA} = \begin{cases} \sum_{m=1}^{k-1} \frac{V}{m} \binom{k-2}{m-1} \psi_i^{m-1} \left( \sum_{j=1}^{i-1} \psi_j \right)^{k-1-m} \\ - \sum_{j=1}^{i-1} S_j \left( \Big( \sum_{l=1}^{j} \psi_l \Big)^{k-1} - \Big( \sum_{l=1}^{j-1} \psi_l \Big)^{k-1} \right), & i > j \\ \sum_{m=0}^{k-2} \frac{V}{m+2} \binom{k-2}{m} \psi_i^{m} \left( \sum_{j=1}^{i-1} \psi_j \right)^{k-2-m} - S_i, & i = j \\ -S_i, & i < j \end{cases}$$

$$\begin{aligned} \pi_i^{2APA} =& V \left( \sum_{j=1}^{i-1} \psi_j \right)^{k-1} + \sum_{m=2}^{k} \frac{V(1+\alpha)}{m} \binom{k-1}{m-1} \psi_i^{m-1} \left( \sum_{j=1}^{i-1} \psi_j \right)^{k-m} \\ & + (k-1) \left( 1 - \sum_{j=1}^{i} \psi_j \right) \sum_{m=1}^{k-1} \frac{V\alpha}{m} \binom{k-2}{m-1} \psi_i^{m-1} \left( \sum_{j=1}^{i-1} \psi_j \right)^{k-1-m} - S_i \end{aligned} \tag{H.3}$$

$$M_{ij}^{2APA} = \begin{cases} V\left(\sum_{j=1}^{i-1}\psi_j\right)^{k-1} + \sum_{m=2}^{k}\frac{V(1+\alpha)}{m}\binom{k-1}{m-1}\psi_i^{m-1}\left(\sum_{j=1}^{i-1}\psi_j\right)^{k-m} \\ +(k-1)\left(1-\sum_{j=1}^{i}\psi_j\right)\sum_{m=1}^{k-1}\frac{V\alpha}{m}\binom{k-2}{m-1}\psi_i^{m-1}\left(\sum_{j=1}^{i-1}\psi_j\right)^{k-1-m} - S_i, & i>j \\ \sum_{m=2}^{k}\frac{V(1+\alpha)}{m}\binom{k-2}{m-2}\psi_i^{m-2}\left(\sum_{j=1}^{i-1}\psi_j\right)^{k-m} \\ +(k-2)\left(1-\sum_{j=1}^{i}\psi_j\right)\sum_{m=2}^{k-2}\frac{V\alpha}{m}\binom{k-2}{m-2}\psi_i^{m-2}\left(\sum_{j=1}^{i-1}\psi_j\right)^{k-2-m} - S_i, & i=j \\ \sum_{m=1}^{k-1}\frac{V\alpha}{m}\binom{k-1}{m}\psi_i^{m-1}\left(\sum_{j=1}^{i-1}\psi_j\right)^{k-1-m} - S_i, & i<j \end{cases}$$

Finally, as discussed in Chapter 5, the parity of $L$ affects the spectra of Jacobian and consequently the power spectra we use to describe the effects of demographic noise. That is the clearest in the 2-player APA game, where, as shown in Chapter 5, Jacobian has antisymmetric structure $J_{ij} = -J_{ji}$ and consequently has purely imaginary spectra coming in conjugated pairs. Being Jacobian of the system with a constraint $\sum_i \psi_i = 0$, it needs to have a zero eigenvalue, thus when $L$ is odd, all other eigenvalues are imaginary, conjugated pairs, but when $L$ is even, there are two zero eigenvalues. For $k > 2$ the effect of $L$ parity is in the number of real non-zero eigenvalues – when $L$ is even there is an additional negative real eigenvalue. This results in a higher value of the plateau in the low $\omega$ power spectra. However, we expect a unique $L \to \infty$ limit. In both parity cases present in Fig H.1, we see agreement with our previous conclusions, the plateau for small $\omega$ increases with $L$ so we expect that the power spectra is $1/\omega^2$ in the large $L$ limit.

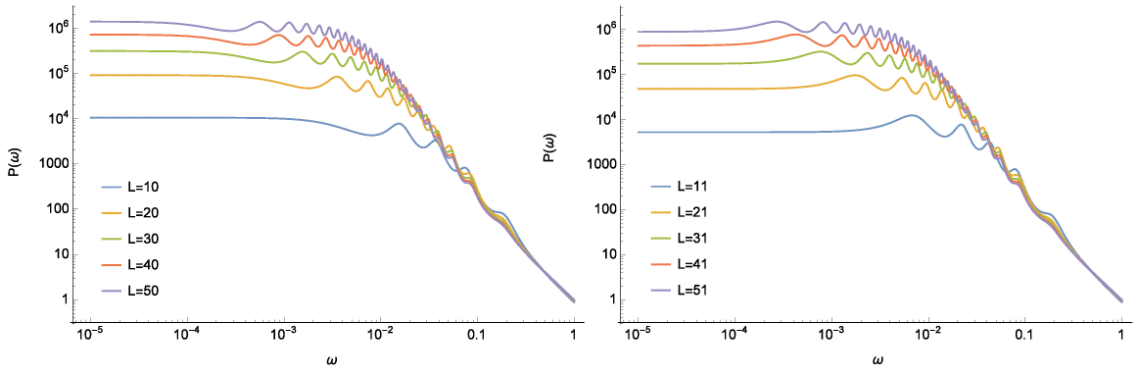


FIGURE H.1: **3-player APA power spectra for different strategy number parity.**

**APA without reward splitting.** Another possibility to study the discrete APA game that would be insightful for the $L \to \infty$ limit is to look at a discrete game in which there is no reward splitting when the highest bid is not unique. This game has the fitness that is the discretized version of the continuous fitness function and thus the fixed point distribution is identical to the discretized fixed point distribution of the continuous game. An example of the two fixed point distributions we see in Figure H.2 along with the power spectra analysis for different strategy number. We note that the power spectra do not have any resonant frequencies (i.e. no pronounced peaks in the power spectra). But, we note that the plateau value for small $\omega$ increases with $L$ suggesting $P(\omega)$ divergence at $\omega = 0$ in the $L \to \infty$ limit, as for other games shown in Chapter 5. This observation is consistent with the expectation that the spectra of the continuous operator have an accumulation point at 0 as previously remarked.

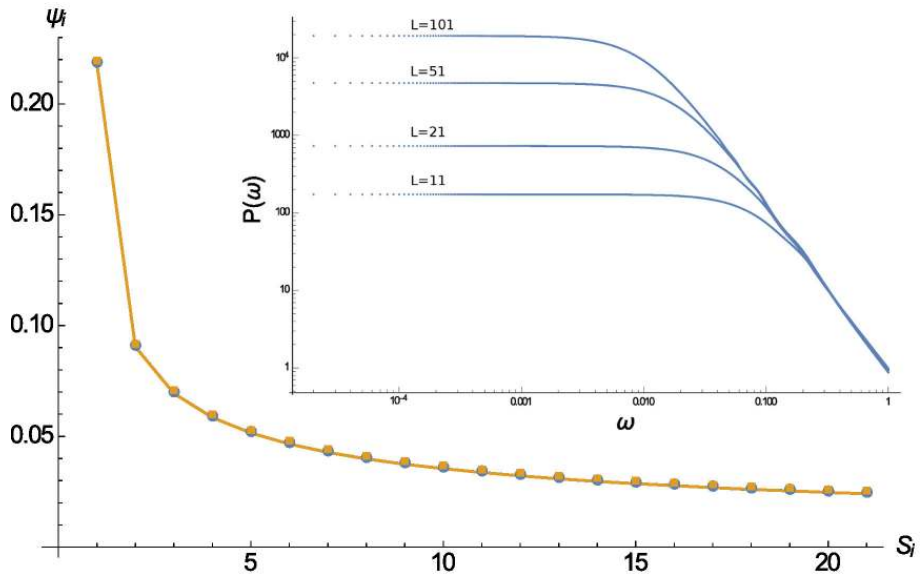


FIGURE H.2: **3-player APA game with no reward splitting.** We compare fixed-point distribution of the game with discrete strategy space (orange) and the discretised fixed point fo the game with continuous strategy space (blue) for $L = 21$ strategies between 0 and V. In the insert we present the power spectra for different strategy number of this 3-player game.

# Appendix I

# SAPA game on finite domain

Here we address the fixed point distribution of Second-price All Pay Auctions on finite domain $[0, A]$. The two player game, e.g. War of Attrition, was analysed by Bishop and Cannings [109] and it has been proven that only if $A$ is attainable, i.e. the domain includes the maximal bidding value, the evolutionary stable strategy exist, but not all pure strategies from the domain are played in the evolutionary stable population. Below, we investigate whether this is also true for the fixed point of the introduced evolutionary dynamics and extend the results to the k-player game. The fitness of playing a strategy $s$ against $k-1$ players with mixed strategy $\psi(s)$ is:

$$\pi(s) = V\phi^{k-1}(s) - s + \int_0^s ds'\phi^{k-1}(s'),$$

where for simplicity we'll use $y(s) = \phi^{k-1}(s)$. Repeating the requirement $\pi(s) = 0$ (as again assuming constant $c$ and enforcing normalisation condtions on $\phi(s)$, e.g. $\phi(0) = 0$ leads to conclusion that $c = 0$) for all $s \in [0, A]$ we obtain:

$$y(s) = 1 - K\exp\left(-\frac{s}{V}\right)$$

the conditions $y(0) = 0$ and $y(A) = 1$ lead to two different values of the constant $K$ thus we realize that a continuous function $y(s)$ can not be a solution on the $[0, A]$ domain. Thus we first assume that $y(s)$ is discontinuous at $A$ (we practically assume there's a delta peak

at A in the distribution $\psi(s)$ that takes care of the normalization on the finite domain):

$$y(s) = \begin{cases} 1 - \exp\left(-\frac{s}{V}\right), & s < A \\ 1, & s = A \end{cases}$$

To check it this assignment is consistent, we calculate the fitness of playing the strategy $A$, as playing any other startegy $s < A$ leads to zero fitness by $y(s)$ construction.

$$\begin{aligned} \pi(A) &= Vy(A) - A + \int_0^A dsy(s) \\ &= V - A + \int_0^A ds\left(1 - \exp\left(-\frac{s}{V}\right)\right) \\ &= V - A + A + V\left(\exp\left(-\frac{A}{V}\right) - 1\right) \\ &= V\exp\left(-\frac{A}{V}\right) \end{aligned}$$

We realize that bidding $A$ would then always lead to a positive fitness as opposed to bidding any other value $A - \epsilon$ that leads to fitness zero. This means that agents would not have incentives to play strategies just below the highest bidding value. We thus investigate if a gap in the strategy space $(B, A)$ would resolve this and lead to a fixed point $\psi(s)$ such that $\pi(s) = 0$ for every $s$ in domain (where $\psi(s) > 0$) as required. We then assume the $y(s)$ is:

$$y(s) = \begin{cases} 1 - \exp\left(-\frac{s}{V}\right), & s \leq B \\ 1 - \exp\left(-\frac{B}{V}\right), & s \in (B, A) \\ 1, & s = A \end{cases}$$

As before, playing strategy $s \in [0, B]$ leads to zero fitness by construction. Also as we assume there are no players bidding values between $B$ and $A$, we only proceed by calculating $\pi(A)$:

$$\begin{aligned}\pi(A) &= V - A + \int_0^B ds\left(1 - \exp\left(-\frac{s}{V}\right)\right) + \int_B^A ds\left(1 - \exp\left(-\frac{B}{V}\right)\right) \\ &= V - A + B + V\left(\exp\left(-\frac{B}{V}\right) - 1\right) + \left(1 - \exp\left(-\frac{B}{V}\right)\right)(A - B) \\ &= (V + B - A)\exp\left(-\frac{B}{V}\right)\end{aligned}$$

Requiring $\pi(s) = 0$ leads to conclusion that $B = A - V$, or that strategies that are less than V smaller than the maximal bidding strategy are not favoured in the SAPA game. We finish by ensuring that playing a strategy $s \in (B, A)$ is not useful for an agent.

$$\begin{aligned}\pi(s) &= V\left(1 - \exp\left(-\frac{B}{V}\right)\right) - s + \int_0^B ds\left(1 - \exp\left(-\frac{s}{V}\right)\right) + \int_B^s ds\left(1 - \exp\left(-\frac{B}{V}\right)\right) \\ &= V\left(1 - \exp\left(-\frac{B}{V}\right)\right) - s + B + V\left(\exp\left(-\frac{B}{V}\right) - 1\right) + (s - B)\left(1 - \exp\left(-\frac{B}{V}\right)\right) \\ &= (B - s)\exp\left(-\frac{B}{V}\right)\end{aligned}$$

that leads always to negative fitness thus agents prefer playing $s \leq B$ or $s = A$. Finally, the fixed point distribution is:

$$\psi(s) = \theta(A - V - s)\frac{1}{V(k-1)}\left(1 - \exp\left(-\frac{s}{V}\right)\right)^{\frac{2-k}{k-1}}\exp\left(-\frac{s}{V}\right) + \omega\delta(s - A)$$

where the fraction of agents bidding the highest value $\omega$ is calculated to ensure that $\psi(s)$ is normalized:

$$\omega = 1 - \left(1 - \exp\left(-\frac{A - V}{V}\right)\right)^{\frac{1}{k-1}}$$

When $A \leq V$ and $k = 2$ this results in an unimodal fixed point distribution centred at $A$, while for $A > V$ fraction of agents bidding highest value $A$ monotonically decreases, decreasing faster for higher number of participants $k$.

# Bibliography


1. Beddington, J. *et al.* Foresight: the future of computer trading in financial markets: final project report (2012).
2. Buti, S., Rindi, B. & Werner, I. M. Dark Pool Trading Strategies, Market Quality and Welfare. *Journal of Financial Economics* (2016).
3. O'Hara, M. & Ye, M. Is market fragmentation harming market quality? *Journal of Financial Economics* **100,** 459–474 (2011).
4. Mendelson, H. Consolidation, fragmentation, and market performance. *Journal of Financial and Quantitative Analysis* **22,** 189–207 (1987).
5. Chowdhry, B. & Nanda, V. Multimarket Trading and Market Liquidity. *The Review of Financial Studies* **4,** 483 (1991).
6. Madhavan, A. Consolidation, Fragmentation, and the Disclosure of Trading Information. *The Review of Financial Studies* **8,** 579 (1995).
7. Biais, B., Glosten, L. & Spatt, C. Market microstructure: A survey of microfoundations, empirical results, and policy implications. *Journal of Financial Markets* **8,** 217–264 (2005).
8. Bennett, P. & Wei, L. Market structure, fragmentation, and market quality. *Journal of Financial Markets* **9,** 49 –78 (2006).
9. Degryse, H., de Jong, F. & Kervel, V. v. The Impact of Dark Trading and Visible Fragmentation on Market Quality*. *Review of Finance* **19,** 1587 (2015).
10. Wah, E. & Wellman, M. P. *Latency arbitrage, market fragmentation, and efficiency: a two-market model* in *Proceedings of the fourteenth ACM conference on Electronic commerce* (2013), 855–872.
11. Bullock, S. & Cliff, D. Complexity and emergent behaviour in ICT systems (2004).

12. Vicsek, T., Czirók, A., Ben-Jacob, E., Cohen, I. & Shochet, O. Novel type of phase transition in a system of self-driven particles. *Physical Review Letters* **75,** 1226 (1995).

13. Cavagna, A. *et al.* From empirical data to inter-individual interactions: unveiling the rules of collective animal behaviour. *Mathematical Models and Methods in Applied Sciences* **20,** 1491–1510 (2010).

14. Bialek, W. *et al.* Statistical mechanics for natural flocks of birds. *Proceedings of the National Academy of Sciences* **109,** 4786–4791 (2012).

15. Helbing, D. & Molnar, P. Social force model for pedestrian dynamics. *Physical Review E* **51,** 4282 (1995).

16. Moussaïd, M., Helbing, D. & Theraulaz, G. How simple rules determine pedestrian behavior and crowd disasters. *Proceedings of the National Academy of Sciences* **108,** 6884–6888 (2011).

17. Galam, S., Gefen, Y. & Shapir, Y. Sociophysics: A new approach of sociological collective behaviour. I. mean-behaviour description of a strike. *Journal of Mathematical Sociology* **9,** 1–13 (1982).

18. Fernández-Gracia, J., Suchecki, K., Ramasco, J. J., San Miguel, M. & Eguíluz, V. M. Is the Voter Model a model for voters? *Physical Review Letters* **112,** 158701 (2014).

19. Castellano, C., Fortunato, S. & Loreto, V. Statistical physics of social dynamics. *Reviews of modern physics* **81,** 591 (2009).

20. Schelling, T. C. Dynamic models of segregation†. *Journal of Mathematical Sociology* **1,** 143–186 (1971).

21. Epstein, J. M. & Axtell, R. *Growing artificial societies: social science from the bottom up* (Brookings Institution Press, 1996).

22. Challet, D. & Zhang, Y.-C. Emergence of cooperation and organization in an evolutionary game. *arXiv preprint adap-org/9708006* (1997).

23. Arthur, W. B. Inductive reasoning and bounded rationality. *The American Economic Review* **84,** 406–411 (1994).

24. Moro, E. The minority game: an introductory guide. *Advances in Condensed Matter and Statistical Physics,* 263 –286 (2004).

25. Challet, D., Marsili, M. & Zhang, Y.-C. Stylized facts of financial markets and market crashes in minority games. *Physica A: Statistical Mechanics and its Applications* **294,** 514–524 (2001).

26. Johnson, N. F., Hui, P. M., Jonson, R. & Lo, T. S. Self-Organized Segregation within an Evolving Population. *Physical Review Letters* **82,** 3360–3363 (16 1999).

27. Huang, Z.-G., Zhang, J.-Q., Dong, J.-Q., Huang, L. & Lai, Y.-C. Emergence of grouping in multi-resource minority game dynamics. *Scintific Reports* **2:703** (2012).

28. Hanaki, N., Kirman, A. & Marsili, M. Born under a lucky star? *Journal of Economic Behavior & Organization* **77,** 382–392 (2011).

29. Brock, W. A. & Hommes, C. H. A rational route to randomness. *Econometrica: Journal of the Econometric Society,* 1059–1095 (1997).

30. Kirman, A. P. & Vriend, N. J. in *Interaction and Market Structure* (eds Gatti, D., Gallegati, M. & Kirman, A.) 33–56 (Springer Berlin Heidelberg, 2000).

31. Wellman, M. P. *et al.* Designing the market game for a trading agent competition. *IEEE Internet Computing* **5,** 43–51 (2001).

32. Cai, K. *et al. Overview of CAT: A market design competition* tech. rep. (Technical Report ULCS-09-005, Department of Computer Science, University of Liverpool, Liverpool, UK, 2009. Version 2.0, 2009).

33. Niu, J., Cai, K., Parsons, S., McBurney, P. & Gerding, E. What the 2007 TAC Market Design Game tells us about effective auction mechanisms. *Journal of Autonomous Agents and Multi-Agent Systems* **21 (2),** 172 –203 (2010).

34. Robinson, E., McBurney, P. & Yao, X. Co-learning Segmentation in Marketplaces. *Adaptive and Learning Agents,* 1–20 (2012).

35. Niu, J., Cai, K., Parsons, S., Fasli, M. & Yao, X. A Grey-Box Approach to Automated Mechanism Design. *Electronic Commerce Research and Applications* **11,** 24–35 (2012).

36. Shi, B., Gerding, E. H., Vytelingum, P. & Jennings, N. R. An equilibrium analysis of market selection strategies and fee strategies in competing double auction marketplaces. *Autonomous Agents and Multi-Agent Systems* **26,** 245–287 (2013).

37. Krumme, C., Llorente, A., Cebrian, M., Pentland, A. S. & Moro, E. The predictability of consumer visitation patterns. *Scientific Reports* **3** (2013).

38. Nagarajan, G., Meyer, R. L. & Hushak, L. J. Segmentation in the informal credit markets: the case of the Philippines. *Agricultural Economics* **12(2),** 171 –181 (1995).

39. Lillo, F., Moro, E., Vaglica, G. & Mantegna, R. N. Specialization and herding behavior of trading firms in a financial market. *New Journal of Physics* **10** (2008).

40. Smith, A. *An Inquiry into the Nature and Causes of the Wealth of Nations* (ed Cannan, E.) (Library of Economics and Liberty, 1904).

41. Wua, R.-S. & Choub, P.-H. Customer segmentation of multiple category data in e-commerce using a soft-clustering approach. *Electronic Commerce Research and Applications* **10(3),** 331–341 (2011).

42. Weinstein, A. *Handbook of Market Segmentation: Strategic Targeting for Business and Technology Firms* ISBN: 9780789021571 (Haworth Press, 2004).

43. Kim, T. & Lee, H.-Y. External validity of market segmentation methods. *European Journal of Marketing* **45,** 153–169. ISSN: 0309-0566 (Feb. 2011).

44. Ellison, G., Fudenberg, D. & Möbius, M. Competing auctions. *Journal of the European Economic Association* **2,** 30–66 (2004).

45. Caillaud, B. & Jullien, B. Chicken & egg: Competition among intermediation service providers. *RAND Journal of Economics,* 309–328 (2003).

46. Sato, Y. & Crutchfield, J. P. Coupled replicator equations for the dynamics of learning in multiagent systems. *Physical Review E* **67** (2003).

47. Quigley, B. J., López, D. G., Buckling, A., McKane, A. J. & Brown, S. P. The mode of host–parasite interaction shapes coevolutionary dynamics and the fate of host cooperation. *Proceedings of the Royal Society of London B: Biological Sciences,* rspb20120769 (2012).

48. Stouffer, D. B. & Bascompte, J. Compartmentalization increases food-web persistence. *Proceedings of the National Academy of Sciences* **108,** 3648–3652 (2011).

49. Tokita, K. & Yasutomi, A. Emergence of a complex and stable network in a model ecosystem with extinction and mutation. *Theoretical Population Biology* **63,** 131 –146 (2003).

50. Bascompte, J., Jordano, P., Melián, C. J. & Olesen, J. M. The nested assembly of plant–animal mutualistic networks. *Proceedings of the National Academy of Sciences* **100,** 9383–9387 (2003).

51. Allender, C. J., Seehausen, O., Knight, M. E., Turner, G. F. & Maclean, N. Divergent selection during speciation of Lake Malawi cichlid fishes inferred from parallel radiations in nuptial coloration. *Proceedings of the National Academy of Sciences* **100,** 14074–14079 (2003).

52. Ford, E. B. & Huxley, S. J. S. *Polymorphism and taxonomy* (Oxford University Press, 1940).

53. Kirkpatrick, M. & Ravigné, V. Speciation by natural and sexual selection: models and experiments. *The American Naturalist* **159,** S22–S35 (2002).

54. Bhattacharyay, A & Drossel, B. Modeling coevolution and sympatric speciation of flowers and pollinators. *Physica A: Statistical Mechanics and its Applications* **345,** 159–172 (2005).

55. Reiter, J. G., Kanodia, A., Gupta, R., Nowak, M. A. & Chatterjee, K. Biological auctions with multiple rewards. *Proceedings of Royal Society B* **282** (2015).

56. Maynard Smith, J. & Price, G. R. The logic of animal conflict. *Nature* **246,** 15 (1973).

57. Smith, J. M. The theory of games and the evolution of animal conflicts. *Journal of Theoretical Biology* **47,** 209–221 (1974).

58. Rose, M. R. Cheating in evolutionary games. *Journal of Theoretical Biology* **75,** 21 –34 (1978).

59. Haigh, J. & Rose, M. R. Evolutionary game auctions. *Journal of Theoretical Biology* **85,** 381 –397 (1980).

60. Bishop, D. T. & Cannings, C. Models of animal conflict. *Advances in Applied Probability* **8,** 616 (1976).

61. Traulsen, A., Claussen, J. C. & Hauert, C. Coevolutionary Dynamics: From Finite to Infinite Populations. *Phys. Rev. Lett.* **95,** 238701 (23 2005).

62. Traulsen, A., Claussen, J. C. & Hauert, C. Coevolutionary dynamics in large, but finite populations. *Phys. Rev. E* **74,** 011901 (1 2006).

63. Taylor, C., Fudenberg, D., Sasaki, A. & Nowak, M. A. Evolutionary game dynamics in finite populations. *Bulletin of Mathematical Biology* **66,** 1621–1644 (2004).

64. Rogers, T., McKane, A. J. & Rossberg, A. G. Demographic noise can lead to the spontaneous formation of species. *EPL (Europhysics Letters)* **97,** 40008 (2012).

65. Chakraborti, A., Toke, I. M., Patriarca, M. & Abergel, F. Econophysics review: II. Agent-based models. *Quantitative Finance* **11,** 1013–1041 (2011).

66. Bak, P., Paczuski, M. & Shubik, M. Price variations in a stock market with many agents. *Physica A: Statistical Mechanics and its Applications* **246,** 430–453 (1997).

67. Chiarella, C. & Iori, G. A simulation analysis of the microstructure of double auction markets*. *Quantitative Finance* **2,** 346–353 (2002).

68. Mike, S. & Farmer, J. D. An empirical behavioral model of liquidity and volatility. *Journal of Economic Dynamics and Control* **32,** 200–234 (2008).

69. Cont, R. & Bouchaud, J.-P. Herd behavior and aggregate fluctuations in financial markets. *Macroeconomic Dynamics* **4,** 170–196 (2000).

70. Lux, T. & Marchesi, M. Volatility clustering in financial markets: a microsimulation of interacting agents. *International Journal of Theoretical and Applied Finance* **3,** 675–702 (2000).

71. Peter R. Wurman, M. P. W. & Walsh, W. E. A Parametrization of the Auction Design Space. *Games and Economic Behavior* **35,** 304–338 (2001).

72. Parsons, S., Marcinkiewicz, M., Niu, J. & Phelps, S. Everything you wanted to know about double auctions, but were afraid to (bid or) ask. *City University of New York: New York2005* (2006).

73. Ladley, D. Zero intelligence in economics and finance. *The Knowledge Engineering Review* **27,** 273–286 (2012).

74. Duffy, J. Agent-based models and human subject experiments. *Handbook of Computational Economics* **2,** 949–1011 (2006).

75. Farmer, J. D., Patelli, P. & Zovko, I. I. The predictive power of zero intelligence in financial markets. *Proceedings of the National Academy of Sciences of the United States of America* **102,** 2254–2259 (2005).

76. Gode, D. K. & Sunder, S. Allocative Efficiency of Markets with Zero-intelligence Traders: Market as a Partial Substitute for Individual Rationality. *Journal of Political Economy* **101(1),** 119–137 (1993).

77. Camerer, C. & Ho, T. H. Experience-weighted Attraction Learning in Normal Form Games. *Econometrica* **67(4),** 827–874 (1999).

78. Ho, T. H., Camerer, C. & Chong, J.-K. Self-tuning experience weighted attraction learning in games. *Journal of Economic Theory* **133,** 177–198 (2007).

79. Anufriev, M., Arifovic, J., Ledyard, J. & Panchenko, V. Efficiency of continuous double auctions under individual evolutionary learning with full or limited information. *Journal of Evolutionary Economics* **23,** 539–573. ISSN: 1432-1386 (2013).

80. Parsons, S., Rodriquez-Aguilar, J. A. & Klein, M. Auctions and bidding: a guide for computer scientists. *ACM Computer Surveys* **43 (2)** (2011).

81. Galla, T. & Farmer, J. D. Complex dynamics in learning complicated games. *Proceedings of the National Academy of Sciences of the United States of America* **110(4),** 1232 –1236 (2013).

82. Goeree, J. K. & Hommes, C. H. Heterogeneous beliefs and the non-linear cobweb model. *Journal of Economic Dynamics and Control* **24,** 761–798 (2000).

83. Eilers, P. H. C. & Goeman, J. J. Enhancing scatterplots with smoothed densities. *Bioinformatics* **20(5),** 623–628 (2004).

84. Binder, K. Critical Properties from Monte Carlo Coarse Graining and Renormalization. *Physical Review Letters* **47,** 693–696 (9 1981).

85. Kampen, N. V. *Stochastic Processes in Physics and Chemistry* Revised and enlarged edition (Elsevier, Amsterdam, 1997).

86. Zwanzig, R. *Nonequilibrium Statistical Mechanics* (OUP USA, 2001).

87. Freidlin, M. I. & Wentzell, A. D. in *Random Perturbations of Dynamical Systems* 15–43 (Springer, 1984).

88. Nicole, R. & Sollich, P. Mean field approach to segregation of traders toward double auction markets (in prep.).

89. Toth, B., Palit, I., Lillo, F. & Farmer, J. D. Why is equity order flow so persistent? *Journal of Economic Dynamics and Control* **51,** 218–239 (2015).

90. van Kampen, N. G. *Stochastic Processes in Physics and Chemistry* (1992).

91. Clerk-Maxwell, J. On the dynamical evidence of the molecular constitution of bodies. *Nature* **11,** 357–359 (1875).

92. McAllister, P. H. Adaptive approaches to stochastic programming. *Annals of Operations Research* **30,** 45–62 (1991).

93. Mookherjee, D. & Sopher, B. Learning behavior in an experimental matching pennies game. *Games and Economic Behavior* **7,** 62–91 (1994).

94. Ben-Akiva, M. E. & Lerman, S. R. *Discrete choice analysis: theory and application to travel demand* (MIT press, 1985).

95. Anderson, S. P., De Palma, A. & Thisse, J. F. *Discrete choice theory of product differentiation* (MIT press, 1992).

96. Erev, I. & Roth, A. E. Predicting how people play games: Reinforcement learning in experimental games with unique, mixed strategy equilibria. *American Economic Review,* 848–881 (1998).

97. Chen, Y. & Tang, F.-F. Learning and incentive-Compatible Mechanisms for Public Goods Provision: An Experimental Study. *Journal of Political Economy* **106,** 633–662 (1998).

98. Camerer, C. & Ho, T.-H. Experience-weighted attraction learning in coordination games: Probability rules, heterogeneity, and time-variation. *Journal of Mathematical Pychology* **42,** 305–326 (1998).

99. Toth, B. & Scalas, E. The value of information in financial markets: An agent-based simulation. *arXiv preprint arXiv:0712.2687* (2007).

100. Toth, B., Scalas, E., Huber, J. & Kirchler, M. The value of information in a multi-agent market model. *The European Physical Journal B* **55,** 115–120 (2007).

101. Huber, J. 'J'-shaped returns to timing advantage in access to information–Experimental evidence and a tentative explanation. *Journal of Economic Dynamics and Control* **31,** 2536–2572 (2007).

102. Hennes, D., Bloembergen, D., Kaisers, M., Tuyls, K. & Parsons, S. *Evolutionary advantage of foresight in markets* in *Proceedings of the 14th annual conference on Genetic and evolutionary computation* (2012), 943–950.

103. Gordon, M. J. *The investment, financing, and valuation of the corporation* (RD Irwin, 1962).

104. Kalimullina, L. & Schöbel, R. *The J-Curve and Transaction Taxes: Insights from an Artificial Stock Market* in *Advances in Artificial Economics* (Springer, 2015), 91–103.

105. Brewer, P. J., Huang, M., Nelson, B. & Plott, C. R. On the behavioral foundations of the law of supply and demand: Human convergence and robot randomness. *Experimental Economics* **5,** 179–208 (2002).

106. Huber, J., Kirchler, M. & Sutter, M. Is more information always better?: Experimental financial markets with cumulative information. *Journal of Economic Behavior & Organization* **65,** 86–104 (2008).

107. Bloembergen, D., Hennes, D., McBurney, P. & Tuyls, K. Trading in markets with noisy information: An evolutionary analysis. *Connection Science* **27,** 253–268 (2015).

108. Vickrey, W. Counterspeculation, auctions, and competitive sealed tenders. *The Journal of finance* **16,** 8–37 (1961).

109. Bishop, D. T. & Cannings, C. A generalised war of attrition. *Journal of Theoretical Biology* **70,** 85 (1978).

110. Haigh, J. T. & Cannings, C. The n-person war of attrition. *Acta Applicandae Mathematicae* **14** (1989).

111. Chatterjee, K., Reiter, J. G. & Nowak, M. A. Evolutionary dynamics of biological auctions. *Theoretical Population Biology* **81,** 69 (2012).

112. Andersson, M. Female choice selects for extreme tail length in a widowbird. *Nature* **299,** 818–820.

113. Viability costs of male tail ornaments in a swallow. *Nature* **339,** 132–135 (1989).

114. Emlen, D. J. The Evolution of Animal Weapons. *Annual Review of Ecology, Evolution, and Systematics* **39,** 387–413 (2008).

115. Marden, J. H. & Waage, J. K. Escalated damselfly territorial contests are energetic wars of attrition. *Animal Behaviour* **39,** 954–959 (1990).

116. Bladon, A. J., Galla, T. & McKane, A. J. Evolutionary dynamics, intrinsic noise, and cycles of cooperation. *Phys. Rev. E* **81,** 066122 (6 2010).

117. Taylor, P. D. & Jonker, L. B. Evolutionary Stable Strategies and game dynamics. *Mathematical Biosciences* **40,** 145 (1978).

118. Hofbuer, J., Schuster, P. & Sigmund, K. A note on evolutionary stable strategies and game dynamics. *Journal of Theoretical Biology* **81,** 609 (1979).

119. Zeeman, E. C. in *Global Theory of Dynamical Systems: Proceedings of an International Conference Held at Northwestern University, Evanston, Illinois, June 18–22, 1979* (eds Nitecki, Z. & Robinson, C.) 471–497 (Springer Berlin Heidelberg, Berlin, Heidelberg, 1980).

120. Chalub, F. A.C. C. & Souza, M. O. The frequency-dependent Wright–Fisher model: diffusive and non-diffusive approximations. *Journal of Mathematical Biology* **68,** 1089–1133 (2014).

121. Aalto, E. The Moran Model and Validity of the diffusion approximation in population genetics. *Journal of Theoretical Biology* **140,** 317–326 (1989).

122. Lombardo, P., Gambassi, A. & Dall'Asta, L. Nonmonotonic effects of migration in subdivided populations. *Physical Review Letters* **112,** 148101 (2014).

123. Lombardo, P., Gambassi, A. & Dall'Asta, L. Fixation properties of subdivided populations with balancing selection. *Physical Review E* **91,** 032130 (2015).

124. Emlen, D. J. The evolution of animal weapons. *Annual Review of Ecology, Evolution, and Systematics,* 387–413 (2008).

125. Wing, G. M. *A primer on integral equations of the first kind: the problem of deconvolution and unfolding* (Siam, 1991).

126. Boland, R. P., Galla, T. & McKane, A. J. How limit cycles and quasi-cycles are related in systems with intrinsic noise. *Journal of Statistical Mechanics: Theory and Experiment* **2008,** P09001 (2008).

127. Attal, S. Operator and Spectral Theory.

128. Robert, A. *Linear algebra: examples and applications* (World Scientific, 2005).

129. Cheung, Y.-W. & Friedman, D. Individual learning in normal form games: Some laboratory results. *Games and Economic Behavior* **19,** 46–76 (1997).

130. Challet, D. & Marsili, M. Criticality and market efficiency in a simple realistic model of the stock market. *Physical Review E* **68,** 036132 (3 2003).

131. Verhulst, P. F. Recherches mathématiques sur la loi d'accroissement de la population. *Nouveaux Mémoires de l'Académie Royale des Sciences et Belles-Lettres de Bruxelles* **18,** 14–54 (1845).

132. Yuexin Jiang Daniel I. Bolnick, M. K.A.E.G.A.E.M.A. M. Assortative Mating in Animals. *The American Naturalist* **181,** E125–E138 (2013).

133. Gillespie, D. T. A general method for numerically simulating the stochastic time evolution of coupled chemical reactions. *Journal of Computational Physics* **22,** 403 – 434. ISSN: 0021-9991 (1976).

134. Adams, R. A. & Essex, C. *Calculus: a complete course* (Pearson Canada 7th ed. Toronto, 2010).

135. Polyanin, A. D. & Manzhirov, A. V. *Handbook of integral equations* (CRC press, 2008).